# UNIVERSIDAD DE OVIEDO

Programa de Doctorado en Materiales

XEROGELES RESORCINOL-FORMALDEHÍDO: POROSIDAD Y QUÍMICA SUPERFICIAL A MEDIDA

TESIS DOCTORAL

Isabel Díaz Alonso-Buenaposada

Abril 2017
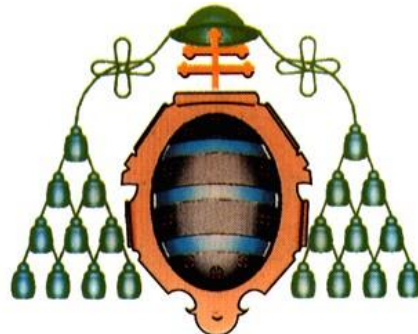
UNIVERSIDAD DE OVIEDO

Programa de Doctorado en Materiales

XEROGELES RESORCINOL-FORMALDEHÍDO: POROSIDAD Y QUÍMICA SUPERFICIAL A MEDIDA

TESIS DOCTORAL

Ana Arenillas de la Puente

José Ángel Menéndez Díaz

Vicerrectorado de Organización
Académica

Universidad de Oviedo

ASTURIAS
CAMPUS DE EXCELENCIA
INTERNACIONAL
| AD FUTURUM |

RESUMEN DEL CONTENIDO DE TESIS DOCTORAL

1.- Título de la Tesis	
Español: Xerogeles Resorcinol-Formaldehído: porosidad y química superficial a medida	Inglés: Resorcinol-Formaldehyde xerogels: tailored porosity and chemical surface.

2.- Autora	
Nombre: Isabel Díaz Alonso-Buenaposada	DNI:
Programa de Doctorado: Materiales (RD99)	
Órgano responsable: Departamento de Ciencia de los Materiales e Ingeniería Metalúrgica	

RESUMEN (en español)

La principal ventaja que presentan los xerogeles orgánicos y de carbono reside en que su porosidad puede ser diseñada a medida para la aplicación en la que se quieran utilizar estos materiales. A pesar de las ventajas que ambos materiales presentan, la mayoría de las aplicaciones se centran en el uso del xerogel de carbono, y deja en un segundo plano a su homólogo orgánico. Sin embargo, este último es un producto mucho más barato ya que no requiere de tratamientos a altas temperaturas. Además, en los últimos años se ha desarrollado y optimizado la utilización de la tecnología microondas en la síntesis de estos materiales permitiendo así su producción de forma económica a nivel industrial e incrementando así su atractivo para ser utilizados directamente en cualquier aplicación. En la presente Tesis Doctoral, se ha estudiado el efecto de la proporción de metanol de la disolución de formaldehído como nueva variable a tener en cuenta a la hora de diseñar las propiedades porosas de estos materiales a medida de la aplicación. Además, se han estudiado las ventajas e inconvenientes que presenta la utilización de catalizadores básicos o ácidos en la disolución precursora del material.
Sin embargo, no sólo las propiedades porosas repercuten sobre la aplicabilidad de estos materiales, sino que su química superficial también juega un papel relevante en este aspecto. Por este motivo, se ha estudiado y modificado la naturaleza química de la superficie de estos materiales para la obtención de xerogeles orgánicos hidrófilos, hidrófobos y superhidrófobos, a través de diferentes tratamientos.
Los resultados obtenidos de estos estudios permiten poder diseñar las propiedades porosas y químicas de los materiales finales obtenidos. Finalmente, este control de las propiedades ha permitido evaluar su utilización diferentes aplicaciones.

RESUMEN (en Inglés)

The main advantage of organic and carbon xerogels is that their porosity can be tailor-made to be used in a specific application. Despite the advantages of both materials, most applications exploit the carbon xerogel, leaving its organic counterpart in the background. However, the latter is a much cheaper product as it does not require treatments at high temperatures. In addition, in recent years the use of microwave technology has been developed and optimized for the synthesis of these materials, allowing them to be produced economically at an industrial level while increasing their appeal as they are ready for direct use.

Vicerrectorado de Organización
Académica

Universidad de Oviedo

ASTURIAS
CAMPUS DE EXCELENCIA
INTERNACIONAL
|AD FUTURUM|

In this Doctoral Thesis, the effect of the methanol content of formaldehyde solution has been studied as a new variable to be taken into account when designing the porous properties of these materials for a specific application. In addition, the advantages and disadvantages of using basic or acid catalysts in the precursor solution of the material have been studied.

However, not only do porous properties affect the applicability of these materials but their surface chemistry also plays a relevant role. For this reason, the chemical nature of the surface of these materials has been studied and modified to obtain hydrophilic, hydrophobic and superhydrophobic organic xerogels, by means of different treatments. The results obtained from these studies have made it possible to optimize the porous and chemical properties of the final materials and to evaluate their effectiveness to different applications.

SR. PRESIDENTE DE LA COMISIÓN ACADÉMICA DEL PROGRAMA DE DOCTORADO EN MATERIALES

A mis padres

Si sólo haces lo que ya sabes hacer

nunca serás más de lo que eres hoy

Índice General

Agradecimientos

En primer lugar, me gustaría expresar mi más sincero agradecimiento a los Dres. J. Ángel Menéndez Díaz y Ana Arenillas de la Puente, directores de la presente Tesis Doctoral. A ti Ángel, por no conformarte y exigirme cada día un poco más, gracias a ti hoy soy mejor profesional. A ti Ana, por motivarme y hacerme sentir enormemente valorada, gracias a ti realmente disfruto con mi trabajo. Gracias a los dos de verdad. También me gustaría agradecer al Dr. Miguel Montes su ayuda a lo largo de este trabajo.

Al Ministerio de Economía y Competitividad así como al 7º Programa Marco UE por su financiación en los proyectos *Desarrollo de materiales orgánicos nanoporosos de estructura porosa controlada, Nuevos súper-aislantes térmicos basados en geles de carbono*, *Producción de xerogeles orgánicos super-hidrófobos* y *Biopolymers from Syngas fermentation*, los cuales han permitido el desarrollo de esta Tesis. También quería agradecer al Consejo Superior de Investigaciones Científicas (CSIC) por permitir la elaboración de este trabajo en el Instituto Nacional del Carbón (INCAR).

Quería dar las gracias a mis compañeros del INCAR, tanto a los que ya no están como a los que acaban de llegar, por hacer que mi estancia en este centro sea una etapa para recordar con una enorme sonrisa. Gracias por las risas en el despacho, las sobremesas, los viajes, los cafés al sol, por vuestro apoyo en los momentos difíciles y por dejarme aprender un poquito de cada uno de vosotros. No sería justo llevarme todo el mérito… Sara, Dani, Jose, Adriá, Sandra, Nuria(s), Tan, Natalia, Fer, y un largo ETC de personas… En esta Tesis hay un trocito de cada uno de vosotros. Gracias.

Aunque todos habéis sido imprescindibles, me gustaría remarcar el papel de Esther por haberme enseñado con cariño y paciencia todo lo necesario en mis comienzos en los laboratorios del INCAR. A Rubén y Ana por valorarme de forma tan desmesurada. Y por supuesto, a María, Héctor y Luis Adrián por estar al pie del cañón en esta recta final. Sois increíbles.

A mis amigos, que estando más cerca o más lejos han sabido darme fuerza y apoyo. Especialmente a mi Sarita, por sentirse orgullosa de mí en cada pequeño paso y por estar a mi lado siempre. A Elisa, David y Marihel por aportar vuestro granito de arena. A mis padrinos, a la tía Carmen y a Lita, por seguir mis pasos de cerca y sentir tan sincero orgullo por mí. Y por supuesto a Miguel, por ser como eres… Gracias por creer en mí tan ciegamente y por hacerme tan feliz.

Finalmente, me gustaría agradecer con toda mi alma el apoyo recibido por mis padres y mi hermano. Siempre habéis luchado por mí, me lo habéis dado TODO, me habéis apoyado y me habéis querido con locura. Aunque no exista manera posible de devolveros todo vuestro esfuerzo, esta Tesis va dedicada a vosotros de manera incondicional. Gracias por todo. **Os quiero**.

Resumen

La principal ventaja que presentan los xerogeles orgánicos y de carbono reside en que su porosidad puede ser diseñada a medida para la aplicación en la que se quieran utilizar estos materiales. A pesar de las ventajas que ambos materiales presentan, la mayoría de las aplicaciones se centran en el uso del xerogel de carbono, y deja en un segundo plano a su homólogo orgánico. Sin embargo, este último es un producto mucho más barato ya que no requiere de tratamientos a altas temperaturas. Además, en los últimos años se ha desarrollado y optimizado la utilización de la tecnología microondas en la síntesis de estos materiales permitiendo así su producción de forma económica a nivel industrial e incrementando así su atractivo para ser utilizados directamente en cualquier aplicación.

En la presente Tesis Doctoral, se ha estudiado el efecto de la proporción de metanol de la disolución de formaldehído como nueva variable a tener en cuenta a la hora de diseñar las propiedades porosas de estos materiales a medida de la aplicación. Además, se han estudiado las ventajas e inconvenientes que presenta la utilización de catalizadores básicos o ácidos en la disolución precursora del material.

Sin embargo, no sólo las propiedades porosas repercuten sobre la aplicabilidad de estos materiales, sino que su química superficial también juega un papel relevante en este aspecto. Por este motivo, se ha estudiado y modificado la naturaleza química de la superficie de estos materiales para la obtención de xerogeles orgánicos hidrófilos, hidrófobos y superhidrófobos, a través de diferentes tratamientos.

Los resultados obtenidos en esta Tesis Doctoral permiten poder diseñar las propiedades porosas y químicas de los xerogeles orgánicos potenciando aún más su versatilidad y por lo tanto sus múltiples aplicaciones.

Abstract

The main advantage of organic and carbon xerogels is that their porosity can be tailor-made to be used in a specific application. Despite the advantages of both materials, most applications exploit the carbon xerogel, leaving its organic counterpart in the background. However, the latter is a much cheaper product as it does not require treatments at high temperatures. In addition, in recent years the use of microwave technology has been developed and optimized for the synthesis of these materials, allowing them to be produced economically at an industrial level while increasing their appeal as they are ready for direct use.

In this Doctoral Thesis, the effect of the methanol content of formaldehyde solution has been studied as a new variable to be taken into account when designing the porous properties of these materials for a specific application. In addition, the advantages and disadvantages of using basic or acid catalysts in the precursor solution of the material have been studied.

However, not only do porous properties affect the applicability of these materials but their surface chemistry also plays a relevant role. For this reason, the chemical nature of the surface of these materials has been studied and modified to obtain hydrophilic, hydrophobic and superhydrophobic organic xerogels, by means of different treatments.

The results obtained in this Doctoral Thesis have made it possible to optimize the porous and chemical properties of the organic xerogels enhancing even more their versatility and their potential use in a wide range of applications.

Índice de Figuras

Índice de Tablas

Abreviaturas y símbolos

ABTS	Sal de diamonio 2,2'-azino-bis (ácido 3-etilbenzotiazolino-6-sulfónico)
ANOVA	Análisis de varianza
APS	Tamaño de Poro Medio
BE	Energía de Enlace
BET	Brunauer-Emmett-Teller
CX	Xerogel de Carbono
Cyt C	Citocromo C
D	Grado de Dilución
DFT	Teoría Funcional de Densidad
DOE	Diseño de Experimentos
Dp	Diámetro de poro
DR	Dubinin-Radushkevich
EBT	Empresa de Base Tecnológica
F	Formaldehído
FTIR	Espectroscopía Infrearroja por Transformada de Fourier
HMDZ	Hexametildisilazano
KE	Energía cinética
MCAT	Microondas y Carbones para Aplicaciones Tecnológicas
MeOH	Metanol
MSR	Metodología de Superficie Respuesta

OX	Xerogel Orgánico
p/p^o	Presión relativa
PZC	Punto de carga cero
R	Resorcinol
R/F	Relación molar Resorcinol/Formaldehído
RF	Xerogel Resorcinol-Formaldehído
RMN	Resonancia Magnética Nuclear
S$_{BET}$	Área superficial equivalente en la ecuación BET (m^2/g)
SEM	Microscopio Electrónico de Barrido
S$_{EXT}$	Área superficial externa (m^2/g)
SHP	Xerogel superhidrófobo
TEM	Microscopio Electrónico de Transmisión
TGA	Análisis Termogravimétrico
TMCS	Trimetilclorosilano
TMMS	Trimetilmetoxisilano
TPD	Desorción por Temperatura Programada
V$_{ads}$	Volumen adsorbido (cm^3/g)
V$_{DUB}$	Volumen total de microporos según la acuación de Dubinin–Radushkevich
V$_{macro}$	Volumen de macroporos (cm^3/g)
V$_{meso}$	Volumen de mesoporos (cm^3/g)
V$_{tot}$	Volumen total de poros (cm^3/g)
XPS	Espectroscopía de fotoelectrones emitidos por rayos X

| θ | Ángulo de contacto sólido-líquido |
| Υ | Tensión superficial (N/m) |

Prólogo

La presente Tesis Doctoral estudia el diseño tanto de las propiedades texturales de los xerogeles resorcinol-formaldehído como de su química superficial. El trabajo desarrollado incluye el estudio de distintas variables que afectan al proceso de síntesis, la incorporación de nuevas técnicas de modificación superficial en estos materiales y el diseño de la combinación óptima de porosidad y mojabilidad para aplicaciones muy diversas: soportes para biomoléculas y materiales desecantes.

Esta memoria está comprendida por: un capítulo de libro, una patente y ocho publicaciones en revistas científicas, algunas aún pendientes de aceptación (Tabla 1), obtenidas a lo largo del periodo de tesis. Para facilitar su comprensión, la tesis se ha dividido en los bloques representados en la Figura 1.

Figura 1. *Estructura de la memoria.*

El **Capítulo 1**, *Introducción*, contiene un breve resumen de lo que se encuentra desarrollado dentro del *Capítulo de libro* que se incluye en este bloque. Aquí se detallan los aspectos más relevantes de los geles de carbono: qué son los xerogeles, su proceso de síntesis, sus propiedades, el efecto de cada una de las variables que afectan en el proceso, la química de los materiales, sus posibles aplicaciones y las perspectivas que tienen de futuro. Además, en este capítulo también se hace un repaso de la utilización de la radiación microondas en la síntesis de diferentes compuestos químicos y los avances que esto supuso en la industria.

El **Capítulo 2**, *Planteamiento de la Tesis*, relata los antecedentes del grupo de investigación MCAT, en el que se ha desarrollado esta Tesis Doctoral, que suponen los cimientos sobre los que se ha desarrollado este trabajo. Estos estudios previos generan la necesidad de abordar los objetivos planteados en el presente trabajo, los cuales desembocan en un único objetivo global: controlar tanto la porosidad como la química superficial de los xerogeles resorcinol-formaldehído para su utilización en múltiples aplicaciones.

El **Capítulo 3**, *Experimental*, describe los procedimientos realizados para la síntesis de los materiales desarrollados a lo largo de la memoria, así como las técnicas experimentales empleadas para su caracterización.

El **Capítulo 4**, *Diseño de las propiedades porosas,* tiene su base en el trabajo desarrollado en el grupo de investigación MCAT durante las Tesis Doctorales anteriores, donde se detalla el efecto que tiene cada una de las variables conocidas hasta entonces sobre el material final obtenido. Sin embargo, la *Publicación I* y *II*, relatan el estudio de una variable nueva que no se había tenido en cuenta hasta la fecha: la proporción de metanol utilizada como estabilizante en la disolución de formaldehído comercial. Estos estudios surgen de la necesidad de resolver la falta de reproducibilidad en los materiales cuando se cambia de proveedor de este reactivo, debido a la falta de homogeneidad entre las distintas casas comerciales.

Una vez controladas todas las variables químicas incluidas en el proceso de síntesis, se estudió la posibilidad de producir materiales con propiedades diferentes mediante la utilización de un catalizador ácido en la disolución precursora en vez de la base comúnmente utilizada (*Publicación III).* El control de las propiedades porosas permitió diseñar una serie de materiales en el rango de mesoporos para evaluar su aplicabilidad como soportes de biomoléculas (*Publicación IV*), permitiendo su recuperación y reutilización.

El **Capítulo 5**, *Diseño de la química superficial*, pretende dar un paso más allá a la hora de diseñar xerogeles orgánicos para distintas aplicaciones, ya que las propiedades químicas de los materiales también repercuten en su eficacia. De esta forma, el capítulo se divide en dos bloques principales. En el primer bloque, se evalúa la capacidad de los xerogeles orgánicos para ser utilizados como materiales desecantes *(Publicación V).* Se observa entonces que, no sólo funcionan de forma prometedora para esta aplicación, sino que presentan mejores resultados que materiales comerciales que se utilizan en la actualidad para este mismo fin. Este hecho dio lugar a una *Patente* y a un segundo estudio (*Publicación VI*) en el que se optimiza la capacidad de adsorción de humedad por parte del material a través del diseño de sus propiedades texturales.

Aunque la química original hidrófila de los xerogeles orgánicos puede ser útil para algunas aplicaciones, como la mencionada anteriormente, puede ser desfavorable para otras posibles aplicaciones como el aislamiento térmico o la adsorción de aceites. Por este motivo, el segundo bloque del Capítulo 5, muestra la obtención de materiales super/hidrófobos mediante la modificación superficial de los materiales orgánicos a través de dos diferentes vías: pasivado con un silano (*Publicación VII*) y con metanol en fase vapor (*Publicación VIII*).

El **Capítulo 6** recoge las *Conclusiones* obtenidas a lo largo de toda la Tesis Doctoral, las cuales responden a los objetivos planteados y dan lugar a la posibilidad de diseñar xerogeles RF con porosidad y química superficial totalmente a medida de la posible aplicación final.

El **Capítulo 7**, *Bibliografía*, recoge todas las referencias bibliográficas citadas a lo largo de la memoria, no incluidas en las publicaciones, sobre las que se sustenta el trabajo aquí desarrollado.

Finalmente, en el **Anexo** se incluyen las contribuciones a congresos derivados del trabajo aquí descrito.

Tabla 1.   *Publicaciones que conforman esta memoria.*

REFERENCIA	TÍTULO	REVISTA
Capítulo de libro	Síntesis de polímeros con microondas	ISBN: 978-9978-395-34-9
Publicación I	Effect of methanol content in commercial formaldehyde solutions on the porosity of RF carbon xerogels	Journal of Non-Crystalline Solids
Publicación II	An underrated variable essential for tailoring the structure of xerogel: the methanol content of commercial formaldehyde solutions	Enviada
Publicación III	Acid-based resorcinol-formaldehyde xerogels synthesized by microwave heating	Enviada
Publicación IV	Protein adsorption and activity on carbon xerogels with narrow pore size distributions covering a wide mesoporous range	Carbon
Publicación V	Desiccant capability of organic xerogels: surface chemistry vs porous texture	Microporous & Mesoporous materials
Publicación VI	On the desiccant capacity of the mesoporous RF-xerogels	Microporous & Mesoporous materials
Patente	Uso de un xerogel orgánico como desecante	ES1641.1201 PTC1641.1201
Publicación VII	Hydrophobic RF xerogels synthesis by grafting with silanes	Enviada
Publicación VIII	Superhydrophobic and Breathable Resorcinol-Formaldehyde Xerogels	Enviada

Capítulo 1

Introducción

1. Introducción

En esta Tesis Doctoral se consideran geles orgánicos a los materiales nanoporosos obtenidos a través de la reacción de polimerización entre un benceno hidroxilado y un aldehído, en un medio de reacción [1]. Los monómeros más comúnmente utilizados para la síntesis de este tipo de materiales son el resorcinol y el formaldehído [2-4] (Figura 2), aunque también se pueden utilizar otros precursores más baratos y/o ecológicos como pueden ser el fenol [5], la hexamina [6], el furfural [7], la urea [8], los taninos [9], etc.
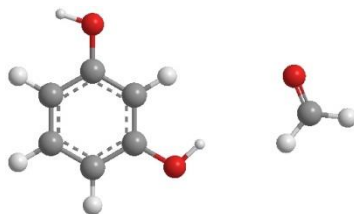
Figura 2.   *Estructura molecular del resorcinol (izq) y el formaldehído (dcha).*

La obtención de dichos materiales tiene lugar a través de una reacción tipo *sol-gel* que se divide en tres etapas principales [10] (Figura 3): i) polimerización, donde los monómeros comienzan a entrecruzarse formando núcleos llamados nódulos, ii) curado, donde se entrecruzan los nódulos formados en la etapa previa y la estructura toma estabilidad, y iii) secado, donde se elimina el exceso de disolvente. El cambio de sol a gel visualmente se traduce en una pérdida de fluidez de la disolución inicial, formándose una fase

viscosa que va tomando consistencia según avanza la reacción hasta formarse finalmente un sólido [11].
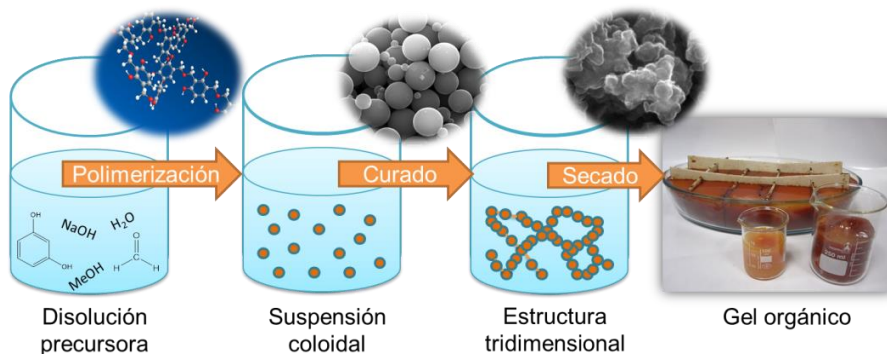
Figura 3.   *Etapas de la síntesis de un gel orgánico.*

Las proporciones de los reactivos utilizados en la disolución precursora determinan tanto la velocidad de polimerización como la forma en que ésta ocurre y, en consecuencia, también la estructura del gel resultante. Por este motivo, en la bibliografía podemos encontrar múltiples estudios que detallan el efecto de cada una de las variables que participan en este proceso sobre la estructura final del gel, tales como: tiempos de síntesis [12], volumen de mezcla utilizado, pH de la disolución precursora [13], tipo de catalizador [14], proporción de disolvente utilizado [4], proporción entre los monómeros [15], porcentaje de estabilizante de la disolución de formaldehído [16], etc. El mayor problema reside en que, no sólo hay gran número de variables, sino que existen sinergias entre ellas, es decir se encuentran interconectadas, de manera que la alteración de cualquiera de ellas modifica de forma directa el comportamiento de las otras. Por este motivo se requiere del uso de programas estadísticos que permitan evaluar de manera global el efecto de todas estas variables y poder así diseñar materiales con porosidad controlada y específica para una aplicación concreta [15, 16].

Una vez completada la fase de curado se procede a la eliminación del disolvente que queda contenido en la estructura del gel (etapa de secado). La metodología empleada en esta etapa determina la estructura, y por tanto las

propiedades, del gel orgánico obtenido. Existen tres métodos de secado dependiendo de las condiciones de operación utilizadas para la eliminación del disolvente [10, 17, 18]: i) condiciones supercríticas, que da lugar a los llamados *aerogeles*, ii) condiciones criogénicas, que da lugar a los llamados *criogeles*, y iii) condiciones subcríticas, que da lugar a los llamados *xerogeles*, materiales en los que se centra esta memoria.

Para la obtención de los xerogeles orgánicos, los materiales son sometidos a un calentamiento moderado (alrededor de 85 ºC). Hasta hace relativamente poco, este proceso se realizaba mediante calentamiento convencional utilizando hornos eléctricos, sin embargo se requerían tiempos prolongados, de aproximadamente 5 días, para completar la síntesis. En 2011, el grupo de investigación MCAT (*Microondas y Carbones para Aplicaciones Tecnológicas*), donde se ha llevado a cabo este trabajo, introdujo el calentamiento con microondas en la síntesis completa del material orgánico [1]. Esto supuso una reducción de los tiempos de síntesis en un 90 %, lo que se traduce en tiempos totales de alrededor de 5 h, y un abaratamiento significativo de los costes de producción.

El producto derivado de este proceso es el llamado *gel orgánico* y presenta una química superficial rica en grupos funcionales oxigenados, baja densidad, baja conductividad térmica y eléctrica, y una porosidad controlable (Figura 4). Si este material se somete a un proceso de carbonización (tratamiento térmico a alta temperatura en atmósfera inerte), se obtiene el llamado *gel de carbono* [19] (Figura 4). El material carbonizado mantiene su meso-macroporosidad respecto a su homólogo orgánico, ya que esta estructura porosa depende de los entrecruzamientos formados en la etapa de síntesis y no se ve afectada por el tratamiento térmico posterior. Sin embargo, su microporosidad aumenta de forma considerable, ya que estos poros son fruto de huecos que dejan los volátiles dentro de los nódulos al desprenderse a altas temperaturas. Si durante este tratamiento térmico, en lugar de utilizar una atmósfera inerte se utilizara un gas reactivo como puede ser el CO_2, se obtendría el llamado *gel activado*, cuya microporosidad es mucho mayor aún

que el carbonizado, pero se asemeja en el resto de sus propiedades [20]. Sin embargo, cualquier tratamiento térmico (carbonización o activación) cambia de forma radical la química del material, pasando de un alto contenido en oxígeno (aproximadamente el 40 % en masa) a estar formado prácticamente por carbono en su totalidad (en torno al 98 % en masa). Como es de esperar, estos cambios tienen repercusión sobre las propiedades del carbonizado, resultando materiales más densos, con buena conductividad eléctrica, gran área superficial y mejor resistencia mecánica. En consecuencia, las distintas propiedades de los materiales orgánicos y carbonizados hacen que las posibles aplicaciones de ambos sean totalmente diferentes.

Figura 4. *a), b) y c) Xerogeles orgánicos con distintas texturas porosas y d) xerogel de carbono.*

Es interesante resaltar, que la mayoría de las aplicaciones encontradas en la bibliografía donde se utilizan este tipo de materiales, hacen uso del gel de carbono [21-23], dejando en un segundo plano al material orgánico. Sin embargo, las cualidades del xerogel orgánico resultan atractivas en campos diferentes a los de su homólogo carbonizado, ya que sus propiedades texturales, así como su morfología, pueden ser diseñadas en la misma medida

que se hacen con el material de carbono. Por ejemplo, su baja conductividad térmica junto con una porosidad apropiada, hacen de estos materiales buenos aislantes térmicos [24]. Asimismo, su alta porosidad y química controlable posibilita su uso como materiales adsorbentes o como soportes para proteínas, donde el diámetro de poro puede ser diseñado de forma específica según el tamaño de la biomolécula que se quiera soportar. Además, como se puede comprobar en las publicaciones científicas recogidas en la presente memoria, los xerogeles orgánicos han demostrado ser prometedores para ser utilizados como materiales desecantes (*Publicación V, Patente* y *Publicación VI*). Además, como se detalla en el Capítulo 5, modificando la química superficial de estos materiales (*Publicación VII y VIII*), se abre una nueva vía a aplicaciones donde se requieren materiales porosos de naturaleza hidrófoba.

La posibilidad de producir estos materiales de forma rápida y barata gracias al empleo de radiación microondas durante toda la etapa de síntesis, en conjunto con la ausencia de una posterior etapa de carbonización/activación, les convierte en materiales económicamente competitivos y escalables a nivel industrial.

Más información acerca de la síntesis de polímeros en microondas, así como de xerogeles de forma más detallada (sus propiedades, cómo afecta cada variable sobre la síntesis, cómo es su química, aplicaciones, perspectivas de futuro, etc.) se puede encontrar en el capítulo del libro *Síntesis de polímeros en microondas,* recogido en el libro *Aplicaciones industriales del calentamiento con energía microondas*, que se presenta a continuación.

CAPÍTULO DE LIBRO

SÍNTESIS DE POLÍMEROS CON MICROONDAS

Síntesis de polímeros con microondas

10

Isabel D. Alonso-Buenaposada, Ana Arenillas

Abstract

During the last 25 years microwave radiation has come to be accepted as a heating source for chemical synthesis due to the number of advantages it offers. These include a reduction in synthesis time, the possibility that it can be used without the need of solvents and, above all, because it is an easy, fast and safe method. Moreover, microwave technology has been shown to be scalable as it is already widely used in the pharmaceutical industry, as a means of synthesising organometallic compounds and polymers, of which vulcanised rubber (industrial scale) and organic gel (R+D scale) are noteworthy examples.

Organic gels are polymeric materials with a great versatility due to the fact that their porosity, surface chemistry and morphology can be tailored for a specific application by controlling the variables which affect the synthesis process. Due to the rigorous control of properties of these materials through a careful manipulation of the variables used during the synthesis, they can be tailored for diverse applications (hydrogen storage, thermal insulation, electrode supercapacitors, adsorbent materials, catalytic supports, etc.).

Keywords: Microwaves, carbon xerogels, polymers, controlled synthesis.

RESUMEN

Durante los últimos 25 años la radiación microondas se ha consolidado como fuente de calor aplicable a la síntesis química debido a sus múltiples ventajas, como son la notable reducción de tiempos de síntesis, la posibilidad de no usar disolventes y sobre todo que es un método fácil, rápido y seguro. Además, la tecnología microondas ha mostrado ser perfectamente escalable, utilizándose en la industria farmacéutica, síntesis de compuestos organometálicos y en la síntesis de polímeros, entre los que destacan a nivel industrial el caucho vulcanizado y a nivel de I+D+i los geles orgánicos.

Los geles orgánicos son materiales poliméricos con una enorme versatilidad debido a que tanto su porosidad, su química superficial y su morfología pueden ser diseñados a medida de la aplicación deseada, controlando las variables que afectan en el proceso de síntesis. Debido al exhaustivo control de las propiedades de estos materiales en función de las variables utilizadas durante la síntesis, las posibles aplicaciones para las que puede ser utilizado son muy diversas (almacenamiento de hidrógeno, aislante térmico, electrodo de supercondensadores, material adsorbente, soporte catalítico, etc.).

1.   INTRODUCCIÓN

Durante los últimos 25 años la radiación microondas se ha consolidado como fuente de calor aplicable a la síntesis química debido a las diferentes ventajas que esta técnica proporciona con respecto al calentamiento convencional.

La principal ventaja que presenta es la reducción de los tiempos de síntesis, ya que en muchos casos la velocidad de la reacción puede llegar a aumentar hasta 2-3 órdenes de magnitud, con respecto al calentamiento convencional (S. Sinnwell & H. Ritter, 2007). Además, el calentamiento directo de las moléculas hace que se produzca de forma más rápida, evitando reacciones secundarias y obteniendo así productos más limpios y con mayor rendimiento. Aunque la mayoría de estas mejoras se le atribuyen a los efectos

térmicos producidos por este tipo de calentamiento, algunos de ellos no se pueden reproducir por calentamiento convencional, por lo que son considerados efectos no térmicos. Estos efectos específicos de la radiación microondas a menudo son asociados al calentamiento dieléctrico (R. Hoogenboom & U.S. Schubert, 2007) en el cual, las moléculas muestran un dipolo permanente que intenta alinearse con el campo electromagnético aplicado, y para ello las moléculas rotan, friccionan y chocan entre ellas, lo cual genera calor. Esto produce un perfil inverso de temperaturas (J. Rydfjord et al., 2013), sobrecalentamiento de los disolventes a presión atmosférica (F. Chemat & E. Esveld, 2001), o el calentamiento selectivo de algunos compuestos que absorben en mayor medida la radiación microondas (N.E. Leadbeater & H.M. Torenius, 2002) . Por este motivo, esta técnica limita su aplicación a medios polares, ya que compuestos apolares no reaccionan ante un campo electromagnético al no contener dipolos permanentes.

Las primeras investigaciones fueron llevadas a cabo con hornos microondas domésticos, lo que hacía que la reproducibilidad de los resultados y la seguridad durante los experimentos fuera escasa, debido a un insuficiente control de la temperatura (A. Loupy, 2006). Hoy en día las condiciones de presión y temperatura se controlan mediante sistemas informáticos para evitar la ruptura de los recipientes o explosiones (R.N. Gedye, F.E. Smith, & K.C. Westaway, 1988; R. Giguere, 1989; R.J. Giguere, T.L. Bray, S.M. Duncan, & G. Majetich, 1986), convirtiéndose así en un método fácil, rápido y seguro. Además, de esta forma se evita el uso de baños de aceite, los cuales son altamente peligrosos y necesitan de largos tiempos para alcanzar la temperatura deseada. El calentamiento por microondas cada vez es más utilizado para llevar a cabo reacciones sin disolvente, donde es un soporte sólido el que absorbe la radiación microondas. Así se evitan los peligros del calentamiento del disolvente y se ahorra la evaporación de estos, siendo así más ecológico.

Además, la tecnología microondas ha mostrado ser escalable para su aplicación a nivel industrial (A. Loupy, 2006)l. Hoy en día ya se utiliza en la

industria farmacéutica (C.O. Kappe & D. Dallinger, 2006), síntesis de compuestos organometálicos (N.E. Leadbeater, 2010) y en la síntesis de polímeros (R. Hoogenboom & U.S. Schubert, 2007; S.E. Mallakpour, A.R. Hajipour, & S. Habibi, 2002; S. Sinnwell & H. Ritter, 2007). Posiblemente, el polímero más común sintetizado con microondas a nivel industrial el caucho vulcanizado, donde caucho crudo se calienta en presencia de azufre y da lugar al caucho de color negro tan cual lo conocemos, más duro y resistente al frío (U. Jung, W.K. Lee, & K.T. Lim, 2011; E. Manaila et al., 2009; I.R. Wayne, 1980).

En la ciencia de los polímeros, la aplicación de tecnología microondas fue previa a la primera publicación en 1986 (R. Gedye et al., 1986) que hablaba de la síntesis orgánica asistida por microondas. En 1979, Gourdenne (A. Gourdenne, A. Maassarani, P. Monchaux, S. Aussudre, & L. Thourel, 1979) publicó un entrecruzamiento entre poliéster insaturado con estireno utilizando tecnología microondas. En 1983 Teffal y Gourdenne (M. Teffal & A. Gourdenne, 1983) publicaron la polimerización de 2-hidroxietil metacrilato tanto en microondas como en condiciones convencionales.
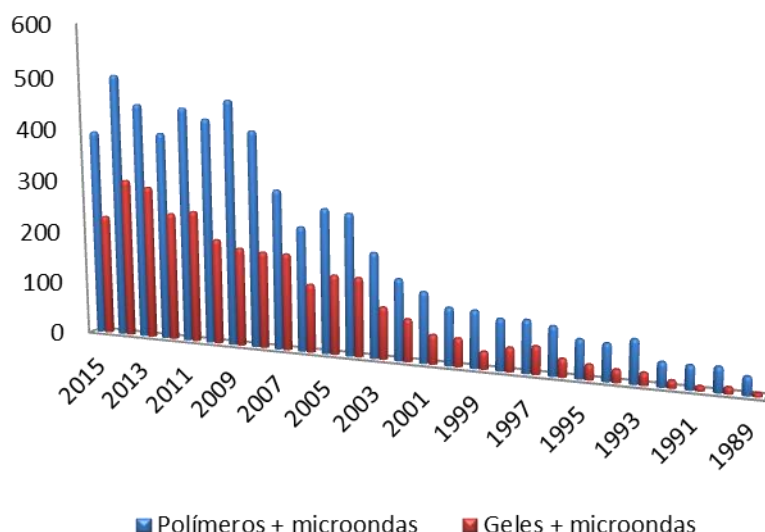
Figura 1. *Representación gráfica del número de publicaciones por año que incluyan polímeros + microondas y geles + microondas.*

Desde entonces la aplicación de microondas para la síntesis de polímeros ha aumentado enormemente como se puede observar en la Figura 1. Las investigaciones se centran principalmente en 3 áreas (R. Hoogenboom & U.S. Schubert, 2007; S. Sinnwell & H. Ritter, 2007): (i) polimerizaciones radicales, donde se produce una adición sucesiva de monómeros gracias a la alta reactividad de los radicales. Es bastante común ya que son compatibles con agua y se evita el uso de disolventes orgánicos. (ii) Polimerizaciones de ciclo abierto, donde el final de una cadena polimérica actúa como centro reactivo, y un monómero cíclico se abre para reaccionar con este, dando un polímero de mayor longitud. Este tipo de reacciones dan lugar a polímeros de alto peso molecular. Y finalmente, (iii) polimerización por etapas, basadas en el acoplamiento de monómeros multifuncionales en etapas independientes, como por ejemplo ocurre en la síntesis de un tipo de polímeros que pasan por un estado sol-gel durante su síntesis y que se denominan geles orgánicos. Dado el gran atractivo que han adquirido durante los últimos años, y la posibilidad de su producción industrial utilizando microondas, los trataremos en más profundidad en este capítulo.

1.1. Geles orgánicos

Los geles orgánicos son materiales nanoporosos obtenidos a partir de la reacción de polimerización entre bencenos hidroxilados (fenol, catecol, resorcinol, hidroquinona, etc.) y aldehídos (formaldehído, furfural, etc.), en un disolvente determinado (agua, metanol, acetona, etc.) según el método de Pekala (R. Pekala, 1989). Tras la polimerización, el gel se somete a una etapa de secado para eliminar el disolvente, y dependiendo del método de secado que se utilice, el gel obtenido va a tener distintas propiedades, y reciben diferente denominación (E.G. Calvo, A. Arenillas, & J. Menéndez, 2011) (Figura 2): (i) el secado en condiciones supercríticas tiene lugar bajo condiciones de presión y temperatura muy altas. Preserva en gran medida las propiedades texturales adquiridas durante la síntesis del gel, pero es extremadamente caro y tarda mucho tiempo en realizarse. Da lugar a los llamados aerogeles (O.

Czakkel, K. Marthi, E. Geissler, & K. László, 2005). (ii) El secado criogénico consiste en congelar el disolvente y eliminarlo por sublimación y posterior desorción. Se obtienen materiales con gran diámetro de poro pero tiene un coste muy alto, necesita de largos tiempos de secado. Además, tiene un procedimiento complicado ya que requiere de intercambio de disolventes. Da lugar a los llamados criogeles (B. Babić, B. Kaluđerović, L. Vračar, & N. Krstajić, 2004). Y finalmente, (iii) el secado en condiciones subcríticas, el cual consiste en evaporación del disolvente mediante aporte de calor, da lugar a los llamados xerogeles (N. Job, F. Sabatier, J.-P. Pirard, M. Crine, & A. Léonard, 2006).
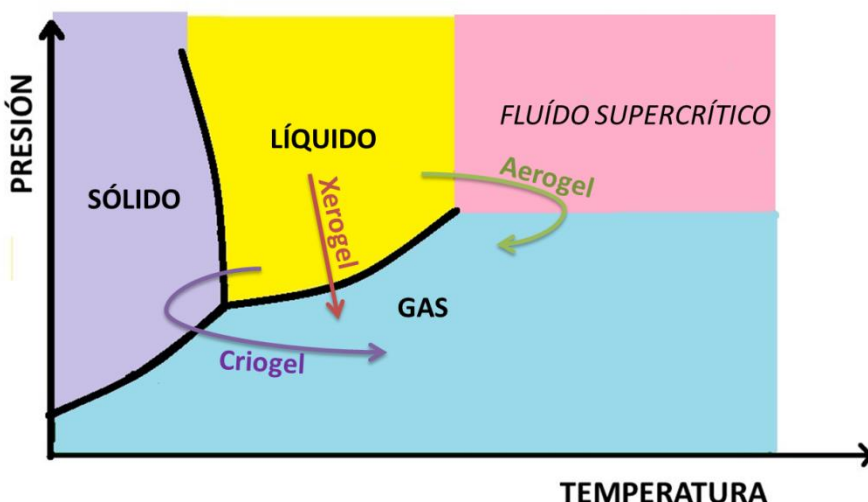
Figura 2. *Esquema de las diferentes condiciones de secado utilizadas en la síntesis de geles orgánicos.*

El secado por evaporación (condiciones subcríticas) presenta varias ventajas frente al secado supercrítico o criogénico como por ejemplo, la sencillez, y bajo coste del método, así como el ahorro de tiempo comparado con los otros dos métodos de secado (L. Zubizarreta, A. Arenillas, J. A. Menéndez, et al., 2008). Por otra parte, cuando el disolvente en el interior de los poros se evapora rápidamente, los poros son sometidos a tensiones altas pudiendo provocar un colapso parcial de la estructura. Para reducir estas fuerzas capilares, algunos autores (E. Gallegos-Suárez, A.F. Pérez-Cadenas, F.J. Maldonado-Hódar, & F. Carrasco-Marín, 2012; K. Kraiwattanawong, H.

Tamon, & P. Praserthdam, 2011) intercambian el disolvente por uno con menor tensión superficial, como puede ser el hexano o la acetona, de forma que la tensión producida entre el disolvente y la superficie del poro se minimiza. De todos modos, controlando adecuadamente las condiciones de secado, se pueden obtener geles de carbono con porosidad controlada y un gran volumen de poros, incluso utilizando un medio acuoso y sin hacer ningún intercambio de disolvente previamente a la etapa de secado (N. Job, R. Pirard, J. Marien, & J.-P. Pirard, 2004; N. Job et al., 2006).

La principal ventaja que presentan estos materiales reside en la capacidad de diseñar su estructura porosa a medida para cada aplicación de forma específica, pudiéndose obtener materiales en un amplio rango de volúmenes y tamaños de poro.

2.   SÍNTESIS DE XEROGELES

Hoy en día, el proceso de síntesis más común para xerogeles orgánicos consiste en la polimerización de los monómeros resorcinol y formaldehído en medio acuoso. Es bastante frecuente la utilización de catalizadores, como pueden ser el NaOH o Na_2CO_3 (C. Moreno-Castilla & F.J. Maldonado-Hódar, 2005; N. Rey-Raap, J. Angel Menéndez, & A. Arenillas, 2014b), los cuales aceleran la reacción de polimerización y modifican la porosidad del material.

Inicialmente los xerogeles eran sintetizados por calentamiento convencional en su totalidad. Posteriormente, se introdujo el calentamiento con radiación microondas sólo en la etapa de secado (N. Tonanon et al., 2006; L. Zubizarreta, A. Arenillas, J. A. Menéndez, et al., 2008). Hoy en día la síntesis completa de los xerogeles orgánicos puede llevarse a cabo utilizando un horno microondas como único dispositivo, lo que facilita enormemente el proceso de síntesis. Además, al utilizar esta técnica la síntesis completa se reduce a 5 h, frente a los 4-5 días que se necesitan cuando se utiliza calentamiento convencional (E.G. Calvo, E.J. Juárez-Pérez, J.A. Menéndez, & A. Arenillas, 2011; Á.H. Moreno et al., 2013). Las variables físicas del proceso de síntesis,

como pueden ser la temperatura o el tiempo de síntesis, afectan en las propiedades porosas del material pero ofrecen ciertos márgenes, lo que es una gran ventaja a la hora de escalar este proceso a nivel industrial. Hoy en día la empresa Xerolutions S.L. (www.xerolutions.com) ha llevado a cabo este proceso de escalado para la producción de xerogeles de carbono en microondas con porosidad a medida para su aplicación como electrodos para supercondensadores.

El proceso de síntesis de los xerogeles orgánicos comprende 3 etapas: polimerización, curado y secado. El mecanismo de polimerización entre el resorcinol y el formaldehído puede observarse en la Figura 3. El resorcinol es un compuesto bencílico trifuncional con dos grupos hidroxilo en las posiciones 1 y 3, lo que permite la adición del formaldehído en las posiciones 2, 4 y 6. En la primera etapa tiene lugar una reacción de adición favorecida en medio básico, ya que el anión del resorcinol es una molécula mucho más reactiva que la molécula no cargada, favoreciendo así la adición del formaldehído en una primera etapa y la formación de derivados hidroximetílicos.
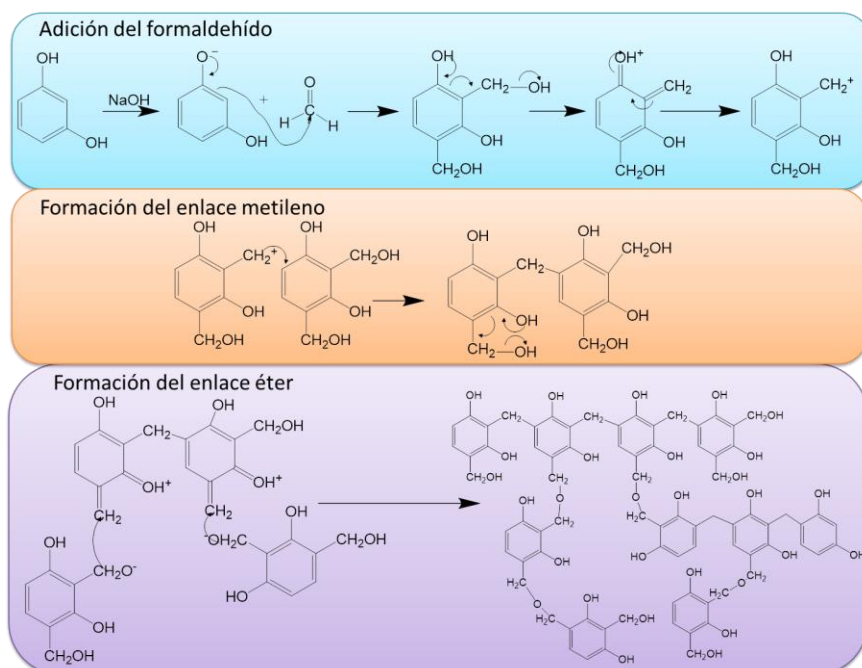
Figura 3. *Mecanismo de polimerización entre el resorcinol y formaldehído.*

En la segunda etapa tiene lugar la condensación de dichos derivados hidroximetílicos, estando esta etapa más favorecida en medio ácido. Esta condensación da lugar a entrecruzamientos que en función del pH y las concentraciones de los reactivos iniciales, darán lugar a materiales con diferente porosidad.

Este proceso conlleva un cambio en la viscosidad de la disolución, pasando de ser una disolución líquida a convertirse en un sólido con la forma del recipiente en el que se encuentre (reacción sol-gel). Al llevarse a cabo en un dispositivo microondas, es posible registrar en tiempo real la energía consumida por el microondas. De esta forma, es posible determinar el punto exacto en el que ocurre el cambio de fase sol-gel (punto de gelación, ver Figura 4), ya que la representación de la energía acumulada frente al tiempo da lugar a dos rectas de diferente pendiente, y cuyo punto de corte corresponde a ese cambio de fase del material (E. G. Calvo et al., 2011; E.J. Juárez-Pérez, E.G. Calvo, A. Arenillas, & J.A. Menéndez, 2010). Gracias a este procedimiento, se puede detener el proceso de síntesis en el momento preciso pudiendo así controlar la viscosidad del medio de reacción. La determinación del punto de gelación resulta de gran utilidad cuando se quieren sintetizar geles de carbono con formas específicas (esferas, monolitos, etc.) para aplicaciones concretas que exijan determinada morfología (J.A. Menéndez, E.J. Juárez-Pérez, E. Ruisánchez, E.G. Calvo, & A. Arenillas, 2012; L. Zubizarreta, J.A. Menéndez, J.J. Pis, & A. Arenillas, 2009).
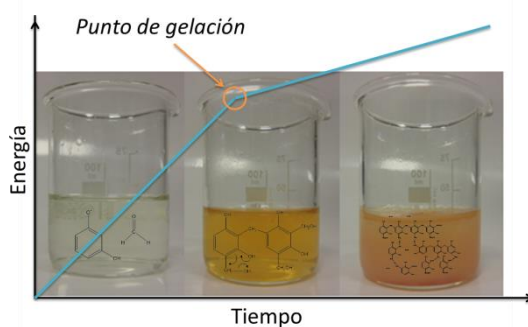
Figura 4. *Determinación del punto de gelación.*

Posteriormente a la etapa de polimerización se encuentra la etapa de curado, en la cual se favorecen los entrecruzamientos de la estructura del gel orgánico, y el polímero formado se estabiliza. Y finalmente, en la etapa de secado, los restos de disolvente que hayan quedado retenidos en la estructura se eliminan mediante evaporación.

De esta forma se obtiene el gel orgánico utilizando únicamente un horno microondas, lo cual presenta muchas ventajas frente a la síntesis por calentamiento convencional, como que el proceso de calentamiento es mucho más rápido, volumétrico, selectivo al agua que hay que evaporar, se utiliza un único dispositivo compacto y de bajo coste y es perfectamente escalable.

Para obtener el llamado gel de carbono, el gel orgánico obtenido tras la síntesis en microondas se somete a un calentamiento a 700ºC en atmósfera inerte. Tras este tratamiento, el material sufre un cambio tanto en las propiedades químicas como en las porosas (S.A. Al-Muhtaseb & J.A. Ritter, 2003). El gel orgánico tiene un alto contenido en oxígeno (65 % carbono, 5% hidrógeno, y 30% oxígeno) en forma de grupos fenólicos a lo largo de la superficie del material, mientras que el gel de carbono tiene una estructura ordenada puramente carbonosa (carbono en más de un 95 %). El material final experimenta un gran desarrollo de la microporosidad, manteniendo prácticamente constante la meso-macroporosidad diseñada durante la síntesis en microondas, sufriendo un ligero aumento en la densidad real. Todos estos cambios hacen que las propiedades finales del gel orgánico y el carbonizado difieran enormemente, por lo tanto serán utilizados en distintos tipos de aplicaciones.

3.   PROPIEDADES DE LOS XEROGELES

Una de las mayores ventajas que ofrecen los xerogeles de carbono es su gran versatilidad, ya que la porosidad del material puede ser controlada a medida de la aplicación deseada. Esto se hace a través del control de las variables químicas y físicas que intervienen en el proceso de síntesis, pudiendo obtener materiales con propiedades muy dispares cuando estas se modifican.

Las variables físicas como el volumen de mezcla precursora empleada, la temperatura o el tiempo total utilizado durante la síntesis, afectan a la porosidad del material aunque en menor medida que las variables químicas (J.A. Menéndez et al., 2012; N. Rey-Raap et al., 2014b; N. Rey-Raap, J.A. Menéndez, & A. Arenillas, 2014). Esto es una ventaja a la hora de escalar el proceso a nivel industrial ya que permite ciertos márgenes en su ejecución.

Las variables químicas no sólo tienen una enorme influencia sobre la porosidad final del material, sino que además son dependientes entre sí, lo que exige un control preciso de las variables empleadas a la hora de diseñar la porosidad de un material (N. Rey-Raap, J. Angel Menéndez, & A. Arenillas, 2014a).

La estructura interna de los xerogeles se podría dividir en: (i) huecos en el interior de los nódulos que tienen un diámetro inferior a 2 nm, los cuales se conocen como microporos y (ii) huecos entre los nódulos, los cuales se denominan mesoporos, si su diámetro está en el rango de 2-50 nm y macroporos cuando el tamaño de los huecos es superior a 50 nm, La microporosidad se controla principalmente con tratamientos post-síntesis que se realizan sobre material, ya que casi no se ve afectada por el proceso de síntesis. Por otro lado, la meso-macroporosidad viene determinada por la cantidad y tamaño de nódulos que se forman durante la síntesis, por lo que va a depender de las principales variables químicas a tener en cuenta, que son: la concentración y tipo de catalizador, las proporciones de reactivos utilizados, la proporción de estabilizante inherente en la disolución de formaldehído utilizada, y la proporción de disolvente empleado como medio de reacción.

Cabe destacar que todas estas variables están interconectadas, y el efecto final de cada una de ellas en la porosidad del material dependerá de todas las demás. Sin embargo, la Figura 5 muestra de forma esquemática el efecto general de cada una de estas variables químicas.
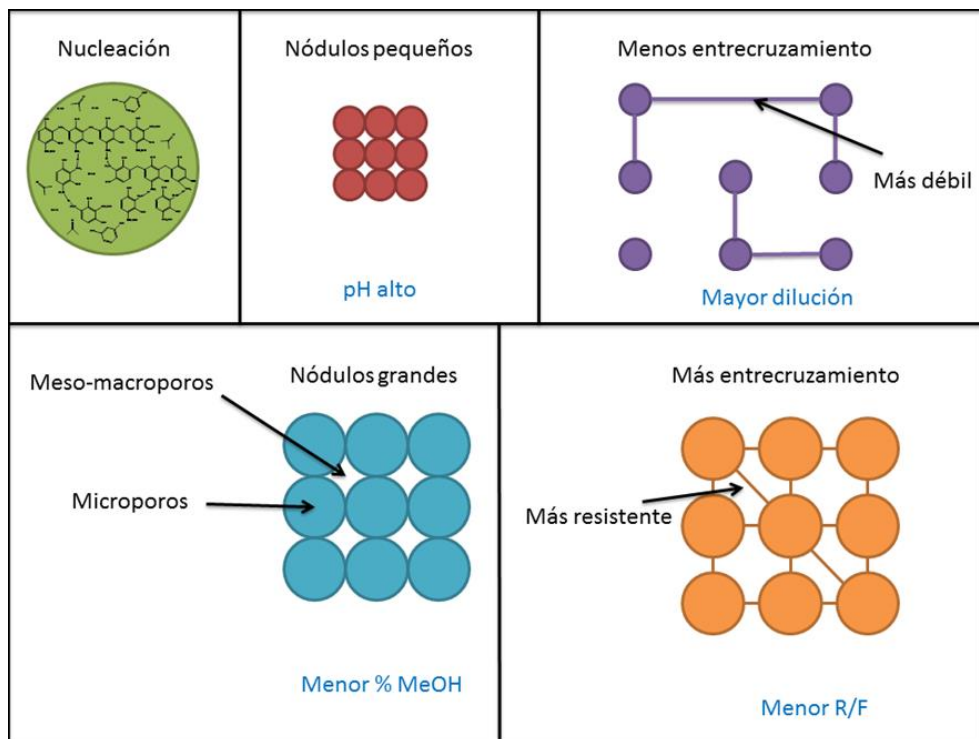
Figura 5. *Representación esquemática de diferentes tipos de estructura interna de xerogeles orgánicos.*

3.1.   El catalizador

3.1.1. El efecto del pH

El pH del medio de reacción está determinado por la cantidad de catalizador utilizado (N. Job et al., 2004; L. Zubizarreta, A. Arenillas, A. Domínguez, J.A. Menéndez, & J.J. Pis, 2008). Atendiendo a la Figura 3, se observa que la reacción de polimerización está favorecida en medios básicos, con la formación del anión del resorcinol. Esta reacción da lugar a agregados muy ramificados, produciendo partículas poliméricas (nódulos) más pequeñas y entrecruzadas entre sí. Por el contrario, en condiciones de pH bajo, los derivados hidroximetílicos tardan más en formarse, generando así una estructura con nódulos de mayor tamaño y conectados en menor medida.

Por este motivo el pH de la disolución inicial es un factor determinante en la obtención de geles con distintas propiedades, ya que afecta al tamaño de los nódulos o partículas poliméricas. Como se ha mencionado anteriormente, los huecos entre nódulos son los que determinan la meso y macroporosidad, por este motivo el pH de la disolución precursora tiene un efecto directo en el tamaño de los poros del material carbonoso final.

3.1.2. Tipo de catalizador

No sólo es importante la cantidad de catalizador añadida a la mezcla precursora (efecto del pH) sino que la naturaleza del catalizador también va a influir sobre las propiedades finales del gel. Dado que cada catalizador tiene una fuerza (pKa) diferente, la cantidad necesaria a añadir sobre la disolución para alcanzar un mismo valor de pH será distinta. En consecuencia, la concentración y tipo de heteroátomos que se añaden a la disolución también son diferentes, los cuales afectan a la estructura final del material.

Aunque hay diferentes estudios sobre el tema (E.G. Calvo, 2015; N. Cohaut, A. Thery, J. Guet, J. Rouzaud, & L. Kocon, 2007; N. Job, C.J. Gommes, R. Pirard, & J.-P. Pirard, 2008; K. Kraiwattanawong, S.R. Mukai, H. Tamon, & A.W. Lothongkum, 2007), parece ser que la variación de la especie catiónica tiene mayor repercusión que la aniónica. Esto puede ser debido a la diferencia de tamaños que suele haber entre estas especies, ya que si enfrentamos un carbonato frente a un hidroxilo (comúnmente utilizadas en bibliografía) (E.G. Calvo, C. Ania, L. Zubizarreta, J. Menéndez, & A. Arenillas, 2010; C. Moreno-Castilla & F.J. Maldonado-Hódar, 2005), el primero genera poros de mayores dimensiones debido a los impedimentos estéricos que genera durante la síntesis. Por otro lado, cuando comparamos un carbonato o un hidroxilo de sodio con su homóloga sal de potasio, las diferencias son despreciables (E.G. Calvo, 2015; N. Job et al., 2008).

3.2. *Relación resorcinol-formaldehído*

Las proporciones de los reactivos utilizados durante la síntesis son otro factor determinante sobre la porosidad. Estas proporciones van a afectar sobre el número y el tamaño de los nódulos formados durante la reacción sol-gel, la etapa de curado y el colapso parcial que puede tener lugar durante la etapa de secado. En consecuencia, los huecos entre los nódulos variarán de tamaño, afectando así a su mesoporosidad y macroporosidad (N. Rey-Raap, A. Arenillas, & J.A. Menéndez, 2015).

La mayoría de los autores utilizan proporciones estequiometrias resorcinol-formaldehído, pero de acuerdo a Feng et al. (Y. Feng et al., 2013) un aumento de la concentración de formaldehído desplaza el equilibrio de la reacción hacia los productos. Esto sugiere que los nódulos se formarán más rápidamente, permaneciendo durante más tiempo en la primera etapa de nucleación. Por lo tanto, se formará un menor número de nódulos pero de mayor tamaño. Por contraposición, una insuficiente cantidad de formaldehído dará lugar a la formación de nódulos de pequeño tamaño y muy entrecruzados.

3.3. *Grado de dilución*

Otro factor importante es el grado de dilución, que se puede definir como el cociente molar del medio de reacción empleado (agua, metanol, etc.) frente a los monómeros (resorcinol y formaldehído) (N. Job et al., 2004; N. Rey-Raap, A. Arenillas, & J.A. Menéndez, 2016). El efecto del grado de dilución o de la proporción de reactivos utilizado, como también aparece en la bibliografía, es bastante controvertido, posiblemente debido a las diferencias que hay en el método de síntesis y secado que se utiliza en cada caso (N. Job, A. Théry, et al., 2005; N. Rey-Raap et al., 2014a; H. Tamon, H. Ishizaka, M. Mikami, & M. Okazaki, 1997). Para el calentamiento con microondas la reacción sol-gel tiene lugar de una forma mucho más rápida que con el calentamiento convencional, por lo que el disolvente no tiene tiempo suficiente para evaporarse y la mayoría queda retenido en la estructura. Esto afecta tanto a la reacción de

polimerización, como al secado, modificando a la estructura porosa del material.

Una menor dilución conlleva una mayor proporción de RF en la disolución, y por consiguiente da lugar a la formación de un mayor número de nódulos de menor tamaño. Por el contrario, un aumento de la dilución lleva a la formación de menos nódulos pero de mayor tamaño. Por otro lado, si la dilución es grande, los entrecruzamientos entre nódulos serán escasos, generando materiales con baja resistencia mecánica. Si la dilución fuera aún mayor, pudiera llegar incluso a no obtenerse el gel si la separación entre los nódulos es lo suficientemente grande como para evitar su entrecruzamiento (N. Rey-Raap, A. Arenillas, et al., 2015).

3.4. *Proporción de metanol como estabilizante de la disolución de formaldehído*

Las disoluciones de formaldehído comerciales contienen cierta proporción de metanol que se utiliza como estabilizante ya que, mediante la formación de hemiacetales/acetales (Figura 6) evita que el formaldehído polimerice consigo mismo y precipite, y así se asegura que la concentración de formaldehído en la disolución permanezca invariable en el tiempo (I.D. Alonso-Buenaposada, N. Rey-Raap, E.G. Calvo, J. Angel Menéndez, & A. Arenillas, 2015). El problema reside en que dependiendo de la casa comercial con la que se trabaje, esta proporción puede variar desde un 0.6 % hasta un 15 %. Ya que las propiedades físicas del agua y el metanol no son las mismas (punto de ebullición, punto dieléctrico, tensión superficial, etc.) esta proporción afecta al proceso de síntesis y por lo tanto a la porosidad (I.D. Alonso-Buenaposada, 2014).
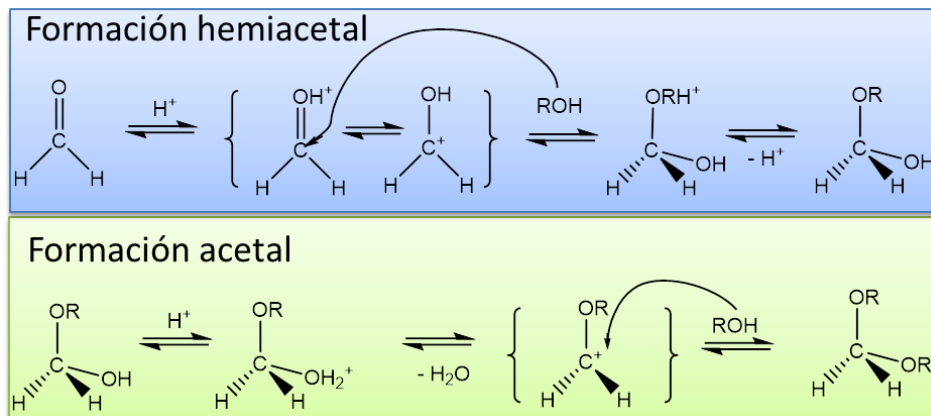
Figura 6. *Mecanismo de estabilización del formaldehído.*

Cuando el metanol reacciona con la molécula de formaldehído para formar el hemiacetal, esa molécula deja de estar disponible para reaccionar con el resorcinol, por lo que un aumento en la proporción de metanol provoca un efecto similar al de una disminución en la proporción de formaldehído. Además, la reacción de formación de los acetales esta favorecida en medios ácidos por lo tanto, a pH más ácidos no sólo hay menor proporción de aniones resorcinol para reaccionar, sino que también hay menor proporción de formaldehído, ya que este se encuentra en forma de hemiacetal. Esto da lugar a la formación de nódulos más pequeños, los cuales dan lugar a materiales con poros de menor tamaño.

Por lo tanto, una disminución de la proporción de metanol provoca un aumento del volumen total y del tamaño de poro y en consecuencia, una disminución de la densidad y un aumento de la porosidad. Aunque la proporción de metanol sobre el volumen total de la disolución pudiera parecer despreciable en un principio, un cambio del 0.6 al 12.5% puede llegar a provocar un cambio de hasta dos órdenes de magnitud en el tamaño de poro, dependiendo del resto de variables químicas empleadas en la síntesis (I.D. Alonso-Buenaposada et al., 2015). En consecuencia, muestras macroporosas de bajo pH pueden llegar incluso a convertirse en mesoporosas cuando se aumenta la proporción de metanol.

En la Figura 7 se observa la influencia de alguna de las variables químicas mencionadas hasta el momento. Como se puede apreciar en las imágenes, las propiedades porosas de los xerogeles de carbono cambian radicalmente en función de las condiciones de síntesis empleadas.
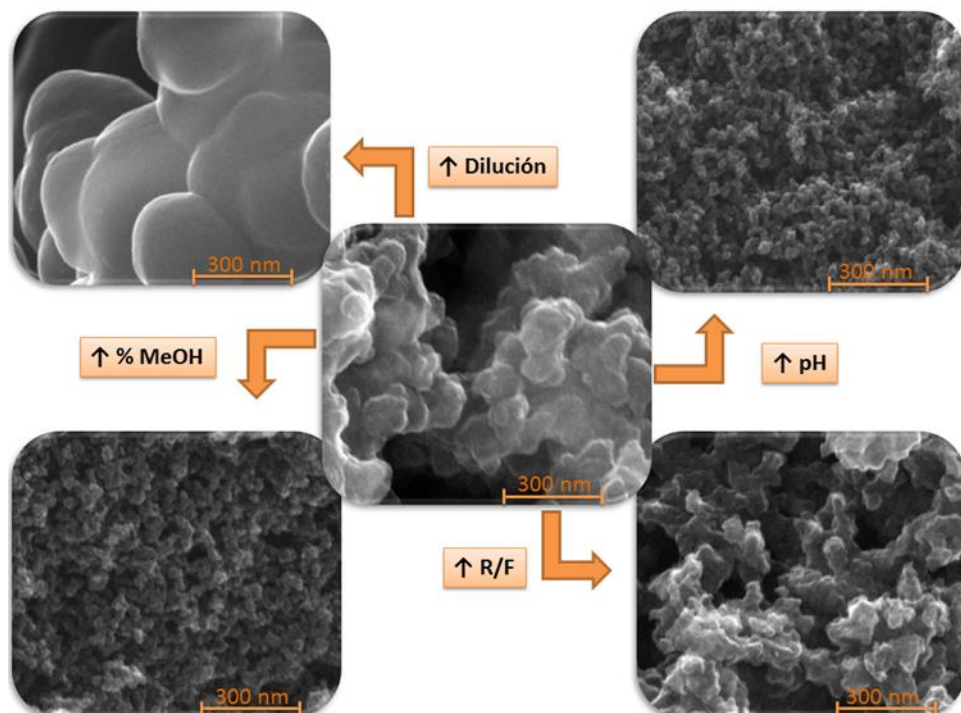
Figura 7. *Influencia de alguna de las variables químicas sobre la microestructura de xerogeles RF.*

3.5. Desarrollo de la microporosidad

Cuando se precisa de un mayor volumen de microporos, el gel se somete a distintos tratamientos post-síntesis como pueden ser la carbonización, la activación física o la activación química, ya que las condiciones de síntesis apenas tienen influencia sobre la microporosidad (L. Zubizarreta, A. Arenillas, A. Domínguez, et al., 2008).

Cuando el gel orgánico se carboniza (tratamiento a 700-900 ºC en atmósfera inerte) se genera un material con una estructura carbonosa de alta

pureza, compuestos principalmente por carbono, térmicamente estable, con la meso-macroporosidad que se ha diseñado en la síntesis del xerogel orgánico pero con un aumento en el volumen de microporos. Así, el área superficial (S_{BET}), pasa de tener alrededor de 200 m^2 g^{-1} en el caso del xerogel orgánico, a desarrollar un área superficial específica de 600 m^2 g^{-1}, manteniendo invariable su meso-macroporosidad. Factores como la temperatura o la velocidad de calentamiento durante la carbonización afectan de forma significativa sobre la generación de porosidad del material, por lo que varios estudios se han centrado en la optimización de estas variables (A. Moreno, A. Arenillas, E. Calvo, J. Bermúdez, & J. Menéndez, 2013). Recientes estudios han demostrado que la carbonización puede llevarse a cabo también por radiación microondas (D. Espinosa-Iglesias et al., 2015). Aunque esta técnica permite la obtención de materiales con mesoporosidad desarrollada, las propiedades químicas de estos materiales son diferentes a las obtenidas por calentamiento convencional.

El tipo de atmosfera utilizada (inerte o reactiva) afecta tanto a la porosidad como a la química superficial del material obtenido (C. Lin & J.A. Ritter, 1997). Cuando se sustituye la utilización de un gas inerte por un gas reactivo como CO_2 el desarrollo de la microporosidad es mayor, pudiendo llegar a obtener áreas superiores a los 2000 m^2 g^{-1} cuando se optimizan los tiempos y temperaturas de reacción (E.G. Calvo, N. Ferrera-Lorenzo, J. Menéndez, & A. Arenillas, 2013; M.S. Contreras et al., 2010). En este caso dejaría de llamarse carbonización para pasar a llamarse proceso de activación física.

Los geles también pueden ser activados químicamente, mediante reacción química con distintos agentes activantes como el KOH (E.G. Calvo et al., 2013; N. Rey-Raap, E.G. Calvo, A. Arenillas, & J.Á. MENÉNDEZ, 2012; L. Zubizarreta, A. Arenillas, J.-P. Pirard, J.J. Pis, & N. Job, 2008; L. Zubizarreta, A. Arenillas, J.J. Pis, J.-P. Pirard, & N. Job, 2009) o H_3PO_4. (M. Jagtoyen, J. Groppo, & F. Derbyshire, 1993). Este tratamiento se puede hacer tanto sobre el gel orgánico como sobre el gel de carbono, y se puede llevar a cabo con radiación microondas (L. Zubizarreta, A. Arenillas, A. Domínguez, et al., 2008).

No obstante, la porosidad generada en cada uno de los casos es totalmente diferente. Cuando la activación química se realiza tras el proceso de carbonización, se obtienen materiales con una microporosidad bastante desarrollada (valores de S_{BET} en torno a 1500 m^2 g^{-1}) y siempre se preserva, la meso-macroporosidad definida durante la síntesis del gel orgánico. Por el contrario, si se activa directamente un xerogel orgánico se puede llegar a modificar total o parcialmente la meso-macroporosidad creada durante la síntesis, pero se consiguen microporosidades mucho más elevadas (S_{BET} > 2000 m^2 g^{-1}) (E. G. Calvo et al., 2011).

3.6. *Química de los materiales*

Las propiedades químicas del gel orgánico y el carbonizado son diferentes ya que, tras el tratamiento térmico no sólo se ve alterada su estructura porosa sino que la composición química del material también cambia. El gel orgánico tiene un alto contenido en oxígeno (65 % carbono, 5 % hidrógeno, y 30 % oxígeno) en forma de principalmente grupos fenólicos a lo largo de la superficie del material, mientras que el gel de carbono apenas tiene oxígeno en su composición (carbono en más de un 95 % de su peso). El gel de carbono obtenido no tiene impurezas ya que es un producto sintético, y cuya composición va a depender de los monómeros utilizados en la síntesis.

A parte de la influencia obvia que tiene la naturaleza de los monómeros utilizados para la polimerización, se pueden alterar las propiedades químicas del material mediante activación, oxidación o mediante procesos de dopado. También es frecuente la utilización de surfactantes (N. Rey-Raap, S. Rodríguez-Sánchez, et al., 2015), los cuales alteran la porosidad del material de diferentes formas dependiendo de su naturaleza, y en muchas ocasiones quedan retenidos en su estructura, cambiando así su química.

El interés en modificar la química superficial del polímero reside en potenciar la conductividad eléctrica del material (J.E. Thomas et al., 2010), en introducir una fase activa cuando se utiliza en áreas como la catálisis (C.

Moreno-Castilla & F.J. Maldonado-Hódar, 2005; C. Moreno-Castilla, F.J. Maldonado-Hódar, J. Rivera-Utrilla, & E. Rodríguez-Castellón, 1999) o en aplicaciones energéticas (E.G. Calvo et al., 2013; J. Zhang, F.D. Nie, W.F. Yu, Q.X. Guo, & G.Y. Zeng, 2009). Este proceso de dopado puede tener lugar de tres formas: (i) mediante mezcla directa del metal en la disolución precursora, (ii) utilizando un derivado del resorcinol que ya contenga el heteroátomo que se quiera introducir en la estructura, y (iii) depositando el elemento sobre la estructura del gel final mediante tratamientos post-síntesis. Dependiendo de la naturaleza y cantidad del heteroátomo que se quiera introducir, la temperatura de utilización de material final, etc. el método a utilizar será distinto.

4.   APLICACIONES DE LOS XEROGELES

Todas las características de los xerogeles mencionadas a lo largo de este capítulo muestran el gran atractivo que tienen estos materiales para su utilización en diversas aplicaciones. El hecho de que tanto la porosidad como la química superficial puedan ser diseñadas a medida, hace que su utilización pueda ser destinada a un gran número de aplicaciones muy diferentes entre sí ya que, dependiendo de estas propiedades, los geles tendrán distinta área superficial, volumen de poros, densidad, conductividad eléctrica y térmica, etc.

Se pueden diferenciar dos grandes grupos, dependiendo si se aplica el gel orgánico de forma directa o tras su tratamiento térmico, ya que las propiedades del material son totalmente distintas (Figura 8). El gel orgánico es un material muy poco denso, de baja conductividad térmica y eléctrica, y con una química rica en oxígeno. Geles orgánicos con diámetro de poro menor de 50 nm y bajas densidades pueden tener propiedades de aislante térmico. Su alta porosidad y la química controlable hace que se puedan utilizar como absorbentes de metales pesados o que puedan utilizarse como soportes para enzimas diseñando el diámetro de poro de forma específica según el tamaño de la enzima.
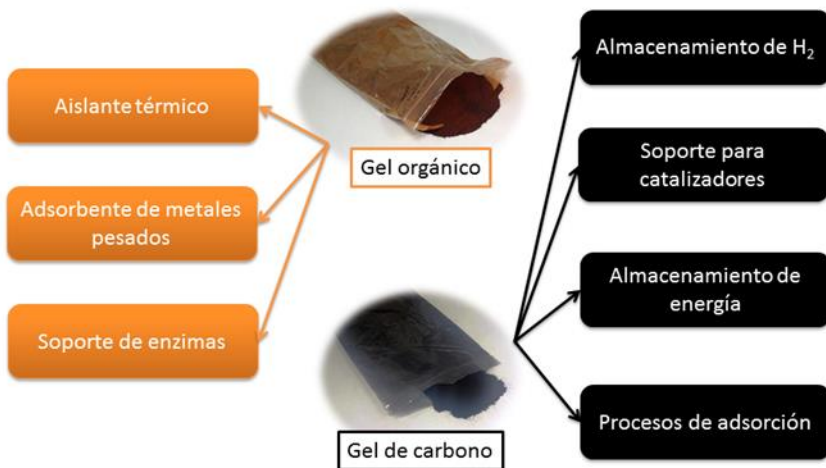
Figura 8. *Diferentes aplicaciones de los geles orgánicos y de carbono.*

Por otro lado, el gel de carbono tiene una estructura más ordenada, es un material conductor, térmicamente estable y tiene una composición carbonosa de alta pureza. Cuando se utilizan estos materiales en procesos de adsorción, con poros suficientemente grandes se minimizan las limitaciones por difusión (N. Job, B. Heinrichs, et al., 2005). Sin embargo, cuando su utilización va dirigida a almacenamiento de hidrogeno, se requiere de un gran desarrollo de la microporosidad del material, con un tamaño de microporos concreto (L. Zubizarreta, A. Arenillas, & J.J. Pis, 2009; L. Zubizarreta et al., 2010). Si se utiliza como material para electrodos en supercondensadores, además de una gran microporosidad, se requiere que tenga cierto volumen de mesoporos para facilitar la difusividad del electrolito (E. Calvo et al., 2013; E.G. Calvo, N. Rey-Raap, A. Arenillas, & J. Menéndez, 2014). En el caso de que se desee aplicar como soporte para catalizadores, necesita una estructura porosa adecuada al soporte y dispersión de las partículas metálicas que comprenden la reacción catalítica, por lo tanto va a depender de cada reacción catalítica de forma concreta (C. Moreno-Castilla & F.J. Maldonado-Hódar, 2005; C. Moreno-Castilla et al., 1999). De acuerdo a esto, las propiedades tanto físicas como químicas de los xerogeles se diseñan a medida según las necesidades de cada aplicación.

5. PERSPECTIVAS DE FUTURO

Como ya se mencionó anteriormente, los xerogeles resorcinol-formaldehído han sido estudiados en detalle durante los últimos años (Figura 1). Uno de los problemas principales que presentaban estos materiales era los largos tiempos que se requerían para su síntesis, cuando se utilizaba el calentamiento convencional. Este problema ya fue solventado por E. G. Calvo (E. G. Calvo et al., 2011) al reducir en un 90 % el tiempo de síntesis cuando se empleaba calentamiento con microondas. Por otro lado, aunque el uso de los monómeros resorcinol-formaldehído está ampliamente extendido en la síntesis de xerogeles de carbono, existe cierta tendencia ser sustituidos por otros más baratos y ecológicos.

En la bibliografía se pueden encontrar sustituyentes del resorcinol como fenol (C. Scherdel, R. Gayer, & G. Reichenauer, 2012), cresol (R. Zhang, Z.J. Hu, S.L. Jin, X. Shao, & M.L. Jin, 2013; Y. Zhu, H. Hu, W.-C. Li, & X. Zhang, 2006), taninos (N. Rey-Raap, A. Szczurek, et al., 2015) o celulosa (B. Grzyb et al., 2010). Entre estos, los taninos se consideran la opción más viable a escala industrial debido a que son más ecológicos, más baratos y no son tóxicos en su manejo (F.L. Braghiroli et al., 2014). El formaldehído es el aldehído alifático más simple que existe en la química. Su reactividad y sus pequeñas dimensiones le dotan de gran atractivo en la síntesis de xerogeles. No obstante es un producto irritante, contaminante, inflamable, tóxico y cancerígeno, por lo que su manejo debe ser minimizado, y su aplicación en productos está altamente restringida. Sustituyentes como furfural (K. Kraiwattanawong, S. Mukai, H. Tamon, & A. Lothongkum, 2008) o hexamina (D. Liu, J.-H. Lei, L.-P. Guo, & K.-J. Deng, 2011) ya pueden encontrarse en la bibliografía, aunque aún requieren de un estudio más exhaustivo para obtener propiedades similares a las que hoy en día tienen los xerogeles de carbono basados en formaldehído.

6. REFERENCIAS

➢ Al-Muhtaseb, S. A., & Ritter, J. A. (2003). Preparation and Properties of Resorcinol–Formaldehyde Organic and Carbon Gels. Advanced Materials, 15(2), 101-114. doi: 10.1002/adma.200390020

➢ Alonso-Buenaposada, I. D. (2014). Efecto de la proporción de metanol en disoluciones de formaldehído sobre la porosidad de xerogeles de carbono R/F. Trabajo Fin de Máster. Universidad de Oviedo.

➢ Alonso-Buenaposada, I. D., Rey-Raap, N., Calvo, E. G., Angel Menéndez, J., & Arenillas, A. (2015). Effect of methanol content in commercial formaldehyde solutions on the porosity of RF carbon xerogels. Journal of non-crystalline solids, 426(0), 13-18. doi: http://dx.doi.org/10.1016/j.jnoncrysol.2015.06.017

➢ Babić, B., Kaluđerović, B., Vračar, L., & Krstajić, N. (2004). Characterization of carbon cryogel synthesized by sol–gel polycondensation and freeze-drying. Carbon, 42(12), 2617-2624.

➢ Braghiroli, F. L., Fierro, V., Izquierdo, M. T., Parmentier, J., Pizzi, A., & Celzard, A. (2014). Kinetics of the hydrothermal treatment of tannin for producing carbonaceous microspheres. Bioresource Technology, 151, 271-277. doi: http://dx.doi.org/10.1016/j.biortech.2013.10.045

➢ Calvo, E., Lufrano, F., Staiti, P., Brigandì, A., Arenillas, A., & Menéndez, J. (2013). Optimizing the electrochemical performance of aqueous symmetric supercapacitors based on an activated carbon xerogel. Journal of Power Sources, 241, 776-782.

➢ Calvo, E. G. (2015). El catalizador: otra variable a considerar en la síntesis inducida por microondas de xerogeles resorcinol-formaldehído. Paper presented at the XIII Reunión del Grupo Español del Carbón, Alicante, España.

➢ Calvo, E. G., Ania, C., Zubizarreta, L., Menéndez, J., & Arenillas, A. (2010). Exploring New Routes in the Synthesis of Carbon Xerogels for Their Application in Electric Double-Layer Capacitors†. Energy & Fuels, 24(6), 3334-3339.

➢ Calvo, E. G., Arenillas, A., & Menéndez, J. (2011). Designing Nanostructured Carbon Xerogels: INTECH Open Access Publisher.

➢ Calvo, E. G., Ferrera-Lorenzo, N., Menéndez, J., & Arenillas, A. (2013). Microwave synthesis of micro-mesoporous activated carbon xerogels for high performance supercapacitors. Microporous and Mesoporous Materials, 168, 206-212.

➢ Calvo, E. G., Juárez-Pérez, E. J., Menéndez, J. A., & Arenillas, A. (2011). Fast microwave-assisted synthesis of tailored mesoporous carbon xerogels. Journal of Colloid and Interface Science, 357(2), 541-547. doi: http://dx.doi.org/10.1016/j.jcis.2011.02.034

➢ Calvo, E. G., Rey-Raap, N., Arenillas, A., & Menéndez, J. (2014). The effect of the carbon surface chemistry and electrolyte pH on the energy storage of supercapacitors. RSC Advances, 4(61), 32398-32404.

➢ Cohaut, N., Thery, A., Guet, J., Rouzaud, J., & Kocon, L. (2007). The porous network in carbon aerogels investigated by small angle neutron scattering. Carbon, 45(6), 1185-1192.

➢ Contreras, M. S., Páez, C. A., Zubizarreta, L., Léonard, A., Blacher, S., Olivera-Fuentes, C. G., . . . Job, N. (2010). A comparison of physical activation of carbon xerogels with carbon dioxide with chemical activation using hydroxides. Carbon, 48(11), 3157-3168. doi: http://dx.doi.org/10.1016/j.carbon.2010.04.054

➢ Czakkel, O., Marthi, K., Geissler, E., & László, K. (2005). Influence of drying on the morphology of resorcinol–formaldehyde-based carbon gels. Microporous and Mesoporous Materials, 86(1), 124-133.

➢ Chemat, F., & Esveld, E. (2001). Microwave Super-Heated Boiling of Organic Liquids: Origin, Effect and Application. Chemical engineering & technology, 24(7), 735-744.

➢ Espinosa-Iglesias, D., Valverde-Sarmiento, C., Pérez-Cadenas, A. F., Bautista-Toledo, M. I., Maldonado-Hódar, F. J., & Carrasco-Marín, F. (2015). Mesoporous carbon-xerogels films obtained by microwave assisted carbonization. Materials Letters, 141, 135-137. doi: http://dx.doi.org/10.1016/j.matlet.2014.11.052

➢ Feng, Y., Wang, J., Ge, L., Jiang, B., Miao, L., & Tanemura, M. (2013). Pore size controllable preparation for low density porous nano-carbon. Journal of Nanoscience and Nanotechnology, 13(10), 7012-7015. doi: 10.1166/jnn.2013.8063

➢ Gallegos-Suárez, E., Pérez-Cadenas, A. F., Maldonado-Hódar, F. J., & Carrasco-Marín, F. (2012). On the micro- and mesoporosity of carbon aerogels and xerogels. The role of the drying conditions during the synthesis processes. Chemical Engineering Journal, 181–182, 851-855. doi: http://dx.doi.org/10.1016/j.cej.2011.12.002

➢ Gedye, R., Smith, F., Westaway, K., Ali, H., Baldisera, L., Laberge, L., & Rousell, J. (1986). The use of microwave ovens for rapid organic synthesis. Tetrahedron Letters, 27(3), 279-282. doi: 10.1016/S0040-4039(00)83996-9

➤ Gedye, R. N., Smith, F. E., & Westaway, K. C. (1988). The rapid synthesis of organic compounds in microwave ovens. Canadian Journal of Chemistry, 66(1), 17-26.

➤ Giguere, R. (1989). Organic Synthesis: Theory and Application. JAI Press: Greenwich, 1, 103-172.

➤ Giguere, R. J., Bray, T. L., Duncan, S. M., & Majetich, G. (1986). Application of commercial microwave ovens to organic synthesis. Tetrahedron Letters, 27(41), 4945-4948.

➤ Gourdenne, A., Maassarani, A., Monchaux, P., Aussudre, S., & Thourel, L. (1979). Cross-Linking of Thermosetting Resins by Microwave-Heating-Quantitative Approach. Paper presented at the Abstracts of papers of the american chemical society.

➤ Grzyb, B., Hildenbrand, C., Berthon-Fabry, S., Bégin, D., Job, N., Rigacci, A., & Achard, P. (2010). Functionalisation and chemical characterisation of cellulose-derived carbon aerogels. Carbon, 48(8), 2297-2307. doi: http://dx.doi.org/10.1016/j.carbon.2010.03.005

➤ Hoogenboom, R., & Schubert, U. S. (2007). Microwave-Assisted Polymer Synthesis: Recent Developments in a Rapidly Expanding Field of Research. Macromolecular Rapid Communications, 28(4), 368-386.

➤ Jagtoyen, M., Groppo, J., & Derbyshire, F. (1993). Activated carbons from bituminous coals by reaction with H 3 PO 4: the influence of coal cleaning. Fuel processing technology, 34(2), 85-96.

➤ Job, N., Gommes, C. J., Pirard, R., & Pirard, J.-P. (2008). Effect of the counter-ion of the basification agent on the pore texture of organic and carbon xerogels. Journal of non-crystalline solids, 354(40–41), 4698-4701. doi: http://dx.doi.org/10.1016/j.jnoncrysol.2008.06.102

➤ Job, N., Heinrichs, B., Ferauche, F., Noville, F., Marien, J., & Pirard, J.-P. (2005). Hydrodechlorination of 1, 2-dichloroethane on Pd–Ag catalysts supported on tailored texture carbon xerogels. Catalysis today, 102, 234-241.

➤ Job, N., Pirard, R., Marien, J., & Pirard, J.-P. (2004). Porous carbon xerogels with texture tailored by pH control during sol–gel process. Carbon, 42(3), 619-628. doi: http://dx.doi.org/10.1016/j.carbon.2003.12.072

➤ Job, N., Sabatier, F., Pirard, J.-P., Crine, M., & Léonard, A. (2006). Towards the production of carbon xerogel monoliths by optimizing convective drying conditions. Carbon, 44(12), 2534-2542.

➤ Job, N., Théry, A., Pirard, R., Marien, J., Kocon, L., Rouzaud, J.-N., . . . Pirard, J.-P. (2005). Carbon aerogels, cryogels and xerogels: Influence of the drying method on the textural properties of porous carbon materials. Carbon, 43(12), 2481-2494. doi: http://dx.doi.org/10.1016/j.carbon.2005.04.031

➢ Juárez-Pérez, E. J., Calvo, E. G., Arenillas, A., & Menéndez, J. A. (2010). Precise determination of the point of sol–gel transition in carbon gel synthesis using a microwave heating method. Carbon, 48(11), 3305-3308. doi: http://dx.doi.org/10.1016/j.carbon.2010.05.013

➢ Jung, U., Lee, W. K., & Lim, K. T. (2011). Vulcanization efficiency of non-polar rubber compounds by microwave. Polymer (Korea), 35(3), 228-231.

➢ Kappe, C. O., & Dallinger, D. (2006). The impact of microwave synthesis on drug discovery. Nature Reviews Drug Discovery, 5(1), 51-63.

➢ Kraiwattanawong, K., Mukai, S., Tamon, H., & Lothongkum, A. (2008). Control of mesoporous properties of carbon cryogels prepared from wattle tannin and furfural. Journal of Porous Materials, 15(6), 695-703. doi: 10.1007/s10934-007-9155-x

➢ Kraiwattanawong, K., Mukai, S. R., Tamon, H., & Lothongkum, A. W. (2007). Preparation of carbon cryogels from wattle tannin and furfural. Microporous and Mesoporous Materials, 98(1-3), 258-266. doi: 10.1016/j.micromeso.2006.09.007

➢ Kraiwattanawong, K., Tamon, H., & Praserthdam, P. (2011). Influence of solvent species used in solvent exchange for preparation of mesoporous carbon xerogels from resorcinol and formaldehyde via subcritical drying. Microporous and Mesoporous Materials, 138(1), 8-16.

➢ Leadbeater, N. E. (2010). Microwave heating as a tool for sustainable chemistry: CRC Press.

➢ Leadbeater, N. E., & Torenius, H. M. (2002). A study of the ionic liquid mediated microwave heating of organic solvents. The Journal of organic chemistry, 67(9), 3145-3148.

➢ Lin, C., & Ritter, J. A. (1997). Effect of synthesis pH on the structure of carbon xerogels. Carbon, 35(9), 1271-1278. doi: http://dx.doi.org/10.1016/S0008-6223(97)00069-9

➢ Liu, D., Lei, J.-H., Guo, L.-P., & Deng, K.-J. (2011). Simple hydrothermal synthesis of ordered mesoporous carbons from resorcinol and hexamine. Carbon, 49(6), 2113-2119. doi: http://dx.doi.org/10.1016/j.carbon.2011.01.047

➢ Loupy, A. (2006). Microwaves in organic synthesis: Wiley-VCH; John Wiley, distributor].

➢ Mallakpour, S. E., Hajipour, A. R., & Habibi, S. (2002). Microwave-assisted synthesis of new optically active poly (ester-imide) s containing N, N′-(pyromellitoyl)-bis-L-phenylalanine moieties. Journal of applied polymer science, 86(9), 2211-2216.

➢ Manaila, E., Martin, D., Stelescu, D. Z., Craciun, G., Ighigeanu, D., & Matei, C. (2009). Combined effects of microwaves, electron beams and

polyfunctional monomers on rubber vulcanization. Journal of Microwave Power and Electromagnetic Energy, 43(3), 43326-43334.

➢ Menéndez, J. A., Juárez-Pérez, E. J., Ruisánchez, E., Calvo, E. G., & Arenillas, A. (2012). A microwave-based method for the synthesis of carbon xerogel spheres. Carbon, 50(10), 3555-3560. doi: http://dx.doi.org/10.1016/j.carbon.2012.03.027

➢ Moreno-Castilla, C., & Maldonado-Hódar, F. J. (2005). Carbon aerogels for catalysis applications: An overview. Carbon, 43(3), 455-465. doi: http://dx.doi.org/10.1016/j.carbon.2004.10.022

➢ Moreno-Castilla, C., Maldonado-Hódar, F. J., Rivera-Utrilla, J., & Rodríguez-Castellón, E. (1999). Group 6 metal oxide-carbon aerogels. Their synthesis, characterization and catalytic activity in the skeletal isomerization of 1-butene. Applied Catalysis A: General, 183(2), 345-356.

➢ Moreno, A., Arenillas, A., Calvo, E., Bermúdez, J., & Menéndez, J. (2013). Carbonisation of resorcinol–formaldehyde organic xerogels: effect of temperature, particle size and heating rate on the porosity of carbon xerogels. Journal of Analytical and Applied Pyrolysis, 100, 111-116.

➢ Moreno, Á. H., de La Puente, A. A., Calvo, E. G., Rey-Raap, N., Bermúdez, J. M., & Díaz, J. A. M. (2013). Xerogeles de carbono competitivos diseñados para aplicaciones específicas. Avances en Ciencias e Ingeniería, 4(1), 109-120.

➢ Pekala, R. (1989). Organic aerogels from the polycondensation of resorcinol with formaldehyde. Journal of Materials Science, 24(9), 3221-3227.

➢ Rey-Raap, N., Angel Menéndez, J., & Arenillas, A. (2014a). RF xerogels with tailored porosity over the entire nanoscale. Microporous and Mesoporous Materials, 195, 266-275. doi: 10.1016/j.micromeso.2014.04.048

➢ Rey-Raap, N., Angel Menéndez, J., & Arenillas, A. (2014b). Simultaneous adjustment of the main chemical variables to fine-tune the porosity of carbon xerogels. Carbon, 78, 490-499. doi: 10.1016/j.carbon.2014.07.030

➢ Rey-Raap, N., Arenillas, A., & Menéndez, J. A. (2015). Resorcinol-formaldehyde carbon gels. SYNTHESIS, APPLICATIONS AND POTENTIAL HEALTH EFFECTS, 31.

➢ Rey-Raap, N., Arenillas, A., & Menéndez, J. A. (2016). A visual validation of the combined effect of pH and dilution on the porosity of carbon xerogels. Microporous and Mesoporous Materials, 223, 89-93. doi: http://dx.doi.org/10.1016/j.micromeso.2015.10.044

➢ Rey-Raap, N., Calvo, E. G., Arenillas, A., & MENÉNDEZ, J. Á. (2012). High surface area carbon xerogels-Microwave vs. conventional activation with KOH. Chimica Oggi-Chemistry Today, 30, 3.

➢ Rey-Raap, N., Menéndez, J. A., & Arenillas, A. (2014). Optimization of the process variables in the microwave-induced synthesis of carbon xerogels.

Journal of Sol-Gel Science and Technology, 69(3), 488-497. doi: 10.1007/s10971-013-3248-6

➢ Rey-Raap, N., Rodríguez-Sánchez, S., Alonso-Buenaposada, I. D., Calvo, E. G., Menéndez, J. A., & Arenillas, A. (2015). The enhancement of porosity of carbon xerogels by using additives. Microporous and Mesoporous Materials, 217(0), 39-45. doi: http://dx.doi.org/10.1016/j.micromeso.2015.06.003

➢ Rey-Raap, N., Szczurek, A., Fierro, V., Menéndez, J. A., Arenillas, A., & Celzard, A. (2015). Towards a feasible and scalable production of bio-xerogels. Journal of Colloid and Interface Science, 456, 138-144. doi: http://dx.doi.org/10.1016/j.jcis.2015.06.024

➢ Rydfjord, J., Svensson, F., Fagrell, M., Sävmarker, J., Thulin, M., & Larhed, M. (2013). Temperature measurements with two different IR sensors in a continuous-flow microwave heated system. Beilstein journal of organic chemistry, 9(1), 2079-2087.

➢ Scherdel, C., Gayer, R., & Reichenauer, G. (2012). Porous organic and carbon xerogels derived from alkaline aqueous phenol–formaldehyde solutions. Journal of Porous Materials, 19(3), 351-360. doi: 10.1007/s10934-011-9481-x

➢ Sinnwell, S., & Ritter, H. (2007). Recent advances in microwave-assisted polymer synthesis. Australian Journal of Chemistry, 60(10), 729-743.

➢ Tamon, H., Ishizaka, H., Mikami, M., & Okazaki, M. (1997). Porous structure of organic and carbon aerogels synthesized by sol-gel polycondensation of resorcinol with formaldehyde. Carbon, 35(6), 791-796.

➢ Teffal, M., & Gourdenne, A. (1983). Activation of radical polymerization by microwaves—I. Polymerization of 2-hydroxyethyl methacrylate. European Polymer Journal, 19(6), 543-549.

➢ Thomas, J. E., Humana, R. M., Zubizarreta, L., Arenillas, A., Menéndez, J., Corso, H. L., & Visintin, A. (2010). Ni-Doped Carbons as a Carbon Support for Metal Hydride Electrodes†. Energy & Fuels, 24(6), 3302-3306.

➢ Tonanon, N., Wareenin, Y., Siyasukh, A., Tanthapanichakoon, W., Nishihara, H., Mukai, S. R., & Tamon, H. (2006). Preparation of resorcinol formaldehyde (RF) carbon gels: Use of ultrasonic irradiation followed by microwave drying. Journal of non-crystalline solids, 352(52–54), 5683-5686. doi: http://dx.doi.org/10.1016/j.jnoncrysol.2006.09.017

➢ Wayne, I. R. (1980). Method and apparatus for microwave vulcanization of extruded rubber profiles: Google Patents.

➢ Zhang, J., Nie, F. D., Yu, W. F., Guo, Q. X., & Zeng, G. Y. (2009). Effect of drying methods on structure of RDX/RF composite energetic materials. Hanneng Cailiao/Chinese Journal of Energetic Materials, 17(1), 23-26.

➢ Zhang, R., Hu, Z. J., Jin, S. L., Shao, X., & Jin, M. L. (2013) Synthesis of monolithic macroporous carbon xerogels from phenol, m-cresol, furfural and phosphoric acid by sol-gel approach. Vol. 750-752. Advanced Materials Research (pp. 1804-1811).

➢ Zhu, Y., Hu, H., Li, W.-C., & Zhang, X. (2006). Cresol–formaldehyde based carbon aerogel as electrode material for electrochemical capacitor. Journal of Power Sources, 162(1), 738-742. doi: http://dx.doi.org/10.1016/j.jpowsour.2006.06.049

➢ Zubizarreta, L., Arenillas, A., Domínguez, A., Menéndez, J. A., & Pis, J. J. (2008). Development of microporous carbon xerogels by controlling synthesis conditions. Journal of non-crystalline solids, 354(10-11), 817-825. doi: 10.1016/j.jnoncrysol.2007.08.015

➢ Zubizarreta, L., Arenillas, A., Menéndez, J. A., Pis, J. J., Pirard, J. P., & Job, N. (2008). Microwave drying as an effective method to obtain porous carbon xerogels. Journal of non-crystalline solids, 354(33), 4024-4026. doi: http://dx.doi.org/10.1016/j.jnoncrysol.2008.06.003

➢ Zubizarreta, L., Arenillas, A., Pirard, J.-P., Pis, J. J., & Job, N. (2008). Tailoring the textural properties of activated carbon xerogels by chemical activation with KOH. Microporous and Mesoporous Materials, 115(3), 480-490. doi: http://dx.doi.org/10.1016/j.micromeso.2008.02.023

➢ Zubizarreta, L., Arenillas, A., & Pis, J. J. (2009). Carbon materials for H2 storage. International Journal of Hydrogen Energy, 34(10), 4575-4581. doi: http://dx.doi.org/10.1016/j.ijhydene.2008.07.112

➢ Zubizarreta, L., Arenillas, A., Pis, J. J., Pirard, J.-P., & Job, N. (2009). Studying chemical activation in carbon xerogels. Journal of Materials Science, 44(24), 6583-6590.

➢ Zubizarreta, L., Menéndez, J. A., Job, N., Marco-Lozar, J. P., Pirard, J. P., Pis, J. J., . . . Arenillas, A. (2010). Ni-doped carbon xerogels for H2 storage. Carbon, 48(10), 2722-2733. doi: 10.1016/j.carbon.2010.03.068

➢ Zubizarreta, L., Menéndez, J. A., Pis, J. J., & Arenillas, A. (2009). Improving hydrogen storage in Ni-doped carbon nanospheres. International Journal of Hydrogen Energy, 34(7), 3070-3076. doi: http://dx.doi.org/10.1016/j.ijhydene.2009.01.040.

Capítulo 2

Planteamiento de la tesis

2. Planteamiento de la tesis

2.1. Antecedentes

Los xerogeles resorcinol-formaldehído han sido ampliamente estudiados durante las últimas décadas debido a las grandes ventajas que ofrecen (como se detalla en la *Introducción*). Inicialmente, estos materiales eran sintetizados por calentamiento convencional, lo que implicaba largos tiempos en el proceso de producción y en consecuencia, un encarecimiento del producto final. Para solventar este problema, el grupo de investigación MCAT (*Microondas y Carbones para Aplicaciones Tecnológicas*) donde se desarrolla esta Tesis Doctoral, introdujo el calentamiento con microondas en la etapa de secado, para posteriormente aplicarlo a la síntesis del material orgánico en su totalidad. Esto supuso una reducción de los tiempos de síntesis en un 90 %, lo que implica un enorme ahorro energético y abre una vía a la posibilidad de producir estos materiales a escala industrial. Este novedoso proceso dio lugar a *Xerolutions S.L.*, (www.xerolutions.com) la EBT spin-off del grupo anteriormente mencionado, que produce xerogeles de carbono como material para electrodos de supercondensadores.

La principal ventaja que presentan los xerogeles RF, con respecto a otros materiales porosos, reside en que su textura puede ser diseñada a medida para la aplicación final deseada mediante el control de las variables que afectan al proceso de síntesis. Aunque las variables físicas (temperatura,

potencia del microondas, tiempos de gelación, curado y secado, etc.) afectan a la porosidad final del material, no lo hacen de forma tan relevante como las variables químicas, las cuales son además dependientes entre sí (*Introducción*). El control de todas variables del proceso permite obtener materiales de diferente porosidad en un amplio rango de anchuras de poro de forma reproducible, lo que dota a los xerogeles de carbono de propiedades físicas y mecánicas totalmente controladas y diferentes.

A pesar de que se tenía controlado el efecto de las variables químicas conocidas hasta entonces (el pH, el grado de dilución y la proporción R/F), se observó que al cambiar de suministrador de la disolución de formaldehído, las propiedades finales de los xerogeles no eran predecibles. La única diferencia entre los reactivos comerciales residía en la concentración de metanol utilizado como estabilizante en la disolución. Nunca antes en la bibliografía se había hecho alusión al efecto de este aditivo, siendo en ocasiones incluso obviado en la parte experimental. De esta forma surge la necesidad de estudiar el primer objetivo planteado en la Tesis.

2.2. Objetivos

El **PRIMER OBJETIVO** de la presente Tesis consistió en determinar el efecto de la proporción de metanol de la disolución de formaldehído sobre la porosidad de los xerogeles de carbono *(Publicaciones I y II).* Estos estudios demostraron la necesidad de considerar esta nueva variable a la hora de diseñar la porosidad de los xerogeles a medida de una aplicación.

Aunque el rango de porosidades que se habían logrado hasta la fecha era muy amplio, como **SEGUNDO OBJETIVO** se estudió la posibilidad de modificar las propiedades mediante la utilización de ácido nítrico como acelerador de la reacción en vez del hidróxido sódico utilizado hasta entonces *(Publicación III).*

Esta mejora del control de las propiedades porosas fue utilizada para diseñar materiales con diferentes tamaños de poro en el rango de mesoporos con el fin estudiar su aplicabilidad como soportes para biomoléculas *(Publicación IV).*

Además de la textura porosa del material, su química superficial también tiene especial relevancia a la hora de ser utilizado en cualquier aplicación. De hecho, la mayoría de las publicaciones encontradas en la bibliografía utilizan el xerogel de carbono en vez del orgánico, lo que requiere de una etapa de carbonización, que cambia totalmente la química del material, y encarece el producto final. Sin embargo, los xerogeles orgánicos presentan unas propiedades texturales similares a los carbonizados pero con una química superficial diferente, además de unos costes de producción relativamente bajos debido al uso del calentamiento con microondas, siendo así candidatos más que interesantes para su utilización en múltiples aplicaciones.

Como ya es sabido, los xerogeles orgánicos resorcinol-formaldehído tienen una química superficial rica en grupos funcionales oxigenados, lo que implica que esta propiedad junto a su porosidad los convierte en materiales potenciales para su utilización como desecantes. Por este motivo, el **TERCER OBJETIVO** fue estudiar la capacidad de este material de actuar como desecante frente a otros comúnmente utilizados *(Publicación V)* y su optimización para éste mismo fin *(Publicación VI y Patente).*

Esta elevada hidrofilia puede ser muy beneficiosa para algunas aplicaciones. No obstante, la adsorción de humedad puede ser un inconveniente para otras aplicaciones como puede ser el aislamiento térmico o la utilización de estos materiales para la retención de aceites en aguas. Por este motivo, el **CUARTO OBJETIVO** de esta tesis fue modificar la química superficial de los xerogeles orgánicos resorcinol-formaldehído para convertir la naturaleza de estos materiales en hidrófoba *(Publicación VII y Publicación VIII).*

Todos estos objetivos mencionados nos llevan a un **OBJETIVO GLOBAL:** diseñar tanto la textura porosa como la química superficial de los

xerogeles resorcinol-formaldehído para que puedan ser utilizados en múltiples aplicaciones.

Capítulo 3

Experimental

3. EXPERIMENTAL

3.1. Reactivos

Tabla 2. *Inventario de reactivos utilizados en esta memoria.*

Compuesto	Casa comercial	Características
Resorcinol	Indspec	99.6 % pureza
Formaldehído	Química S.A.U.	37 % formaldehído[a]
Metanol	AnalaR Normapur	100 % pureza
NaOH	AnalaR Normapur	99.9 % pureza
NaOH	Titripac, Merck	0.1 M
HNO$_3$	Merck	65 % en peso
HMDZ	Basf	100 %
Citocromo C	Sigma-Aldrich	Corazón bovino, ref C2037
ABTS	Sigma-Aldrich	98 % pureza
H$_2$O$_2$	VWR Chemicals Normapur	30 %

(a) Se analizaron las concentraciones de metanol en las disoluciones utilizadas y resultaron entre 0.6 - 1.5 %

3.2. Diseño de las propiedades texturales

3.2.1. Síntesis de xerogeles orgánicos

Para la realización de esta Tesis se han utilizado resorcinol (R) y formaldehído (F) como monómeros precursores de la reacción de polimerización. Para la preparación de la disolución precursora, el resorcinol se disuelve en agua desionizada mediante agitación magnética hasta su total disolución. En otro vaso de precipitados, se mezcla formaldehído con metanol. Ambas disoluciones se mezclan y se agita durante unos minutos para asegurar homogeneidad en la disolución final, la cual tiene un pH aproximado de 3. Para modificar el pH de la disolución precursora se utilizan disoluciones de hidróxido sódico (NaOH) de diferentes molaridades, o ácido nítrico (HNO_3) en el caso de la Publicación III, hasta alcanzar el pH final deseado. La concentración de cada reactivo depende de los valores elegidos para cada una de las variables que se tienen en cuenta en este trabajo: el pH, relación molar entre el resorcinol y el formaldehído, el grado de dilución (Ecuación 1) y el porcentaje de metanol que contiene la disolución de formaldehído. En la Ecuación 1, H_2O y *MeOH* hace referencia a los moles totales de agua y metanol añadidos directamente, mientras que $H_2O_{(f)}$ y $MeOH_{(f)}$ son los moles el agua y metanol contenidos en la disolución de formaldehído, *R* son los moles de resorcinol y *F* los de formaldehído puro.

$$D = \frac{H_2O + MeOH + H_2O_{(f)} + MeOH_{(f)}}{R+F}$$
(Ecuación 1)

La mezcla precursora obtenida se introduce en un horno microondas multimodo que opera a una frecuencia de 2450 MHz, a 85 ºC durante 10000 s (2 h y 47 min), donde tienen lugar las etapas de gelado y curado. Este gel obtenido se trocea para facilitar la evaporación de agua y se seca en este mismo horno microondas hasta que ha perdido la mitad de su masa. Los tiempos de secado son diferentes dependiendo de las propiedades del gel

sintetizado. De esta forma, la síntesis completa de un xerogel orgánico dura aproximadamente 5 horas, lo que supone una gran ventaja frente a la síntesis con calentamiento convencional, donde se requieren 5 días. Esto conlleva un enorme ahorro energético y ofrece así una vía para que los xerogeles RF puedan ser sintetizados a escala industrial de forma simple y barata.

3.2.2. Carbonización

La carbonización es la etapa donde el gel orgánico pasa a tener una estructura carbonosa térmicamente estable, compuesta fundamentalmente por carbono, dando lugar así al llamado *gel de carbono*. La producción de estos geles tiene lugar mediante tratamiento térmico de 2 h a 700 ºC con una rampa de calentamiento de 50 ºC min^{-1} bajo atmósfera de N_2 (100 mL min^{-1}) en un horno eléctrico horizontal tubular (Carbolite MTF 12/38/400). Finalmente la muestra se deja enfriar hasta alcanzar la temperatura ambiente.

3.3. Estadística aplicada al proceso de síntesis

Como se ha mencionado en la *Introducción*, existe un gran número de variables que influyen sobre las propiedades finales de los geles RF y que, además, se encuentran interconectadas entre sí. Por este motivo, la optimización del proceso de síntesis requiere de la aplicación de técnicas estadísticas que permiten evaluar de forma global el efecto de cada una de las variables del proceso, así como la sinergia existente entre ellas. De esta manera, se pueden obtener conclusiones fiables a partir de un número de muestras reducido.

Para ello se ha utilizado el programa *Design Expert ®* y se ha aplicado la Metodología de Superficie de Respuesta (MSR o *Response Surface Methodology, RSM*) la cual engloba tres fases: i) diseño de experimentos, ii) aplicación del modelo y iii) técnicas de optimización. Fijando previamente el objetivo, las variables que se quieren estudiar y las que se utilizan como respuesta, el Diseño de Experimentos *(Design Of Experiments, DOE)*

determina el número y tipo de experimentos mínimos necesarios para llevar a cabo el estudio de forma fiable. Tras la realización de los experimentos, se aplica un análisis de varianza (*Analysis of Variance, ANOVA*) a cada una de las variables respuestas en función del modelo estadístico que mejor se ajuste a los resultados experimentales obtenidos. Este análisis te aporta también información sobre la relevancia de cada una de las variables por separado (determinado por el valor de *p-value*) y la sinergia que hay entre ellas. El modelo estadístico seleccionado (lineal, cuadrático, cúbico, etc.) ha de ajustarse en la mayor medida posible a los resultados experimentales ya que a partir de él, se pueden determinar las variables necesarias para obtener geles con unas propiedades porosas concretas.

3.4. Diseño de la química superficial de los xerogeles orgánicos

Los xerogeles RF tienen una química superficial rica en grupos fenólicos que les dotan de naturaleza hidrófila. Esto es debido a que los grupos hidroxilo generan puentes de hidrógeno con el agua, atrayéndola así hacia la superficie. Para modificar la química superficial de estos materiales y hacerlos hidrófobos, se llevaron a cabo los siguientes procedimientos.

3.4.1. Pasivado de xerogeles orgánicos con silanos

Este procedimiento consiste en la sustitución de los grupos OH que cubren la superficie de los geles orgánicos por grupos $-Si(CH_3)_3$ mediante la reacción indicada en la Figura 5. En esta reacción, el nitrógeno del hexametildisilazano (HMDZ) extrae el protón del OH fenólico. Este grupo aniónico actúa como nucleófilo gracias al par electrónico del oxígeno y ataca a los átomos de silicio del HMDZ mediante un mecanismo SN_2. De esta forma se obtienen enlaces $-O-Si(CH_3)_3$, los cuales hacen que la superficie quede cubierta por grupos apolares que le dotan de hidrofobicidad.
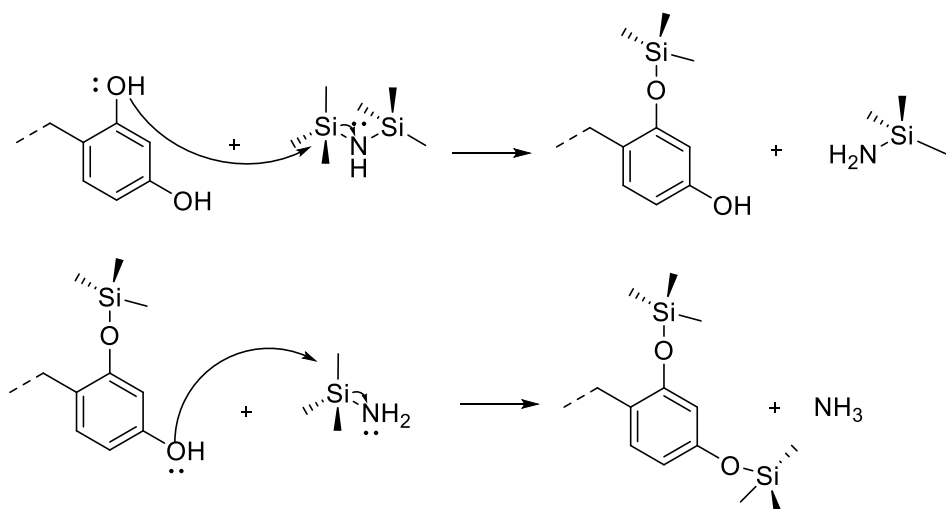
Figura 5.   *Reacción de pasivación de la superficie de los xerogeles RF con HMDZ.*

Para llevar a cabo esta modificación superficial, se muelen 8 gramos de xerogel orgánico por debajo de 212 µm para asegurar su máxima impregnación. Posteriormente, sobre este sólido se añaden 100 mL de hexametildisilazano (HMDZ) y esta mezcla se agita a 80 ºC y presión atmosférica. Para determinar el tiempo óptimo de reacción, se extraen pequeñas alícuotas de material a diferentes tiempos de reacción y se secan en estufa durante una noche a 80 ºC. El grado de hidrofobicidad se determina a través de la medida del ángulo de contacto (Sección 3.7.3) sobre la superficie de un pellet de este material.

3.4.2. Pasivado de xerogeles orgánicos con metanol

Este procedimiento consiste en la sustitución de los grupos OH que cubren la superficie de los geles orgánicos por grupos metoxi (-O-CH$_3$) mediante la reacción de condensación de alcoholes indicada en la Figura 6. De esta forma, la superficie queda cubierta por grupos metoxi, dejando el extremo apolar hacia el exterior y dotando así al material de naturaleza hidrófoba.
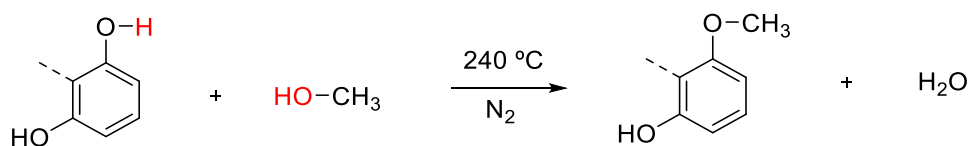
Figura 6. *Reacción de pasivación de la superficie de los xerogeles RF con metanol.*

Para llevar a cabo esta modificación superficial, se muelen 2 g de gel orgánico por debajo de 212 μm y se secan en la estufa durante una noche a 100 ºC para eliminar cualquier humedad residual. Una vez seco, se coloca en el interior de un reactor de cuarzo lo más extendido posible. Un flujo de nitrógeno de 100 mL min^{-1} se borbotea en metanol líquido a 80 ºC en un recipiente cerrado. De esta manera, el flujo de N$_2$ se encuentra saturado de metanol, en esas condiciones, y se introduce al interior del reactor que se encuentra en un horno (Carbolite MTF 12/38/400) a 240 ºC. Esta reacción se llevó a cabo a diferentes tiempos de reacción para hallar el mínimo tiempo necesario para permitir la modificación superficial de hidrófilo a hidrófobo. Antes de caracterizar el grado de hidrofobicidad, las muestras se almacenan en la estufa durante 1 h a 80 ºC para eliminar cualquier metanol residual que pudiera contener la muestra.

3.5. Caracterización de la textura porosa

De acuerdo con la Unión Internacional de Química Pura y Aplicada (IUPAC), textura se define como la geometría detallada del espacio hueco en el interior de las partículas. La textura de un sólido poroso viene determinada por tres parámetros: tamaño de partícula, área superficial y porosidad. Las propiedades que definen la porosidad de un material son: volumen total de poros, forma y tamaño medio de poros, y distribución de tamaño de poros, es decir, el volumen correspondiente a cada intervalo de diámetro de poro.

La caracterización textural suele incluir la determinación de los siguientes parámetros:

➢ Superficie específica: área superficial por unidad de masa de sólido.

➤ Volumen específico de poros: volumen total de poros por unidad de masa de sólido.

➤ Tamaño o anchura de poro: depende de la geometría del poro (cilíndricos, forma de rendija, etc.).

➤ Distribución de tamaño de poros: volumen de poros presentes en una muestra sólida, entre unos determinados tamaños de poro.

Los poros se pueden clasificar en función de su geometría o anchura. La clasificación de los poros atendiendo a su anchura aceptada por la IUPAC, distingue tres grupos de poros:

➤ Microporos: poros con una anchura menor de 2 nm.

➤ Mesoporos: poros con una anchura entre 2 y 50 nm.

➤ Macroporos: poros con una anchura superior a 50 nm.

Ya que cada técnica de caracterización abarca un rango concreto de anchuras de poro, a lo largo de esta Tesis se utilizaron 3 técnicas distintas que en su conjunto nos dan una idea global de la textura porosa total del material: i) isotermas de adsorción de nitrógeno, ii) medidas de densidad real y aparente y iii) porosimetría de mercurio.

3.5.1. Desgasificado

Como paso previo a la caracterización porosa, es necesario dejar la muestra libre de cualquier molécula adsorbida en su superficie. Para ello se somete a un proceso de desgasificado a 120 ºC en vacío (0.1 mbar) durante una noche.

3.5.2. Isotermas de adsorción de nitrógeno

Esta técnica permite evaluar los microporos de mayor tamaño y parte de la mesoporosidad más estrecha de nuestros materiales.

En el caso de materiales porosos, como son los xerogeles RF, toma especial relevancia conocer tanto el volumen y la distribución del tamaño de poro, como el área específica de que estos presentan (Figura 7). Para determinar estos parámetros se realizaron medidas de adsorción de nitrógeno en un *Tristar 3020 (Micromeritics)* a 196 ºC (77 K).
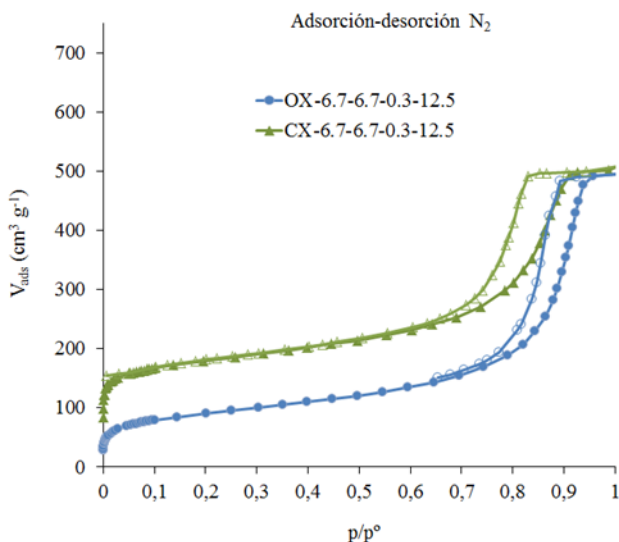
Figura 7. *Isoterma de adsorción-desorción de N_2 a 77 K de un gel orgánico y su correspondiente gel carbonizado.*

En esta Tesis, los métodos empleados para obtención de información a través de esta técnica fueron: i) el método de Brunauer, Emmet y Teller, conocido como BET, donde calcula el área específica a partir de la cantidad de gas adsorbido para formar una monocapa de gas y calculando el área que ocupa (sabiendo que una molécula de nitrógeno ocupa 0.162 nm^2), (ii) método Dubinin-Radushkevich, DR, utilizado para conocer el volumen y anchura media de los microporos presentes en una muestra; y, (iii) método DFT (Density Functional Theory), que permite calcular la distribución de volúmenes de poro.

3.5.3. Densidad real o de helio

Se entiende como densidad real a la relación masa/volumen en la cual se excluyen todos los poros de la muestra. Por ello, se ha utilizado gas helio ya que, además de su carácter inerte sobre nuestra muestra, su pequeño tamaño le permite acceder a todos los poros y así excluir esa porosidad en el resultado final.

Para llevar a cabo esta medida, se pesa la muestra y se introduce en una cubeta de 1 cm^3 en el interior del equipo *Micrometics Accupyc 1340*. Mediante dosificación controlada de He y medidas de presión una vez alcanzado el equilibrio, el equipo determina el volumen que ocupa la muestra. A través de la relación, obtenemos la densidad real del material.

3.5.4. Densidad aparente y porosidad

Se entiende como densidad aparente a la relación masa/volumen en la que se tiene en cuenta la porosidad y pequeñas cavidades de la muestra pero se excluye cualquier tipo de relieve que la muestra pueda tener. Para ello se ha utilizado el equipo *GeoPyc 1360* de la casa *Micromeritics*. Esta técnica permite comparar la densidad de materiales en todo el rango de porosidad, de forma no destructiva.

De forma previa al análisis, la muestra es tamizada entre 2-3 mm para trabajar siempre con el mismo tamaño de partícula. Posteriormente, en una cámara de 19.1 mm de diámetro, se introducen 0.8 g de *DryFlo*, que es un sólido pulverulento de la casa *Micromeritics* que se comporta como un fluido. Se hace un blanco de la medida en el que el *DryFlo* es sometido a una fuerza de 38 N durante 20 ciclos. Posteriormente, una cantidad de muestra tal que corresponda aproximadamente a un 25 % del volumen total, se mezcla con el *DryFlo* y se somete a las mismas condiciones de presión y ciclos que el blanco. El volumen de fluido desplazado corresponde al volumen de nuestra muestra. Sabiendo la masa de muestra introducida, obtenemos la densidad aparente. A partir de este valor de densidad aparente y el valor de densidad real (apartado

anterior), también se puede obtener el valor de porosidad de la muestra (Ecuación 2):

$$Porosidad\ (\%) = \left[1 - \left(\frac{densidad\ aparente}{densidad\ real}\right)\right] \times 100 \qquad \textbf{(Ecuación 2)}$$

3.5.5. Porosimetría de mercurio

Esta técnica permite evaluar los mesoporos de mayor tamaño (de 5.5 a 50 nm) y los macroporos (de 50 a 10000 nm). El fundamento de la porosimetría de mercurio parte de que, en condiciones normales, el mercurio es un líquido que no moja los sólidos, por lo que envuelve la muestra, pudiéndose calcular así el volumen aparente de muestra. Por lo tanto, sabiendo la masa de la muestra, se puede obtener también una densidad aparente análoga a la que se obtiene en el *Geopyc* (apartado anterior) pero con otra metodología. Cuando esta mezcla de mercurio y muestra es sometida a una presión de hasta 228 MPa, el mercurio penetra en los poros del material de diámetro mayor a 5.5 nm, dándonos así información de poros en el rango de 5.5 nm - 1 mm. La caracterización del sistema poroso con esta técnica se basa en aumentar la presión de inyección y medir el volumen de mercurio que entra en la muestra, obteniéndose una curva de *intrusión*. Cuando se alcanza el punto de máxima presión, el mercurio ya no puede penetrar más en los poros del material, por lo que se va bajando la presión y el mercurio sale de esos poros, obteniéndose así la curva de *extrusión*. Sabiendo el volumen de mercurio introducido en la muestra, conoceremos la porosidad del material, es decir el volumen de poros en la muestra, así como la distribución de tamaños de poro (Figura 8).

En esta tesis, el equipo utilizado para este análisis fue el *AutoPore IV* de *Micromeritics*. La muestra se analiza en forma de partículas de 2-3 mm de diámetro para evitar posibles diferencias debidas a la morfología. La cantidad de muestra utilizada es calculada previamente para conseguir alrededor de un 55 % de *stem* (porcentaje de mercurio del vástago del penetrómetro que se mete dentro de la porosidad de la muestra en condiciones de alta presión),

teniendo en cuenta el volumen del dilatómetro utilizado, la porosidad de la muestra y su densidad, las cuales han sido determinadas previamente según el apartado anterior. El equipo realiza medidas desde presión atmosférica hasta 228 MPa con un tiempo de equilibrio de 10 s y las muestras se evacuan hasta una presión de 6.7 Pa. La tensión superficial y el ángulo de contacto del mercurio son de 485 mN m^{-1} y 130 º, respectivamente.
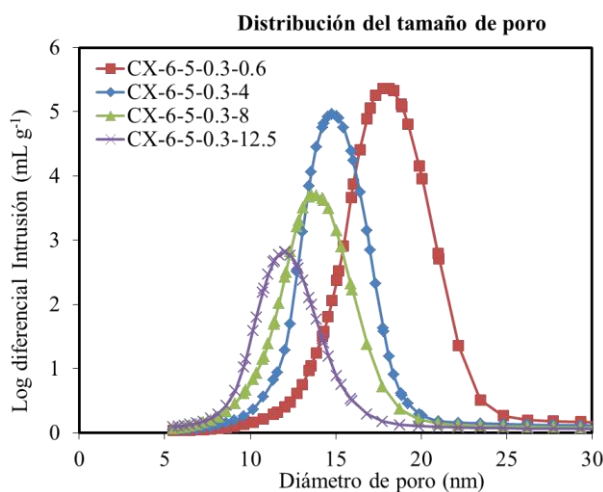
Figura 8. *Distribución del tamaño de poro de cuatro xerogeles de carbono obtenida por porosimetría de mercurio*

3.6. Análisis químico y estructural

3.6.1. Microscopía electrónica de barrido (SEM)

Para observar la morfología de los xerogeles (relieve, textura, tamaño y forma de grano) se utilizó un microscopio electrónico de barrido (SEM, del inglés *Scanning Electron Microscope*) el cual permite obtener imágenes de alta resolución de la superficie de los materiales (Figura 9). En este tipo de microscopios, un haz de electrones incide sobre la muestra objeto de estudio produciendo distintos tipos de interacciones entre la materia y los electrones incidentes. Fruto de las interacciones, se generan distintos tipos de señales que son recogidas por diferentes detectores. La muestra a analizar debe ser sólida,

seca y conductora. Los xerogeles, fueron depositados en forma de partículas sobre una cinta de adhesiva de carbono de doble cara fijada a una chincheta de aluminio.
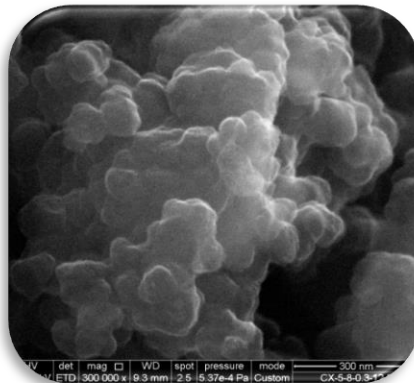
Figura 9. *Imagen de un xerogel de carbono obtenida a través de SEM.*

En este trabajo se ha utilizado un microscopio electrónico de barrido de emisión de campo (FESEM) Quanta FEG 650. Entre los detectores que posee dicho equipo cabe destacar el detector de electrones secundarios, ETD, (*Everhart-Thornley* detector) que permite obtener imágenes topográficas de alta resolución. Se ha trabajado a alto vacío, con un voltaje de aceleración de 25 kV y un tamaño de spot de 2.5.

3.6.2. Microscopía electrónica de transmisión (TEM)

La microscopía electrónica de transmisión (TEM, del inglés *Transmission Electron Microscopy)* al igual que el SEM, utiliza un haz de electrones que incidirá sobre la muestra. En este caso, la muestra debe ser ultrafina y la señal recogida es la que corresponde a aquellos electrones que han atravesado la muestra, aportando así información sobre la estructura interna de la muestra. En esta Tesis se ha utilizado el microscopio electrónico de transmisión modelo *JEOL-2000-EX-II* de 200 keV.

3.6.3. Resonancia magnética nuclear (RMN) de sólidos

La resonancia magnética nuclear (RMN) es una espectroscopía de absorción en la que determinados núcleos (con spin nuclear ≠ 0) son sometidos a un campo magnético intenso y absorben energía cuando se les irradia a una frecuencia característica llamada *pulso*. Estos núcleos generan diferentes señales consecuencia de las interacciones que tenga con su entorno, obteniendo así información estructural (Figura 10).
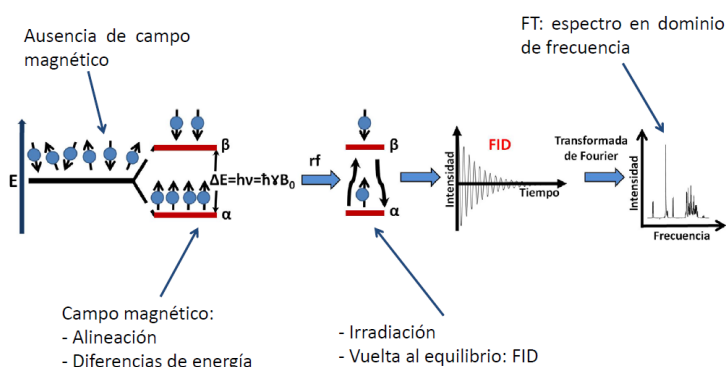
Figura 10.   *Esquema del mecanismo de RMN.*

En el caso concreto de esta Tesis, se realizaron análisis de espectroscopía RMN de estado sólido para ^1H y ^{13}C y estudios de imagen obtenida por RMN para ^1H. Las medidas se llevaron a cabo en un espectrómetro *Bruker Avance 400* (Bruker BioSpin, Rheinstetten) y para la obtención de imágenes, se acopló un accesorio de microimagen al espectrómetro previamente mencionado. En RMN de sólidos, se requiere de métodos altamente específicos para cada tipo de material, ya que la señal resultante es tremendamente compleja. Por este motivo, detalles de las condiciones de análisis se incluyen en la *Publicación II*.

3.6.4. Análisis elemental

Esta técnica tiene como objetivo determinar los porcentajes en masa de carbono (C), hidrógeno (H), nitrógeno (N) y azufre (S) contenidos en la muestra. Para ello se realiza una combustión completa de la muestra mediante

tratamiento térmico a alta temperatura (1050 ºC) en una atmósfera de oxígeno diluido en helio. Los productos obtenidos tras la combustión (CO_2, H_2O, NO_x y SO_3) fluyen hacia un tubo de reducción donde los distintos óxidos de nitrógeno son reducidos a N_2. La cuantificación del CO_2, H_2O y SO_3 tiene lugar de manera específica en los correspondientes detectores de infrarrojos, mientras que el N_2 se analiza en un detector TCD (*Thermal Conductivity Detector*). El equipo utilizado para llevar a cabo esta determinación fue un analizador *LECO TruSpec Micro.*

3.6.5. Análisis inmediato

El análisis inmediato tiene como objetivo determinar el contenido de humedad, cenizas y materia volátil de la muestra. La humedad se determina a partir de la pérdida de masa experimentada por tratamiento térmico hasta 105 ºC, manteniendo esta temperatura hasta transcurrida una hora o hasta alcanzar una masa constante (lo que más tiempo implique). Por otro lado, se consideran cenizas al producto solido inorgánico que resulta de la incineración de la muestra a una temperatura de 815 ºC en atmósfera de aire. La material volátil es el porcentaje de pérdida de masa cuando se somete la muestra, en un crisol provisto de tapa, a un tratamiento térmico a 900 ºC, durante 7 minutos. El análisis inmediato se llevó a cabo en un equipo termogravimétrico LECO TGA 701 (Norma ASTM D7582-10).

3.6.6. Punto de carga cero (pH_{PZC})

El objetivo de esta técnica es determinar la naturaleza de la química superficial de nuestro sólido. El punto de carga cero (pH_{PZC}) corresponde al pH al cual el número de cargas positivas y negativas es análogo, de manera que la carga total de la superficie es cero. Si el pH del medio (agua) es menor que el pH_{PZC} del sólido, la superficie estará cargada positivamente. De la misma forma, si el medio es más básico (pH mayor) que la superficie del sólido, el material estará cargado negativamente. Así, midiendo el pH de la disolución

sobrenadante de esta suspensión sólido-agua obtenemos información sobre la acidez o basicidad de los grupos superficiales de nuestro material.

Para llevar a cabo este análisis, se pesan 200 mg de muestra y se añade un volumen conocido de agua desionizada. Tras 48 h de estabilización bajo agitación magnética, se hace una medida del pH de la mezcla. A continuación, se añade un volumen conocido de agua sobre esta primera mezcla y tras 24 h de agitación se mide de nuevo el pH de la mezcla. Este procedimiento se repite a lo largo de varios días hasta que el pH se modifica considerablemente. Los primeros resultados deberían ser muy análogos entre sí por lo que el pH_{PZC} de nuestro material se calcula con la media de estos primeros datos.

3.6.7. Desorción térmica programada (TPD)

Los análisis de desorción térmica programada (TPD, del inglés *Temperature Programmed Desorption*) aportan información sobre la química superficial de nuestro material. Al ser sometido a tratamiento térmico en atmósfera inerte, los grupos funcionales presentes en la superficie dan lugar a diferentes reacciones de descomposición. Los grupos oxigenados de carácter ácido, como pueden ser ácidos carboxílicos, lactonas, etc., se desorben en forma de CO_2, mientras que los grupos oxigenados básicos como los fenoles, éteres o carbonilos, desorben en forma de CO. Cada tipo de grupo funcional lo hace a una temperatura característica pudiendo identificar así su presencia en la muestra.

Las TPDs de este trabajo se han llevado a cabo en un analizador *AutoChem II 2920* de *Micromeritics* completamente automatizado para la quimisorción en estudios de alta precisión en adsorción química y reacciones a temperatura programada. Cuando fue requerido, se le acopló un espectrómetro de masas, *Onmistar Pfeiffer,* donde son analizados los gases desorbidos, previa calibración con gases conocidos. Para llevar a cabo este procedimiento, se coloca la muestra sobre lana de cuarzo en un reactor de cuarzo en forma de

U y se calienta a 1000 ºC, con una rampa de 10 ºC min^{-1}, bajo flujo constante (50 ml min^{-1}) de argón como gas de arrastre.

3.6.8. Análisis termogravimétrico (TGA)

El análisis termogravimétrico (TGA, del inglés *Thermogravimetric Analysis*) permite registrar de forma continua la variación de masa que experimenta una muestra a medida que aumenta la temperatura. De esta forma se obtiene información tanto sobre la humedad retenida por las muestras como de su estabilidad con la temperatura.

Este análisis se llevó a cabo en un analizador *TGA Q5000IR* de *TA Instruments*, a presión atmosférica y en flujo de aire (100 mL min^{-1}), desde temperatura ambiente hasta 1000 ºC y a una velocidad de calentamiento de 5 ºC min^{-1}.

3.6.9. Espectroscopía Infrarroja por Transformada de Fourier (FTIR)

La espectroscopía infrarroja por transformada de Fourier (FTIR, del inglés, *Fourier Transform Infrared Spectroscopy*) es una técnica que permite determinar los diferentes grupos funcionales que se encuentran en la estructura de la muestra. Al incidir la radiación infrarroja sobre la muestra, una parte es absorbida y otra pasa a su través, siendo detectada por el equipo que lo traduce en forma de espectro. Cada banda observada corresponde a la vibración del enlace de un grupo funcional concreto, y aparece a una longitud de onda determinada, pudiendo así determinarse su presencia en la muestra.

Para la elaboración de este trabajo se han obtenido espectros FTIR en un rango de longitudes de onda de 400 a 4000 cm^{-1} con un equipo a Nicolet IR 8700 y un deterctor DTGS (Sulfato de triglicina deuterada) a una resolución de 4 cm^{-1} a través de 64 barridos. Para preparar los pellets que se utilizan en esta técnica, de mezcla la muestra en polvo y desgasificada en proporción 1:100 con KBr en un mortero de ágata durante 10 minutos para asegurar homogeneidad. Con aproximadamente 0.125 g de esta mezcla se hace una pastilla de 13 mm

de diámetro por compresión a 8 Tons. La pastilla obtenida se desgasifica de nuevo antes de realizar el análisis para evitar bandas características de humedad.

3.6.10. Espectroscopía fotoelectrónica de rayos X (XPS)

La espectroscopía fotoelectrónica de rayos X (XPS, del inglés *X-ray Photoelectron Spectroscopy*) es una técnica semi-cuantitativa de carácter superficial que nos aporta información sobre la energía de cada nivel electrónico y, por tanto, sobre la naturaleza de cada átomo emisor. Esta técnica se basa en la excitación de los niveles más internos de los átomos mediante un haz de rayos X, que provoca así la emisión de fotoelectrones. Este efecto se consigue cuando la energía del haz incidente supera a la energía de ligadura del electrón con el átomo (*BE, binding energy*) y a la energía de extracción necesaria para llevar al electrón del nivel de Fermi al vacío circundante. La energía en exceso de este proceso es transferida al electrón como energía cinética (*KE, kinetic energy*). De esta manera, el espectro XPS representa la intensidad de la señal (número de electrones emitidos) en función de la BE.

Para llevar a cabo esta técnica se ha utilizado un espectroscopio *SPECS* equipado con un analizador *Phoibos 100* utilizando una fuente de rayos X Mg Kα no monocromática (1254.6 eV) con una potencia de 100 W. Al ser una técnica superficial que requiere del uso de alto vacío (10^{-7} Pa) las muestras deben ser previamente desgasificadas (según Apartado 3.5.1.) para evitar contaminación de cualquier compuesto adsorbido sobre la superficie. Los porcentajes atómicos (% en átomos) de los elementos presentes en la capa superior del material (aproximadamente los primeros 10 nm de profundidad) se calculan considerando las áreas integradas de los picos de XPS principales. Para obtener los espectros de alta resolución de C_{1s} se utilizó una energía de 10 eV. La deconvolución de los picos se llevó a cabo utilizando la función Gaussian-Lorentzian por medio del algoritmo de Marquardt.

3.7. Estudios de interacción xerogel/agua

3.7.1. Medidas de adsorción de humedad

Para evaluar la capacidad de adsorción de humedad de los materiales, se almacenan 0.8 g de muestra en un recipiente sellado en condiciones de 100 % humedad y 25 ºC y se registra el aumento de peso que experimenta con el tiempo. Para realizar estudios comparativos es fundamental que los materiales a estudiar tengan el mismo tamaño de partícula y se utilice un volumen similar de muestra.

3.7.2. Isotermas de adsorción de vapor de agua

Esta técnica nos aporta información sobre qué cantidad de vapor de agua es capaz de adsorber la muestra en su superficie y a qué velocidad lo hace. La muestra se expone a cambios en la humedad relativa que la rodea, mediante dosificación controlada de vapor de agua, permitiendo a la muestra alcanzar el equilibrio antes de realizar la siguiente dosificación. Determinando la presión de equilibrio en las condiciones del análisis y la dosificación de vapor de agua realizada, se determina la cantidad de vapor de agua adsorbida (curva de adsorción). En este caso, la adsorción de agua es función tanto de las propiedades porosas de la muestra, como de su química superficial. Una vez llegado a la presión de saturación, se reduce paulatinamente la presión relativa del vapor de agua, obteniéndose la curva de desorción.

Este análisis se llevó a cabo en un equipo multigas *Hydrosorb 1000* (*Quantachrome*) a 25 ºC.

3.7.3. Medidas del ángulo de contacto

Para determinar la afinidad de una superficie con el agua líquida se mide el ángulo de contacto que forma la interfase de una gota de agua con la superficie del material. Si el material tiene afinidad por el agua, la gota tiende a esparcirse sobre la superficie procurando así tener el máximo contacto entre

ambas fases. Para estos materiales, se forman ángulos de contacto de entre 0 y 90 º y se denominan materiales *hidrófilos* (Figura 11). Si por el contrario el agua no tiene afinidad por la superficie del material, la gota minimiza la superficie de contacto. Estos materiales forman ángulos de contacto entre 90 y 180 º y se denominan *hidrófobos*. Dentro de este grupo, si el ángulo de contacto es superior a 150 º se denominan *superhidrófobos* y muestran una repulsión extrema al agua.

Figura 11. *Medida del ángulo de contacto de un xerogel hidrófobo (izq) y otro hidrófilo (dcha) con una gota de agua.*

Para llevar a cabo este análisis es necesario que la superficie del material sea totalmente plana. Para ello, el material es previamente molido por debajo de 212 µm. Con este material, se preparan pellets de 10 mm de diámetro sometiéndolos a una presión de 10 Tons durante 25 s. Sobre la superficie de estos materiales, se deposita con una jeringuilla de vidrio una gota de agua de aproximadamente 6 mm de diámetro (Figura 12). La determinación del ángulo de contacto se lleva a cabo con un tensiómetro óptico de la casa *Krüss 62/G40*. El ángulo de contacto se determina en 3 gotas diferentes, como mínimo, y se hace la media para obtener un valor representativo.

Figura 12. *Método de medida de ángulo de contacto.*

3.8. Estudios de interacción xerogel/biomoléculas

En la presente tesis se exploró la posibilidad de utilizar los xerogeles de carbono (CX) como soportes de biomoléculas con el objetivo de obtener un sistema biocatalítico insoluble que sea estable bajo condiciones severas y que permita su reutilización durante varios ciclos de uso manteniendo su actividad. En este sentido, se seleccionó el Citocromo C (cyt c) de corazón bovino (Figura 13) como proteína modelo para realizar los estudios de inmovilización debido a su estabilidad y pureza.
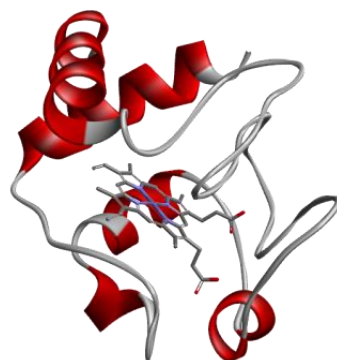
Figura 13. *Modelización de una molécula de Citocromo C.*

3.8.1. Inmovilización de citocromo C en xerogeles de carbono

Para llevar a cabo este proceso se preparan disoluciones de 0.5 g L^{-1} de cyt c a distintos valores de pH (3, 6 y 10) utilizando disoluciones tampón con una fuerza iónica total de 100 mM. Previamente a los estudios de inmovilización, los CX son tamizados a un tamaño de partícula entre 1 y 2 mm, y son estabilizados durante 24 h en la disolución tampón correspondiente. Para los experimentos de adsorción, 10 mg de CX se suspenden en 5 mL de disolución de cyt c y se agita a 200 rpm a 30 ºC en una incubadora (*TH 15* modelo de *Edmund Bühler GmbH*) durante 96 h. La cantidad de cyt c inmovilizada es determinada mediante espectrometría UV-vis (con un espectrofotómetro *Shimadzu UV-2401 PC*) a través del cambio en el pico máximo de absorbancia a una longitud de onda de 410 nm ($\varepsilon = 10^5$ M^{-1} cm^{-1}). También se realizaron medidas de un blanco para estudiar la estabilidad de la proteína en la disolución tampón a las condiciones experimentales.

3.8.2. Estudios de actividad catalítica

La actividad peroxídica del Citocromo C es evaluada a través de la oxidación del ABTS^{TM} (sal de diamonio 2,2'-azino-bis (ácido 3-etilbenzotiazolino-6-sulfónico)). Para llevar a cabo este estudio, se preparan disoluciones de ABTS (1 mM) a valores de pH entre 2 y 10 (todos con una fuerza iónica de 100 mM). Para determinar la actividad del cyt c libre se mezclan cantidades equivalentes (1.9 mL) de ABTS y H_2O_2 (10 mM) en una cubeta de UV. Sobre esta disolución, se añaden 0.2 mL de disolución de cyt c obteniéndose así un volumen final de reacción de 4 mL. El avance de la reacción es controlado mediante el aumento en la absorbancia a 420 nm ($\varepsilon = 36000$ M^{-1} cm^{-1}) de forma continua.

Cuando el cyt c está soportado sobre los CX, se suspenden 10 mg de biocatalizador sólido en viales que contienen una mezcla de 5 mL de ABTS (1 mM, en tampón de pH 4) y 5 mL de H_2O_2 (10 mM, en tampón pH 4) obteniendo un volumen total de reacción de 10 mL, el cual es sometido a agitación

constante. A tiempos conocidos, se van extrayendo alícuotas de la disolución sobrenadante y se evalúa su absorbancia a 420 nm. Después de ser medida, la disolución se devuelve a su vial original. La actividad de la enzima soportada se calcula a partir de la pendiente de la absorbancia frente a la gráfica del tiempo. Además, se estudió la capacidad de reutilización de los biocatalizadores derivados mediante la evaluación de su actividad después de sucesivos ciclos de reacción donde se reemplazan las disoluciones de ABTS y H_2O_2 cuando la oxidación ha sido completada. Previo a cada ciclo de uso, los biocatalizadores son lavados mediante agitación vortex con 5 mL de disolución tampón de pH 6 (100 mM).

Capítulo 4

Diseño de las propiedades porosas

Este capítulo incluye

Publicación I	Effect of methanol content in commercial formaldehyde solutions on the porosity of RF carbon xerogels
Publicación II	An underrated variable essential for tailoring the structure of xerogel: the methanol content of commercial formaldehyde solutions
Publicación III	Acid-based resorcinol-formaldehyde xerogels synthesized by microwave heating
Publicación IV	Protein adsorption and activity on carbon xerogels with narrow pore size distributions covering a wide mesoporous range

4. Diseño de las propiedades porosas

Una de las grandes ventajas de los xerogeles RF es la posibilidad de diseñar sus propiedades texturales para que sean utilizados de forma óptima en distintas aplicaciones. Aunque las variables físicas (temperatura y tiempo de síntesis, volumen de mezcla, etc. [12]) influyen sobre la porosidad final del gel, no sirven para un control fino y diseño de las propiedades finales. Además, permiten ciertos márgenes de modificación sin alterar la estructura del material final. Sin embargo, pequeñas modificaciones en las variables químicas (pH, proporción de monómeros R/F utilizada, etc. [12, 16, 25]) afectan de forma directa al proceso de polimerización, formándose así una estructura tridimensional diferente dependiendo de las variables utilizadas.

Cuando hablamos de la textura porosa de los xerogeles entendemos que su estructura está formada por un conjunto de esferas a las que llamamos *nódulos* que se encuentran entrecruzadas entre sí formando una red sólida. Los meso-macroporos (definidos en *Experimental*) corresponden al espacio que se encuentra entre estos nódulos, mientras que los microporos son huecos localizados en su interior. De esta manera, cuanto más grandes sean los nódulos mayor es el espacio que hay entre ellos y mayor es el tamaño de meso-macroporo, dando lugar a materiales poco densos; por contra, cuanto más cerca estén los nódulos entre sí, más entrecruzamientos habrá, y el material resultante tendrá mayor resistencia mecánica (Figura 14).
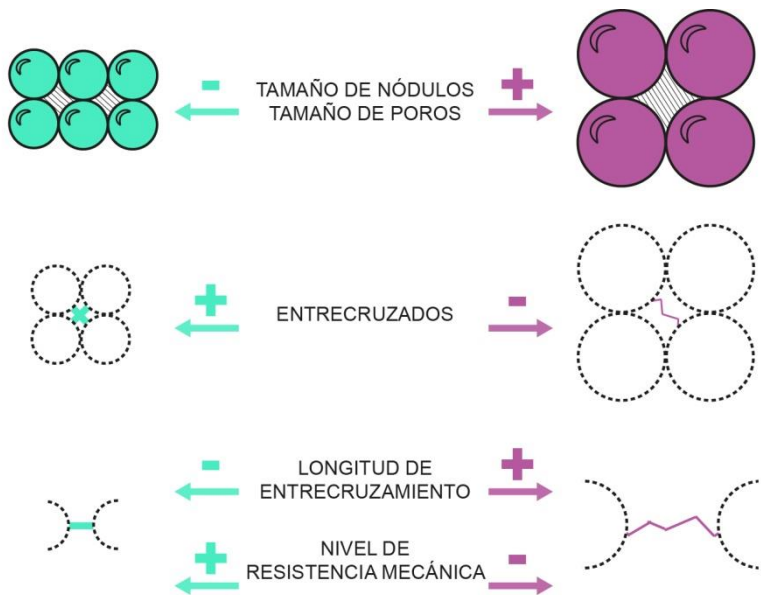
Figura 14. *Esquema de distintos tipos de estructuras dependiendo del tamaño de los nódulos y sus entrecruzamientos.*

Como ya se mencionó en la *Introducción*, el efecto de variables como el pH, el grado de dilución y la proporción de monómeros utilizada, ya han sido anteriormente estudiadas y muestran una gran repercusión sobre la porosidad final del material. En este capítulo se estudia el efecto de la proporción de metanol de la disolución de formaldehído como nueva variable química a tener en cuenta en la síntesis de xerogeles orgánicos, así como el efecto de sustituir el catalizador básico de la disolución precursora por otro de naturaleza ácida. Este control más exhaustivo de las propiedades porosas ha sido utilizado para el diseño de xerogeles de carbono como soporte para biomoléculas.

El **objetivo general** de este capítulo es lograr el control total de las propiedades texturales de los xerogeles de carbono para poder diseñarlos a la medida de cualquier aplicación.

4.1. Efecto de la proporción de metanol de la disolución de formaldehído

El formaldehído es un gas incoloro que se comercializa en disoluciones acuosas normalmente al 37 % en peso debido a que concentraciones mayores de este producto generarían la condensación del formaldehído consigo mismo, precipitando como para-formaldehído, y produciría enormes variaciones de la concentración de este compuesto en disolución [26].

Para evitar su precipitación, se añade cierta proporción de metanol como estabilizante, de forma que mediante la producción de hemiacetales evita la polimerización del formaldehído consigo mismo, y por tanto, mantiene concentraciones constantes de este reactivo con el tiempo (Figura 15).
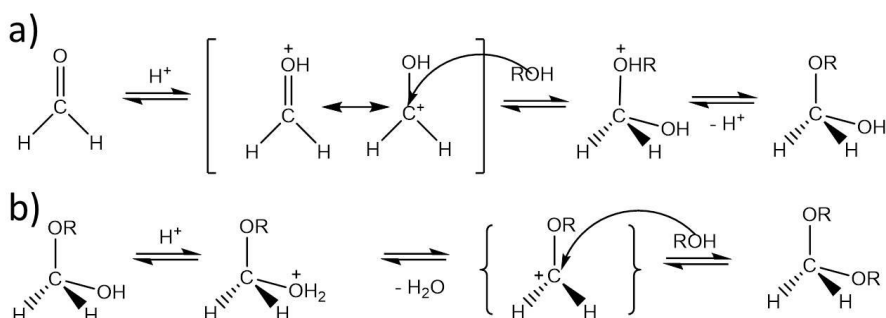
Figura 15. *Mecanismo de estabilización del formaldehído a través de a) hemiacetales y b) acetales.*

Entre las distintas empresas que comercializan con disoluciones de formaldehído se observa una gran variación en la concentración de metanol contenida en el producto. De hecho, algunas casas comerciales indican la presencia de metanol con objetivos estabilizantes pero en ningún momento indican la cantidad de este compuestos en la disolución (Tabla 3).

Tabla 3. *Porcentaje de formaldehído y metanol de distintas casas comerciales.*

CASA COMERCIAL	FORMALDEHÍDO	% METANOL
Fernández Rapado	36.5-37.5	≤ 1.3
Oxidal	37-40	10-15.0
Panreac	35-40	9-14
Solvech	35-40	9-15
Spi-Chem	37	No especificado
Merck Chemicals	37	10
Sigma-aldrich	37	10-15

Esta ausencia de homogeneidad pudiera derivar en una alteración de la estructura del xerogel orgánico diseñado debido a que el agua y el metanol presentan propiedades físicas y químicas diferentes que pudieran afectar en el proceso de síntesis, como pueden ser:

➢ El valor de la constante dieléctrica: 80.4 para el agua y 32.6 para el metanol [27, 28]. Esta diferencia pudiera afectar a la cantidad de energía microondas que absorbe el material durante la síntesis.

➢ El punto de ebullición: 100 ºC para el agua y 65 ºC para el metanol [29]. Esta diferencia pudiera afectar al proceso de síntesis ya que se lleva a cabo a 85 ºC, por encima del punto de ebullición de uno de los compuestos y por debajo del otro, lo que podría llevar a la evaporación del metanol pero no del agua, afectando así a las condiciones generales de la síntesis.

➢ La tensión superficial: 75.8 para el agua y 23.8 para el metanol [29]. Esta propiedad afecta en la fase de secado por calentamiento donde los poros experimentan una elevada tensión superficial en la fase sol-líquido, pudiendo causar el colapso la estructura porosa. Según esto, los geles con una mayor proporción de metanol en su composición se verían menos afectados por este fenómeno, produciéndose un menor colapso en la estructura porosa.

Las diferencias entre las propiedades del agua y el metanol, así como la formación de hemiacetales en la disolución por efecto del metanol, pudieran traducirse en que al cambiar de casa comercial de disolución de formaldehído los resultados pudieran verse alterados respecto a los predecibles utilizando una disolución de formaldehído con una concentración de metanol conocida.

Por estos motivos, en esta Tesis Doctoral se ha evaluado el efecto de distintas concentraciones de metanol en la disolución de formaldehído sobre las propiedades porosas del gel final.

4.1.1. Objetivos

Los objetivos planteados para realizar el estudio fueron:

➢ Evaluar el efecto de distintas proporciones de metanol contenidas en la disolución de formaldehído comercial respecto a:

  o Las propiedades texturales de los xerogeles obtenidos.

  o Las propiedades químicas de los xerogeles obtenidos.

  o La influencia de otras variables químicas utilizadas en la síntesis.

➢ Encontrar una hipótesis que explique estos comportamientos observados.

➢ Hacer un estudio estadístico que prediga el diseño de las propiedades porosas de nuevos materiales teniendo en cuenta esta nueva variable.

4.1.2. Estudio

Para llevar a cabo estos estudios se sintetizaron un total de 150 xerogeles de carbono variando: i) el porcentaje de metanol contenido en la disolución de formaldehído entre 0.6 y 12.5 %, ii) el pH de la disolución precursora entre 4 y 7, iii) el grado de dilución entre 5 y 8 y iv) las proporciones R/F entre 0.3 y 0.7.

Estas condiciones fueron seleccionadas acorde a estudios previos de la bibliografía [15, 30] y las proporciones de metanol abarcan el rango de

porcentajes que suelen emplear las distintas casas comerciales (Tabla 3). La necesidad de realizar un número tan elevado de experimentos reside en el diseño de una superficie respuesta fiable para predecir nuevas recetas que nos proporcionen la porosidad deseada para nuevas aplicaciones, considerando esta nueva variable.

4.1.3. Resultados

Los detalles experimentales y la discusión de los resultados obtenidos se hallan en la *Publicación I y II*, incluida al final de este capítulo. Los principales resultados de este estudio se detallan a continuación:

➢ Una disminución de la proporción de metanol implica un aumento del tamaño y volumen de poros, un aumento de su porosidad total y por tanto, una disminución de la densidad aparente del material.

➢ El efecto de proporción de metanol sigue la misma tendencia, pero tiene diferente magnitud, dependiendo de las otras variables químicas utilizadas en el proceso. Se propusieron diferentes hipótesis y mecanismos de reacción que explican este efecto.

➢ Este efecto es consecuencia de la formación de hemi/acetales en la disolución consecuencia de la reacción del metanol con el formaldehído. Un aumento de la concentración de metanol conlleva una menor proporción de formaldehído en forma libre, entorpeciendo así la reacción de polimerización.

➢ El efecto de la proporción de metanol repercute únicamente sobre la síntesis del material orgánico y no sobre el proceso de carbonización.

➢ La composición química de todos los materiales obtenidos mostró ser muy similar. Se observaron cambios muy sutiles que se achacaron a las presencia de distintos grupos funcionales dependiendo de si hay más o menos entrecruzamientos en la síntesis.

4.1.4. Conclusión

La proporción de metanol contenida en la disolución de formaldehído comercial afecta de forma muy relevante sobre la textura porosa del gel. Por lo tanto, se hace necesario tenerla en cuenta a la hora de diseñar materiales a medida de una aplicación (Figura 16).
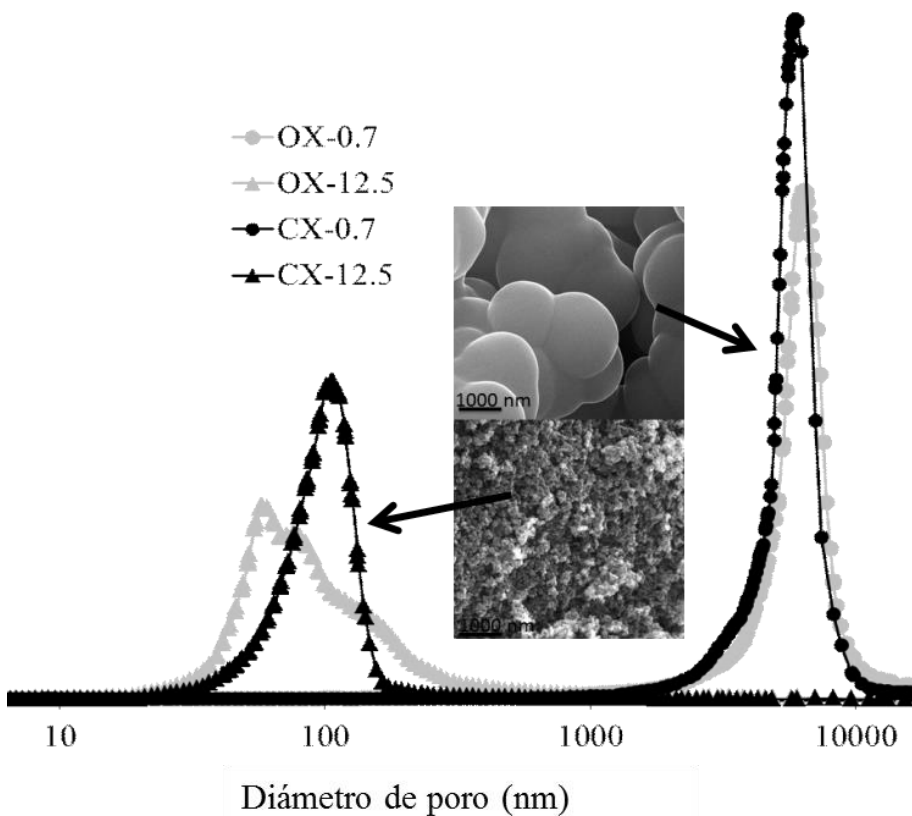
Figura 16. *Efecto de la proporción de metanol sobre dos muestras OX y CX.*

PUBLICACIÓN I

EFFECT OF METHANOL CONTENT IN COMMERCIAL FORMALDEHYDE SOLUTIONS ON THE POROSITY OF RF CARBON XEROGELS

Isabel D. Alonso-Buenaposada, Natalia Rey-Raap, Esther G. Calvo, J. Angel Menéndez, Ana Arenillas, *Journal of Non-Crystalline Solids, 426 (2015) 13-18.*

Effect of methanol content in commercial formaldehyde solutions on the porosity of RF carbon xerogels

CrossMark

Isabel D. Alonso-Buenaposada, Natalia Rey-Raap, Esther G. Calvo, J. Angel Menéndez, Ana Arenillas *

Instituto Nacional del Carbón, CSIC, Apartado 73, 33080 Oviedo, Spain

ABSTRACT

Methanol is used commercially as a stabilizer in solutions of formaldehyde to prevent its precipitation. However, the methanol content of commercially available formaldehyde solutions differs from one supplier to another. The pH, dilution and R/F ratio have been demonstrated to be interdependent variables that can be manipulated to tailor the porous properties of RF carbon xerogels. This work considers the methanol contained in formaldehyde solutions as a new variable to be studied in conjunction with those just mentioned. For the purpose of this study, the influence of methanol on the final porous properties of RF carbon xerogels has been evaluated. It was found that carbon xerogels synthesized using formaldehyde solutions with lower concentrations of methanol showed a higher total pore volume and pore size, and in turn, a lower density and a greater porosity. The porosity of RF carbon xerogels could therefore be radically modified depending on the commercial formaldehyde solution used for their synthesis.

Keywords: carbon xerogel, formaldehyde, methanol, controlled porosity

1. **INTRODUCTION**

Carbon gels are nanoporous materials obtained by the polymerization of hydroxylated benzenes and aldehydes in the presence of a solvent following Pekala´s method [1]. Most carbon gels presented in the literature are synthesized using resorcinol and formaldehyde as precursors and water as solvent [2-5], although other precursors and reaction media can be used [6-9].

The process follows four main steps from the initial mixture of precursors to the final carbon gel [10]. First of all, polymerization and gelation take place, causing the solution to turn gradually into a solid state. Then, an ageing step generates crosslinking reactions that result in a stable polymeric structure. Next, the solvent is removed in a drying step. Finally, the dry material is subjected to high temperature treatment to produce the carbon gel.

The drying step can be performed by one of three different methods, each of which generates different properties in the final gel: supercritical drying, freeze-drying and evaporative drying. These give rise to aerogels, cryogels and xerogels, respectively [5, 11-16]. In this particular study, microwave radiation was used as heating source from the beginning to the end of the process, i.e. for accelerating the polymerization and crosslinking reactions, and also for the evaporative drying [17, 18]. This has been demonstrated to be a cost-effective process since it offers the possibility of synthesizing carbon gels on a large scale via a simple and fast procedure to yield very competitive and highly valued materials [17-22].

Over the last ten years, carbon xerogels have emerged as materials with a great added value owing to the fact that their porosity can be controlled and designed by selecting the appropriate synthesis variables, both physical (i.e. temperature, time of synthesis, etc.) [2, 19] and chemical (i.e. pH, dilution, ratio R/F, etc) [23-26]. In addition, it has been demonstrated that all these variables are interdependent, making it necessary to study several variables at the same time, for which the application of statistical programs and a global assessment of the results are required.

Methanol is used commercially as a stabilizer in formaldehyde solutions, and generates hemiacetal/acetal compounds which prevent the precipitation of the formaldehyde. The study of the influence of the proportion of methanol present in commercial formaldehyde solutions has attracted a great deal of attention owing to the fact that these solutions differ greatly in methanol content from one supplier to another. As an example, Table 1 shows different chemical suppliers and the percentages of methanol in their commercial formaldehyde solutions. It can be seen that the concentrations of methanol may differ substantially. It is well known that the physical and chemical properties of water and methanol also differ (i.e. dielectric constant, boiling point, surface tension, etc.) [27], and accordingly may have an influence in certain stages of the synthesis, such as the polymerization or drying steps. Indeed, RF gels synthesized with methanol as solvent have already been reported in the bibliography, and these carbon gels exhibit quite different properties to those synthesized in water [10, 28, 29].

Thus, the proportion of methanol in the formaldehyde solution is believed to affect the final porous properties of the RF xerogel. Accordingly, the aim of this work is to assess the influence that methanol contained in commercial formaldehyde solutions has on the final porous properties of RF carbon xerogels.

Table 1. Variation of the methanol content in different available commercial solutions of formaldehyde.

SUPPLIER	Methanol concentration (wt. %)
Fernández Rapado	<1.3
Panreac	9-14
Solvech	9-15
Merck Chemicals	10
Oxidal	10-15
Sigma-Aldrich	10-15
Spi-Chem	non specified

2. EXPERIMENTAL

2.1. Synthesis of carbon xerogels

Carbon xerogels were synthesized by the polymerization of resorcinol (R) and formaldehyde (F), using deionized water as solvent and NaOH as catalyst of the reaction. First of all, resorcinol (Indspec, 99.6 wt. %) was dissolved in deionized water in an unsealed glass beaker under magnetic stirring until completely dissolved. In another beaker, formaldehyde (Química S.A.U., 37 wt. % formaldehyde, 0.6 wt. % methanol, 62.4 wt. % water) was mixed with methanol (AnalaR Normapur, 99.9 %) under stirring in order to obtain formaldehyde solutions with different proportions of stabilizer. Afterwards, both solutions were mixed and stirred until a homogeneous solution was obtained. Then, two different NaOH solutions were used in order to achieve the desired pH: a NaOH 5 M solution prepared from solid NaOH (AnalaR Normapur, 99.9 %) and a NaOH 0.1 M solution (Titripac, Merck).

The proportions of each reagent depend on the dilution ratio (D), the R/F ratio, the pH and the percentage of methanol selected for each experiment. The dilution ratio is defined as the molar ratio of the total solvent to the reactants. Total solvent refers to the water and methanol contained in the formaldehyde solution and the amount of deionized water and methanol added, whilst reactants refers only to the resorcinol and formaldehyde.

In the present work, dilutions between 5 and 8, R/F ratios from 0.3 to 0.7, pH values between 4 (pH with no catalyst added) and 7, and percentages of methanol from 0.6 (already contained in the commercial formaldehyde solution employed) to 12.5, were used. These limits were selected taking into account other studies found in the bibliography [23]. The range of the methanol percentages was selected from the different commercial formaldehyde solutions available (see Table 1).

Each precursor solution was placed in a in-lab modified multimode microwave oven at 85 ºC for the whole synthesis process (polymerization and curing steps) during ca. 3 hours. More details about the microwave cavity and the operating conditions used are described elsewhere [18, 23, 24]. The polymer was then dried also by microwave heating until a mass loss of over 50 wt. % was recorded, giving rise to the organic xerogel. The xerogel was then carbonized in a tubular reactor (Carbolite MTF 12/38/400) for 2 h at 700 ºC under a N_2 flow (150 mL min^{-1}) to yield the desired carbon gel end product.

The sample nomenclature selected throughout this study is as follows: "CX-pH-D-R/F-M" where the CX is the abbreviation for the carbon xerogels and the pH, D, R/F and M are 4 numerical values corresponding to the pH of the precursor solution, the dilution ratio, the R/F molar ratio and the percentage of methanol contained in the formaldehyde solution, respectively.

2.2. Sample characterization

Porosity and morphology of the samples studied were characterized by means of nitrogen adsorption-desorption isotherms, mercury porosimetry and scanning electron microscopy (SEM). Before any characterization, the xerogels were outgassed (Micromeritics VAcPrep 0.61) at 0.1 mbar and 120 ºC overnight, in order to remove humidity and other physisorbed gases.

The nitrogen adsorption-desorption isotherms were measured at -196 ºC in a Tristar 3020 (Micromeritics). S_{BET} was determined from the N_2 adsorption branch and, in all cases, the number of points used to apply BET equation was superior to 5. Vmicro was estimated by the Dubinin-Raduskevich method. N_2 adsorption-desorption isotherms were only used to obtain information about microporosity (S_{BET}, Vmicro and mean micropore size). Parameters such as porosity (%), pore size distribution (PSD), bulk density and mesopore/macropore volumes (Vmeso, Vmacro), were determined by mercury porosimetry, with the equipment AutoPore IV 9500 (Micromeritics), which is able to measure from atmospheric pressure to 228 MPa. In the case of mesopores

characterisation, the lower limit for the apparatus used was 5.5 nm. Likewise, Vmacro refers to porosity ranging from 50 to 10000 nm. The surface tension and contact angle were taken to be 485 mN m^{-1} and 130 º, respectively, and the stem volume was between 45-58 % in all the analysis performed. Initially, in the low pressure step, the samples were evacuated to 6.7 Pa and the equilibration time used was 10 seconds. Subsequently, the pressure was gradually increased to the maximum value and the subsequent mercury intrusion evaluated.

Micrograph of the carbon xerogels were also obtained on a Zeiss DSM 942 scanning electron microscopy. For this characterisation samples were attached to an aluminum tap using conductive double-sided adhesive tape. An accelerating voltage of 25 kV and a secondary electron detector EDT Everhart-Thornley, was used in all analysis.

2.3.   *Experimental design*

As is well known, the final porous properties of carbon gels are affected by several variables which are interrelated [12, 18, 23, 24]. Therefore, the selection of the variables for tailoring the final properties is crucial. The biggest challenge in this study was to ensure that most of the possible combinations of pH, D, R/F and % MeOH were covered, taking into account that this is a four-dimensional study and an exponential number of combinations of variables is possible for each experiment.

Accordingly, an experimental design was constructed based on Response Surface Methodology (RSM), using a Design Of Experiments (DOE) which allowed the largest possible number of combinations to be covered by the smallest possible number of experiments. The range for the variables studied were: pH values between 4 and 7, a dilution (D) between 5 and 8, a R/F ratio from 0.3 to 0.7 and a percentage of methanol in the precursor solution from 0.6 to 12.5 %, according to the concentrations provided by different suppliers of formaldehyde solutions (Table 1). A D-optimal design was applied to 146 experiments, from which a statistical model was obtained for the different

responses of the system, with special attention to the characterisation of mesoporosity by using an analysis of variance (ANOVA). The data were adjusted to a cubic function with an R-squared value from 0.95 for samples obtained using 0.6 % of MeOH, to 0.81 when using 12.5 %. The p-value obtained from the ANOVA was always smaller than 0.05, indicating that the fit of data is significant and therefore the model applied is correct. The design matrix was generated by using a Design-Expert 9.0 Trial version from Stat-Ease Inc.

3. RESULTS AND DISCUSSION

In order to present the large amount of results obtained in a clear manner, a sample (CX-6-5-0.3) obtained from a precursor solution with a pH of 6, a dilution ratio of 5 and a R/F molar ratio of 0.3 was taken as a reference. The pH, dilution ratio and R/F molar ratio were varied with respect to the reference sample. The other variables used were kept constant during the synthesis process. Every combination of variables was prepared using four different methanol concentrations (i.e. from 0.6 to 12.5 wt. %). A selection of the resulting samples is presented in Table 2.

As can be seen, a decrease in the concentration of methanol leads to an increase in the total pore volume (up to 218 %), pore size (up to 400 nm) and porosity (up to 64 %) and, as a consequence, to a decrease in density (up to 37 %). This strong influence is graphically shown in Figure 1. The corresponding variations for the reference samples are shown in Figure 1a, where it can be seen that the total pore volume increases as the concentration of methanol decreases.

Table 2. *Porosity parameters, derived from mercury porosimetry, of carbon xerogels obtained from 4 different recipes and in each case with 4 different methanol concentrations.*

	Sample	V_{tot} (cm³/g)	V_{meso} (cm³/g)	V_{macro} (cm³/g)	Pore diameter (nm)	Bulk density (g/cm³)	Porosity (%)
REFERENCE	CX-6-5-0.3-12.5	0.53	0.53	0.00	12	0.74	38
	CX-6-5-0.3-8	0.69	0.69	0.00	14	0.70	47
	CX-6-5-0.3-4	0.78	0.78	0.00	15	0.64	49
	CX-6-5-0.3-0.6	0.89	0.89	0.00	18	0.59	52
DIFFERENT PH	CX-5-5-0.3-12.5	0.90	0.88	0.02	22	0.50	44
	CX-5-5-0.3-8	1.37	0.82	0.54	46	0.46	64
	CX-5-5-0.3-4	1.94	0.11	1.83	101	0.35	67
	CX-5-5-0.3-0.6	2.55	0.03	2.52	420	0.30	72
DIFFERENT DILUTION	CX-6-8-0.3-12.5	1.50	1.18	0.33	47	0.43	63
	CX-6-8-0.3-8	1.53	0.14	1.39	65	0.43	64
	CX-6-8-0.3-4	1.58	0.04	1.55	124	0.42	64
	CX-6-8-0.3-0.6	-	-	-	-	-	-
DIFFERENT R/F	CX-6-5-0.7-12.5	0.28	0.28	0.00	13	0.95	26
	CX-6-5-0.7-8	0.33	0.33	0.00	13	0.92	30
	CX-6-5-0.7-4	0.46	0.46	0.00	14	0.80	36
	CX-6-5-0.7-0.6	0.89	0.86	0.03	21	0.60	52
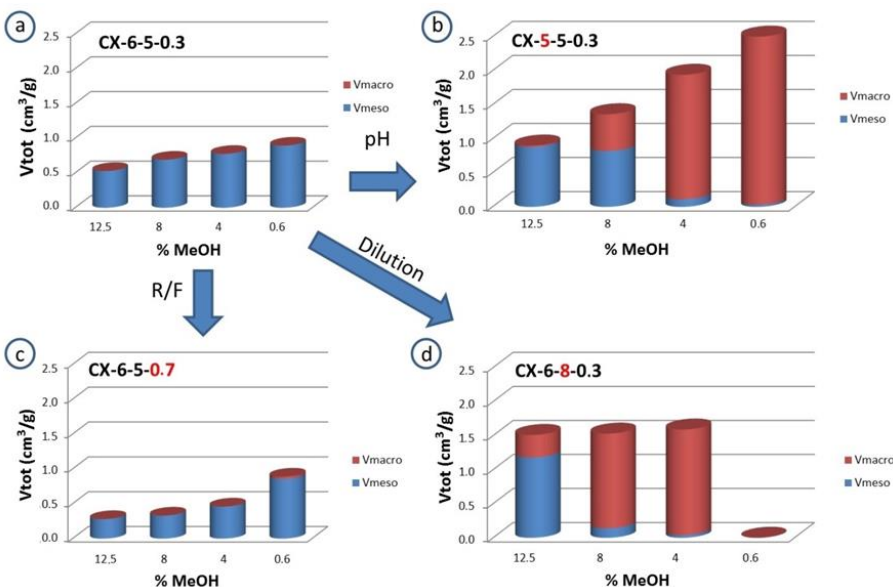
Figure 1. *Influence of methanol concentration on the meso-macroporosity and total pore volume developed in carbon xerogels in combination with variation of the pH, R/F ratio and dilution of the precursor solution.*

The same trend is also observed for the different pH, R/F molar ratio and dilution ratios (Figures 1b, 1c and 1d, respectively). However, the contribution of the mesopore and macropore volume to the total volume of pores is different as it depends on all the other chemical variables selected. Figure 1a shows mesoporous materials and, in this case, methanol only affects the volume of mesopores, since these samples do not have any macroporosity. However, Figure 1b shows samples with different a pH (i.e. a precursor solution pH of 5). Here it can be seen that not only is the total pore volume three times larger when 0.6 wt. % of methanol is applied instead of 12.5 wt. %, but also that the type of porosity has changed radically. In this case, the sample obtained with 0.6 wt. % of methanol is a macroporous material, while that obtained with 12.5 wt. % of methanol is mesoporous. These results show that a change in the proportion of methanol affects the porosity of the resulting material considerably.

Figure 1c displays samples where the R/F molar ratio has been increased with respect to the reference ones. In this case, the increase in pore volume obtained is not directly proportional to the decrease in methanol, since

the increase, when the methanol decreases from 4 to 0.6 wt. % is higher than in the case of the other formulations (see Table 2). In Figure 1d samples with different dilution ratios are shown. As can be observed, the total pore volume increases only slightly with the decrease in methanol content, but the type of pores obtained changes drastically in that the material obtained is predominantly mesoporous when 12.5 wt. % of methanol solution is used, but totally macroporous when 4 wt. % of methanol is employed. It was not possible to synthesize carbon xerogels with 0.6 wt. % of methanol under the conditions used in this study, since gelation did not take place, and the precursor solution remained in a sol state.

It is well known that the pH of the precursor solution has a strong effect on the porosity of carbon xerogels. Higher pH values enhance polymerization, leading to an increase in the number of clusters of lower size and as a consequence, a decrease in the pore size [18, 23, 24, 27, 30, 31]. For this reason, in Figure 2a, which corresponds to samples obtained with a pH value of 6, pore sizes are in the mesopore range (i.e. pores between 5 and 25 nm, depending on the sample) whereas in Figure 2b, corresponding to samples with a pH of 5, pores of hundreds of nm may develop. Therefore, as the pH of the precursor solution decreases, not only does the pore size increase but also the total pore volume. Moreover, in both cases, a decrease in the methanol concentration generates an increase in the pore size, which is much higher when a lower pH is used (i.e. the pore size can be increased from 22 to 420 nm merely by decreasing the methanol content of the sample obtained with a precursor solution pH of 5).
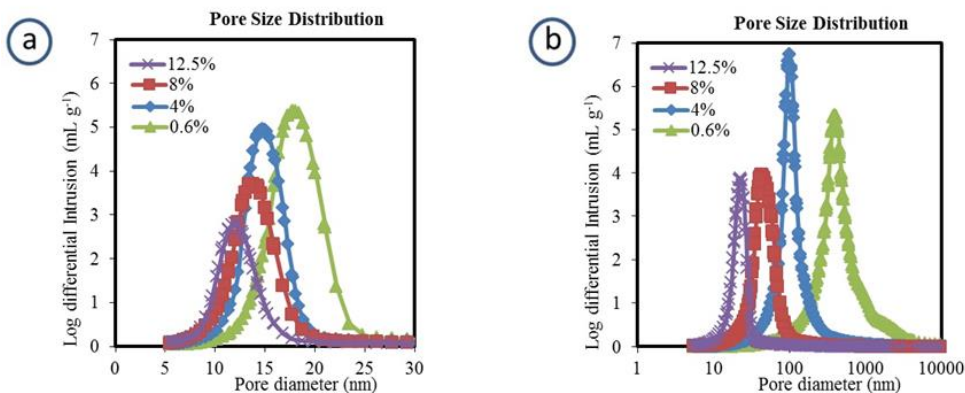
Figure 2. *Variation of the pore size distribution of carbon xerogels due to different methanol proportions for two different precursor solution pH values: a) pH=6 and b) pH=5.*

The R/F molar ratio is considered another important variable for controlling the porosity of carbon xerogels. It has been demonstrated that, provided that the rest of the variables are kept constant, an excess of formaldehyde promotes the formation and growth of clusters and produces a greater number of interconnections [12, 24]. A decrease in the R/F ratio displaces the reaction equilibrium to the products, giving rise to an increase in the rate of reaction and in the size of the clusters. The SEM micrographs in Figure 3 show the effect of this variable on the size of the clusters in the carbon xerogel and, in turn, on the final porosity. Thus, from the left to the right, it can be seen that an increase in the R/F ratio leads to a decrease in the pore size and smaller clusters are formed. However, when the two rows corresponding to two different methanol concentrations are compared, it is observed that the effect of the methanol concentration is even greater than the influence of the R/F ratio, as it is very difficult to distinguish differences between the R/F ratios when 12.5 wt. % is the percentage of methanol used.
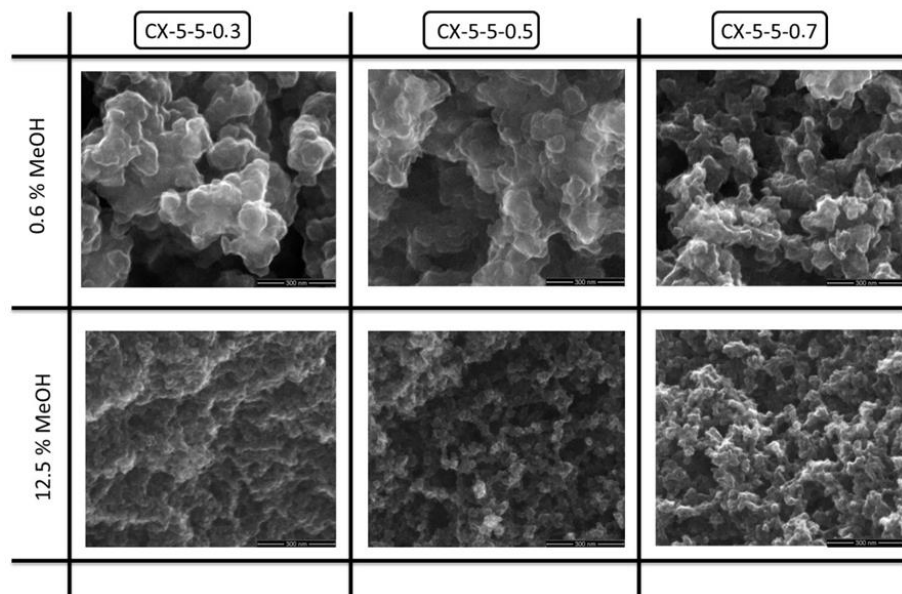
Figure 3. *SEM images showing the influence of the R/F molar ratio and methanol concentration in the formaldehyde solution on the size of the clusters formed and therefore on the final porosity of carbon xerogels.*

It has been demonstrated that chemical variables are interdependent [23, 24] and therefore, they must be studied simultaneously. As it is not possible to represent the variations and interdependence of four variables at the same time (i.e. pH, dilution, R/F ratio and percentage of methanol), Figure 4 only represents the combined effect of pH and dilution ratio on the mesopore volume for two different concentrations of methanol.
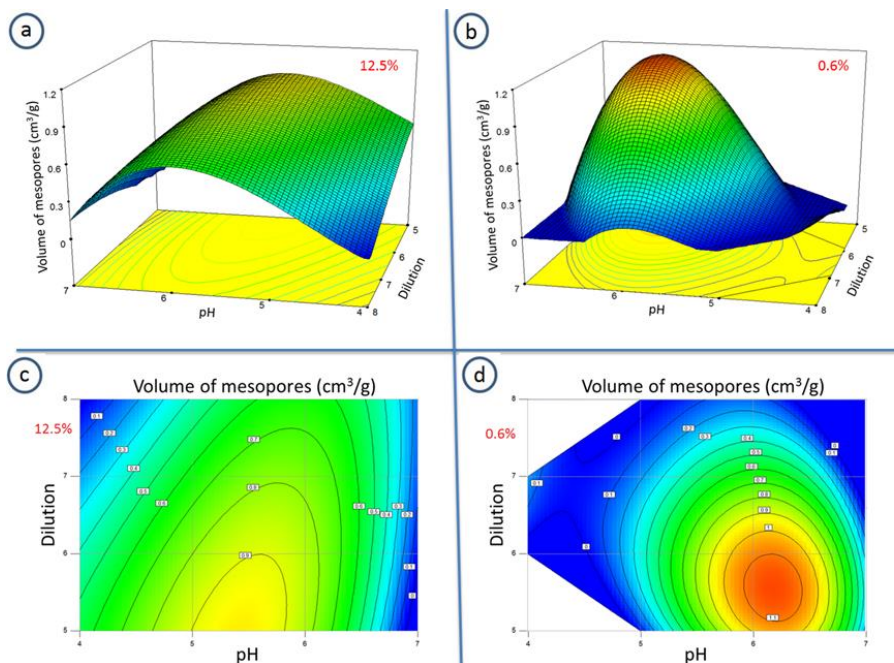
Figure 4. *Three-dimensional surface plot and contour plot showing the combined effect of the dilution ratio and pH on the mesopore volume for two different methanol concentrations (R/F ratio fixed at 0.3).*

The dilution ratio used in the precursor solution affects the final porosity of carbon xerogels in that the greater the dilution ratio, the greater the distance between the clusters of polymers formed, leading to materials with wider pores [23, 24]. The R/F ratio was fixed at 0.3 for this study, as illustrated in Figure 4, because it has been observed to yield a large mesopore volume, not only in this work but also in previous published studies [24]. Figures 4a and 4b show a three-dimensional surface plot with 0.6 and 12.5 wt. % of methanol, respectively. Figure 4c and 4d display the corresponding contour plots for the same methanol concentrations. In these graphs, it can again be observed that a decrease in the concentration of methanol produces an increase in the mesopore volume. Moreover, the maximum is displaced to a higher value of pH and the area corresponding to mesopore volume has been reduced.

It is not possible to synthesize samples with 0.6 wt. % of methanol under the conditions of this work, when the pH and dilution are low, since the precursor solution would boil and the process would get out of control. Neither

was it possible to synthesize samples with a low pH and a high dilution ratio because more than 3 h would be needed to reach the gelation point, making the process too costly. For this reason these areas are not represented on the graph (Figure 4d).

At some points on the plot, a decrease in pore volume seems to occur. However, the decrease observed is due to an enlargement of the pores, as a consequence of which some mesopores become macropores, leading to a decrease in the mesopore volume. This can also be observed in Figures 1b and 1d, where the type of porosity has been drastically modified. In other regions of the graph in Figure 4, an increase in the mesopore volume is apparent, as occurs in Figures 1a and 1c.

All the samples were characterized by nitrogen adsorption in order to evaluate the microporosity developed in each case, besides the possible influence of methanol on this type of porosity. However, the microporosity of all the carbon xerogels remained more or less unchanged. Thus, all the samples in Table 1 present a similar BET surface area of ca. 600 m^2/g, and a mean micropore size of ca. 0.9 nm. It can be inferred from this that the presence of methanol influences the size of the clusters and, in turn the meso-macroporosity of the carbon xerogels, though not the micropores that form inside the clusters.

The reason for the influence of methanol content on the final size of the clusters formed is related to the role that methanol plays in the stabilization of formaldehyde solutions. The oxygen in the carbonyl group from formaldehyde is protonated under acidic conditions, which leads to the formation of hemiacetal. However, a sufficient amount of methanol allows the reaction to form acetals, which are more stable compounds [28]. Therefore, an increase in the concentration of methanol results in the formation of more hemiacetals, leaving less formaldehyde available to participate in the sol-gel reaction. This result is somewhat similar to the effect produced by the decrease in the R/F ratio in the formulation of carbon xerogels that leads to the formation of smaller clusters.

Polymeric structures with small clusters give rise to small voids between clusters and hence to samples with smaller pores and a lower pore volume.

The drying step during the synthesis of organic xerogels aims the elimination of the excess solvent used as the polymerization media. Its effect on the porosity is due to the surface tensions occurring during solvent elimination and the consequent shrinkage of the structure. This surface tension depends on the kind of porosity present and on the type of solvent used during the synthesis. Carbonization process aims to remove volatiles and labile/residual components making the material thermally stable. The designed meso-macroporous structure of the xerogels during the synthesis process remains unchanged, only microporosity markedly increases due to the removal of volatile matter that generates new micropores. Thus, S_{BET} value is around 200-300 m^2 g^{-1} for the organic xerogels compared to about 600 m^2 g^{-1} after the carbonization process.

Regarding the influence of methanol content in the formaldehyde solutions on shrinkage and yields during drying and carbonization steps, results show that these depend on the kind of organic xerogel treated. The higher the methanol content the higher the shrinkage during drying (i.e. ca. 10 and 40 % of shrinkage when formaldehyde solutions with 0.6 % and 12.5 % are used, respectively). This could be due to the fact that more formaldehyde is inhibited in the presence of methanol and the structure created are less crosslinked and therefore less mechanically resistant. In the carbonization step some further shrinkage can occur due to the release of volatiles, however this is similar in all cases (ca. 50 %). Concerning the yields obtained during the synthesis and carbonization processes, the results obtained shows that the variations are not very relevant (i.e. all yields between 40-50 wt %) and they are dependent on the composition of the precursor solution. The higher the R/F ratio the lower the yield obtained in the synthesis due to the lower amount of F available. In the same way, for the same R/F ratio used, the higher the methanol content in the formaldehyde solution the lower the yield obtained due to the formation of more hemiacetals inhibiting the polymerization reactions. Finally the carbonization

process leads also slightly lower yields when methanol is included in the initial formulation, maybe because the non-reacted molecules are lost during the thermal process. Finally, it is worth to mention that methanol content has more influence on shrinkage and porosity of the final materials than on carbon yield.

4. CONCLUSIONS

In this study it has been demonstrated that the concentration of methanol present in commercial formaldehyde solutions has a significant influence on the porosity of RF carbon xerogels synthesized in a microwave oven. Provided that the rest of the variables used in the synthesis process are kept constant, carbon xerogels synthesized with a lower concentration of methanol show a higher total pore volume and pore size and, as a consequence, a lower density and a higher porosity. This effect occurs to different degrees depending on the other variables used in the synthesis process. In some cases, the type of porosity changes dramatically and samples obtained by the same recipe may present meso or macroporosity depending on the concentration of methanol in the commercial formaldehyde solution. On the other hand microporosity does not seem to be influenced by the presence of methanol. In short, the concentration of methanol can be considered a highly useful novel chemical variable for tailoring the porosity of carbon xerogels for specific applications.

5. ACKNOWLEDGEMENTS

6. REFERENCES

1.   Pekala, R., Organic aerogels from the polycondensation of resorcinol with formaldehyde. Journal of Materials Science, 1989. 24(9): p. 3221-3227.

2.   Job, N., et al., Synthesis optimization of organic xerogels produced from convective air-drying of resorcinol–formaldehyde gels. Journal of Non-Crystalline Solids, 2006. 352(1): p. 24-34.

3.   Aguado-Serrano, J., et al., Surface and catalytic properties of acid metal–carbons prepared by the sol–gel method. Applied Surface Science, 2006. 252(17): p. 6075-6079.

4.   Gun'ko, V.M., et al., Synthesis and characterization of resorcinol–formaldehyde resin chars doped by zinc oxide. Applied Surface Science, 2014. 303(0): p. 263-271.

5.   Léonard, A., et al., Evolution of mechanical properties and final textural properties of resorcinol–formaldehyde xerogels during ambient air drying. Journal of Non-Crystalline Solids, 2008. 354(10–11): p. 831-838.

6.   Pérez-Caballero, F., et al., Preparation of carbon aerogels from 5-methylresorcinol–formaldehyde gels. Microporous and Mesoporous Materials, 2008. 108(1–3): p. 230-236.

7.   Szczurek, A., et al., The use of tannin to prepare carbon gels. Part II. Carbon cryogels. Carbon, 2011. 49(8): p. 2785-2794.

8.   Szczurek, A., et al., The use of tannin to prepare carbon gels. Part I: Carbon aerogels. Carbon, 2011. 49(8): p. 2773-2784.

9.   Grishechko, L.I., et al., New tannin–lignin aerogels. Industrial Crops and Products, 2013. 41(0): p. 347-355.

10.   Al-Muhtaseb, S.A. and J.A. Ritter, Preparation and properties of resorcinol–formaldehyde organic and carbon gels. Advanced Materials, 2003. 15(2): p. 101-114.

11.   Kraiwattanawong, K., H. Tamon, and P. Praserthdam, Influence of solvent species used in solvent exchange for preparation of mesoporous carbon xerogels from resorcinol and formaldehyde via subcritical drying. Microporous and Mesoporous Materials, 2011. 138(1-3): p. 8-16.

12.   ElKhatat, A.M. and S.A. Al-Muhtaseb, Advances in Tailoring Resorcinol-Formaldehyde Organic and Carbon Gels. Advanced Materials, 2011. 23(26): p. 2887-2903.

13.   Yamamoto, T., et al., Effect of drying method on mesoporosity of resorcinol-formaldehyde drygel and carbon gel. Drying Technology, 2001. 19(7): p. 1319-1333.

14.   Gallegos-Suárez, E., et al., On the micro- and mesoporosity of carbon aerogels and xerogels. The role of the drying conditions during the synthesis processes. Chemical Engineering Journal, 2012. 181–182(0): p. 851-855.

15.   Szczurek, A., et al., Porosity of resorcinol-formaldehyde organic and carbon aerogels exchanged and dried with supercritical organic solvents. Materials Chemistry and Physics, 2011. 129(3): p. 1221-1232.

16.   Liang, C., G. Sha, and S. Guo, Resorcinol–formaldehyde aerogels prepared by supercritical acetone drying. Journal of Non-Crystalline Solids, 2000. 271(1–2): p. 167-170.

17.   Calvo, E.G., et al., Microwave synthesis of micro-mesoporous activated carbon xerogels for high performance supercapacitors. Microporous and Mesoporous Materials, 2013. 168: p. 206-212.

18.   Calvo, E.G., et al., Fast microwave-assisted synthesis of tailored mesoporous carbon xerogels. Journal of Colloid and Interface Science, 2011. 357(2): p. 541-547.

19.   Rey-Raap, N., J.A. Menéndez, and A. Arenillas, Optimization of the process variables in the microwave-induced synthesis of carbon xerogels. Journal of Sol-Gel Science and Technology, 2014. 69(3): p. 488-497.

20.   Tonanon, N., et al., Preparation of resorcinol formaldehyde (RF) carbon gels: Use of ultrasonic irradiation followed by microwave drying. Journal of Non-Crystalline Solids, 2006. 352(52–54): p. 5683-5686.

21.   Menéndez, J.A., et al., A microwave-based method for the synthesis of carbon xerogel spheres. Carbon, 2012. 50(10): p. 3555-3560.

22.   Menéndez, J.A., et al., Microwave heating processes involving carbon materials. Fuel Processing Technology, 2010. 91(1): p. 1-8.

23.   Rey-Raap, N., J. Angel Menéndez, and A. Arenillas, RF xerogels with tailored porosity over the entire nanoscale. Microporous and Mesoporous Materials, 2014. 195: p. 266-275.

24.   Rey-Raap, N., J. Angel Menéndez, and A. Arenillas, Simultaneous adjustment of the main chemical variables to fine-tune the porosity of carbon xerogels. Carbon, 2014. 78: p. 490-499.

25.   Moreno, A.H., et al., Carbonisation of resorcinol-formaldehyde organic xerogels: Effect of temperature, particle size and heating rate on the porosity of carbon xerogels. Journal of Analytical and Applied Pyrolysis, 2013. 100: p. 111-116.

26.   Al-Muhtaseb, S.A. and J.A. Ritter, Preparation and Properties of Resorcinol–Formaldehyde Organic and Carbon Gels. Advanced Materials, 2003. 15(2): p. 101-114.

27.   Carr, C. and J.A. Riddick, Physical properties of methanol-water system. Industrial & Engineering Chemistry, 1951. 43(3): p. 692-696.

28.   Zubizarreta, L., et al., Development of microporous carbon xerogels by controlling synthesis conditions. Journal of Non-Crystalline Solids, 2008. 354(10-11): p. 817-825.

29.   Kiciński, W., M. Szala, and M. Nita, Structurally tailored carbon xerogels produced through a sol-gel process in a water-methanol-inorganic salt solution. Journal of Sol-Gel Science and Technology, 2011. 58(1): p. 102-113.

30.   Durairaj, R.B., Resorcinol: chemistry, technology and applications. 2005: Springer Science & Business Media.

31.   Job, N., et al., Porous carbon xerogels with texture tailored by pH control during sol–gel process. Carbon, 2004. 42(3): p. 619-628.

PUBLICACIÓN II

AN UNDERRATED VARIABLE ESSENTIAL FOR TAILORING THE STRUCTURE OF XEROGEL: THE METHANOL CONTENT OF COMMERCIAL FORMALDEHYDE SOLUTIONS

Isabel .D. Alonso-Buenaposada, Leoncio Garrido, Miguel A. Montes-Morán, J. Angel Menéndez, Ana Arenillas, *Enviada*.

mCAT

Enviada

INCAR CSIC

An underrated variable essential for tailoring the structure of xerogel: the methanol content of commercial formaldehyde solutions

Isabel D. Alonso-Buenaposada[1], Leoncio Garrido[2], Miguel A. Montes-Morán[1], J. Angel Menéndez[1], Ana Arenillas[1]*

[1]Instituto Nacional del Carbón, CSIC, Apartado 73, 33080 Oviedo, Spain
[2]Departamento de Química Física, Instituto de Ciencia y Tecnología de Polímeros, ICTP-CSIC, Juan de la Cierva 3, 28006 Madrid, Spain

ABSTRACT

Resorcinol-formaldehyde xerogels are polymers whose porosity can be designed for a specific application by the selection of appropriate physical and chemical synthesis variables. Until recently, the methanol content of commercial formaldehyde solutions has never been considered as a chemical variable that must also be taken into account. However, it has been demonstrated that the proportion of methanol might be even more important than other variables for tailoring the porosity of xerogels. Different reaction mechanisms are proposed to explain this heavy dependence of the final structure of RF xerogels. Organic and carbon xerogels synthesized with low concentrations of methanol showed a higher porosity with much larger pore sizes (up to two orders of magnitude) than when using formaldehyde with high concentrations of methanol. This means that extra caution needs to be shown in choosing these commercial products since formaldehyde solutions differ greatly in methanol content from one supplier to another.

Keywords: xerogel, formaldehyde, methanol, controlled porosity.

1. INTRODUCTION

Porous carbon and organic gels synthesized by means of Pekala´s method [1], with resorcinol and formaldehyde as precursors, and water as solvent [2-5], have been the most common type of gels studied until now in preference to other precursors and reaction media [6-11].

Microwave radiation is the most common method used to synthesize this type of material since it is a highly competitive process that requires only 3 h instead of the 5 days needed for conventional heating. Furthermore, the entire process, from gelation and ageing to the final drying step, is carried out in the same device (referred to as one-pot synthesis), reducing the amount of energy needed and, therefore, making the process much more cost-effective.

However, the main attraction of these materials resides in their great versatility. Xerogels are considered materials with a high added value due to the fact that their porosity can be controlled and designed for a specific application by selecting appropriate values for the synthesis variables, whether physical (e.g. temperature, time of synthesis, etc.) [2, 12] or chemical (e.g. pH, dilution, molar ratio resorcinol/formaldehyde, etc) [13-16]. In addition, all these variables are interdependent and an exhaustive study of all of them together requires the use of statistical programs [13, 14, 17].

Until recently, the role of the methanol content in commercial formaldehyde solutions as a chemical variable has been underestimated. Every commercial formaldehyde solution contains a certain proportion of methanol to prevent the formaldehyde from polymerizing and precipitating, and to keep its concentration constant. It has been demonstrated [17] that the proportion of methanol is even more important than other variables for controlling porosity. As formaldehyde solutions differ greatly in methanol content from one supplier to another, this factor must be paid due attention. However, more deeply characterization of the samples obtained only varying the composition of the formaldehyde solution is needed in order to postulate a mechanism and a chemical explanation of what it is occurring.

In this work two different organic and carbon xerogels were synthesized under the same synthesis conditions using formaldehyde solutions with different proportions of methanol. A series of chemical, structural and morphological analyses of the samples obtained were carried out in order to clarify the role of the methanol content. On the basis of the results obtained, a reaction mechanism and chemical explanation for the influence of this chemical variable is proposed.

2. EXPERIMENTAL

2.1. Synthesis of carbon xerogels

Xerogels were synthesized by the polymerization of resorcinol (R) and formaldehyde (F) with water as the reaction media using a solution of NaOH to adjust the pH to the desired value. The variables selected for this study were: a pH of 5, a dilution ratio of 8 (dilution ratio is defined as the molar ratio between the total solvent and reactants. Total solvent refers to the water and methanol contained in the formaldehyde solution and the deionized water that is added and reactants refers to the resorcinol and formaldehyde), and a R/F molar ratio of 0.7.

In order to prepare the organic xerogels, resorcinol (Indspec, 99.6 wt. %) was dissolved in deionized water in an unsealed glass beaker under magnetic stirring. As the formaldehyde solution used (Química S.A.U., 37 wt. % formaldehyde, 0.7 wt. % methanol, 62.3 wt. % water) contains 0.7 wt. % methanol, one of the gels was prepared using this solution directly. The other gel, was prepared by adding methanol (AnalaR Normapur, 99.9 %) to the former formaldehyde solution until a 12.5 wt. % methanol content was obtained. In both cases the formaldehyde solution was then added to the rest of the precursor mixture. It is worth noting that pure methanol was added to the above formaldehyde solution, instead of using other commercial formaldehyde, in order to use exactly the same reagents for the synthesis of the samples studied.

Therefore other factors such as impurities, pH, etc. may be avoided. In order to obtain a pH of 5 in the precursor mixture, 5 M and 1 M solutions were prepared from solid NaOH (AnalaR Normapur, 99.9 %) and added until the desired pH.

Each precursor solution was kept in an in-lab modified multimode microwave oven at 85 ºC for the entire synthesis process (polymerization and curing steps) i.e., ca. 3 hours. The microwave cavity and the operating conditions used are described in detail elsewhere [13, 14, 18]. The polymer was then dried in the same device, by microwave heating, without any pretreatment or intermediate step until a mass loss of over 50 wt. % was reached, giving rise to the final organic xerogel. The xerogel was then carbonized in a tubular reactor (Carbolite MTF 12/38/400) for 2 h at 700 ºC under a N_2 flow (150 mL min^{-1}) to obtain the carbon gel product. Samples, either organic and carbon xerogels were obtained in duplicate to ensure reproducibility.

In this study, the samples labelled OX refer to the organic xerogels, CX samples to the carbon xerogels and 0.7 or 12.5 to the percentage of methanol contained in the formaldehyde solution used in each case.

2.2.   Sample characterization

2.2.1. Porosity

Before characterization, the xerogels were outgassed (Micromeritics VAcPrep 0.61) at 0.1 mbar and 120 ºC overnight in order to remove all humidity and other physisorbed gases.

The porosity of the samples studied was characterized by means of mercury porosimetry on an AutoPore IV 9500 (Micromeritics) device, which is able to measure from atmospheric pressure up to 228 MPa. To characterize mesoporosity the lowest limit of the apparatus considered was 5.5 nm. Likewise, Vmacro refers to porosity ranging from 50 to 10000 nm. The surface tension and contact angle were 485 mN m^{-1} and 130 º, respectively, while the stem

volume was between 45-58 % in all the analyses performed. Initially, in the low pressure step, the samples were evacuated at 6.7 Pa and the equilibration time chosen was 10 seconds. Subsequently, the pressure was gradually increased to its maximum value, after which the mercury intrusion was evaluated. This characterization yielded data about pore size distribution, pore volume and bulk density.

2.2.2. Microscopy

Micrographs of the carbon xerogels were obtained on a Zeiss DSM 942 scanning electron microscope (SEM). For this characterization the samples were previously dried overnight and then attached to an aluminum tap using a conductive double-sided adhesive tape. A voltage of 25 kV and a secondary electron detector EDT Everhart-Thornley, were used in all the analyses.

Transmission electron microscopy (TEM) was carried out on a Jeol 2000 at 180 kV. A very dilute ethanolic suspension was prepared and then deposited on a 200 mesh copper grid with carbon membrane.

2.2.3. X-ray photoelectron spectroscopy (XPS)

The X-ray photoelectron spectra (XPS) of the carbonised xerogels (CX samples) were carried out in a SPECS Phoibos 100 analyser using MgKα X-rays (1254.6 eV) at a power of 100 W and in a residual vacuum of 10^{-7} Pa. Analyser pass energy of 50 eV has been used to collect broad scan spectra (0–1100 eV). The atomic percentages (atom %) of the different elements present in the approx. 10 nm upper layer probed by XPS were calculated from the survey spectra by considering the integrated areas of the main XPS peaks. High resolution spectra of C (1s) were performed using a pass energy of 10 eV. C1s peaks were deconvoluted fitting Gaussian-Lorentzian functions by means of Marquardt algorithm by using proprietary software. The number of peaks considered in the fitting procedure was, on one hand, sufficient to attain a sound fitting [19], and on the other, to account for the different contributions with

physical meaning. The assignment of such contribution was done following previous studies in carbon materials [20-21]. Samples were dried overnight before characterization.

2.2.4. Nuclear Magnetic Resonance (NMR)

The samples were analyzed directly after synthesis and also after being dried overnight under vacuum at room temperature by ^{1}H and ^{13}C solid state NMR spectroscopy and ^{1}H NMR imaging (MRI).

The ^{1}H and ^{13}C NMR measurements were performed on a Bruker Avance 400 spectrometer (Bruker BioSpin, Rheinstetten, Germany) equipped with a 89 mm wide bore, 9.4 T superconducting magnet (at ^{1}H and [13]C Larmor frequencies of 400.14 and 100.61 MHz, respectively). All the reported data were obtained at room temperature. Powdered samples were placed in 4 mm zirconia rotors and a standard Bruker double resonance 4 mm cross-polarization (CP)/magic angle spinning (MAS) NMR probe head was used. The ^{1}H MAS spectra were recorded using single pulse excitation and the ^{13}C CP/MAS spectra were obtained by applying a 3 ms CP contact time and sideband suppression (seltics). The recycle delays in the ^{1}H and ^{13}C experiments were 5 and 3 s, respectively. The MAS spinning rates varied between 5.0 and 7.0 kHz. ^{13}C NMR spectra were obtained by high-power proton decoupling at 75 kHz. In all cases, the NMR spectra were evaluated using the manufacture's Top-Spin™ spectrometer software package. All the free-induction decays were subjected to the standard Fourier transformation procedure with line broadening ([13]C: 50-100 Hz; [1]H: 20 Hz) and phasing. The chemical shifts were externally referenced to adamantane ([13]C δ: 29.5 ppm; [1]H δ: 1.63 ppm) secondary to tetramethylsilane (^{13}C and [1]H δ: 0.0 ppm).

The proton NMR imaging measurements were performed on the spectrometer described above fitted with a microimaging accessory. The maximum possible amplitude available for the magnetic field gradients was 97.3 G cm^{-1}. Cylindrical monoliths of each sample cut into pieces of about 10 mm in

length were prepared and analyzed by ^{1}H MRI after being dried overnight under vacuum at room temperature (Figure 1). Glass tubes with an outer diameter of 20 mm and a height of 8 cm were employed as sample holders. The cylindrical samples were fully impregnated with cyclohexane under vacuum, and loaded into an NMR probe fitted with a radiofrequency coil insert of diameter 25 mm. All measurements were performed at 25 ± 0.2 ºC.
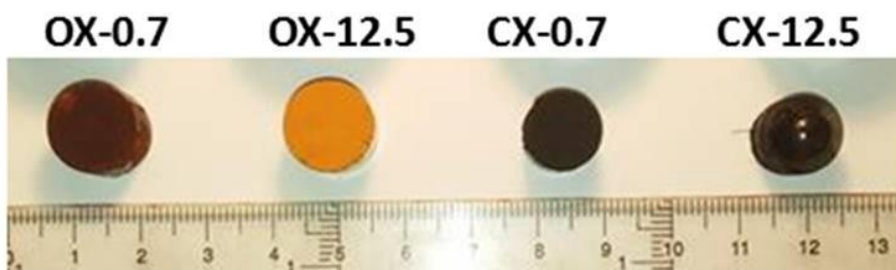
Figure 1. *Samples of the xerogels prepared for the MRI study.*

Scout images were recorded using a two-dimensional multislice gradient-echo pulse sequence with an echo time (TE) of 1.86 ms and a repetition time (TR) of 300 ms. The images were obtained in three orthogonal planes, 1 mm thick, with a field of view (FOV) of 25 x 25 mm^2 and an isotropic resolution of 128 x 128 pixels. To characterize the morphological features of the xerogels, fully relaxed (TR > 5 x T1) multislice/multispin-echo images at echo times between 5 and 40 ms were recorded. Eight transaxial images with a slice thickness of 0.5 mm, a gap between slices of 0.4 mm, and an in-plane isotropic resolution of 78 x 78 µm^2 were obtained. T1 measurements were performed using an inversion-recovery pulse sequence. The images were processed using ImageJ software (National Institute of Health, Bethesda, US).

2.2.5. Fourier Transform Infrared Spectroscopy

The chemical surface characterization of the powdered samples was carried out by Fourier Transform Infrared Spectroscopy (FTIR). Samples were dried overnight before characterization. The spectra were recorded in the 525

and 4000 cm^{-1} range on a Nicolet IR 8700 spectrometer fitted with a DTGS detector (deuterated triglycine sulphate) at a 4 cm^{-1} resolution in 64 accumulated scans. The samples were analyzed twice. In order to prepare the tablets, the samples and KBr (previously dried overnight) were mixed in a proportion of 1:100 in an agate mortar for 10 minutes until a homogeneous mixture was obtained. Around 0.125 g of this mixture was subjected to 8 tons of pressure in a 13 mm diameter matrix.

3. RESULTS AND DISCUSSION

Two samples synthesized under the same conditions, except for the methanol content in the formaldehyde solution (i.e., 0.7 and 12.5), were studied by means of different techniques. The pore size distribution of each sample, both before and after carbonization: OX and CX respectively, is shown in Figure 2. It can be seen that a decrease in the methanol content of the formaldehyde solution causes an increase in the pore diameter of up to two orders of magnitude. Moreover, an increase in the methanol content produces an increase in the bulk density of the material from 0.34 to 0.41 g/cm^3 for OX-0.7 and OX-12.5, respectively (Table 1), leading to radically different material. These variations may result from a change of supplier or if a different batch of formaldehyde from the same supplier is used. The differences in methanol content are of crucial importance since the main advantage of organic and carbon gels are that they allow porosities to be tailored for specific applications.

Table 1. *Textural properties of the samples obtained by mercury porosimetry.*

Sample	Pore volume (cm^3 g^{-1})	Bulk density (g cm^3)	% Porosity
OX-0.7	2.02	0.34	69
OX-12.5	1.61	0.41	66
CX-0.7	2.13	0.32	69
CX-12.5	1.53	0.43	65
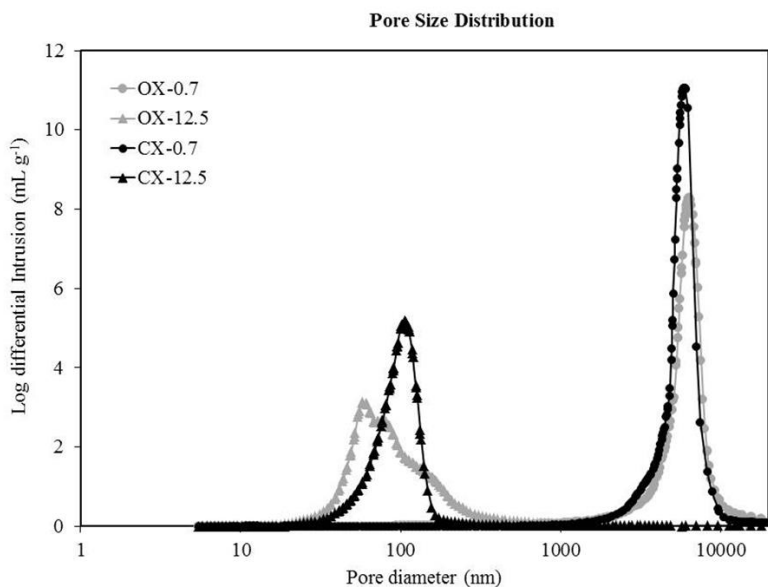
Figure 2. *Pore size distribution obtained by mercury porosimetry for the samples studied.*

To investigate possible differences in the chemical structure of xerogels, solid state NMR spectroscopy and FTIR measurements were carried out. Figure 3a shows the ^{13}C CP/MAS NMR spectra corresponding to samples OX-0.7 and OX-12.5. The spectra are not significantly different and show 5 main resonances centered at 151.7; 132.4; 120.5; 103.7, and 28.3 ppm. The 151.7 peak corresponds to phenolic carbons from the substituted resorcinol. Due to the fact that aromatic rings can be substituted by one, two or three bridges with respect to the adjacent rings, this gives rise to asymmetric resonances. The peak at 132.4 corresponds to carbons in meta position with respect to both phenols, whereas the peak at 120.5 ppm corresponds to mono and bi-substituted aromatic carbons in ortho position relative to the phenol group. The peak at 103.7 ppm corresponds to the carbons between the phenolic OH and the wide peak at 28.3 is assigned to different CH_2 bridges [22].
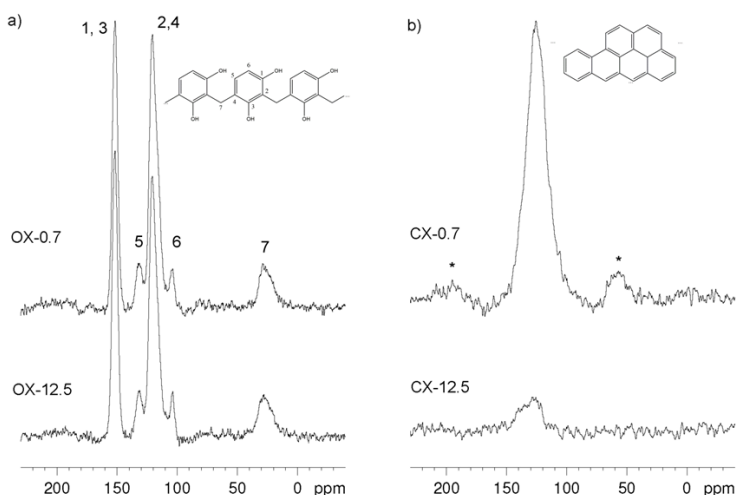
Figure 3. ^{13}C *CP/MAS NMR spectra with proton decoupling and sideband suppression corresponding to the samples studied: a) organic xerogels and b) carbon xerogels. Asterisks indicate residual spinning side bands and the structures assigned to the peaks appear in the inset.*

The ^{13}C CP/MAS NMR spectra of samples CX-0.7 and CX-12.5 are shown in Figure 3b. In this case, there is only one peak centered at ca. 127 ppm that can be assigned to C-C sp^2 bonds (the other peaks in the top trace are spinning sidebands that have not been completely suppressed). As CP/MAS experiments favor the detection of carbons with nearby protons, a comparison of the spectra of samples OX and CX, suggests that the CX samples have a lower proton density than the OX ones, especially, sample CX-12.5 (which has lower signal intensity than the rest). It should also be pointed out that the spectra of the OX samples are the result of averaging 1,000 scans, while those of CX represent an average of 10,000 scans.

Figure 4 shows the ^1H MAS spectra of the organic samples (OX) analyzed before and after drying. The spectra in Figure 4a correspond to sample OX-0.7. A narrow peak at 4.62 ppm only appears in the sample prior to drying (top trace), and the broad peak at 3.94 ppm shifts to 3.49 after drying (bottom trace). Likewise, Figure 4b illustrates the spectra corresponding to sample OX-12.5. In this case, only one peak at 4.06 ppm is visible before

drying. After drying, there is only one broad peak at 3.87 ppm is observed. In both cases, the narrow linewidth of the peaks observed in the xerogels before drying suggests that they are associated to protonated species with a high mobility. The broad peaks observed in the dried samples (bottom traces in Figure 4) could be associated to protons with a low mobility (protons bound to the polymer network). The carbonized samples were also characterized. However, the differences between the pristine and dried samples are very small, reflecting the weak hydrophilic character of the CX samples due to the absence of surface groups (Figures S1 and S2 in the supplementary material).
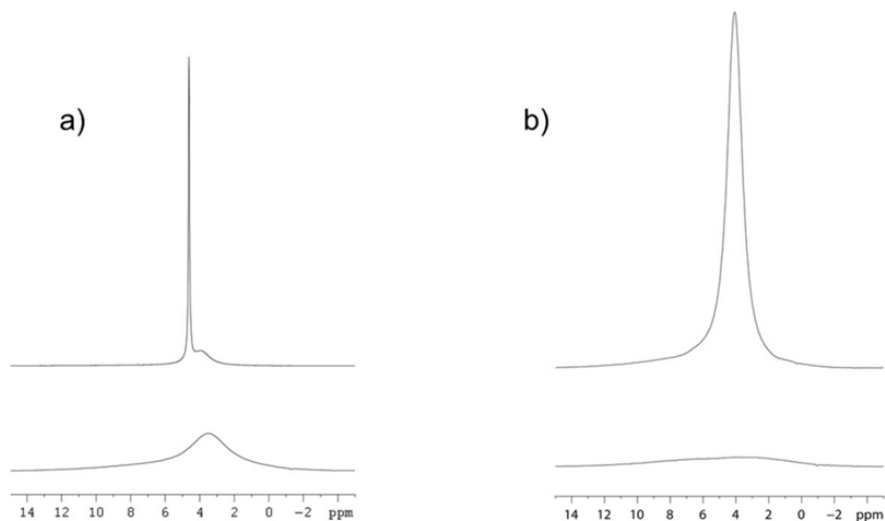
Figure 4. ^{1}H MAS NMR spectra corresponding to a) OX-0.7 and b) OX-12.5 samples, before (top trace) and after (bottom trace) drying.
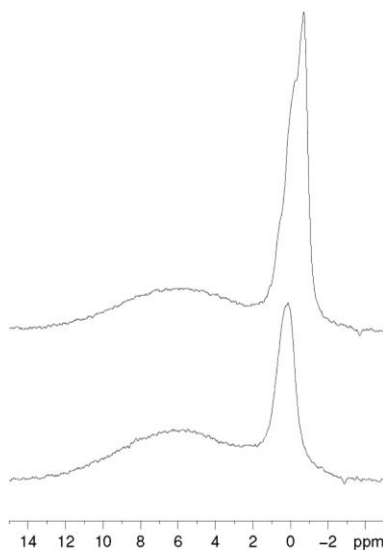
Figure S1. [1]H MAS spectra corresponding to sample CX-0.7 before (top trace) and after (bottom trace) drying. The spectra were acquired with the same conditions and are plotted with the same vertical scale. A broad peak centered at about 6 ppm is observed in both spectra. The narrow peak shows changes after drying, the peak at 0.13 ppm is observed in the two spectra, while the peak at -0.71 ppm is only visible in the untreated sample.
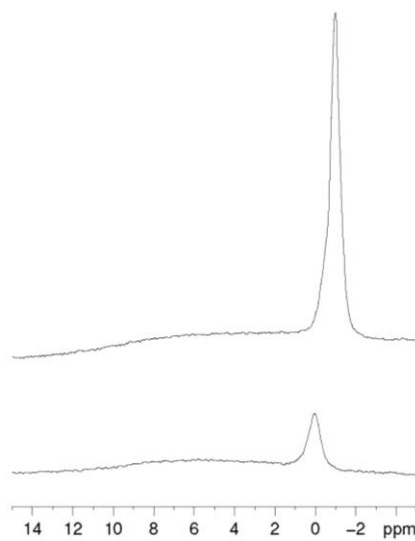
**Figure S2.** [1]H MAS spectra corresponding to sample CX-12.5 before (top trace) and after (bottom trace) drying. The spectra were acquired with the same conditions and are plotted with the same vertical scale. A broad peak centered at about 5.5 ppm is observed in both spectra. The intensity of the narrow peak decreases after drying, and shifts from -0.99 to 0.02 ppm.

The FTIR spectra of the OX xerogels are presented in Figure 5. Both spectra exhibit a broad band between 3700 and 3000 cm^{-1} associated with O-H stretching vibrations, due to phenol groups with a high concentration of hydroxyl groups on their surfaces, providing these materials with a high hydrophilicity. The band at 2931 cm^{-1} can be assigned to aliphatic stretching vibrations (CH_2). The band located at 1474 cm^{-1} corresponds to CH_2 deformation vibrations and the one at 1613 cm^{-1} to the aromatic ring stretching vibration (C=C). Stretching vibration bands at 1217 and 1092 cm^{-1} indicate the presence of methylene ether bridges C-O-C) [23, 24]. It should also be noted that, in the case of NMR, FTIR revealed identical bands in both organic samples, indicating similar chemical compositions. Elemental chemical analysis also (Table 2) corroborated the similar compositions of the OX samples. The carbonized samples (CX) were also analyzed, and again their chemical composition seems to be independent of the amount of methanol used (Table 2). The CX samples have a carbon content of ca. 95 wt %. The FTIR spectra of the CX samples reveal a poor surface chemistry, a feature typical of a carbonized material (see Figure S3). It is also worth noting that in no case do these xerogels (OX and CX samples) show signs of impurity content.
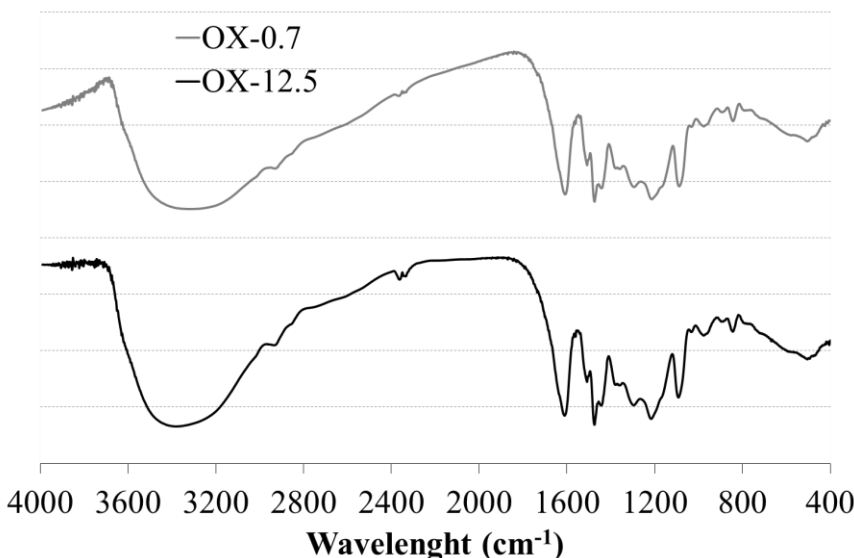
Figure 5. *Chemical characterization of the organic samples from FTIR spectra.*

Table 2. Elemental analysis results for the organic and carbon xerogels (dry basis).

	OX-0.7	OX-12.5	CX-0.7	CX-12.5
C (±0.2, wt. %)	62.5	63.2	93.7	93.4
H (±0.2, wt. %)	5.0	4.8	1.8	1.7
N (±0.2, wt. %)	0.3	0.3	0.5	0.6
O (±0.2, wt. %)	32.2	31.7	4.0	4.3
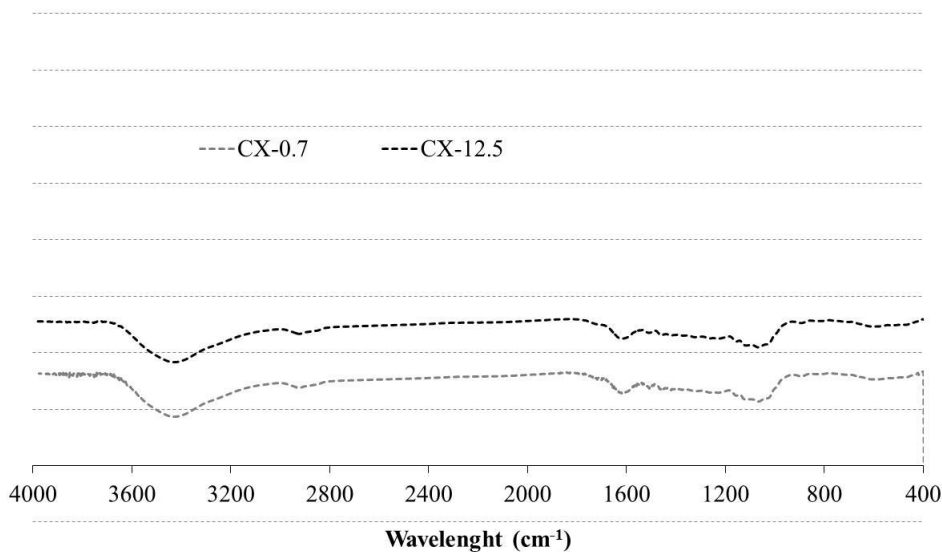
Figure S3. FTIR spectra for the carbonized samples CX-0.7 and CX-12.5 (note, it was used the same scale as Figure 5 for comparison proposes).

It is clear from Figure 4 that all of these organic materials are sensitive to air humidity since water is easily absorbed by their surfaces. Furthermore, Figure 5 shows a high hydroxyl group content on the surface of these organic materials which endows them with a high hydrophilicity. What is more, their porosity provides them with a good water storage capacity, giving rise to a material with outstanding desiccant properties [25]. The FTIR spectra of the CX

samples (data not shown) were characteristic of high temperature carbon materials, i.e., there being no bands detected.

As differences in porosity are a result of different reaction mechanisms, and possibly different functional groups in the chemical structure, XPS was also performed as being a more sensitive technique for the characterization of the surface chemistry of the materials. It should be noted that the OX samples could not be characterized by this technique, due to their high volatiles content (i.e. 50 wt %) which may cause damage to the XPS equipment.

XPS analyses of the CX carbons brought about a similar atomic composition, namely 89.5 % of C and 10.5 % of O. As expected, a higher concentration of oxygen is thus present on the outermost layers of the carbon materials when compared to the bulk, as probed by the elemental analysis shown in Table 2. This higher surface oxygen content helps to depict some differences between the two CX materials, hence on the possible influence of the methanol content on the final properties of the materials. The deconvolution process of the high resolution C1s profiles is shown in Figure 6. Four different peaks were considered for the fitting of the original signals (cross symbols). The main peak corresponding to C (sp^2) was located at 284.5 eV (B.E.). C-OR (R including H) moieties are known to give a peak displaced by approx. 1.5-2 eV of the C (sp^2) band. Two additional peaks could be present at +3.5 and +4.5 eV of the main band, normally assigned to R-C=O and O=C-OR (R including H) species, respectively. The convolved profile of all these components is also included in Figure 6 (continuous line) to indicate the soundness of the fitting procedure. The relative areas of the different components are collected in Table 3.
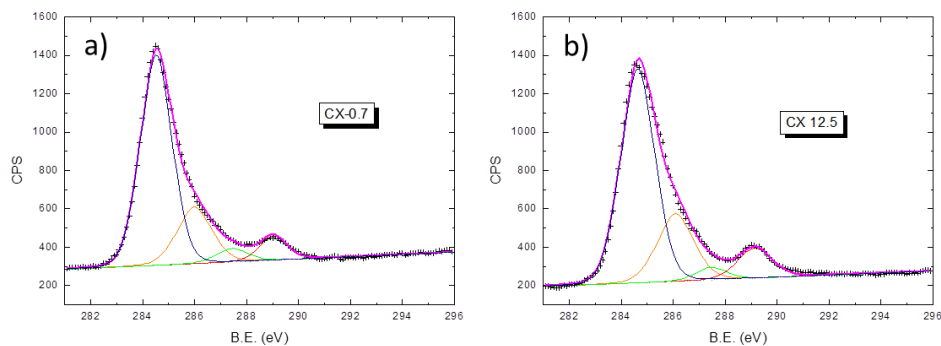
Figure 6. *C1s high resolution XPS spectra of CX-0.7 (a) and CX-12.5 (b).*

Table 3. *Analysis of the C1s high resolution XPS of the carbonised gels.*

Sample	Relative contribution of the fitting peaks (%)			
	C=C	C-OR	RC=O	O=C-OR
CX-0.7	68.2	20.4	4.4	7.0
CX-12.5	64.9	22.2	3.5	9.4

It was notice that both samples (CX-12.5 and CX-0.7) present a very similar chemistry. The most relevant difference between them is the relative contribution of O=C-OR functionalities, with a higher presence in the sample CX-12.5. These would suggest that this carbon material, prepared using the formaldehyde solution containing a higher content of MeOH, leads to the formation of a slightly higher number of ester bonds which are most likely related to high levels of crosslinking between the nodules. This would agree with a more condensed structure, leading narrow pores as it is observed in the porosity characterization mentioned above, besides the SEM and TEM observations that would be discussed later.

Figure 7 shows structural differences between the carbonized samples. These differences arise from the polymerization process, and so are also

observed in the OX samples. However the RF xerogels (i.e. OX samples) provide photographs of a much lower quality as they contain nearly 50 wt % volatiles and are not good conductor materials. Consequently, only photographs of CX are shown in this study. The SEM photographs reveal significant differences between their internal structures since, on the same scale, large well-defined clusters are recorded for CX-0.7 whereas only small nodules are observed in the case of CX-12.5. TEM also reveals very different patterns, as it is difficult for electrons to penetrate through the sample in the analysis of CX-0.7 due to the large size and thickness of the nodules. Nevertheless this technique is suitable for the characterization of CX-12.5 as its nodules are thinner and homogeneous throughout the sample and therefore, electrons are able to pass through the sample. All of the techniques applied show clearly that these two samples have totally different structures.
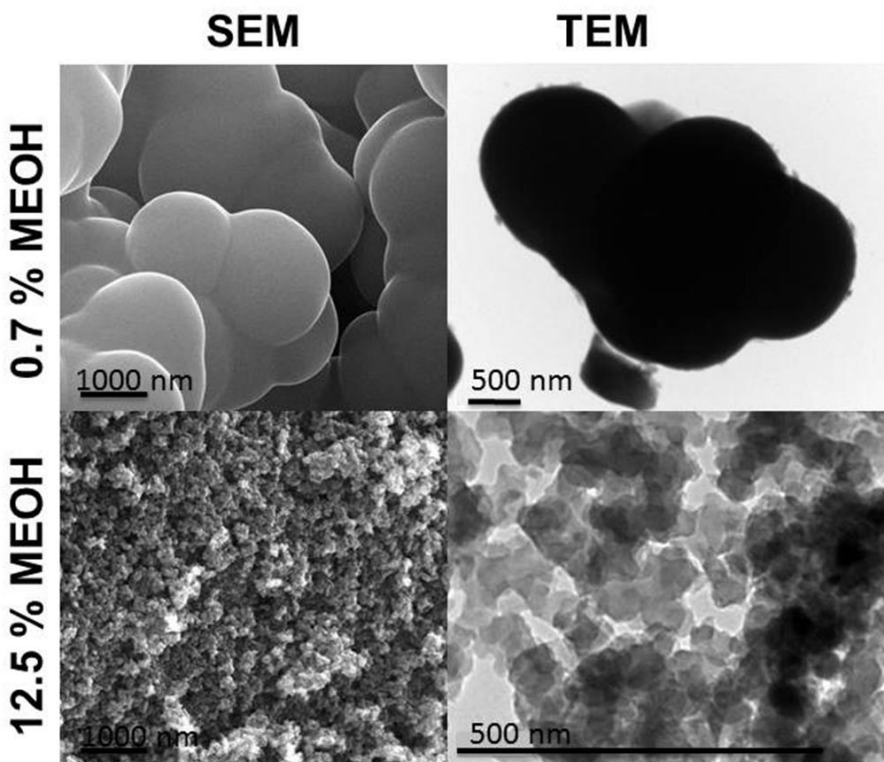

Figure 7. Microphotograhs of the carbon xerogels obtained from SEM and TEM characterization.

Magnetic resonance imaging (MRI) methods allow the non-destructive evaluation of a specimen, providing contrasting images based on its chemical, structural and morphological characteristics [26-28]. Moreover, longitudinal studies and a direct comparison between the results obtained by means of MRI and other techniques applied to the same set of samples are also possible.

In this work, the proton MRI study of carbon xerogels impregnated with a fluid (cyclohexane) provides valuable information about their morphological characteristics and could contribute to a better understanding of the effect of the initial concentration of methanol on the synthesis of carbon xerogels. Although MRI is not a very sensitive technique and the degree of spatial resolution does not allow a satisfactory discrimination between submicron structures, it nevertheless enables the open porosity (the porosity in the sample connected to the outside) and, therefore, its regional variations at a macroscopic scale to be mapped [29-31]. Figure 8 shows four representative transaxial proton images corresponding to the four types of synthesized xerogels vacuum impregnated with cyclohexane. In these images, the sample is at the centre, surrounded by cyclohexane. The values of image signal intensity reflected in the different shades of grey are proportional to the amount of cyclohexane protons at each location. Thus, the contrasting shades of each image represent regional variations in the amount of cyclohexane and, in turn, in the open porosity of the sample. The bright rim around the samples corresponds to 100 % cyclohexane. It can be seen that the images corresponding to the xerogels prepared with an initially lower content of methanol (0.7 % w/w) have a courser appearance than those prepared with higher methanol content (12.5 % w/w). This is in agreement with the electron microscopy observations (TEM and SEM) described previously, and with the data in Table 1, since an increase in the methanol content indicates an increase in density, which naturally entails a decrease in porosity.
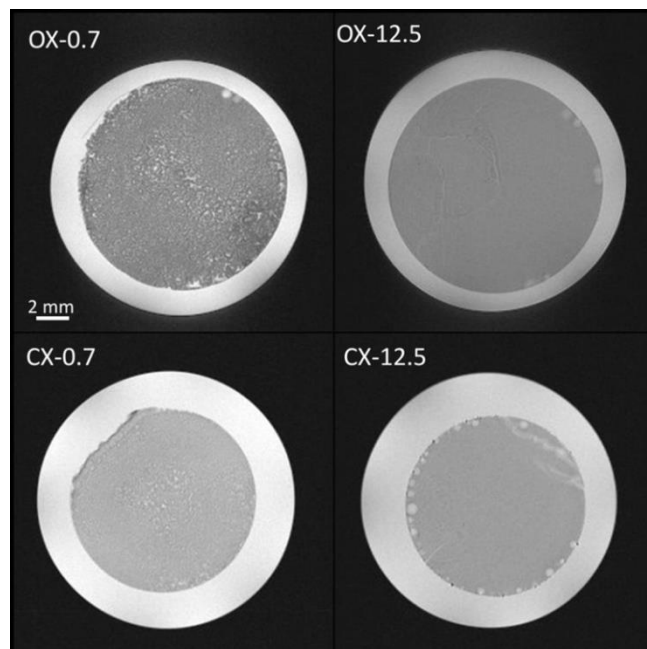
Figure 8. *Proton MRI of xerogels vacuum impregnated with cyclohexane. Images acquired with an echo time of 5 ms and a repetition rate of 6 s. The images represent transaxial cross-sections of the cylindrical xerogel samples.*

Different reaction mechanisms are proposed based on a detailed chemical and structural analysis. First, however, it should be mentioned that methanol is added to the formaldehyde solutions in order to prevent the formaldehyde from polymerizing itself and subsequent precipitation. As illustrated in Figure 9, the reaction of methanol with formaldehyde is favored in acidic media, giving rise to mainly hemiacetals (Figure 9a) and to acetals (Figure 9b) if the reaction continues any length of time. The reaction between resorcinol and formaldehyde only takes places if the formaldehyde remains in its free form or in other words, when it is not in a hemiacetal or acetal form. An increase in the methanol content leads to an increase in the hemiacetal form, preventing the resorcinol molecules from finding free formaldehyde molecules to react with (Figure 9b).
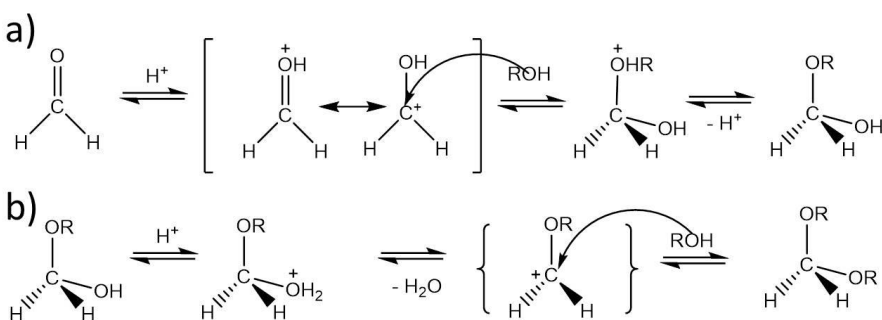
Figure 9. *Reaction mechanisms proposed for the stabilization of formaldehyde by the addition of methanol and the formation of hemiacetals (a) and acetals (b).*

Furthermore, the greater the amount of free formaldehyde available, the smaller the number of interconnections formed between large-size nodules, as is corroborated by Figures 5-6. On the other hand, the smaller the concentration of free formaldehyde, the larger the number of interconnections formed between the small size nodules. It can also be said that, a similar pattern is observed when there is a reduction in the R/F molar ratio [14]. The lower the R/F ratio is, the higher the proportion of methanol present since more formaldehyde is consumed in the reaction media which will lead to the effects of the methanol being more prominent.

It is well known that all chemical variables involved in carbon xerogel synthesis are interdependent. However, although the effect of methanol is always apparent, the extent of the effect depends on the other variables. For example, the start of the reaction is favored when the pH of the initial precursor solution (ca. 3) is increased due to the addition of the basic catalyst. The formation of the resorcinol anions to initiate the addition reaction is favored (see Figure 10). As the kinetics of the reaction increases, small clusters are formed, giving rise to materials with a small pore size. If the kinetics of the reaction is increased, the methanol content is not as important as it would be at a low pH. In this case, crosslinking reactions that counteract the growth of nodules are favored. Consequently the availability of formaldehyde due to methanol content has less influence on the porosity of the material. In short, methanol content has

more effect when the kinetics of the reaction is slow or, in other words, when low amount of catalyst is used.
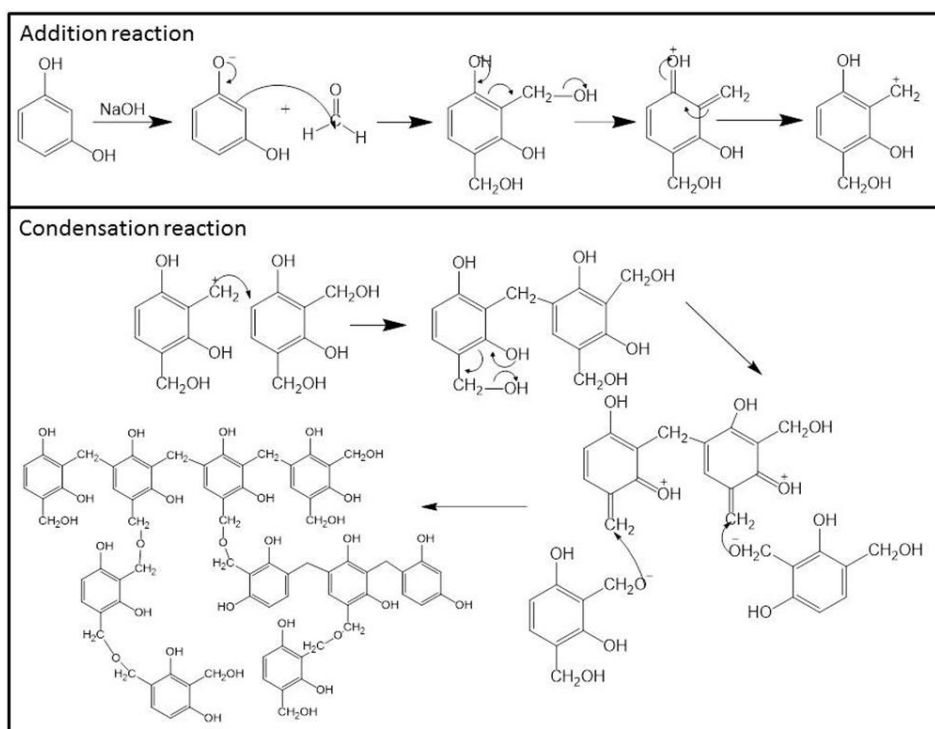
Figure 10. *Polymerization steps of resorcinol and formaldehyde with basic catalyst.*

The effect of the dilution ratio has also been widely studied in the literature. However, there are some differences between authors possibly due to the different synthesis methods or drying methods employed [13, 32, 33]. Under microwave heating, the sol-gel reaction proceeds faster than under conventional heating, leaving the solvent no time to evaporate and so it is retained inside the structure and this may alter the structure somewhat. A lower dilution degree implies a higher proportion of reactants in the solution and, therefore, an increase in the number of smaller size nodules formed. On the other hand, an increase in the dilution ratio will cause the formation of a smaller number of nodules of larger size. Furthermore, a high dilution ratio will lead to a lower degree of crosslinking and materials with poorer mechanical properties. If the

dilution ratio is increased even further, gel will not be able to form since the nodules will be too far apart to crosslink [34].

CONCLUSIONS

The concentration of methanol present in commercial formaldehyde solutions has a significant influence on the porosity of RF xerogels. The bulk chemical composition remains analogous in spite of some differences in the structure and possibly some functional groups. Different reaction mechanisms have been proposed to explain the strong dependence of the final structure of RF xerogels on the presence of methanol. Methanol reacts with formaldehyde, generating hemiacetal molecules which are not able to react with resorcinol. Therefore, the greater the amount of methanol, the smaller the amount of formaldehyde that will be available to participate in reactions, which means that resorcinol molecules will have difficulty finding formaldehyde in its free form to react with. In short, organic and carbon xerogels synthesized with a lower concentration of methanol show a higher level of porosity with larger pore sizes (by up to two orders of magnitude) than when formaldehyde with high concentrations of methanol is used. Consequently, in order to obtain accurate bespoke materials, apart from the already established chemical variables (i.e., pH of the precursor solution, R/F ratio, dilution ratio, etc) it is necessary to take into account the composition of the formaldehyde solution and especially the percentage of methanol.

ACKNOWLEDGEMENTS

REFERENCES

1.   Pekala R (1989) Organic aerogels from the polycondensation of resorcinol with formaldehyde. J. Mater. Sci. 24:3221-3227.

2.   Job N et al (2006) Synthesis optimization of organic xerogels produced from convective air-drying of resorcinol–formaldehyde gels. J. Non-Cryst. Solids 352:24-34.

3.   Léonard A et al (2008) Evolution of mechanical properties and final textural properties of resorcinol–formaldehyde xerogels during ambient air drying. J. Non-Cryst. Solids 354:831-838.

4.   Shen J, Hou J et al (2005) Microstructure control of RF and carbon aerogels prepared by sol-gel process. J. Sol-Gel Science and Technology 36:131-136.

5.   Feng J, Feng J, Zhang C (2011) Shrinkage and pore structure in preparation of carbon aerogels. J. Sol-Gel Science and Technology 59:371-380.

6.   Pérez-Caballero F et al (2008) Preparation of carbon aerogels from 5-methylresorcinol–formaldehyde gels. Microporous Mesoporous Mater. 108:230-236.

7.   Szczurek A et al (2011) The use of tannin to prepare carbon gels. Part II. Carbon cryogels. Carbon 49:2785-2794.

8.   Rey-Raap N et al (2015) Towards a feasible and scalable production of bio-xerogels. J. Colloid Interface Sci. 456:138-144.

9.   Moreno-Castilla C, et al (2011) Surface characteristics and electrochemical capacitances of carbon aerogels obtained from resorcinol and pyrocatechol using boric and oxalic acids as polymerization catalysts. Carbon 49:3808-3819.

10.   Zubizarreta L, Arenillas A, Pis JJ (2008) Preparation of Ni-doped carbon nanospheres with different surface chemistry and controlled pore structure. Applied Surface Science 254:3993-4000.

11.   Szczurek A et al (2016) Structure and properties of poly(furfuryl alcohol)-tannin polyHIPEs. Eur. Polymer Journal. 78:195-212.

12.   Rey-Raap N, Menéndez JA, Arenillas A (2014) Optimization of the process variables in the microwave-induced synthesis of carbon xerogels. J. Sol-Gel Sci. Technol. 69:488-497.

13.   Rey-Raap N, Menéndez JA, Arenillas A (2014) RF xerogels with tailored porosity over the entire nanoscale. Microporous Mesoporous Mater. 195:266-275.

14.   Rey-Raap N, Menéndez JA, Arenillas A. (2014) Simultaneous adjustment of the main chemical variables to fine-tune the porosity of carbon xerogels. Carbon 78:490-499.

15.　Moreno AH et al (2013) Carbonisation of resorcinol-formaldehyde organic xerogels: Effect of temperature, particle size and heating rate on the porosity of carbon xerogels. J. Anal. Appl. Pyrol. 100:111-116.

16.　Al-Muhtaseb SA, Ritter JA (2003) Preparation and Properties of Resorcinol–Formaldehyde Organic and Carbon Gels. Advanced Materials. 15:101-114.

17.　Alonso-Buenaposada ID et al (2015) Effect of methanol content in commercial formaldehyde solutions on the porosity of RF carbon xerogels. J. Non-Cryst. Solids. 426:13-18.

18.　Calvo EG et al (2011) Fast microwave-assisted synthesis of tailored mesoporous carbon xerogels. J. Colloid Interface Sci. 357:541-547.

19.　Singh B, Hesse R, Linford MR (2015) Good practices for XPS (and other types of) peak fitting. Vacuum Tecnology & Coating 12:25-31.

20.　Figueiredo JL, Pereira (2010) MFR The role of surface chemistry in catalysis with carbons. Catalysis Today 150:2-7.

21.　Estrade-Szwarckopf H (2004) XPS photoemission in carbonaceous materials: a "defect" peak beside the graphitic asymmetric peak. Carbon 42:1713-1721.

22.　Mulik S, Sotiriou-Leventis C, Leventis N (2007) Time-Efficient Acid-Catalyzed Synthesis of Resorcinol− Formaldehyde Aerogels. Chem. Mater. 19:6138-6144.

23.　Wickenheisser M et al (2015) Hierarchical MOF-xerogel monolith composites from embedding MIL-100(Fe,Cr) and MIL-101(Cr) in resorcinol-formaldehyde xerogels for water adsorption applications. Microporous Mesoporous Mater. 215:143-153.

24.　Awadallah-F A, Elkhatat AM, Al-Muhtaseb SA (2011) Impact of synthesis conditions on meso-and macropore structures of resorcinol–formaldehyde xerogels. J. Mater. Sci. 46:7760-7769.

25.　Alonso-Buenaposada ID et al (2016) Desiccant capability of organic xerogels: surface chemistry vs porous texture. Microporous Mesoporous Mater. 232:70-76.

26.　Blümich B, Callaghan PT (1995) In Principles of nuclear magnetic resonance microscopy. Oxford University Press, Oxford, Magnetic Resonance in Chemistry 33:322-322.

27.　Blumich B In NMR imaging of materials. OUP Oxford. Vol. 2000, 57.

28.　Stapf S, Han SI (2006) In NMR imaging in chemical engineering. John Wiley & Sons.

29.　Ackerman JL et al (1987) In The use of NMR imaging to measure porosity and binder distributions in green-state and partially sintered ceramics. Massachusetts General Hospital, Boston (USA). Radiology Dept.; Argonne

National Lab., IL (USA); Aluminum Co. of America, Alcoa Center, PA. Alcoa Technical Center.

30.   Garrido L (1999) Nondestructive evaluation of biodegradable porous matrices for tissue engineering. Tissue engineering methods and protocols 35-45.

31.   Marcos M et al (2006) NMR relaxometry and imaging of water absorbed in biodegradable polymer scaffolds. Magnetic resonance imaging 24:89-95.

32.   Job N et al (2005) Carbon aerogels, cryogels and xerogels: Influence of the drying method on the textural properties of porous carbon materials. Carbon 43:2481-2494.

33.   Tamon H et al (1997) Porous structure of organic and carbon aerogels synthesized by sol-gel polycondensation of resorcinol with formaldehyde. Carbon 35:791-796.

34.   Rey-Raap N, Arenillas A, Menéndez JA (2015) Formaldehyde in the synthesis of resorcinol-formaldehyde carbon gels. In Formaldehyde: Synthesis, applications and potential health effects. Patton A. Ed.; Nova Science Publishers.; pp 31-60.

4.2. Utilización de catalizadores ácidos en la disolución precursora

Los xerogeles RF se sintetizan a través de una reacción de polimerización entre el resorcinol y el formaldehído que se suele favorecer mediante la adición de compuestos que aceleran la reacción y que, en consecuencia, modifican la estructura porosa del gel orgánico final [31]. La disolución precursora tiene un pH inicial de alrededor de 3. Mediante la adición de un catalizador básico, siendo NaOH y Na_2CO_3 los más comunes [32-36], el pH se puede aumentar hasta un valor máximo (en torno a 7) que da lugar a un material no poroso [30].

Existen en la bibliografía estudios [37-40], aunque escasos, que utilizan ácidos en vez de bases como catalizadores de la reacción de polimerización con el fin de reducir de forma significativa los tiempos de síntesis del material orgánico. Sin embargo, estos materiales son exclusivamente macroporosos, y gran parte de las aplicaciones requieren de mesoporosidad.

En esta Tesis Doctoral se ha evaluado el efecto de sustituir el catalizador básico común por uno de naturaleza ácida sobre las propiedades porosas y químicas de los xerogeles obtenidos mediante radiación microondas.

4.2.1. Objetivos

Los objetivos planteados para realizar el estudio fueron:

➢ Evaluar el efecto de la adición de un ácido en la disolución precursora sobre la porosidad de los xerogeles sintetizados con radiación microondas.

➢ Evaluar el efecto de la adición de un ácido en la disolución precursora sobre la química de los xerogeles sintetizados con radiación microondas.

➢ Evaluar las diferencias entre la utilización de un catalizador básico o ácido sobre las variables químicas que afectan en la porosidad de los materiales.

➢ Evaluar la posibilidad de diseñar materiales con mesoporosidad a medida con catalizador ácido.

4.2.2. Estudio

Para llevar a cabo este estudio se compararon xerogeles orgánicos catalizados con ácido nítrico e hidróxido sódico a diferentes valores de dilución, proporción de monómeros R/F y porcentajes de metanol de la disolución de formaldehído.

4.2.3. Resultados

Los detalles experimentales y la discusión de los resultados obtenidos se hallan en la *Publicación III*, incluida al final de esta sección. Los principales resultados de este estudio se detallan a continuación:

➢ La adición de un catalizador básico o ácido desarrolla la red tridimensional del material a través de distintos mecanismos de reacción que se observan a escala macroscópica.

➢ El efecto de cada una de las variables químicas que repercuten sobre la porosidad final de los xerogeles sigue la misma tendencia independientemente del catalizador utilizado.

➢ Los materiales obtenidos muestran la misma composición química independientemente del catalizador utilizado.

➢ La adición de un catalizador ácido logra tamaños de poro mayores que uno básico.

➢ La obtención de materiales mesoporosos sólo se logra incrementando la concentración de metanol de la disolución de formaldehído.

➢ El control de las propiedades porosas es menos minucioso con la adición de ácidos, ya que ligeras variaciones en cualquiera de sus variables implican grandes cambios en la porosidad.

➢ La utilización de catalizadores ácidos evita la introducción de heteroátomos metálicos (impurezas) en la estructura del gel.

➢ La reacción con catalizadores ácidos es más rápida.

4.2.4. Conclusión

Es posible obtener materiales con propiedades porosas y químicas similares independientemente de la naturaleza del catalizador utilizado en la disolución precursora, a pesar de que sigan diferente mecanismo de reacción. El diseño de la porosidad a través del control de las variables químicas es mucho más preciso cuando se utilizan catalizadores básicos. Sin embargo, con catalizadores ácidos no se introduce ningún heteroátomo metálico en la estructura del gel (impurezas), la reacción se produce más rápidamente y se pueden obtener materiales mesoporosos en muy poco tiempo variando la concentración de metanol (Figura 17).
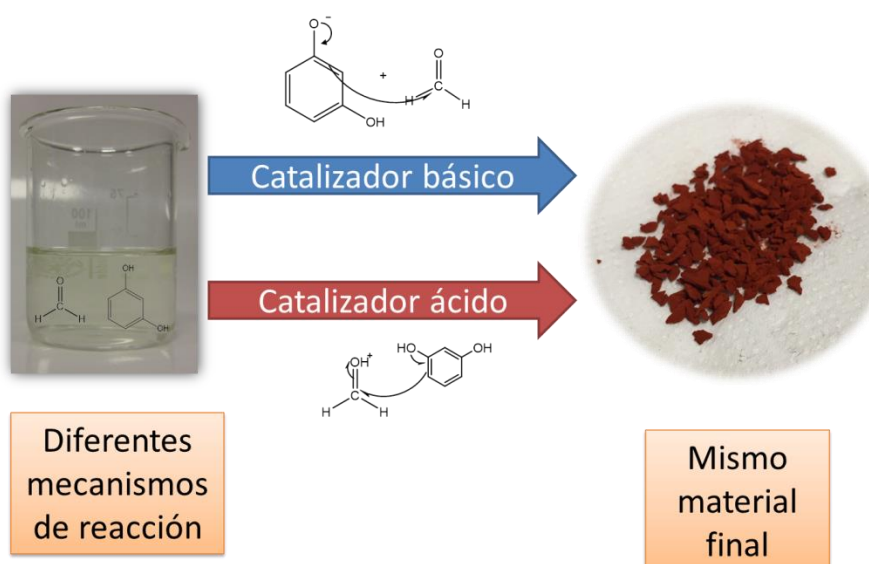
Figura 17. *Esquema resumen del efecto de utilizar un catalizador básico o ácido en la síntesis de xerogeles RF.*

PUBLICACIÓN III

ACID-BASED RESORCINOL-FORMALDEHYDE XEROGELS SYNTHESIZED BY MICROWAVE HEATING

Isabel .D. Alonso-Buenaposada, Natalia Rey-Raap, Esther G. Calvo, J. Angel Menéndez, Ana Arenillas, *Enviada*.

Enviada

Acid-based resorcinol-formaldehyde xerogels synthesized by microwave heating

Isabel D. Alonso-Buenaposada, Natalia Rey-Raap*, Esther G. Calvo, J. Angel Menéndez, Ana Arenillas

Instituto Nacional del Carbón, CSIC, Apartado 73, 33080 Oviedo, Spain

ABSTRACT

The polymerization reaction that takes place between resorcinol and formaldehyde is spontaneous but slow. For this reason, compounds are often used to increase the reaction rate and reduce the synthesis time. These compounds can be basic or acidic and their nature and concentration can be used to modify the mechanisms of the reaction and the final properties of the materials. In this work the differences in the final properties of the organic xerogels obtained with basic or acid boosters have been studied. It was found that, irrespective of the nature of the booster, none of the end-product materials showed any differences in their chemical properties. Moreover, the concentrations of the components of the precursor solution (i.e. monomers, water and methanol) were observed to have the same effect on the porous properties of the materials regardless of whether an acidic or a basic booster was used. However, differences in the porous properties were observed. It was found that the methanol content was crucial to tailor the porosity over the entire nanoscale when an acidic booster is used. These results are of great importance as acidic boosters allows to decrease synthesis time and, hence, to produce more competitive materials.

Keywords: Organic xerogels, pH, microwave heating, porosity, resorcinol, formaldehyde

1. INTRODUCTION

Resorcinol-formaldehyde (RF) gels are porous materials obtained by means of a polymerization reaction [1-3]. These materials have aroused widespread interest among the scientific community over the past two decades due to their excellent properties and diverse applications [3-8]. Some of the most notable features of these materials include their high purity, low density, controllable porous structure and the possibility of doping them with metals or other substances [6, 8-10]. Another reason for the growing interest in these polymeric materials has been the development of a simple and fast synthesis process based on microwave technology, which has led to a reduction in the synthesis time and manufacturing costs [11, 12]. From this process, the so-called xerogels are obtained instead of the well-known aerogels, which are unfeasible to synthesize at an industrial scale [3]. Therefore, it is now possible for companies to take benefit from the advantageous characteristics of RF xerogels without incurring excessive production costs. However, as in all industrial processes, more research is needed to further reduce the synthesis time and, in turn, increase the competitiveness of the material produced. In the context of microwave-assisted synthesis, one of the possibilities to further minimize production time is to accelerate the chemical reaction that takes place during the synthesis process [13].

Generally, RF gels are synthesized by a sol-gel process via the polycondensation of resorcinol and formaldehyde in an aqueous solution [3]. Another compound, the so-called booster throughout this publication, is commonly used to regulate the pH of the precursor solution and accelerate the formation of the polymeric structure [3, 9, 14]. Usually, the compounds employed to promote the polymerization reaction between the resorcinol and formaldehyde are basic, being Na_2CO_3 and NaOH the most widely used bases [4, 15-18]. However, some acid compounds such as perchloric, acetic, nitric or oxalic acids have also been employed in the synthesis of RF gels [4, 16, 19-21]. Some of these studies have demonstrated that acidic boosters lead to an

increase in the reaction rate in comparison with basic boosters and, hence, the synthesis time is reduced [16, 20]. Another factor to bear in mind is the incorporation of impurities in the carbon structure [13, 17-19]. Calvo et al. recently shown that the most common basic boosters provide impurities, which cause corrosion and slagging in steel reactors operating at high temperatures [18]. These reactors are typically employed in the carbonization process of RF gels, which give rise to carbon gels. Therefore, the selection of an acid booster may contribute to avoid the incorporation of metals.

Nevertheless, despite the abovementioned advantages, the vast amount of literature on basic boosters overshadows the few reports focused on acidic boosters (the reader is referred to some of these relevant publications on acid-based RF gels [1, 13, 16, 19]). From those studies, two main items should be highlighted: i) almost all acid-based RF gels synthesized are mainly macroporous materials but with lower densities than that of basic-based gels, and ii) from the best of our knowledge, all the studies reported to date, are based on the synthesis of aerogels rather than xerogels, the latter being those currently synthesized at an industrial scale by means of microwave heating. Consequently, although several attempts to synthesized acid-based aerogels have been made, there is still an ongoing need for a method for producing RF xerogels using acidic boosters, which gives rise to materials with tailored porosity over the entire nanoscale.

Therefore, the aim of the present work is to synthesize acid-based RF xerogels by means of microwave heating in order to i) obtain materials with tailored porosity and ii) increase the competitiveness of these materials by reducing synthesis time. It is well-known that the porosity of basic-based RF xerogels can be minutely tuned by selecting the appropriate composition of the precursor solution: pH, dilution ratio, R/F molar ratio and even, as recently demonstrated, the methanol content in commercial formaldehyde solutions [14, 21-25]. Accordingly, in this work the influence of the aforementioned variables on the chemical and porous properties of acid-based RF xerogels synthesized by microwave heating has been studied. All of the synthesized xerogels were

characterized from the point of view of their chemical and porous structure to determine the effect of each variable. Moreover, basic-based RF xerogels have also been synthesized to ascertain possible differences in properties due to the booster employed.

2. EXPERIMENTAL SECTION

2.1. Synthesis of organic xerogels

A wide spectrum of resorcinol-formaldehyde xerogels was synthesized by microwave heating and by modifying chemical variables such as the pH of the precursor solution, the amount of solvent (water), the R/F molar ratio and the amount of methanol contained in the commercial formaldehyde solution. Briefly, the synthesis of the organic xerogels proceeded as follows: a mixture of resorcinol (Indspec, 99.6 wt. %), distilled water, formaldehyde (Química S.A.U., aqueous solution with 37 wt. % formaldehyde and 1.5 wt. % methanol), and some extra methanol, if necessary (AnalaR Normapur, 99 %) was prepared. The initial pH of the precursor solution, which had a value of ca. 3.0 in almost all cases, was measured and then adjusted to the desired final pH in order to obtain acid-based and basic-based xerogels. To this end, nitric acid (Merck, 65 wt. % HNO_3) and sodium hydroxide (1 M NaOH made up of solid NaOH, AnalaR Normapur, 99.9 %) were used as boosters to adjust the pH of the precursor solutions, respectively.

Resorcinol, formaldehyde, methanol and water were added in the required proportions depending on the values of dilution ratio (D = total solvent / reactant molar ratio), R/F molar ratio and percentage of methanol desired. These values were selected on the basis of results reported in previous published works on the synthesis of basic-based RF xerogels, in order to obtain materials with different porous properties [14, 25].

Each precursor solution prepared was introduced into the microwave oven at 85 ºC for about 5 hours, following the experimental method describe elsewhere [11]. Once the synthesis was completed, the organic xerogels were subjected to a heat treatment at 100 ºC overnight to remove any traces of reagent and obtain completely stable samples.

The nomenclature of each sample indicates the synthesis conditions employed; OXA and OXB denoting Organic Xerogel prepared with an Acid booster and Organic Xerogel prepared with a Basic booster, respectively, and the following numbers referring to the pH, dilution ratio, R/F molar ratio and the percentage of methanol content, in that order.

2.2. Characterization techniques

The chemical composition of the RF xerogels was evaluated in order to identify possible discrepancies between the samples synthesized via the acid and basic routes. Therefore, ultimate (i.e. carbon, hydrogen, nitrogen and oxygen contents) and proximate (i.e. moisture, ash and volatile matter contents) measurements were carried out in a LECO-TF-900 and LECO-CHNS-932 microanalyzer, respectively.

Fourier Transform Infrared Spectroscopy (FTIR) was also performed. The spectra were recorded in the 525 and 4000 cm^{-1} range on a Nicolet IR 8700 spectrometer fitted with a DTGS detector (deuterated triglycine sulphate) at a resolution of 4 cm^{-1} over 64 accumulated scans. All the samples were analyzed twice. In order to prepare the pellets, the samples and KBr (previously dried overnight) were mixed in a proportion of 1:100 in an agate mortar for 10 minutes until a homogeneous mixture was obtained. Around 0.125 g of this mixture was subjected to 8 tons of pressure in a 13 mm-diameter matrix.

In addition, in order to study the chemical properties of the xerogels in greater depth the pH of the point of zero charge (pH_{PZC}) was determined by the reverse mass titration method described elsewhere [26].

The porous structure of the RF xerogels was evaluated by the following techniques: (i) nitrogen adsorption-desorption isotherm analysis and; (ii) mercury porosimetry. Prior to performing these analyses, the samples were degassed at 120 ºC under a vacuum of 0.1 mbar overnight. N_2 adsorption-desorption isotherms were performed at -196 ºC using a Tristar II 3020 (Micromeritics) analyzer. The specific surface area was calculated by the Brunauer-Emmett-Teller (BET) method. The Dubinin-Raduskevich (D-R) model was used to obtain information about the microporosity (V_{DUB-N2}). The total pore volume (Vp) was calculated from the amount of nitrogen adsorbed at a relative pressure of 0.99. The mesopore volume obtained by this technique ($Vmeso-N_2$) was calculated as the difference between Vp and the V_{DUB-N2}. The pore Size Distribution (PSD) of the RF xerogels was determined by applying the DFT method to the nitrogen adsorption branch. However, as several of the samples displayed large mesopores and in some cases, macropores, mercury intrusion porosimetry was also used to obtain a more reliable measurement of the pore size distribution. The device used was an AutoPore IV 9500, Micromeritics that is able to operate in a pressure range from atmospheric pressure to 228 MPa. The surface tension and contact angle values for Hg in all the characterizations were 0.485 N m^{-1} and 130 º, respectively. By means of this technique, based on the Washburn intrusion theory, the following parameters were calculated: mesopore and macropore volume (Vmeso and Vmacro, respectively), average pore size (d_{pore}), percentage of porosity and bulk density. It should be noted that the lowest detectable limit of the device is 5.5 nm, so that, Vmeso refers to a pore size range of between 50 and 5.5 nm.

The morphology of all samples was examined using a Quanta FEG 650 scanning electron microscope. Samples were previously attached to an aluminum tap using conductive double-sided adhesive tape. An accelerating voltage of 25 kV and a secondary electron detector EDT (Everhart-Thornley) were used in all analysis.

3. RESULTS AND DISCUSSION

3.1. Chemical properties

The chemical composition of acid-based (OXA) and basic-based (OXB) RF xerogels synthesized was analysed. Given that, as expected, the composition of all materials studied was similar, only the results of four samples are shown in Table 1, as an example.

Table 1. *Elemental analysis of the acid and basic RF xerogels.*

Booster	Acid (HNO₃)		Basic (NaOH)	
Sample	**OXA-2.0-3.7-0.5-12.5**	**OXA-2.0-2.7-0.5-1.5**	**OXB-5.4-7.7-0.3-12.5**	**OXB-6.5-6.0-0.5-12.5**
C (± 0.3, wt. %)	65.8	66.1	64.7	66.3
H (± 0.3, wt. %)	4.3	4.6	4.9	4.5
N (± 0.3, wt. %)	0.3	0.3	0.3	0.3
O (± 0.3, wt. %)	29.6	29.0	30.1	28.9

All samples contain c.a. 65.5 wt. % of carbon, 4.5 wt. % of hydrogen and 30 wt. % of oxygen. No nitrogen is considered to be present since 0.3 wt. % is within the range of analysis error and the precursors (i.e., R and F) have no nitrogen. It should also be noted that the same nitrogen content was obtained for all the samples which means that the nitrogen content did not increase (at least substantially) as a result of using HNO_3 for the synthesis. Moreover, all the samples showed c.a. 46 % of volatile material, 5 % of moisture and no mineral residue at all. Therefore, irrespective of the nature of the booster employed to fix the pH, the chemical composition obtained was similar for all samples, inasmuch as the same main reagents were used to prepare the precursor solutions. However, it is well-known that the nature of the booster modifies the mechanism of the polymeric reaction [3, 10]. Accordingly, structural differences may be expected between OXA and OXB samples. Conversely, as shown in Figure 1, the FTIR spectra of acid (series OXA) and basic (series OXB) samples

are quite similar (note that only four samples are shown in Figure 1, as an example).
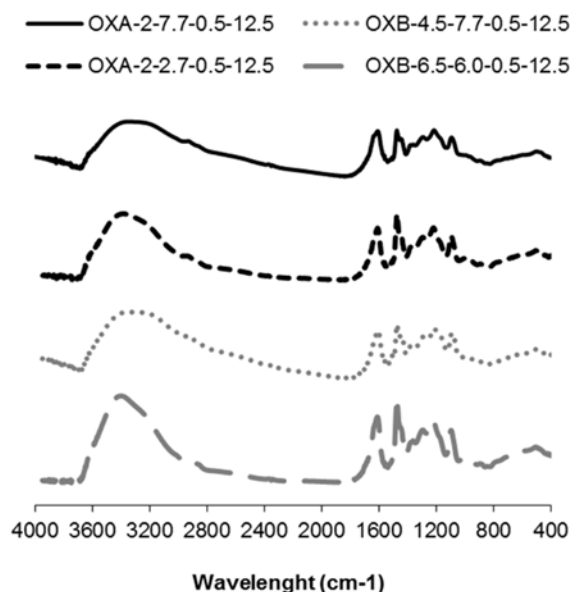
Figure 1. *FTIR spectra of the RF xerogels synthesized by the addition of an acid (HNO_3) or basic (NaOH) booster.*

All the samples exhibit a wide band between 3700 and 3000 cm^{-1}, associated with O-H stretching vibrations, while another band located at 1474 cm^{-1}, corresponds to CH_2 deformation vibrations [5]. Moreover, the band at 1613 cm^{-1} is due to aromatic ring stretching vibrations (C=C) whereas the bands at 1217 and 1092 cm^{-1} indicate the presence of methylene ether bridges C-O-C. These similarities found in the chemical properties of the RF xerogels synthesized from precursor solutions with boosters of different nature can be attributed to the two steps involved in the polymerization reaction between resorcinol and formaldehyde: (i) addition and (ii) condensation reaction [2]. In general, the mechanism of the addition reaction depends largely on the nature of the compound used to adjust the pH of the precursor solution, whilst the condensation reaction is independent of the booster, as shown in Figure 2.
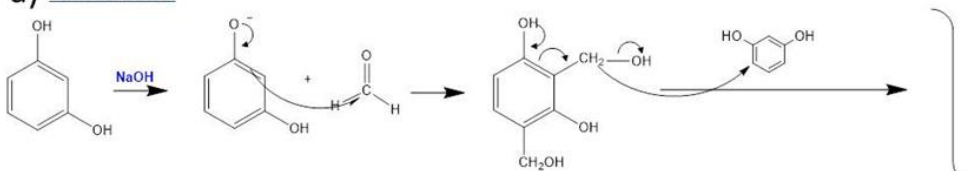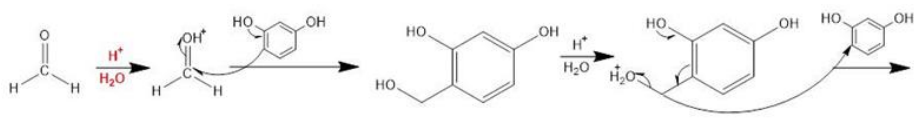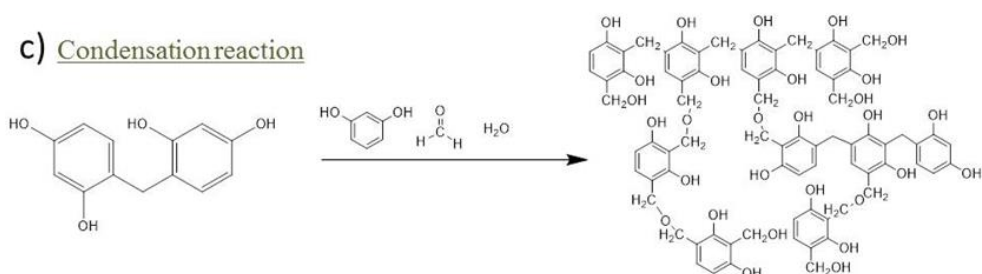
Figure 2. *Mechanism of the polymerization reaction between resorcinol and formaldehyde under basic and acid routes.*

When a basic booster is used, the resorcinol is deprotonated (Figure 2a), giving rise to resorcinol anions which trigger a nucleophilic attack from the second, fourth or sixth positions of the resorcinol towards the formaldehyde [2, 3, 23]. On the other hand, when an acid compound is used, the first step is favoured by the protonation of the formaldehyde (Figure 2b), which makes the carbonyl carbon more electrophilic and causes an identical SN_2 attack from the resorcinol [1]. As a result of these two mechanisms, hydroxymethyl derivatives are obtained, which are the necessary monomers for polymerization to occur. A series of consecutive condensation reactions then take place, in which the hydroxymethyl derivatives lose OH groups and form benzyl-type cations [24]. Each cation reacts with a benzene ring of another molecule, giving rise to methylene and ether bonds until a three-dimensional cross-linked polymer is formed, as shown in Figure 2c. The results of FTIR shown in Figure 1, are in

good agreement with the above detailed mechanisms, as all the materials have similar chemical properties, whichever booster was used.

3.2. Porous properties

The most interesting characteristic of basic-based RF xerogels is that it is possible to design their porous properties to fit the requirement of specific applications, by modifying the main chemical variables: pH, D, R/F molar ratio and % of methanol. The effect of the pH is the most studied variable [9, 12, 14, 16]. Values of pH usually ranged between 3.0, which is the initial pH value of most of the precursor solutions, and 7.0 [12, 24]. Generally, an increase in the concentration of the basic booster, i.e. an increase in the pH value, results in materials with smaller pore size, as shown in Figure 3a. Therefore, one might assume an increase in pore size as the pH drops below 3.0. However, contrary to expected, pore size of samples synthesized with an acidic booster decreases with pH, as shown in Figure 3b. It is evident from these results that the polymerization reaction depends largely on the amount and nature of catalyst added. Each booster favours its corresponding addition reaction (Figure 2a and 2b), which leads to the formation of a large number of clusters and, hence, to materials with pores of smaller size. However, it should be noted that the use of a basic or an acidic booster results in meso-macroporous materials or exclusively macroporous materials, respectively. These results are consistent with other published studies where it was shown that the use of acidic booters gives rise to materials of larger pore size [13]. Therefore, it seems necessary to modify the concentration of the remaining reagents (i.e. R/F molar ratio, D and percentage of methanol) to find out if it is possible to obtain porous materials over the entire nanoscale by using acidic boosters.
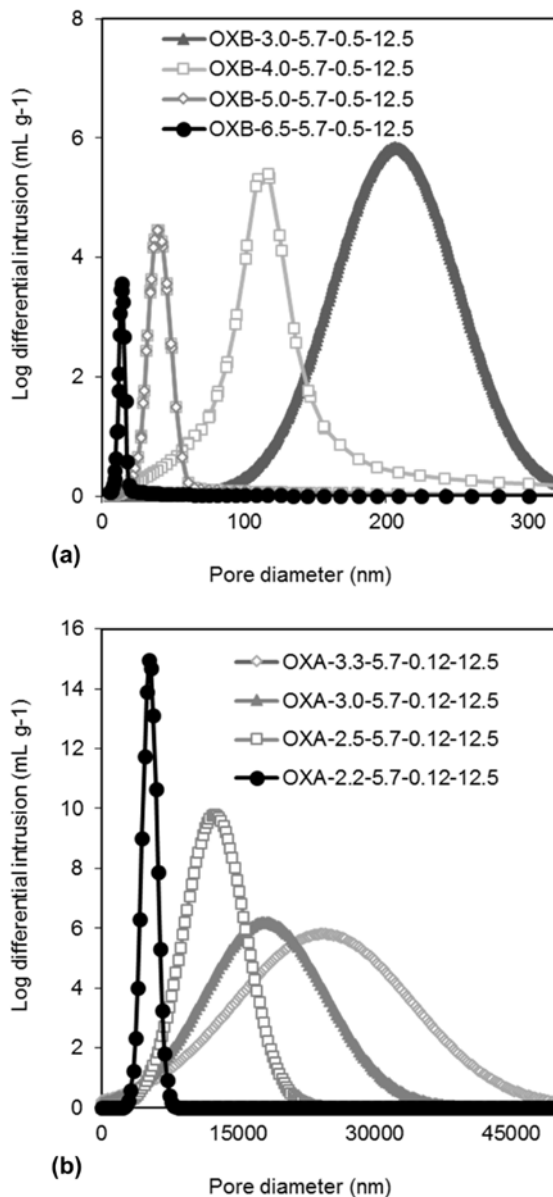
Figure 3. Influence of the pH value on the pore size distribution of RF xerogels synthesized by adding basic (a) or acid (b) boosters.

Initially, two set of samples (OXB and OXA) were synthesized from precursor solutions with different R/F molar ratio. The effect of this variable on pore size and total pore volume is shown in Figure 4. Regardless of the nature of the booster, a decrease in the concentration of either of the main reagents (resorcinol and formaldehyde) leads to a decrease in the reaction rate since the

precursors are prevented from locating each other. As a consequence, an increase in the pore size is observed, and a minimum value of pore size is obtained when the stoichiometric ratio (R/F = 0.5) is employed. On the other hand, an excess of formaldehyde (i.e., a low R/F molar ratio) creates more interconnections between clusters, leading to a highly branched structure [14, 21]. The mechanical strength of these RF xerogels is greater so that no shrinkage occurs during the drying step, which results in a larger total pore volume (Figure 4). Therefore, whereas same pore size can be obtained using different R/F molar ratios, large pore volumes are achieved only if the R/F molar ratio is below 0.5. The effect of modifying the R/F molar ratio is similar for both the OXA and OXB series. However, the porous properties of samples synthesized by using an acidic booster are within the range of macroporosity, while OXB are within the range of mesoporosity. This effect, as explained above, is due to the amount and nature of the booster, which means that pH value has more effect on the porous properties than the R/F molar ratio.

(a)
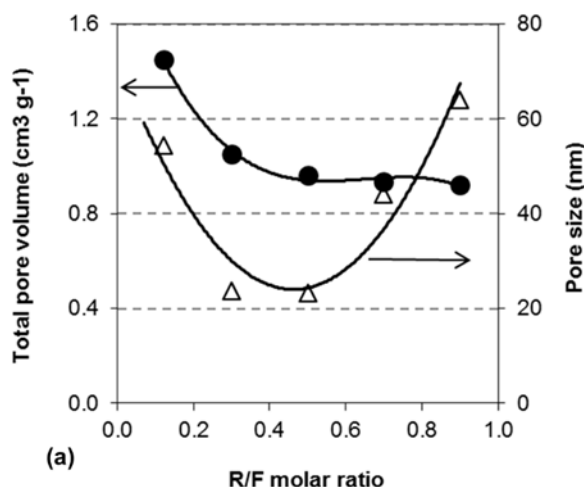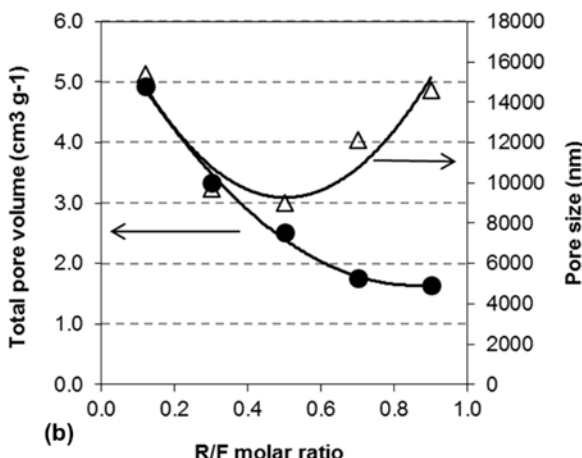
Figure 4. *Effect of the variation of the R/F molar ratio on the pore size (▲) and total pore volume (●) when (a) a basic (NaOH) or (b) an acid (HNO₃) booster is used to prepare the precursor solution.*

Another important chemical variable which must be taken into account when designing the porosity of RF xerogels is the dilution ratio (D). In order to evaluate the effect of this parameter, the pore size distribution obtained by subjecting the samples with different dilution ratios to mercury porosimetry is shown in Figure 5. The same trend can be observed by both the OXA and OXB series: the larger the dilution ratio is, the larger the pore size obtained. This is because an increase in the dilution ratio leads to a greater volume of water among the clusters, which in turn, results in an increase in the distance between clusters, and therefore, larger pores [22, 24]. As in the case of basic compounds, the OXA series shows an upper limit for D values and, when it is exceeded, the sol–gel reaction fails to take place as the large amount of water prevents the precursor solution from reaching its gelation point [24].
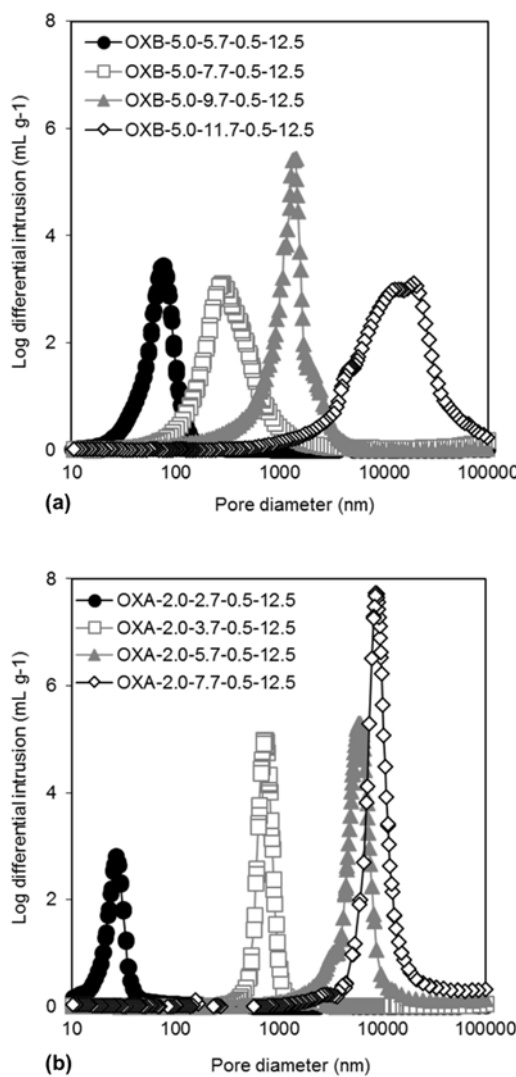
Figure 5. *Influence of the dilution ratio on the pore size distribution of RF xerogels synthesized by adding basic (a) or acid (b) boosters.*

Finally, the influence of the concentration of methanol on the porous properties of RF xerogels prepared from acidic and basic precursor solutions was evaluated. Methanol is added to formaldehyde solutions in order to prevent the formaldehyde from polymerizing and subsequently precipitating. It was only recently that the methanol content of the formaldehyde solution was recognised as a chemical variable that affected the porosity of RF xerogels [25]. Hemiacetals and acetals are formed in a reversible reaction that prevents the

formation of clusters owing to the fact that the reaction between resorcinol and formaldehyde only takes place if the formaldehyde remains in its free form [3]. Consequently, an increase in the methanol content leads to an increase in the formation of hemiacetals which prevents the resorcinol molecules from finding free formaldehyde molecules to react with. Moreover, the formation of hemiacetal compounds is favoured in acidic media [25], which suggest that the formation, growth and crosslinking of the polymeric structure depend to a great extent on the methanol content and the booster used to prepare the precursor solution. In fact, structural differences were observed by SEM images, as shown Figure 6. In Figure 6a and 6b it can be appreciated the characteristic morphology of basic-based RF xerogels. However, by using an acidic booster, the typical morphology is replaced by a capsule-like or cellular morphology with pores enclosed by thin polymeric walls.
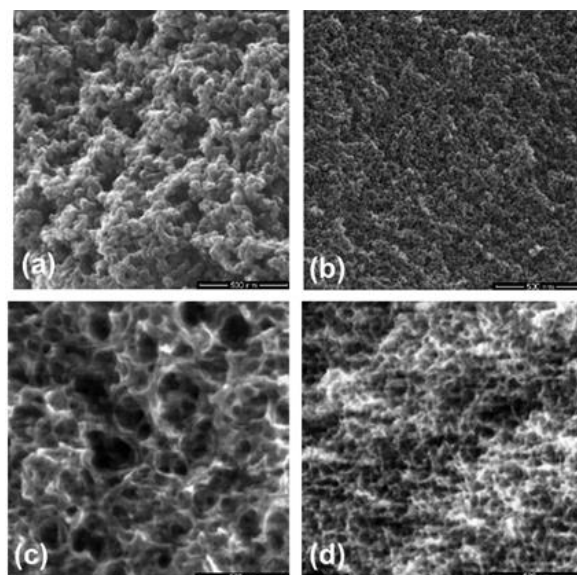
Figure 6. SEM images of RF xerogels synthesized from precursor solutions with different concentration of reagents: (a) OXB-5.4-7.7-0.3-12.5, (b) OXB-6.5-6.0-0.5-12.5, (c) OXA-2.0-2.7-0.5-1.5 and (d) OXA-2.0-2.7-0.5-20.0.

However, even though differences in the polymeric structures have been found, the effect of methanol content on the reactivity of resorcinol (or the availability to polymerize) is independent of the nature of the booster used

(acidic or basic). Therefore, similar effects on the final porous properties are observed, as shown in Figure 7. Materials synthesized with low concentrations of methanol have larger pore volumes both in the OXA and OXB series of samples.
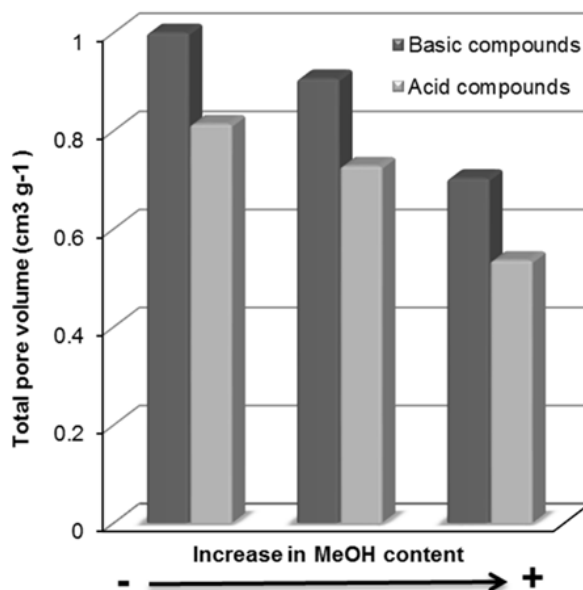
Figure 7. *Influence of the methanol content of the formaldehyde solutions on the porosity of RF xerogels synthesized using a basic (NaOH) or an acid (HNO₃) booster in the precursor solution.*

As explained in detail in previous studies [10, 14, 24, 25], the formation, growth and crosslinking of the polymeric structure depend on the concentrations of all the reagents used to prepare the precursor solution. Accordingly, it is possible to obtain RF xerogels with a desired pore size whether an acid or basic booster is used, if the concentration of all the reagents are properly selected, as shown in Table 2. However, it is worth noting that the variation of the percentage of methanol in OXA series, results in mesoporous materials, which are generally achieved only by using basic boosters. In other words, the variation of the methanol content is essential in the case of acid-based RF xerogels in order to obtain mesoporous materials.

Table 2. *The porous properties of the RF xerogels synthesized under different chemical conditions*

SAMPLE	[a]V_{tot} (cm^3 g^{-1})	V_{meso} (cm^3 g^{-1})	V_{macro} (cm^3 g^{-1})	[a]Pore diameter (nm)	[a]Bulk density (g cm^{-3})	[a]Porosity (%)	S_{BET} (m^{2}g^{-1})	$V_{meso-N2}$ (cm^3 g^{-1})
OXB-4.5-7.7-0.5-12.5	2.67	0.03	2.64	775	0.2	86	120	0.05
OXB-5.4-7.7-0.3-12.5	1.47	0.81	0.65	41	0.44	65	180	0.36
OXB-6.2-8.6-0.5-12.5	0.64	0.51	0.13	22	0.61	53	269	0.47
OXB-6.5-6.0-0.5-12.5	0.41	0.36	0.04	14	0.76	40	303	0.52
OXA-2.0-3.7-0.5-12.5	1.01	0	1.01	735	0.56	56	0	0
OXA-2.0-2.7-0.5-1.5	0.81	0.65	0.17	41	0.63	50	110	0.33
OXA-2.0-2.7-0.5-12.5	0.73	0.67	0.06	26	0.67	49	226	0.66
OXA-2.0-2.7-0.5-20	0.54	0.48	0.06	14	0.70	37	354	0.73

[a]obtained from mercury porosimetry

[b]obtained from N_2 adsorption isotherms

In short, an appropriate combination of pH, R/F molar ratio, dilution ratio and methanol content leads to materials with similar porous properties irrespective of the mechanism of the polymerisation reaction (Figure 2). However, acidic boosters, should result in lower synthesis time and, hence, in to more competitive materials. In order to verify this advantage, the evolution of the pH of 4 precursor solutions was registered at ambient temperature and plotted in Figure 8.
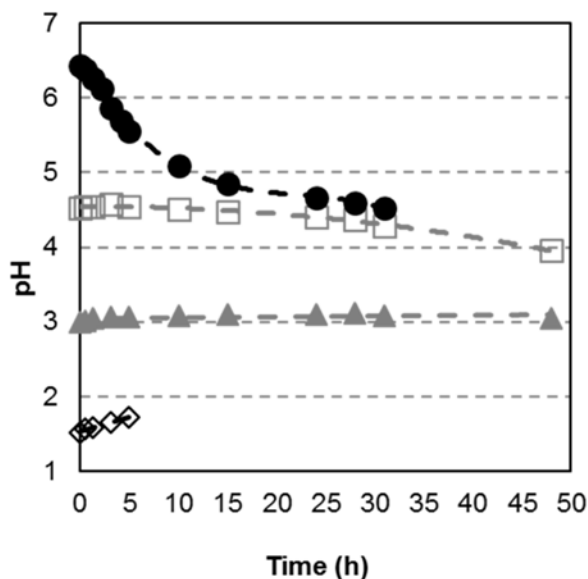
Figure 8. *Evolution of the pH of the precursor solutions with time up to the point of gelation for the following initials pH: 1.5, 3 (with no compound to modify the pH), 4.5 and 6.5.*

From Figure 8 it can be inferred that, even at ambient temperature, the precursor solution reacts and its pH value changes with time. Moreover, although each solution has a different initial pH, the general trend is for all of them to acquire the same final pH (c.a. pH of 3), which can be considered as the equilibrium pH for this type of materials. This pH value matches the pH_{PZC} of all the final RF xerogels obtained (i.e. pH_{PZC}=3 for all organic xerogels), indicating that, although the type and concentration of the booster may have a great effect on the mechanism and rate of the polymerisation reaction, respectively, the final nature of the material obtained is similar. It can also be observed that the acidic solutions get to the gelation point faster than the basic ones even if they are farther from the equilibrium pH (e.g., the precursor mixture with a pH = 1.5 only shows a few points in Figure 8). In fact, a solution with a pH of 0.85 was prepared and no data at all could be recorded owing to its instant gelation. Therefore, the main difference between what an acid or a basic booster has to offer is that the acid mechanism (Figure 2b) is more favoured and so the reaction is much faster than when a basic one is used. Extra evidence for this is provided in the video of the supplementary material.

5. CONCLUSIONS

In this work resorcinol-formaldehyde (RF) xerogels have been synthesized by means of microwave heating and by using basic and acidic booster to adjust the pH of the precursor solutions. It was found that, regardless of the booster used, materials with similar chemical composition were obtained. Conversely, the nature of the booster had a great influence on the porous properties. It has been observed that basic boosters led to meso-macroporous materials while acid boosters resulted in exclusively macroporous materials. However, it has been demonstrated that the properties of acid-base RF xerogels can be also tailored by the appropriate selection of the concentration of all reagents, which are defined by the R/F molar ratio, the dilution ratio and the methanol content. Among these three variables, the methanol content has shown to be crucial to obtained mesoporous materials via an acid route. Moreover, acid boosters has the advantage that it prevents the incorporation of impurities into the carbonaceous structure (i.e. alkaline metals) and accelerates the polymerization reaction, leading to more competitive materials.

ACKNOWLEDGEMENTS

BIBLIOGRAPHY

[1] M.A. Aegerter, N. Leventis, M.M. Koebel, Aerogels handbook, Springer2011.

[2] S.A. Al-Muhtaseb, J.A. Ritter, Preparation and properties of resorcinol-formaldehyde organic and carbon gels, Adv. Mater. 15 (2003) 101-114.

[3] N. Rey-Raap, A. Arenillas, J.A. Menéndez, Formaldehyde in the Synthesis of Resorcinol-Formaldehyde Carbon Gels in: A. Patton (Ed.),

Formaldehyde: Synthesis, Applications and Potential Health Effects, Nova Science2015.

[4] C. Alegre, D. Sebastián, M.E. Gálvez, R. Moliner, M.J. Lázaro, Sulfurized carbon xerogels as Pt support with enhanced activity for fuel cell applications, Appl. Catal., B 192 (2016) 260-267.

[5] S. Álvarez, R.S. Ribeiro, H.T. Gomes, J.L. Sotelo, J. García, Synthesis of carbon xerogels and their application in adsorption studies of caffeine and diclofenac as emerging contaminants, Chem. Eng. Res. Des. 95 (2015) 229-238.

[6] C. Moreno-Castilla, F.J. Maldonado-Hódar, Carbon aerogels for catalysis applications: An overview, Carbon 43 (2005) 455-465.

[7] N. Rey-Raap, M.L.C. Piedboeuf, A. Arenillas, J.A. Menendez, A.F. Leonard, N. Job, Aqueous and organic inks of carbon xerogels as models for studying the role of porosity in lithium-ion battery electrodes, Mater Design 109 (2016) 282-288.

[8] X. Lu, J. Shen, H. Ma, B. Yan, Z. Li, M. Shi, M. Ye, A cost-effective way to maintain metal-doped carbon xerogels and their applications on electric double-layer capacitors, J. Power Sources 201 (2012) 340-346.

[9] S.J. Taylor, M.D. Haw, J. Sefcik, A.J. Fletcher, Gelation mechanism of resorcinol-formaldehyde gels investigated by dynamic light scattering, Langmuir 30 (2014) 10231-10240.

[10] M. Alshrah, M.P. Tran, P. Gong, H.E. Naguib, C.B. Park, Development of high-porosity resorcinol formaldehyde aerogels with enhanced mechanical properties through improved particle necking under CO_2 supercritical conditions, J. Colloid Interface Sci. 485 (2017) 65-74.

[11] N. Rey-Raap, J.A. Menéndez, A. Arenillas, Optimization of the process variables in the microwave-induced synthesis of carbon xerogels, J. Sol-Gel Sci. Technol. (2013) 1-10.

[12] E.G. Calvo, E.J. Juarez-Perez, J.A. Menendez, A. Arenillas, Fast microwave-assisted synthesis of tailored mesoporous carbon xerogels, J. Colloid Interface Sci. 357 (2011) 541-7.

[13] M.L. Rojas-Cervantes, Some strategies to lower the production cost of carbon gels, J. Mater. Sci. 50 (2014) 1017-1040.

[14] N. Rey-Raap, J.A. Menéndez, A. Arenillas, Simultaneous adjustment of the main chemical variables to fine-tune the porosity of carbon xerogels, Carbon 78 (2014) 490-499.

[15] M.L.C. Piedboeuf, A.F. Léonard, K. Traina, N. Job, Influence of the textural parameters of resorcinol-formaldehyde dry polymers and carbon xerogels on particle sizes upon mechanical milling, Colloids Surf., A 471 (2015) 124-132.

[16] D. Fairén-Jiménez, F. Carrasco-Marín, C. Moreno-Castilla, Porosity and surface area of monolithic carbon aerogels prepared using alkaline carbonates and organic acids as polymerization catalysts, Carbon 44 (2006) 2301-2307.

[17] N. Job, C.J. Gommes, R. Pirard, J.P. Pirard, Effect of the counter-ion of the basification agent on the pore texture of organic and carbon xerogels, J. Non-Cryst. Solids 354 (2008) 4698-4701.

[18] E.G. Calvo, J.A. Menéndez, A. Arenillas, Influence of alkaline compounds on the porosity of resorcinol-formaldehyde xerogels, J. Non-Cryst. Solids 452 (2016) 286-290.

[19] R. Brandt, J. Fricke, Acetic-acid-catalyzed and subcritically dried carbon aerogels with a nanometer-sized structure and a wide density range, J. Non-Cryst. Solids 350 (2004) 131-135.

[20] O. Barbieri, F. Ehrburger-Dolle, T.P. Rieker, G.M. Pajonk, N. Pinto, A. Venkateswara Rao, Small-angle X-ray scattering of a new series of organic aerogels, J. Non-Cryst. Solids 285 (2001) 109-115.

[21] A. Awadallah-F, A.M. Elkhatat, S.A. Al-Muhtaseb, Impact of synthesis conditions on meso- and macropore structures of resorcinol-formaldehyde xerogels, J. Mater. Sci. 46 (2011) 7760-7769.

[22] N. Rey-Raap, A. Arenillas, J.A. Menéndez, A visual validation of the combined effect of pH and dilution on the porosity of carbon xerogels, Micropor. Mesopor. Mater. 223 (2016) 89-93.

[23] J.P. Lewicki, C.A. Fox, M.A. Worsley, On the synthesis and structure of resorcinol-formaldehyde polymeric networks - Precursors to 3D-carbon macroassemblies, Polymer (United Kingdom) 69 (2015) 45-51.

[24] N. Rey-Raap, J.A. Menéndez, A. Arenillas, RF xerogels with tailored porosity over the entire nanoscale, Micropor. Mesopor. Mater. 195 (2014) 266-275.

[25] I.D. Alonso-Buenaposada, N. Rey-Raap, E.G. Calvo, J.A. Menéndez, A. Arenillas, Effect of methanol content in commercial formaldehyde solutions on the porosity of RF carbon xerogels, J. Non-Cryst. Solids 426 (2015) 13-18.

[26] J.A. Menéndez, J. Phillips, B. Xia, L.R. Radovic, On the modification and characterization of chemical surface properties of activated carbon: In the search of carbons with stable basic properties, Langmuir 12 (1996) 4404-4410.

4.3. Xerogeles de carbono como soportes de biomoléculas

Los materiales carbonosos son frecuentemente utilizados como soportes para catalizadores [21, 41]. Sin embargo, el papel que desempeñan estos materiales en el campo de los biocatalizadores es muy limitado, ya que la mayoría de estos materiales porosos se centran en el desarrollo de su microporosidad, cuyo tamaño de poro es demasiado pequeño para poder soportar biomoléculas [42, 43].

La posibilidad de poder obtener xerogeles RF en el rango de los meso-macroporos, donde las biomoléculas pueden ser depositadas, abre una nueva vía para su utilización en este tipo de aplicaciones. Además, el tamaño de poro puede ser diseñado a medida para cada tipo de enzima de forma específica y asegurar así una funcionalidad óptima. La necesidad de su soporte reside en: el alto precio de las biomoléculas, así como su reutilización y recuperación de forma sencilla [44-46].

Por lo tanto, en esta Tesis Doctoral se ha evaluado la posibilidad de inmovilizar Citocromo C en los poros de xerogeles de carbono con distintas propiedades porosas, así como su actividad catalítica y su reutilización.

4.3.1. Objetivos

Los objetivos planteados para realizar el estudio fueron:

➢ Evaluar la inmovilización de Citocromo C en xerogeles de carbono con diferente tamaño de poro y determinar cuál es el material óptimo para este fin.

➢ Evaluar la actividad del Citocromo C una vez depositado en el material.

➢ Evaluar la reutilización de esta biomolécula una vez depositada en el material.

4.3.2. Estudio

Para llevar a cabo este estudio se sintetizaron cuatro xerogeles de carbono que cubren practicamente el rango de mesoporos (desde 5 nm a 55 nm) y se estudió la inmovilización de Citocromo C a tres pHs distintos (3, 6 y 10) para posteriormente evaluar su actividad.

Se seleccionó Citocromo C como molécula modelo debido a su alta pureza, su utilización en otros estudios de la bibliografía [47] y su amplio conocimiento sobre su estructura y propiedades fisicoquímicas [48].

4.3.3. Resultados

Los detalles experimentales y la discusión de los resultados obtenidos se hallan en la *Publicación VI*, incluida al final de este capítulo. Los principales resultados de este estudio se detallan a continuación:

➢ El pH de la disolución tampón utilizada no afecta a la inmovilización de Citocromo C en xerogeles de carbono.

➢ A mayor fuerza iónica de la disolución tampón, mayor cantidad de Citocromo C es inmuvilizado en los xerogeles de carbono.

➢ CX-30 mostró ser el material con mayor capacidad de adsorción mientras que CX-5 el que menor.

➢ Todos los materiales mostraron similar actividad catalítica independientemente del material soporte utilizado y, en consecuencia, de la cantidad de proteína inmovilizada.

➢ CX-5 mostró un comportamiento similar al de la proteína sin soporte, siendo este distinto al del resto de materiales de este estudio. Se concluyó que toda la proteína estaba depositada en la superficie externa y no en el interior de los poros.

➢ Para CX-15, CX-30 y CX-55 un aumento de la concentración de ABTS o su reutilización durante varios ciclos implica un aumento en su actividad catalítica.

4.3.4. Conclusión

El Citocromo C se deposita de forma efectiva dentro de la porosidad de los xerogeles de carbono con tamaño de poro entre 15 y 55 nm, mostrando además una mayor actividad enzimática cuando está soportada en el interior de los poros que cuando se encuentra en su superficie externa, o lo que es lo mismo, en su forma libre. Por lo tanto, los xerogeles de carbono son materiales factibles para ser utilizados como soportes de biomoléculas ya que su porosidad puede ser diseñada a medida de la proteína que se quiera soportar.

PUBLICACIÓN IV

ADSORPTION AND ACTIVITY ON CARBON XEROGELS WITH NARROW PORE SIZE DISTRIBUTIONS COVERING A WIDE MESOPOROUS RANGE

Luis A. Ramírez-Montoya, Alejandro Concheso, Isabel D. Alonso-Buenaposada, Héctor García, J. Angel Menéndez, Ana Arenillas, Miguel A. Montes-Morán, *Carbon, 118 (2017) 743-751*.

Protein adsorption and activity on carbon xerogels with narrow pore size distributions covering a wide mesoporous range

Luis A. Ramírez-Montoya, Alejandro Concheso, Isabel D. Alonso-Buenaposada, Héctor García, J. Angel Menéndez, Ana Arenillas, Miguel A. Montes-Morán[*]

Instituto Nacional del Carbón, INCAR-CSIC, Apartado 73, 33080 Oviedo, Spain

ABSTRACT

Four carbon xerogels (CXs) were used to study the effect of the average pore size (APS) on the adsorption and activity of cytochrome c (cyt c). Pore size distributions of the CXs were relatively narrow with APSs covering the whole mesoporosity range (5, 15, 30 and 55 nm), as determined by mercury porosimetry. Selected techniques verified that all carbons were identical in terms of composition and surface chemistry. The best APS for cyt c adsorption (in terms of capacity) was 30 nm, with loadings of 180 mg of protein (g of support)$^{-1}$. The CX with APS of 15 nm also hosted high amounts of cyt c, followed by the material with 55 nm. The CX with 5 nm APS did not adsorb cyt c. The pH of adsorption had little effect on the final amount adsorbed, thus stressing the hydrophobic nature of the protein/carbon surface interaction. The activity of the resulting materials towards the ABTS oxidation was similar regardless the amount of cyt c adsorbed on their surface/pores. Their performance in successive cycles of re-use was different depending on the carbon support; xerogels bearing APSs ≥ 15 nm presented an increasing activity with increasing the number of cycles.

1. INTRODUCTION

The interaction of proteins with porous substrates is crucial for a number of applications [1,2]. It is however appalling the little role that porous carbons play in this area. A possible explanation might be linked to the scientific and technical interest of the carbon community being traditionally focused on the production of (microporous) activated carbons [3]. Due to the size of most biomolecules of interest, microporosity seems not relevant [3,4]. This situation could be reverted as an increasing interest on protein/porous carbons systems is steadily shown [5,6]. Actually, it was the development of the so-called nanostructured mesoporous carbons [7-9] what steered the scientific research on this particular issue [10-13]. Still, studies on mesoporous carbons are few compared to those carried out on mesoporous silicates or aluminosilicates [14-19], in spite of the well-known strengths of the carbon supports [20,21].

Nevertheless, most studies on the interaction of proteins with mesoporous materials concentrate in a rather narrow range, normally below 20 nm of average pore size. These pore sizes are well below those used in commercial supports (> 50 nm) and there are already studies questioning the suitability of nanostructured mesoporous materials to support proteins for real applications [22-24]. The debate on the effect of pore size on the performance of supported proteins is still far from conclusion due to two different factors. First, there is a lack of studies that evaluate the adsorption of biomolecules on similar supports with pore size distributions (PSDs) covering wider ranges of average pore sizes. Second, most studies focus only on the adsorption process rather than also accounting for the activity of the supported enzymes. The possibility of using a set of carbon materials to evaluate the effect of the pore size on the adsorption and activity of the resulting materials is not straightforward. It should be pointed out here that, due to the sensibility of the protein activity to the surroundings, changes on the surface chemistry or composition of the carbon materials could hinder the effect of their different textural properties [21,22].

Carbon xerogels obtained by the carbonisation of resorcinol (R)/formaldehyde (F) organic gels could be ideal candidates for this purpose [25]. Specifically, it has been demonstrated that the macro and mesoporosity of the carbon xerogels mimics those of the RF organic xerogels, which in turn can be tuned precisely over the entire nanoscale (from 2 nm to 1000 nm) by controlling a number of variables during their synthesis [26]. Microwave heating can be used to speed up the gelation and curing processes of the RF sols, thus lowering costs. Carbon materials resulting from the carbonisation of the RF organic xerogels are highly reproducible solids of very high purity, with negligible ash contents [27].

This work studies the effect of the pore size on the protein loading and activity using four carbon xerogels with relatively narrow PSD. The maxima of such PSD cover the whole range of mesoporosity (from 5 nm to 55 nm). Cytochrome c (cyt c) has been selected as a protein model due to the high purity of the product commercially available, its use in other immobilisation studies [19], and the deep knowledge of its structure and physicochemical properties [18]. Factors that are known to affect the adsorption process and the activity of the supported cyt c have been considered.

2. EXPERIMENTAL

2.1. Synthesis of the carbon xerogels

Four different carbon xerogels (CXs) were prepared for this study by using a method reported previously [25,26]. Essentially, organic xerogels were first synthesised by the polycondensation of resorcinol (Indspec, 99.6 % purity) and formaldehyde (Merck, 37 % aqueous solution, including 0.7 % methanol) (RF) in deionised water and methanol (VWR Chemicals, Normapur >99.9 % purity) using selected conditions (see below). A lab-made microwave device was set to heat the solutions up to 85 ºC for 3 h. Excess water was afterwards eliminated by continuing to heat the gel in the microwave oven until a mass loss

of over 50 % of the initial weight was achieved. Finally, organic xerogels were converted into CXs by heating them (25 g) in a quartz reactor (i.d. 30 mm) placed in a horizontal electrical tube furnace (Carbolite Type MFT 12/38/400), under a nitrogen flow rate of 100 ml min^{-1} up to 700 ºC at 50 ºC min^{-1} and 2 h dwell time. The carbonised RF carbon xerogel particles were cooled down to room temperature under the same nitrogen flow rate. Carbon xerogels were finally milled and sieved down to 1-2 mm particles.

Following previous studies, four variables related to the RF solutions are known to affect the porosity of the organic xerogels OXs (hence of the carbon xerogels CXs). These variables include the R/F ratio, the dilution ratio D (defined as the molar ratio between the total solvent and reactants, see [25]), the pH of the sol and the amount of MeOH contained in the formaldehyde solution (MeOH %). Table 1 gives the values of each variable for the different supports.

Table 1. *Experimental variables used in the preparation of the organic xerogels (OXs) that were carbonised to obtain the different carbon xerogels (CXs).*

Sample	R/F ratio	D[a]	pH	MeOH (%)[b]
CX-5	0.5	5.7	6.5	20
CX-15	0.1	6.7	6.25	10
CX-30	0.15	6.7	5.4	10
CX-55	0.3	8	6	12.5

[a] Dilution ratio (see text)

[b] Methanol content of the formaldehyde solution

2.2. Characterisation of the carbon xerogels

N_2 adsorption-desorption isotherms were performed at -196 ºC in a Micromeritics Tristar II volumetric adsorption system. Prior to measurement, samples were outgassed by heating overnight at 120 ºC under vacuum. The Brunauer–Emmett–Teller and Dubinin-Radushkevich models were selected to determine the BET surface area and micropore volume of the CXs from the nitrogen adsorption data, respectively.

The true density of the CXs (ρ_{He}) was measured with a Micromeritics AccuPyc 1330 pycnometer, using helium as the probe gas. The samples were outgassed at 120 °C overnight prior to analysis. The apparent density (ρ_{Hg}) was determined with mercury on a Micromeritics AutoPore IV apparatus. The samples were also outgassed at 120 °C overnight. The pore volume distributions were evaluated with a mercury porosimeter with a maximum operating pressure of 227 MPa. The percentage of open porosity (s) was calculated as:

$$s = [1-(\rho_{Hg}/\rho_{He})] \times 100 \qquad (1)$$

Elemental analysis of the samples was carried out in LECO apparatuses (LECO CHNS-932 and LECO VTF-900 to determine the oxygen content). The characterisation of the surface chemistry of the CXs included the determination of their point of zero charge (pH_{PZC}) [28], as well as XPS and TPD analyses. XPS measurements were carried out in a SPECS Phoibos 100 analyser using MgKα X-rays (1253.6 eV) at a power of 120 W and in a residual vacuum of 10^{-7} Pa. Measurements were made with the analyser in fixed transmission mode and normal to the plane of the sample. Analyser pass energy of 80 eV was used to collect broad scan spectra (0–1100 eV). The atomic percentages (atom %) of the different elements present in the approx. 10 nm upper layer probed by XPS were calculated from the survey spectra by considering the integrated areas of the main XPS peaks. Representative amounts (around 100 mg) of the CXs were tested. Typical standard deviation of the measurements is within ± 0.5 atom % of the reported values. C (1s) high resolution spectra were obtained using a pass energy of 25 eV. Peaks were deconvoluted fitting Gaussian-Lorentzian functions by means of CasaXPS software. Peak assignment was carried out following previous studies [29,30].

For TPD experiments, ca. 20 mg of the CXs were heated at 10 ºC min^{-1} under a He flow of 50 ml min^{-1} in the quartz reactor of an Autochem II apparatus (Micromeritics). Desorbed gases were analysed using an Omnistar (Pfeiffer Vacuum) mass spectrometer. TPD curves were obtained by plotting the desorbed CO and CO_2 (µmol g^{-1} s^{-1}) vs. the temperature (ºC). TPD curves were

deconvoluted using homemade software, following the criteria reported in previous studies [31,32].

2.3. Immobilisation of biomolecules

Cytochrome c (cyt c) from bovine heart (Sigma-Aldrich, ref C2037) was selected for the immobilisation experiments due to its high purity (≥ 95 %; 12327 Da). Solutions of cyt c (0.5 g L^{-1}) were prepared in different pH buffers: phosphoric acid/sodium phosphate (pH 3), sodium phosphate (pH 6) and sodium carbonate (pH 10). The total ionic strength of all buffer solutions was set to 100 mM. CXs particles of 1-2 mm in size were suspended in the buffer solutions 24 h prior their use as biomolecules supports. In a typical immobilisation experiment, 10 mg of a CX were suspended in 5 mL of the cyt c solution prepared in the selected buffer. This was done in screw top vials that were then orbitally shaken at 200 rpm and kept at 30 ºC in an incubator shaker (TH 15 model form Edmund Bühler GmbH)) for up to 96 h. Aliquots were periodically withdrawn from the supernatant solution to quantify the cyt c content remaining in the liquid phase. Quantification of the cyt c in the solutions was performed by UV-vis spectrometry (Shimadzu UV-2401 PC scanning spectrophotometer). Absorbances at ca. 410 nm (ε = 105 M^{-1} cm^{-1}) were used to determine the concentration of cyt c in a given solution. In addition, Bio-Rad protein assays (Bio-Rad Labs, ref. 500-0002) were carried out to determine the amount of protein present in the initial and final (equilibrium) solutions [33]. This protein quantification methodology is a standard procedure that was performed on separate experiments after 24 h and 96 h of immobilisation time. At least, duplicates of each immobilisation experiment were carried out simultaneously to attain statistical soundness. Also, blank tests (i.e., cyt c solutions without carbon supports) were also performed in order to test the stability of the proteins under the immobilisation test conditions. Once prepared, the resulting solids were maintained in buffer suspensions (pH 6) inside a refrigerator (4 ºC) for further use.

2.4. Activity assays

Cytochrome c, which is known to present peroxidic activity, was tested on the oxidation of 2,2'-Azino-bis(3-ethylbenzthiazoline-6-sulfonic acid) diammonium salt (ABTS^{TM}) (Sigma-Aldrich, ≥ 98 % HPLC) by following spectrophotometrically the absorbance of the band at 420 nm (ε = 36000 M^{-1} cm^{-1}) [32-34]. Unsupported protein assays were carried out with cyt c solutions (0.5 g L^{-1}) in pH 3, 6 and 10 buffers (see above). ABTS solutions (1 mM) were prepared in buffers covering a wider pH interval, from 2-10 (pH 2 and 3 buffers: phosphoric acid/sodium phosphate; pH 4 and 5 buffers: sodium acetate; pH 6, 7 and 8 buffers: sodium phosphate; and pH 10 buffer: sodium carbonate; all 100 mM total ionic strength buffers). Equal amounts (1.9 mL) of the ABTS (1 mM) and H_2O_2 (VWR Chemicals, Normapur, about 30 %) (10 mM) solutions buffered at pH 4 (100 mM total ionic strength) were mixed in a UV cuvette. 0.2 mL of the cyt c solution was finally added to sum a total reaction volume of 4 mL. The change in the absorbance at 420 nm was measured continuously. The activity of the unsupported cyt c was calculated from the slope of the linear part of the absorbance vs. time plot. One unit of cyt c activity (U) is defined as the amount of protein that oxidises 1 μmol of ABTS to coloured products per minute. At least, two experiments under the same conditions were carried out.

In the case of the cyt c supported on the carbon xerogels, 10 mg of the solid particles loaded with cyt c (see Section 2.3) were suspended, at a controlled time, in screw top vials containing a mixture of 5 mL of ABTS (1 mM, pH 4 buffer) and 5 mL of H_2O_2 (10 mM, pH 4 buffer) (i.e., total volume of reaction = 10 mL). Aliquots of the supernatant solution were extracted at selected times to measure the absorbance at 420 nm. After measuring, volumes were returned to the original solution. At least 6 points (i.e., 6 extractions) were carried out in every activity assay. The activity of the cyt c/CX materials was then calculated from the slope of the absorbance vs. time plot. A minimum of two experiments were run in parallel for each activity test.

The reusability of the materials was evaluated by measuring the change in activity after successive cycles of reaction using ABTS as substrate. Both ABTS and H_2O_2 solutions were replaced in each cycle, which was carried out until complete ABTS oxidation. Two successive washes of the biocatalysts were performed under vortex shaking (30 Hz) for 5 min in 5 mL pH 6 buffer (100 mM) before each cycle.

3. RESULTS AND DISCUSSION

3.1. Carbon xerogels characteristics

Figure 1 shows the nitrogen isotherms of the four CXs synthesised in this study. They are all type IV isotherms, which are characteristic of mesoporous materials. The hysteresis loop of samples CX-15, 30 and 55 is very similar, with a sharp decrease of the desorption branch (H1 hysteresis loop type) at p/p^0 values well over 0.8. The hysteresis loop of the CX-55 sample is hardly perceptible, which indicates that mesopores in this sample are too wide to be detected by N_2 adsorption. On the other hand, the hysteresis loop closing point gradually moves to lower p/p^0 values from CX-55 to CX-5, suggesting a decrease of the average mesopore size of those samples. The desorption hysteresis in the isotherm of sample CX-5 is however much less steeper resembling a H4 loop-type. This denotes a wider distribution of mesopores for this particular carbon xerogel. Selected textural parameters obtained (or calculated) from the adsorption isotherms are presented in Table 2. As expected from the isotherms (Figure 1), the micropore volumes (VDR) of all samples are almost identical. Hence, since the BET surface area is mainly controlled by their microporosity, the S_{BET} values of the CXs are very similar.
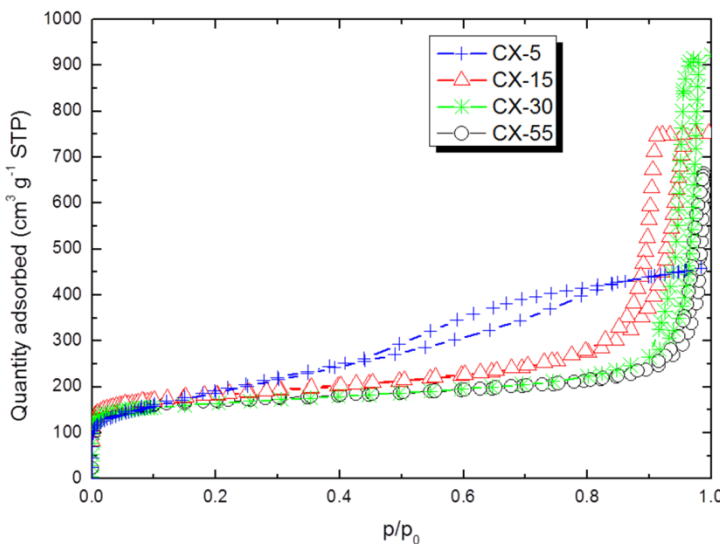
Figure 1. N_2 adsorption/desorption isotherms at -196 ºC of the CXs.

Table 2. Textural parameters of the carbon xerogels.

Sample	S_{BET} $(m^2\ g^{-1})$	V_{total}[a] $(cm^3\ g^{-1})$	V_{DR}[b] $(cm^3\ g^{-1})$	V_{meso}[c] $(cm^3\ g^{-1})$	ρ_{He} $(g\ cm^{-3})$	V_{Hg}[d] $(cm^3\ g^{-1})$	ρ_{Hg} $(g\ cm^{-3})$	s[e] $(\%)$
CX-5	660	0.71	0.23	0.48	1.69	-	1.05	38
CX-15	679	1.16	0.26	0.90	1.75	0.88	0.61	65
CX-30	625	1.42	0.24	1.18	1.78	1.32	0.46	74
CX-55	640	0.78	0.24	0.54	1.74	1.48	0.43	75

[a] Calculated at $p/p^0 = 0.99$

[b] DR: Dubinin-Radushkevich model

[c] $V_{meso} = V_{total} - V_{DR}$

[d] Hg intrusion pore volume corresponding to the pore size distributions shown in Figure 2

[e] Open porosity (eq. 1)

Due to the mesoporous nature of the CXs under study, Hg intrusion was considered a more adequate technique than N_2 adsorption at -196 ºC to ascertain the pore size distributions of the samples (Figure S1 and Figure 2). The mercury pore size distributions of Figure 2 reflect the versatility of the here reported route for the preparation of designed carbon xerogels. Thus, relatively narrow pore size distributions were obtained for the CX-55, CX-30 and, especially, CX-15. The maximum of those distributions (in nm) were used for

sample labelling, i.e., CX-30 corresponds to the carbon xerogel having a pore size distribution with a maximum centred at ca. 30 nm. The pore size distribution of the CX-5 sample reaches the lower limit of the technique (5.5 nm, Figure 2). Still, assuming a curve with a normal distribution shape (similar to those obtained for the rest of carbon xerogels), it seems that the maximum of the mesopore size distribution would be located near 5 nm (see inset in Figure 2). A DFT pore size distribution derived from the nitrogen isotherm of this particular sample would corroborate this (Figure S2), although, as expected from the shape of the isotherm (Figure 1), the N_2 PSD of CX-5 (Figure S2) is wider than that of Hg intrusion (Figure 2). The volume of the pores with sizes comprised within the Hg PSD of Figure 2 was also calculated for CX-15, -30 and -55. Results are included in Table 2. For CX-15, the mesopore volume estimation from N_2 adsorption isotherms agrees very well with the pore volume calculated from Hg intrusion. Those pore volumes start to deviate as the PSD moves to higher values (CX-30). For CX-55, such comparison makes little sense since the maximum of the Hg PSD is located in the macropore region (Figure 2).
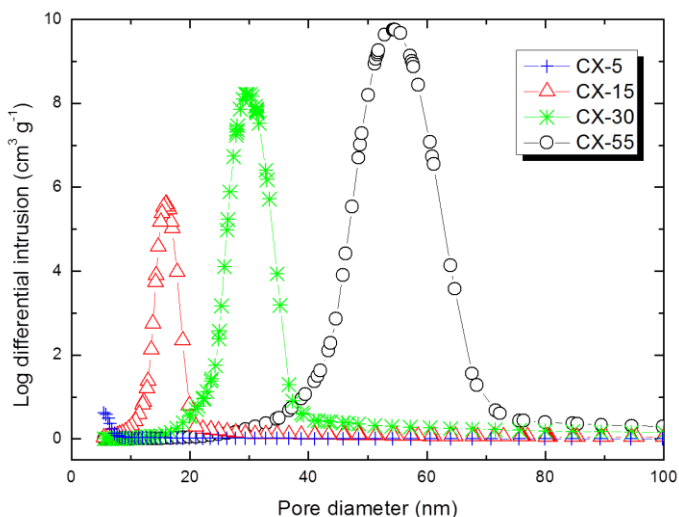
**Figure 2.** *Pore size distributions of the CXs as measured by Hg intrusion porosimetry.*
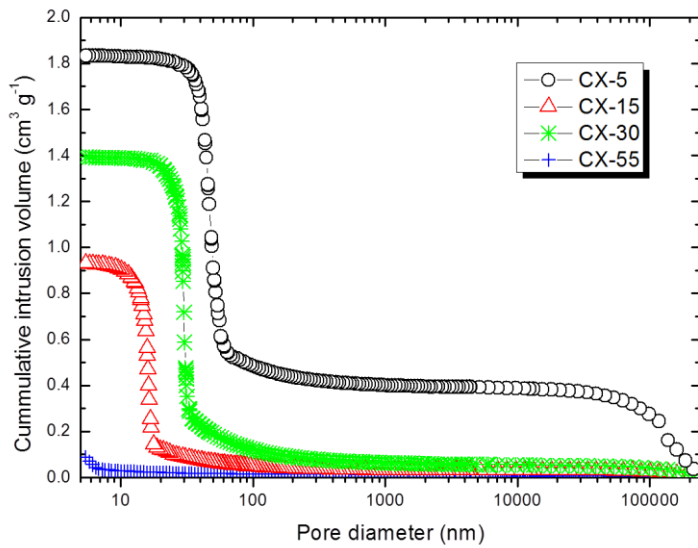
**Figure S1.** *Hg intrusion volumes of the CXs.*
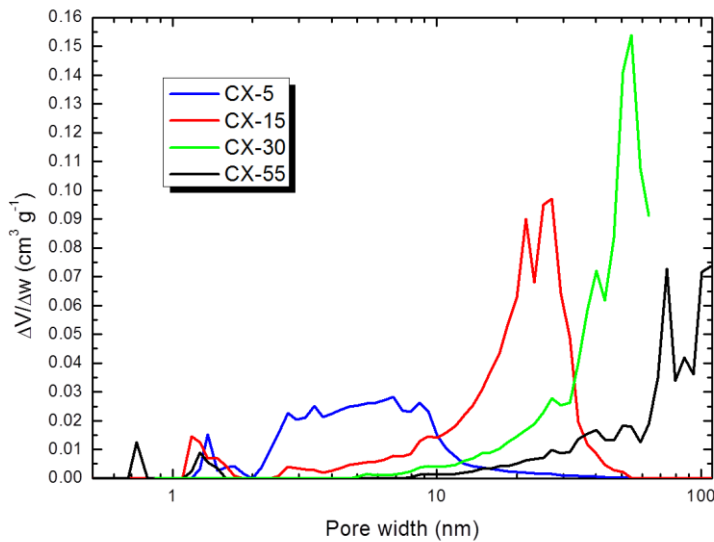
Figure S2. *Pore size distribution of the CXs as determined by DFT modelling of the N_2 adsorption isotherm.*

The different synthesis conditions of the organic xerogels counterparts brought about materials with RF condensed clusters increasing in size and/or having higher inter-cluster distances from CX-5 to CX-55 [35]. As a consequence, the apparent density (ρ_{Hg}) of the carbon xerogels decreases from CX-5 to CX-55 (Table 2). Since the true density (ρ_{He}) is very similar for all the carbons, the percentage of open porosity differs strongly from CX-5 to CX-55 (Table 2).

As for the chemical properties, all techniques rendered similar, if not identical results for all CXs. Thus, starting with the elemental analysis results, all materials were mainly composed of carbon (approx. 95 % for all samples), with small amounts of oxygen (ranging from 3-3.5 %) and hydrogen (1.5 % for all samples). The pH_{PZC} of all carbons was around 8.5.

XPS analyses also showed very similar compositions on the surface of all carbon xerogels (Table 3). Differences in C and O atom% on three of the carbon supports (CX-15, -30 and -55) are within the experimental error of the technique. CX-5 seems to have a slightly higher oxygen concentration on its surface than the rest of CXs. In spite of such a rather low surface oxygen concentration, carbon chemical bonding environment information was obtained by measuring C1s high resolution XPS profiles of the carbon xerogels. They were found to be almost identical for all samples (Figure 3). Figure S3 shows the deconvolution of one of those C1s profiles (that of CX-5), where contributions from C-OR (R including H), C=O and O=C-OR (R including H) were included at +1.5, +2.6 and +4.5 eV of the $C(sp^2)$ peak at 284.4 eV, respectively. The last contribution (O=C-OR) which amounts for ca. 5 % of the total C1s area is possibly overestimated since it exhibits a rather higher peak width (FWHM) than the rest of contributions.
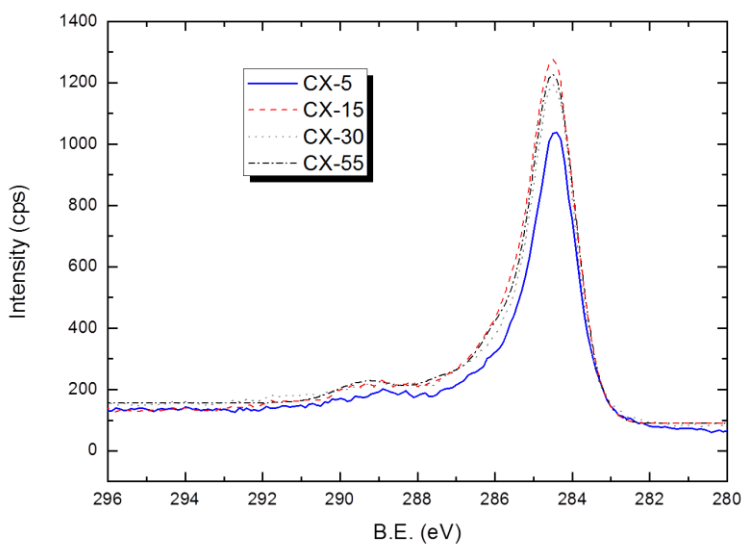
Figure 3. *High resolution C1s XPS profiles of the four carbon supports.*
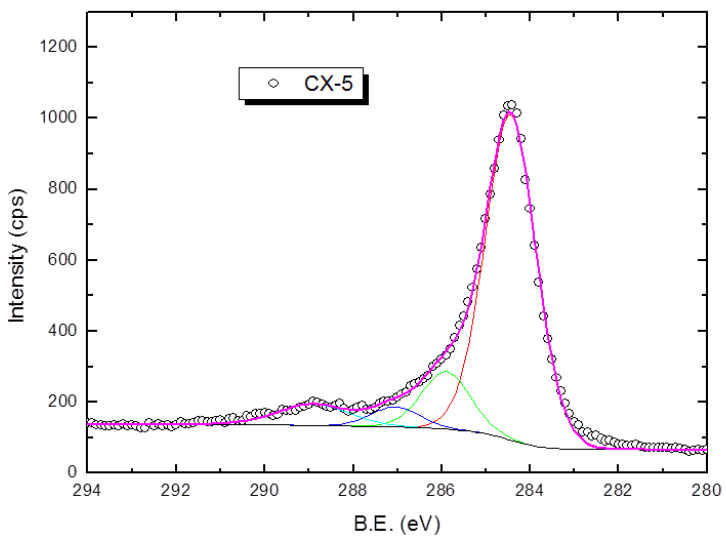
Figure S3. *Deconvolution of the high resolution C1s XPS profile of CX-5.*

Table 3. *XPS and TPD results on the composition of the carbon xerogels.*

Sample	XPS Atom%		TPD CO ($\mu mol\ g^{-1}$)	TPD CO_2 ($\mu mol\ g^{-1}$)
	C	O		
CX-5	94.2	5.8	243	159
CX-15	96.0	4.0	255	247
CX-30	95.8	4.2	277	283
CX-55	95.8	4.2	260	217

TPD analyses were also carried out. The CO and CO_2 profiles of all carbons are shown in Figure 4. The total amounts of CO and CO_2 obtained by integration of the emission profiles for the different carbon xerogels are also collected in Table 3. Values are again very similar between samples. They are very low when compared with the emissions measured for other carbon materials, including activated carbons [30]. Figure S4 shows the deconvolution of the CO and CO_2 profiles of CX-55, which is representative for the rest of them. In the case of the CO TPD profile, five different peaks were selected to contribute to the overall signal. The two peaks at temperatures below 400 ºC are more likely related to the decomposition of carbonyl groups in ketones and aldehydes [30,36]. The three peaks contributing to the maximum CO emission signal (> 400 ºC) are normally ascribed to the decomposition of carboxylic anhydrides (600-610 ºC), phenols (ca. 730 ºC) and carbonyl/quinones (ca. 830 ºC). Analysis of the CO_2 emission signal included four peaks, the main one at 250 ºC corresponding to strongly acidic carboxylic groups. The peaks at approx. 400, 550 and 740 ºC are normally assigned to the decomposition of less acidic carboxylic groups, carboxylic anhydrides and lactones, respectively [30].
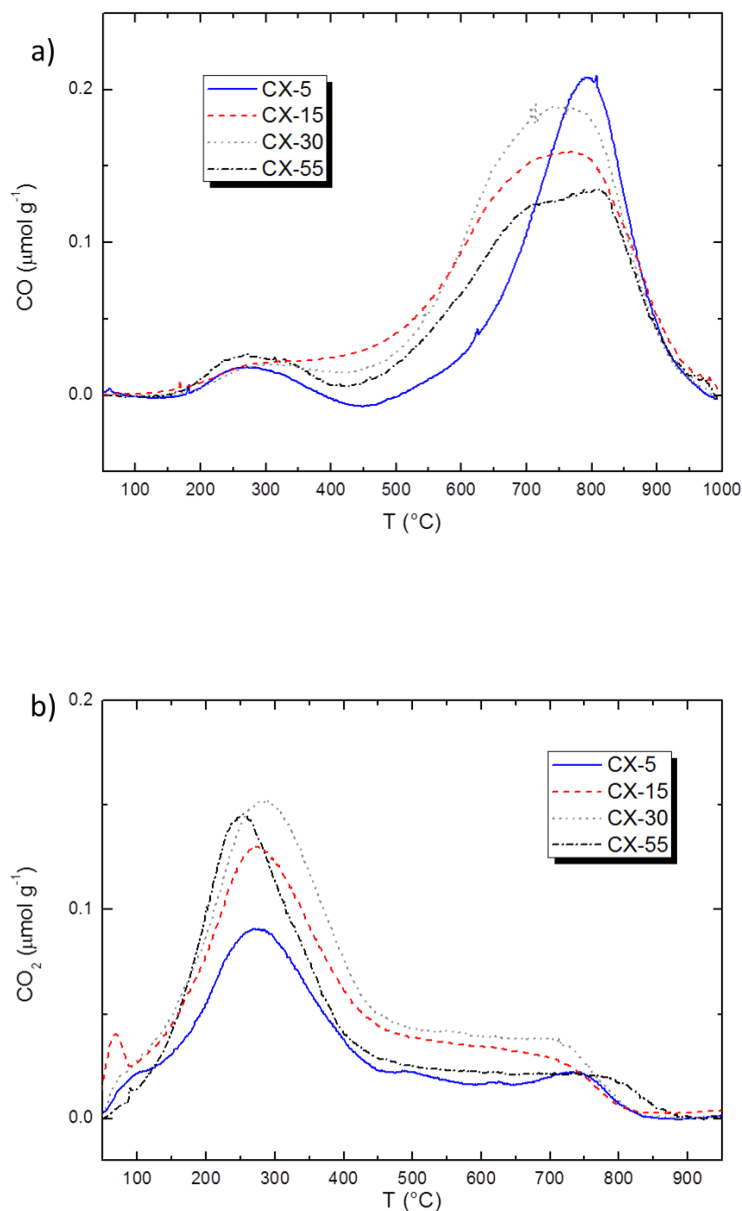
Figure 4. TPD (a) CO and (b) CO$_2$ profiles of the CXs.
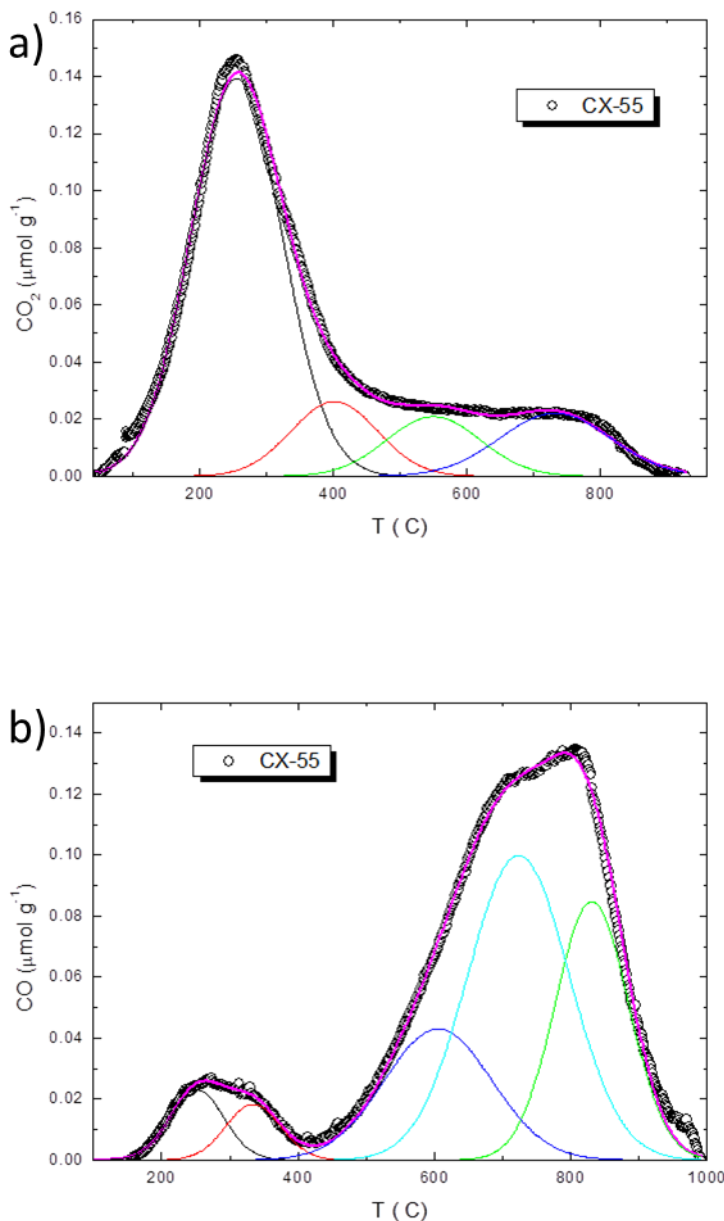
Figure S4. *Deconvolution of the TPD (a) CO and (b) CO$_2$ profiles of the CX-55.*

In summary, the characterisation of the CXs points out that they differ in their textural properties, i.e., mesopore size distribution and mesopore volumes, but do not differ on their surface properties. The surface chemistry of the supports should be considered almost identical. Minor differences should be

attributed to the carbonisation process rather than to the synthesis of the organic xerogels. Therefore, eventual differences in the cyt c adsorption capacities of the CXs and/or the activity of the immobilised cyt c should be ascribed to differences in the textural properties of the carbon supports.

3.2. Immobilisation of Cytochrome c on the carbon xerogels

The adsorption of biomolecules on porous supports could be affected by a number of factors including ionic strength, particle size, temperature, shaking conditions and pH. In order to minimise the number of influencing factors and to concentrate on the effect of pore size of the carbon xerogels, preliminary tests were carried out to fix some of the experimental conditions for the immobilisation tests. Accordingly, ionic strength, temperature, shaking, cyt c concentration, mass of the support/solution volume ratio and particle size were set for all immobilisation experiments, as detailed in Section 2.3. Only the influence of the pH of the cyt c solution on the performance of the supports was thus considered.

Figure 5 shows the capacities of the different supports when using cyt c solutions (0.5 g L^{-1}) in three different buffers (pH 3, pH 6 and pH 10). The protein loadings reported in Figure 5 were measured after 24 and 96 h of immersion of the CXs particles in the cyt c solutions. Both values are spectroscopic determinations, i.e., calculated from the absorbance of the supernatant liquid at 410 nm. Protein uptake values measured by using the Bio-Rad method were found to match the spectroscopic determination (both at 24 h and 96 h, Figure S5), within experimental error. The adsorption experiments were carried out up to 96 h in most cases due to practical considerations, i.e., the increase on the support capacities at higher times of exposure was very low (less than 5 % of the values at 96 h) as tested randomly using some of the carbon xerogels. It should be also noted that the stability of pH 10 unsupported cyt c solutions is compromised beyond 96 h, under the experimental conditions of adsorption used.
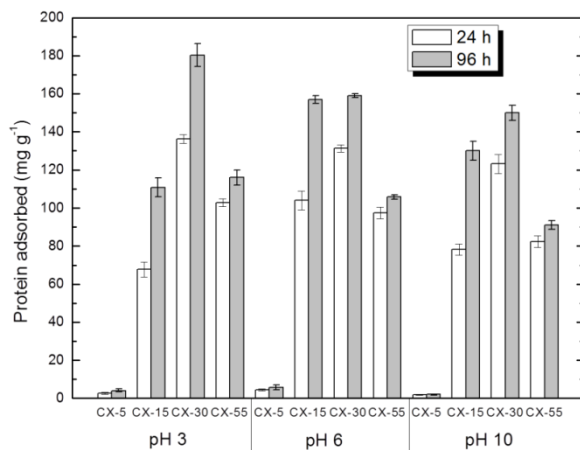
Figure 5. *Cyt c loadings (average values and errors), expressed as mg of biomolecule per gram of support, on the four CXs after 24 and 96 h of adsorption. Experimental conditions: initial concentration of the solutions, 0.5 g cyt c L^{-1}; temperature, 30 ºC; ionic strength of the different buffers, 100 mM.*
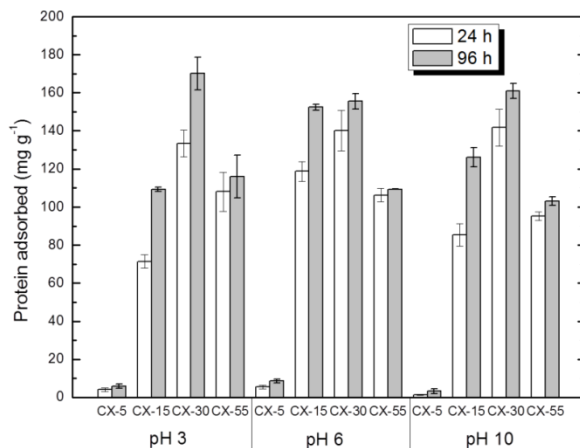

Figure S5. *Cyt c loadings (average values and errors), expressed as mg of biomolecule per gram of support, on the four CXs after 24 and 96 h of adsorption as determined by the Bio-Rad method. Experimental conditions: initial concentration of the solutions, 0.5 g cyt c L^{-1}; temperature, 30 ºC; ionic strength of the different buffers, 100 mM.*

Results of Figure 5 indicate that cyt c is hardly adsorbed at all in CX-5, with capacities well below 10 mg g^{-1}. For this particular support, immobilisation time was extended up to 144 h at pH 6, but the amount adsorbed was virtually the same. In this case, pores of 5 nm seem too tight to host cyt c (4 nm of spherical diameter) [18]. Results obtained on the immobilisation of cyt c on nanostructured mesoporous carbons would contradict this finding. Thus, values as high as ca. 230 mg g^{-1} were obtained on a CMK-3 mesoporous carbon with an average pore size of 4.5 nm [10]. However, a closer inspection of the results reported in that work reveals that such high values were obtained when using solutions with a very high cyt c concentration (4 g L^{-1}). The capacity of the same support when using 0.5 g L^{-1} solutions of is lower, between 150-190 mg g^{-1}. Those values are still more than an order of magnitude higher than the loadings of CX-5. Cyt c loadings on mesoporous silica with average pore sizes around 5 nm are in the 40-80 mg g^{-1} interval [15,18], albeit the pioneering work of Balkus Jr. group [16] reports loadings very similar to ours (6-10 mg g^{-1}). It should be clear that one main difference in our adsorption studies with respect to the use of nanostructured mesoporous systems is the particle size of the supports, i.e., tens of microns in the case of nanostructured mesoporous carbons or silicas vs. 1-2 mm for the CXs used in this work (see Experimental Section). Particle size and even particle shape are known to affect strongly the adsorption of biomolecules [37]. Furthermore, compared with carbon xerogels, the diffusion of the biomolecules in ordered mesoporous carbons would be enhanced by elimination of pore tortuosity. The straight mesoporous channels present in those ordered mesoporous carbons would facilitate the diffusion of the molecules and, therefore, could increase the adsorption capacity of the support.

The maximum capacities (at 96 h) were attained when using the CX-30 carbon xerogel in the three different pH environments; next comes CX-15 and, finally, CX-55. Although the adsorption studies on carbon materials with average pore sizes > 30 nm are very scarce, Vijayaraj et al. found capacities of less than 10 mg g^{-1} for a series of nanostructured carbon materials with average pore sizes of 30, 50 and 150 nm [38], much lower thus than the capacities of the CX-

30 and CX-55 (Figure 5). As just mentioned in the case of CX-5, the immobilisation conditions, particularly the particle size and pore geometry might be crucial to understand the differences between the capacities of CXs and the supports of [38].

Since the CXs differ not only in their average pore size but also in the pore volume, protein adsorption results expressed in a volumetric basis are relevant (Table 4). Pore volumes calculated from Hg intrusion (V_{Hg}, Table 2) were selected for such calculations for all supports but CX-5, for which the mesopore volume estimation from the N_2 isotherm was used (Vmeso, Table 2). An alternative, more intuitive way of depicting the influence of the different pore volumes of the supports is the calculation of the pore filling percentages. An estimation of the cyt c density can be drawn from the protein volume and its molecular mass [39,18]. Thus, taking values of the unit cell of the horse heart cyt c (and assuming that they are essentially the same for the bovine heart cyt c used here) [39], a density of 0.17 g cm^{-3} results. Pore filling percentages can be thus estimated for the different carbon xerogels (Table 4, values in parentheses). These new values indicate that not only CX-30 but also CX-15 are very effective supports for cyt c hosting in terms of pore filling, with values ≥ 75 % for the three pH conditions. The porosity of CX-55, on the other hand, is only partially filled by cyt c.

Table 4. *Average values of the protein loadings (volumetric basis) on CXs at 96 h. Pore filling percentages are in parentheses.*

Sample	Protein loading (mg cm^{-3})		
	pH 3	pH 6	pH 10
CX-5	8 (5%)	12 (7%)	4 (2%)
CX-15	123 (73%)	174 (100%)	144 (85%)
CX-30	137 (80%)	120 (70%)	114 (70%)
CX-55	103 (61%)	71 (42%)	61 (36%)

Results of Figure 5 do not show a clear effect of the pH of the cyt c buffer solution on the final protein uptakes of the carbon xerogels. In any case, the maximum adsorption capacities are not happening at pHs close to the isoelectric point of cyt c (pI = 10.5). This finding contradicts previous results of different proteins adsorption on nanostructured mesoporous carbons [10,11,40]. The little effect of the solution pH on the final cytc loading on the CXs suggests that electrostatic interactions are not playing a significant role in the adsorption in this particular biomolecule/support system. If electrostatic interactions were governing the adsorption, in accordance with the cyt c isoelectric point and the carbon xerogels pH_{PZC} (ca. 8.5), maximum and minimum protein loadings would be expected at pH 10 and pH 3, respectively, which is not the case (Figure 5). At pH 10, the solid surface is negatively charged whereas the cyt c molecules are positively charged. On the other hand, at pH 3, both CXs surface and cyt c molecules would be positively charged. The irrelevance of the electrostatic interactions here might be understood in terms of the high carbon content of the carbon xerogels or, alternatively, the lack of a rich surface chemistry despite of its basic character [41]. For these particular materials, protein/carbon surface hydrophobic interactions would control the adsorption process. Such hydrophobic interactions are known to be strongly affected by the total ionic strength of the protein solution, the higher the ionic strength the higher the level of interaction [42]. To confirm this hypothesis, further immobilisation experiments were carried out on the CX-15 carbon xerogel using cyt c dissolved in a pH 3 phosphoric acid-sodium phosphate buffer of 1 mM ionic strength. The amount adsorbed at 96 h decreased dramatically from 111 mg g^{-1} (100 mM, Figure 5) to 36 mg g^{-1} (1 mM). A similar effect has been reported for the adsorption of cyt c on a nanostructured organosilicate [18]. In any case, this very same argument should be valid for the adsorption of cyt c on nanostructured mesoporous carbons, since they are virtually pure carbon materials with hydrophobic surfaces [8,9,13]. The maximum loadings obtained on those materials when working with solutions pH near the isoelectric point of the proteins is ascribed to the effective molecular diameter of the adsorbate [10,11]. Thus, charged biomolecules would experience adsorbate-adsorbate

repulsive forces that would reduce the amount of protein adsorbed on a given volume.

A final comment on the adsorption results of cyt c on the carbon xerogels shown in Figure 5 is devoted to the differences observed in the protein uptakes measured at 24 h and 96 h. Excluding CX-5 from this discussion, CX-15 and CX-30 show higher protein loadings at 96 h, whereas CX-55 values at 24 h and 96 h are very similar at the three pH buffers, thus suggesting a more favourable kinetics of cyt c adsorption on this meso-macroporous carbon. Results of a more detailed study carried out at pH 10 are shown in Figure 6. Adsorption of cyt c on the three supports was relatively fast during the first hours and slowed down to attain the equilibrium (or, at least, to observe minimum variations in the quantity of protein adsorbed) [43]. The time required to attain the adsorption equilibrium is considerably shorter for CX-55 than for the other two CXs. A closer inspection of the early stages of adsorption is shown in Figure S6. During the first hour of adsorption, the rate of protein loading on both CX-55 and CX-30 is very similar, and significantly faster than the cyt c adsorption on CX-15.
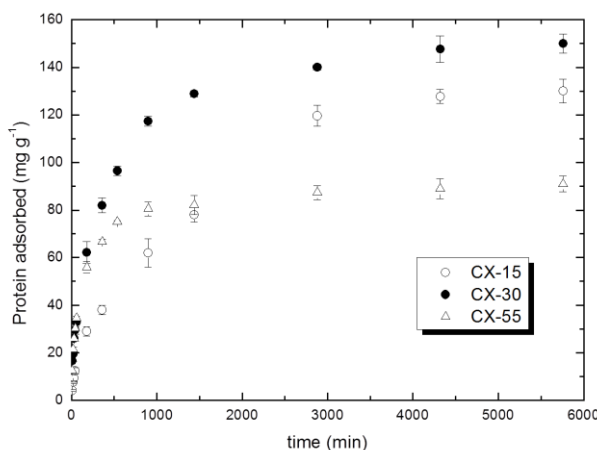
Figure 6. *Kinetics of adsorption of cyt c on CX-15, CX-30 and CX-55. Experimental conditions: initial concentration of the solutions, 0.5 g cyt c L^{-1}; temperature, 30 ºC; pH 10 (100 mM ionic strength).*
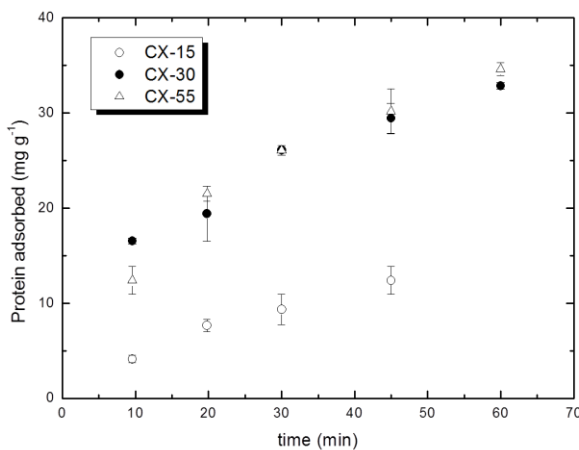
Figure S6. *Detail of Figure 6 corresponding to the initial stages of adsorption.*

Assuming that the adsorption of the cyt c on the CXs was diffusion controlled, two relatively simple models were used to fit the experimental results of Figure 6, namely the homogeneous diffusion model [43,44]:

$$\ln(1-F)= \ln(6\pi^{-2}) - \pi^2 D_p t R^{-2} \qquad (2)$$

and the parabolic diffusion model [44]:

$$F t^{-1}= 4 D_p^{1/2}\pi^{-1/2}R^{-1}t^{-1/2} - D_p R^{-2} \qquad (3)$$

where F is the fractional loading of cyt C on the CX at time t, D_p is the diffusion coefficient of cyt c on the adsorbent and R is the particle radius (0.05 cm for the CXs, assuming spherical particles). The homogeneous diffusion model (eq. 2) was found to fit reasonably well the experimental points of Figure 6 obtained at t ≥ 60 min, whereas the parabolic diffusion model (eq. 3) fitted well almost the whole set of points (Figure S7). Results of the D_p values obtained using both models are collected in Table 5. All coefficients are much lower than

that of unsupported cyt c in aqueous solution ($2 \cdot 10^{-6}$ cm^2 s^{-1} at 30 ºC and 100 mM ionic strength) [45]. The information of the two models is quite different. The homogeneous model establishes no significant differences between the diffusion coefficients of the cyt c on the three supports. This situation corresponds to the last stages of adsorption in which diffusion of cyt c is most likely hindered by previously adsorbed biomolecules. On the other hand, the estimation of the Dp based on the parabolic diffusion model reveals a clear difference between the supports, which in turn correlates with the pore size distributions of the CXs. These Dp values would be then closely linked to the pore diffusion of the cyt c on the supports.
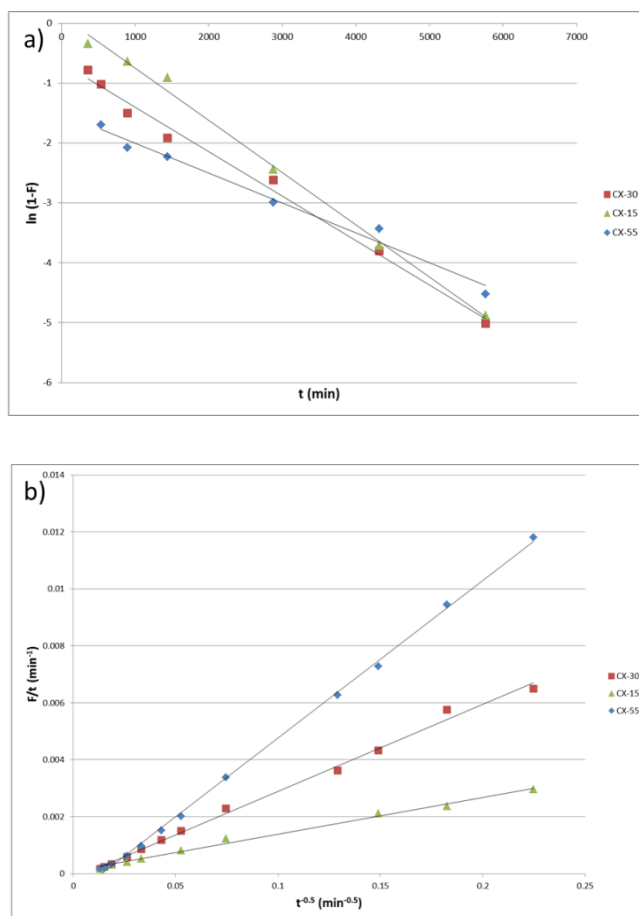
Figure S7. *Curve fitting of the kinetic experimental results of Figure 6: a) homogeneous diffusion model (eq. 2); b) parabolic diffusion model (eq. 3).*

Table 5. *Diffusion coefficients of cyt c adsorption on CXs calculated from the homogeneous and parabolic diffusion models Correlation coefficients of the model fitting are also included.*

Sample	Homogeneous Diffusion (eq. 2)[a]		Parabolic Diffusion (eq. 3)	
	D_p x 10^9 cm^2 s^{-1}	R^2	D_p x 10^9 cm^2 s^{-1}	R^2
CX-15	3.8	0.994	1.4	0.995
CX-30	3.1	0.991	7.7	0.996
CX-55	2.5	0.982	25	0.999

[a] For experimental points obtained at t ≥ 60 min (see text)

3.3. Activity of the supported cyt c

Cyt c is known to catalyse the oxidation of different substrates by H_2O_2 [32-34]. Figure S8 shows the activity profiles of the cyt c used in this work when dissolved in pH 3, pH 6 and pH 10 buffers. Maximum activity values were obtained for the substrates solution buffered at pH 4 [33]. Solutions of cyt c with different pH were tested since it is known that enzymes preserve "memory" of the last aqueous solution they had been dissolved in [46]. As a consequence, in spite of the pH of the solution of the substrates, different enzymatic activities are expected from solutions of the same enzyme prepared at different buffers. This can be seen in Figure S8; the effect of the pH of the cyt c solution is clear, with pH 10 cyt c solutions showing a significantly better performance (using a pH 4 reactants solution) than unsupported cyt c at pH 6 and pH 3.
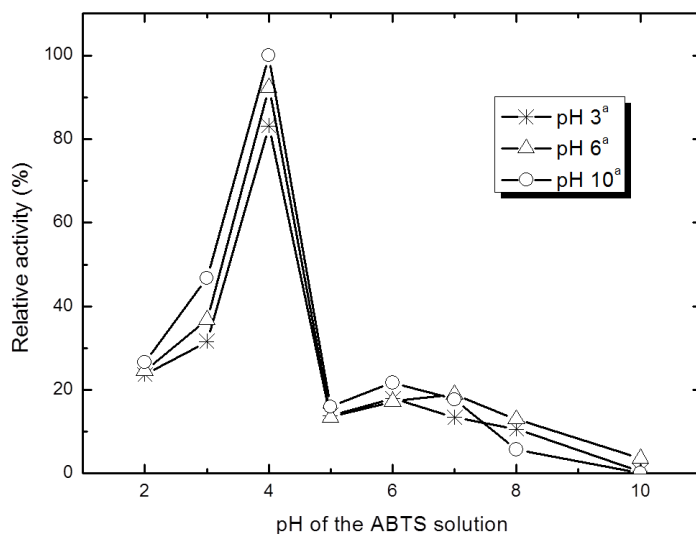
Figure S8. *Activity (expressed as relative activity; 100 % relative activity corresponds to 1.2 Units per mg cyt c) of 0.5 g L^{-1} cyt c solutions at 30 ºC buffered at a three different pH (100 mM). The activity tests were carried out at different pH, as specified in the x axis of the graph.*

Immobilised catalysts reproduced such trend (Figure 7), i.e., maximum activities (at pH 4) were obtained when the adsorption of the cyt c on the CXs was carried out at pH 10. It should be noticed that the activities of cyt c/CX-5 were also tested in spite of the very low protein uptakes on this particular material (Figure 5). This leads us to point out a startling result. For a given immobilisation pH, the activity (per gram of support) of all the cyt c/CXs systems is very similar (Figure 7) regardless the huge differences in their protein loadings (Figure 5). In other words, most of the immobilised cyt c on CX-15, -30 and -55 is not operational. In order to clarify this, increasing amounts of cyt c were loaded on the CX-15 and CX-30 supports and the activities of the resulting materials were tested. Activity results (Figure 8) are expressed both in U (g of support)$^{-1}$ and U (mg cyt c)$^{-1}$. The activity results expressed per gram of support were similar for both supports regardless the amount of cyt c adsorbed on them. However, when Units per mg of cyt c are used, the activities improved significantly at low loading values, especially for the CX-15 materials. These

activity values are still very far from those of unsupported cyt c solutions, ca. 1 U (mg of cyt c)$^{-1}$. Actually, only CX-5 biocatalysts have similar activities per milligram of cyt c than that of unsupported cyt c (Figure S9 and Figure S8). It should be mentioned here that blank tests were also carried out with unloaded (pristine) CXs and no activity was detected. These observations would indicate that either there is a limited accessibility of the substrates to the immobilised proteins or that inactivation of cyt c occurs after immobilisation. A series of tests were then devised to understand the lack of activity of most of the cyt c on the CX-15, 30 and 55.
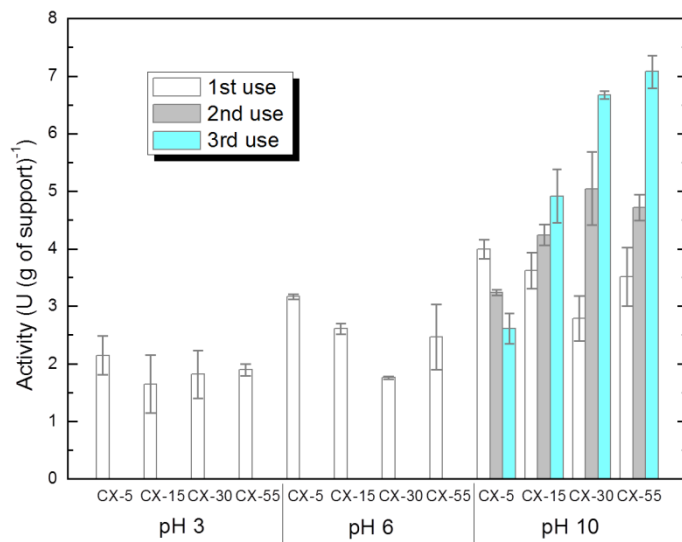
Figure 7. Activities expressed as Units per gram of support. The biocatalysts were prepared by immobilisation of cyt c on CXs at different pH (pH 3, 6 and 10). All the activity tests were carried out at pH 4.
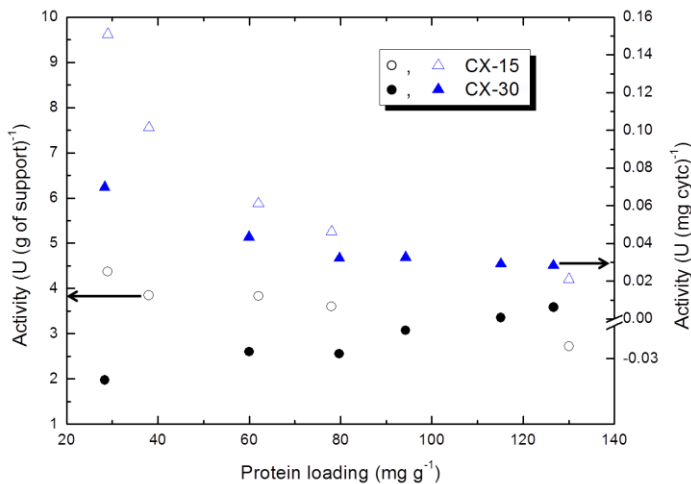
Figure 8. *Activities of CX-15 and CX-30 materials prepared by immobilisation of different quantities of cyt c on them at pH 10. Circles correspond to activities expressed in Units per g of support (left y axis), whereas triangles correspond to activities expressed in Units per mg of cyt c (right y axis). All the activity tests were carried out at pH 4.*
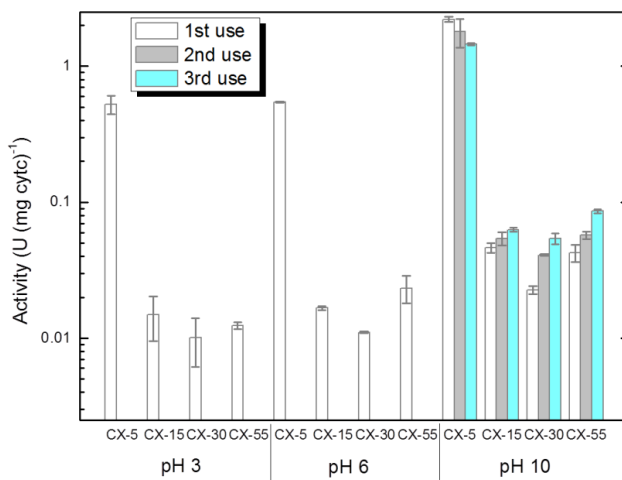
Figure S9. *Same as Figure 7, but activities expressed in Units per mg of cyt c.*

Two cycles of reuse were carried out with the biocatalysts prepared by immobilisation of cyt c solutions buffered at pH 10 (see Section 2.3). Results are also shown in Figure 7. The activity values followed a clear trend, hence increasing substantially after every consecutive cycle for CX-15, CX-30 and CX-55, but decreasing in the case of the CX-5 support. This suggests that successive washings of the heavily loaded supports would "clean" the access to the cyt c stored in the pores. However, it should be mentioned here that such "cleaning" effect would entail a partial lixiviation of the supported enzyme. The amounts of cyt c in the lixiviates were close to the detection limits of the spectrophotometry method used in this work, amounting less than 0.001 mg cyt c mL^{-1} in every wash for all the materials tested. In other words, the amount of cyt c lixiviated from the supports was less than 1 mg of cyt c per gram of support. This number is only relevant for the CX-5 biocatalysts, whose loadings are below 10 mg of cyt c g^{-1} (Figure 5)

A final experiment was carried out with all supports loaded at pH 10 in which the amount of ABTS was increased by an order of magnitude (10 mM) in order to ease the diffusion of the (relative) big reactant inside the porous network. The activity values obtained (Figure 9) show a trend that mimics that already described when successive cycles of reuse were carried out (Figure 7, pH 10). Thus, the CX-15, -30 and -55 systems were more active at higher concentrations of ABTS, whereas the activity of the CX-5 clearly decreased. On the other hand, the activity of unsupported cyt c diminished as the ABTS concentration in the solution increased (see inset in Figure 9).
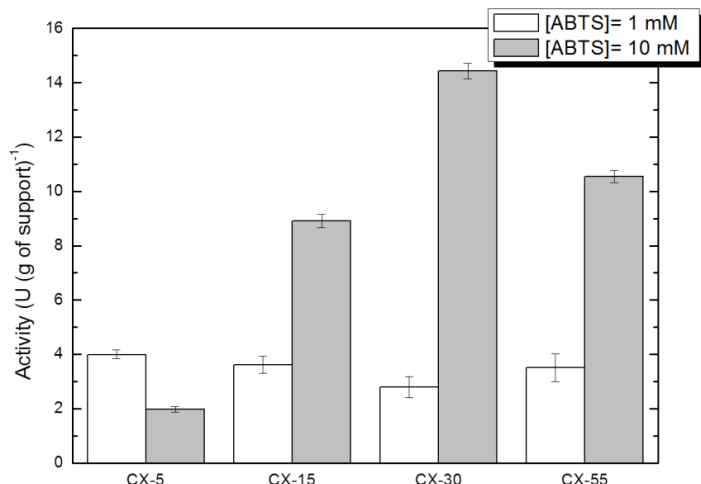
Figure 9. *Effect of the ABTS concentration on the activity (expressed as Units per g of support) of CXs biocatalysts prepared at pH 10. Inset: effect of the ABTS concentration on the activity of unsupported cyt c (0.5 g L^{-1}, 30 ºC, pH 10, 100 mM). All the activity tests (including unsupported cyt c experiments) were carried out at pH 4.*

The outcomes of these two experiments, i.e., the increase of the activity of the CX-15, -30 and -55 in successive re-use cycles (Figure 7) and when, in the first use, the concentration of ABTS is 10 mM (Figure 9), led us to propose the following model of cyt c adsorption. Minimum quantities (ca. 5 mg g^{-1}, Figure 5) of cyt c are adsorbed on the external (geometrical) surface of CX-5 particles. These biomolecules behave essentially as unsupported cyt c, hence the similar dependence on ABTS concentration and the reduction of the supported cyt c activity with reuse due to progressive leaching, which although being very low is more significant for the CX-5 systems. For the rest of supports, the explanation is a bit more complex. Thus, the improvement of the activity of the immobilised cyt c when working at high concentrations of ABTS (Figure 9) would support, in principle, the hypothesis of the limited accessibility of the reactants to the cyt c hosted within the pores. Certainly, an increase of ABTS concentration in the solution should favour the diffusion of the ABTS molecules inside the pores. This simple explanation, however, does not fit with the behaviour observed for the unsupported cyt c solutions (inset of Figure 9). If the activity of the cyt c

located in the pores of the CX-15, -30 and -55 were similar to that of unsupported cyt c, the activity values of the resulting materials should not increase when the concentration of ABTS increases. Moreover, if partial pore clogging is responsible for the low activity (per mg of cyt c) of the supports with pores ≥ 15 nm, this effect should be affected by the relative pore filling percentages (Table 4), with CX-55 biocatalysts having much less restrictions than CX-15 ones, which is not the case.

A model that would explain the activity results observed for the cyt c supported on CX-15, -30 and -55 should include both a gradient in the concentration and in the activity of the adsorbed cyt c molecules. Hence, in all these systems a given amount of cyt c would be adsorbed on their geometrical (external) surfaces, in a similar fashion (and possibly quantity) than in CX-5. Under the initial selected conditions of operation, at relatively low (1 mM) ABTS concentration, the activity of the materials would also be determined by that external layer of adsorbed cyt c. When the ABTS concentration increases (10 mM, Figure 9) diffusion of the substrate is favoured, and trapped cyt c would oxidise ABTS faster. This suggests a high stabilisation of the biomolecules inside the pores that would show a higher activity than cyt c in solution [47]. Alternatively, when successive reuses of the CX-15, CX-30 and CX-55 help to remove the cyt c adsorbed on the outer layers of the carbons (as in the case of CX-5), ABTS (1 mM) would have access to cyt c biomolecules having higher activity as a consequence of their confinement inside the pore network, hence the increase observed (Figure 7, pH 10).

4. CONCLUSIONS

The synthesis of carbon xerogels with narrow PSDs and the control of their average pore size over the whole mesopores range provide an ideal set of materials for studying the interaction of carbon surfaces with proteins. Several novel outcomes derived from this study. Pore sizes well over the size of the protein are more indicated for hosting biomolecules, both in terms of quantity

adsorbed and favourable kinetics. Accordingly, the CX-5 materials (with 5 nm average pore size) adsorbed very little amounts of cyt c (below 10 mg g^{-1}), which was expected to lay on the external surface of the carbon particles. This result is at odds with several studies carried out on nanostructured mesoporous carbons with similar average pore sizes.

The interaction of the basic, highly pure carbon surfaces of the CXs with the proteins was essentially hydrophobic, i.e., it was independent of the pH of the solution used for the immobilisation. This also contradicts previous studies that claimed maximum adsorption capacities when using cyt c solutions buffered at pHs close to the isoelectric point of the protein (10.5 for cyt c). On the contrary, the ionic strength of the cyt c solution influenced considerably the adsorption of the protein on the CXs.

Finally, high protein loadings on the CXs did not entail high catalytic activities of the resulting materials. The activity of cyt c supported on all CXs was essentially the same regardless the pore size and/or pore volume (hence the protein uptakes) of the four supports. Additional studies, however, demonstrated a very different behaviour of the cyt c supported on CX-5, on one side, and on the rest of systems (CX-15, -30 and -55) on the other. Thus, cyt c adsorbed on CX-5 behaved like unsupported cyt c. In the case of the cyt c adsorbed on the rest of CXs, the situation is more complex. Under conventional test conditions, the catalytic activity of all the systems studied was highly controlled by the biomolecules adsorbed on the external surface of the materials. However, when higher concentrations of the substrate (ABTS) were used or when successive cycles of reuse were carried out, a rise on the activity of the cyt c/CX-15, -30 and -55 systems was observed. The combination of results from these last experiments suggested that not only the access of ABTS to the cyt c adsorbed on the pores was favoured, but that the activity of those "trapped" cyt c molecules was higher than that of the protein adsorbed on the external surface of the support and, hence, of the unsupported protein.

ACKNOWLEDGMENTS

REFERENCES

[1] Klibanov AM. Enzyme stabilization by immobilization. Anal Biochem 1979;93:1-25.

[2] Tran DN, Balkus Jr KJ. Perspective of recent progress in immobilization of enzymes. ACS Catal 2011;1:956-968.

[3] Kyotani T. Control of pore structure in carbon. Carbon 2000;38:269-286.

[4] Cho YK, Bailey JE. Immobilization of enzymes on activated carbon: selection and preparation of the carbon support. Biotechnol Bioeng 1979;21:461-476.

[5] Nagy B, Tóth A, Savina I, Mikhalovsky S, Mikhalovska L, Geissler E, Lászlo K. Double probe approach to protein adsorption on porous carbon surfaces. Carbon 2017;112:103-110.

[6] Nagy B, Tóth A, Savina I, Mikhalovsky S, Mikhalovska L, Grillo I, Geissler E, Lászlo K. Small angle neutron scattering study of globular proteins confined in porous carbons. Carbon 2016;106:142-151.

[7] Enterría M, Figueiredo JL. Nanostructured mesoporous carbons: tuning texture and surface chemistry. Carbon 2016;108:79-102.

[8] Liang C. Li Z, Dai S. Mesoporous carbon materials: synthesis and modification. Angew Chem Int Ed 2008;47:3696-3717.

[9] Lee J, Kim J, Hyeon T. Recent progress in the synthesis of porous carbon materials. Adv Mater 2006;18:2073-2094.

[10] Vinu A, Streb C, Murugesan V, Hartmann M. Adsorption of cytochrome c on new mesoporous carbon molecular sieves. J Phys Chem B 2003;107:8297-8299.

[11] Vinu A, Miyahara M, Ariga K. Biomaterial immobilization in nanoporous carbon molecular sieves: influence of solution pH, pore volume, and pore diameter. J Phys Chem B 2005;109:6436-6441.

[12] Vinu A, Hossain KZ, Kumar GS, Ariga K. Adsorption of L-histidine over mesoporous carbon molecular sieves. Carbon 2006;44:530-536.

[13] Vinu A, Hossain KZ, Srinivasu P, Miyahara M, Anandan S, Gokulakrishnan N, Mori T, Ariga K, Balasubramanian VV. Carboxy-mesoporous carbon and its excellent adsorption capability for proteins. J Mater Chem 2007;17:1819-1825.

[14] Díaz JF, Balkus Jr KJ. Enzyme immobilization in MCM-41 molecular sieve. J Mol Catal B:Enzymatic 1996;2:115-126.

[15] Deere J, Magner E, Wall JG, Hodnett BK. Adsorption and activity of cytochrome c on mesoporous silicates. Chem Comm 2001:465-466.

[16] Washmon-Kriel L, Jimenez VL, Balkus Jr KJ. Cytochrome c immobilization into mesoporous molecular sieves. J Mol Cat B:Enzymatic 2000;10:453-469.

[17] Blanco RM, Terreros P, Fernández-Pérez M, Otero C, Díaz-González G. Functionalization of mesoporous silica for lipase immobilization Characterization of the support and the catalysts. J Mol Cat B:Enzymatic 2004;30:83-93.

[18] Hudson S, Magner E, Cooney J, Hodnett BK. Methodology for the immobilization on enzymes onto mesoporous materials. J Phys Chem B 2005;109:19496-19506.

[19] Hudson S, Cooney J, Magner E. Proteins in mesoporous silicates. Angew Chem Int Ed 2008;47:8582-8594.

[20] Rodríguez-Reinoso F. The role of carbon materials in heterogeneous catalysis. Carbon 1998;36:159-175.

[21] Quirós M, García AB, Montes-Morán MA. Influence of the support surface properties on the protein loading and activity of lipase/mesoporous carbon biocatalysts. Carbon 2011;49:406-415.

[22] Bayne L, Ulijn RV, Halling PJ. Effect of pore size on the performance of immobilised enzymes. Chem Soc Rev 2013;42:9000-9010.

[23] Zhao J, Wang Y, Luo G, Zhu S. Immobilization of penicillin G acylase on macro-mesoporous silica spheres. Bioresource Technology 2011;102:529-535.

[24] Lazzara TD, Mey I, Steinem C, Janshoff A. Benefits and limitations of porous substrates as biosensors for protein adsorption. Anal Chem 2011;83:5624-5630.

[25] Rey-Raap N, Menéndez JA, Arenillas A. Simultaneous adjustment of the main chemical variables to fine-tune the porosity of carbon xerogels. Carbon 2014;78:490-499.

[26] Rey-Raap N, Menéndez JA, Arenillas A. RF xerogels with tailored porosity over the entire nanoscale. Mic Mes Mater 2014;195:266-275.

[27] Calvo EG, Juárez-Pérez EJ, Menéndez JA, Arenillas A. Fast microwave-assisted synthesis of tailored mesoporous carbon xerogels. J Coll Interf Sci 2011;357:541-547.

[28] Menéndez JA, Illán-Gómez MJ, León y León CA, Radovic LR. On the difference between the isoelectric point and the point of zero charge of carbons. Carbon 1995;33:1655-1659.

[29] Estrade-Szwarckopf H. XPS photoemission in carbonaceous materials: a "defect" peak beside the graphitic asymmetric peak. Carbon 2004;42:1713-1721.

[30] Figueiredo JL, Pereira MFR, Freitas MMA, Órfão JJM. Characterization of active sites on carbon catalysts. Ind Eng Chem Res 2007;46:4110-4115.

[31] Bonde M, Pontoppidan H, Pepper DS. Direct dye binding-A quantitative assay for solid-phase immobilized protein. Anal Biochem 1992;200:195-198.

[32] Tu AT, Reinosa JA, Hsiao YY. Peroxidative activity of hemepeptides from horse heart cytochrome c. Experientia 1968;24:219-221.

[33] Radi R, Thomson L, Rubbo H, Prodanov E. Cytochrome c-catalyzed oxidation of organic molecules by hydrogen peroxide. Arch Biochem Biophys 1991;288:112-117.

[34] Vazquez-Duhalt R. Cytochrome c as biocatalyst. J Mol Cat B:Enzymatic 1999;7:241-249.

[35] Rey-Raap N, Arenillas A, Menéndez JA. A visual validation of the combined effect of pH and dilution on the porosity of carbon xerogels. Mic Mes Mater 2016;223:89-93.

[36] Moreno-Castilla C, Carrasco-Marín F, Mueden A. The creation of acid carbon surfaces by treatment with $(NH_4)_2S_2O_8$. Carbon 1997;35:1619-1626.

[37] Fan J, Lei J, Wang L, Yu C, Tu B, Zhao D. Rapid and high-capacity immobilization of enzymes based on mesoporous silicas with controlled morphologies. Chem Comm 2003:2140-2141.

[38] Vijayaraj M, Gadiou R, Anselme K, Ghimbeu C, Vix-Gurtel C, Orikasa H, Kyotani T, Ittisanronnachai S. The influence of surface chemistry and pore size on the adsorption of proteins on nanostructured carbon materials. Adv Func Mater 2010;30:2489-2499.

[39] Bushnell GW, Louie GV, Brayer GD. High-resolution three-dimensional structure of horse heart cytochrome c. J Mol Biol 1990;214:585-595.

[40] Sang L-C, Vinu A, Coppens M-O. General description of the adsorption of proteins at their iso-electric point in nanoporous materials. Langmuir 2011;27:13828-13837.

[41] Montes-Morán MA, Suárez D, Menéndez JA, Fuente E. The basicity of carbons. In: Tascón JMD, editor. Novel Carbon Adsorbents. Oxford: Elsevier; 2012. p. 173-203.

[42] Eriksson K-O, Belew M. Hydrophobic interaction chromatography. In: Janson J-C, editor. Protein purification. New Jersey: John Wiley&Sons; 2011(3rd edition). p. 165-181.

[43] Ivanov AE, Kozynchenko OP, Mikhalovska LI, Tennison SR, Jungvid H, Gun'ko VM, Mikhalovsky SV. Activated carbons and carbon-containing poly(vinyl alcohol) cryogels: characterization, protein adsorption and possibility of myoglobin clearance. Phys Chem Chem Phys 2012;14:16267-16278.

[44] Trgo M, Perić J, Medvidović NV. A comparative study of ion exchange kinetics in zinc/lead-modified zeolite-clinoptilolite systems. J Haz Mat 2006;B136:938-945.

[45] Kontturi A-K, Kontturi K, Niinikoski P, Savonen A, Vuoristo M. The effective charge number and diffusion coefficient of cationic cytochrome c in aqueous solution. Acta Chem Scandinavica 1992;46:348-353.

[46] Zaks A, Klibanov AM. Enzyme-catalyzed processes in organic solvents. Proc Natl Acad Sci USA 1985;82:3192-3196.

[47] Sang L-C, Coppens M-O. Effects of surface curvature and surface chemistry on the structure and activity of proteins adsorbed in nanopores. Phys Chem Chem Phys 2011;13:6689-6698.

Capítulo 5

Diseño de la química superficial

Este capítulo incluye

Publicación V	Desiccant capability of organic xerogels:Surface chemistry vs porous texture
Publicación VI	On the desiccant capacity of the mesoporous RF-xerogels
Patente	Uso de un xerogel orgánico como desecante
Publicación VII	Hydrophobic RF xerogels synthesis by grafting with silanes
Publicación VIII	Superhydrophobic and Breathable Resorcinol-Formaldehyde xerogels

5. *Diseño de la química superficial*

A la hora de diseñar xerogeles para una aplicación concreta, además de una porosidad apropiada, se requiere de una química superficial adecuada, la cual va a repercutir notablemente sobre la efectividad de los materiales. La mayoría de las aplicaciones que se encuentran en la bibliografía [21-23, 49, 50] utilizan xerogeles de carbono en vez de su homologo orgánico, lo que requiere de una etapa de carbonización, que cambia totalmente la química del material, y encarece el producto final [2]. Los xerogeles orgánicos tienen una porosidad parecida a los carbonizados pero con una química superficial diferente, lo que les dota de propiedades finales distintas. Además, gracias al uso de la tecnología microondas durante la síntesis, los costes de producción son relativamente bajos, siendo así materiales más que interesantes para ser utilizados en múltiples aplicaciones [1].

Por lo tanto, este capítulo está enfocado al estudio de la aplicabilidad de los xerogeles orgánicos como materiales desecantes y a la modificación de su química superficial para obtener materiales hidrófobos aplicables como materiales adsorbentes de aceites.

El **objetivo general** de este capítulo es lograr el control de la química superficial de los xerogeles RF.

5.1. Xerogeles resorcinol-formaldehído como materiales desecantes

Se entiende por materiales desecantes aquellos que eliminan la humedad que les rodea [51]. De forma general, estos materiales se dividen en 2 grandes bloques dependiendo del mecanismo que utilicen para la adsorción de agua : i) a través de reacciones químicas o ii) a través de interacciones superficiales, como es el caso de los xerogeles RF. Para que los materiales de este segundo bloque funcionen de forma efectiva necesitan tener una superficie *hidrófila* y una gran capacidad de adsorción, dos conceptos muy diferentes [51]. La *hidrofilia* hace referencia a la atracción que tiene el material por el agua (del griego, *hydros* = agua + *philia* = amistad) mientras que la capacidad de adsorción depende principalmente de su porosidad.

Los xerogeles RF son materiales altamente porosos cuya química superficial es rica en grupos funcionales oxigenados que atraen hacia sí las moléculas de agua que les rodean a través de puentes de hidrógeno, siendo así materiales potenciales para su utilización como desecantes.

Por lo tanto, en esta Tesis Doctoral se ha evaluado la capacidad de los xerogeles RF para ser utilizados como materiales desecantes y se ha optimizado el tamaño de poro para lograr una máxima capacidad de adsorción. El estudio exhaustivo de esta aplicación ha derivado en una *Patente* que se encuentra al final de este capítulo.

5.1.1. Objetivos

Los objetivos planteados para realizar el estudio fueron:

➢ Evaluar la capacidad de adsorción de humedad de los xerogeles RF con respecto a otros desecantes comerciales.

➢ Determinar las propiedades texturales óptimas para obtener una máxima capacidad de adsorción.

➢ Evaluar la capacidad de regeneración y reutilización de los xerogeles orgánicos.

5.1.2. Estudio

Para llevar a cabo el primer estudio se sintetizaron dos geles, uno mesoporoso y otro macroporoso, y se comparó su capacidad de adsorción de humedad con respecto al gel de sílice utilizado comúnmente en los desecadores de los laboratorios. Tras determinar que el tamaño de poro óptimo se encontraba en el rango de los mesoporos, para el segundo estudio se sintetizaron seis xerogeles RF con tamaño de poro entre 0 y 80 nm, obtenidos mediante la variación de la concentración de metanol en la disolución de formaldehído utilizada para la síntesis.

5.1.3. Resultados

Los detalles experimentales y la discusión de los resultados obtenidos se hallan en la *Publicación V* y *VI*, incluidas al final de este capítulo. Los resultados obtenidos de este estudio derivaron en una *Patente* que se encuentra a continuación de las publicaciones anteriormente mencionadas. Los principales resultados de este estudio se detallan a continuación:

➢ La química superficial de los xerogeles RF es la misma independientemente de la composición de la mezcla precursora utilizada durante su síntesis. Por lo tanto, las diferencias observadas en la adsorción de humedad son consecuencia exclusivamente de sus propiedades porosas.

➢ Los xerogeles RF muestran mejores resultados como materiales desecantes que el gel de sílice comúnmente utilizado en los laboratorios con este mismo fin.

➢ El tamaño de poro óptimo para esta aplicación es en torno a 8 nm, logrando una ganancia de más de un 80 % de su peso en humedad.

➢ En contra de lo observado en estudios anteriores, la concentración de metanol utilizada afecta sobre la microporosidad del xerogel RF.

➢ Aunque la microporosidad pudiera contribuir a la adsorción de humedad, son los mesoporos los que juegan un papel relevante en esta aplicación.

➢ Los materiales han mostrado ser fácilmente regenerables (temperaturas moderadas) y su eficiencia no disminuye con los ciclos.

5.1.4. Conclusión

Los xerogeles RF han mostrado ser unos excelentes materiales desecantes que absorben más de un 80 % de su peso en humedad, con las ventajas añadidas de que son fácilmente regenerables, ligeros en su utilización, baratos en su producción y resistentes a ácidos debido a su naturaleza orgánica (Figura 18).

Figura 18.   *Esquema resumen del estudio de xerogeles RF como materiales desecantes.*

PUBLICACIÓN V

DESICCANT CAPABILITY OF ORGANIC XEROGELS: SURFACE CHEMISTRY VS POROUS TEXTURE

Isabel D. Alonso-Buenaposada, Esther G. Calvo, Miguel A. Montes-Morán, Javier Narciso, J. Angel Menéndez, Ana Arenillas, *Microporous and Mesoporous Materials, 232 (2016) 70-76.*

Desiccant capability of organic xerogels: Surface chemistry vs porous texture

CrossMark

Isabel D. Alonso-Buenaposada [a], Esther G. Calvo [a], M.A. Montes-Morán [a], J. Narciso [b], J. Angel Menéndez [a], Ana Arenillas [a, *]

[a] Instituto Nacional del Carbón, CSIC, Apartado 73, 33080 Oviedo, Spain
[b] University of Alicante, Department of Inorganic Chemistry, Apartado 99, 03080, Spain

ABSTRACT

Resorcinol-Formaldehyde xerogels are organic polymers that can be easily tailored to have specific properties. These materials are composed of carbon, hydrogen and oxygen, and have a surface that is very rich in oxygen functionalities, and is therefore very hydrophilic. Their most interesting feature is that they may have the same chemical composition but a different porous texture. Consequently, the influence of porous characteristics, such as pore volume, surface area or pore size can be easily assessed. In this work, a commonly used desiccant, silica gel, is compared with organic xerogels to determine their rate and capacity of water adsorption, and to evaluate the role of surface chemistry versus porous texture. It was found that organic xerogels showed a higher rate of moisture adsorption than silica gel. Pore structure also seems to play an important role in water adsorption capacity. The OX-10 sample, whose porosity was mainly composed of micro-mesoporosity displayed a water adsorption capacity two times greater than that of the silica gel, and three times higher than that of the totally macroporous xerogel OX-2100. The presence of feeder pores (mesopores) that facilitate the access to the hydrophilic surface was observed to be the key factor for a good desiccant behaviour. Neither the total pore volume nor the high surface area (i.e. high microporosity) of the desiccant sample, is as important as the mesopore structure.

1. INTRODUCTION

Organic gels are nanoporous materials that are obtained by the polymerization of hydroxylated benzenes and aldehydes in the presence of a solvent following Pekala´s method [1]. Most organic gels presented in literature are synthesized using resorcinol (R) and formaldehyde (F) as precursors and water as solvent [2-5], although other precursors and reaction media can be used [6-9], to produce materials with different properties. In general, three main steps are involved in the formation of the organic gel: gelation, curing and the drying step. Depending on the drying method applied to remove the solvent, gels are classified into three main categories: aerogels, cryogels and xerogels where supercritical drying, freeze-drying and evaporative drying are employed, respectively [5, 10-15]. In this study, microwave radiation was used as heating source throughout the entire synthesis process to produce RF xerogels by means of a simple, fast and cost-effective methodology [16,17].

Over the last few years, organic and carbon xerogels have been demonstrated to be materials of great added value owing to the fact that their porosity can be controlled and designed by adjusting the synthesis variables, both physical (i.e. temperature, time of synthesis, etc.) [2, 16] and chemical (pH, dilution, R/F ratio and percentage of stabilizer contained in the formaldehyde solutions) [17-22]. In addition to the large number of variables that need to be controlled, it has been shown that there exists a synergy between them. For this reason, statistical programs have been applied to allow the simultaneous study of all of these variables, allowing to designed porous properties for specific applications [18, 21].

Not only is an appropriate porosity necessary for obtaining an optimum material for a specific application, but the surface chemistry also plays an important role. Most of the applications of RF xerogels are based on its carbonized form, for example: electrode material for supercapacitors, hydrogen

storage, catalysis, heavy metal adsorbents, etc. [3, 23-28]. As the structure of carbon xerogel is mainly made up of carbon colloidal chains (with a C content of up to 95 %), sometimes the material is doped with heteroatoms, or chemically treated to change the surface chemistry and improve its behavior for a specific application [29-32].

The surface chemistry of organic xerogels is different to that of their carbonized counterparts [20]. When polycondensation between resorcinol and formaldehyde takes place, a high concentration of hydroxyl groups remains on their surfaces. Thus, the chemical composition of a generic RF organic xerogel could be 65 % wt. C, 5 % wt. H and 30 % wt. O. However, heat treatment of organic xerogels to obtain a thermally stable material (i.e. carbon xerogel) causes these labile oxygen surface groups to be released, leading to a more condensed carbonaceous structure consisting of about 95 % wt. C, the remaining being divided between H and O [23]. Therefore the surface chemistries of organic and carbon xerogels are totally different, even though their designed porosities may be similar [33, 34].

Desiccant materials are hygroscopic solids that induce or sustain a state of dryness in the surrounding air [35]. In order to be considered a good desiccant porous material, it not only needs to be hydrophilic but also highly adsorbent, which are two different concepts [35]. Its hydrophilicity refers to its affinity to water, while its adsorption capacity depends mainly on its porosity. For example, some carbon-based materials, though considered as hydrophobic, nevertheless have a high water sorption capacity due to their high porosity, but their rate of adsorption is low because their surface chemistry is not appropriate for attracting moisture.

Generally speaking, there are two types of desiccant materials: (i) substances whose desiccant behavior originates from a chemical hydration reaction, such as P_4O_{10}, $MgSO_4$, and (ii) substances whose desiccant behavior is based on surface interactions like adsorption processes. The latter category includes molecular sieves, silica gels, clays and starches [35-37]. The water adsorption behavior of a sorbent depends on many factors, such as the porous

structure, chemical composition, surface functionality content, presence of charged species, etc. [32].

Desiccants have been used in recent times for a wide range of applications, with the aim of controlling the humidity in the air when a moisture-free ambient is necessary. Other examples include the use of desiccant materials for controlling the level of water in industrial gas streams, in air conditioner systems, for storing and protecting goods in shipping containers against moisture damage (e.g., electronic devices, foods, clothes, etc.) [38].

As mentioned above, silica gel is the most common desiccant as its chemical behavior has been known since the XVII century and it has been used as a dehumidifier since the beginning of the XX century up to this day. Its good moisture adsorption capacity is due to its porous properties and the presence of hydroxyl groups on its surface which give it a hydrophilic nature. Water molecules are attracted by its surface chemistry which is rich in oxygen.

Due to the physical and chemical similarities between silica gels and RF organic gels, the aim of this work is to evaluate the desiccant behavior of two bare RF xerogels with different porosities. The interest shown in these RF xerogels is due to a series of advantages that they offer, such as their light weight, the possibility of modifying their surface chemistry to enable them to adsorb (and eliminate) components other than moisture, their chemical resistance to acids that may be present in the fluids to be treated, and the fact that they do not require neither doping or post-treatment processes, such as carbonization or activation, which makes them more cost-effective.

2. EXPERIMENTAL SECTION

2.1. Synthesis of organic xerogels

The organic xerogels used in this study were synthesized by the polymerization of resorcinol (R) and formaldehyde (F), using deionized water as

solvent and NaOH as catalyst. First of all, resorcinol (Indspec, 99.6 %) was dissolved in deionized water in an unsealed glass beaker under magnetic stirring until completely dissolved. Then, a formaldehyde solution was added until a homogeneous solution was obtained. The R/F molar ratio used was 0.15 and 0.70 for the synthesis of the samples OX-10 and OX-2100, respectively. NaOH solution (0.1 M, Titripac, Merck) was added in each precursor solution dropwise until the desired pH was reached. In this case, a pH of 5.8 and 4.8 were selected for the preparation of samples OX-10 and OX-2100, respectively. The precursor solutions were placed in an open vessel inside a microwave oven at 85 ºC for about 3 hours in order for gelation and ageing to take place. The polymers were then dried also by microwave heating, in the initial vessel, until a mass loss of over 50 % were recorded, the total time of synthesis being less than 5 h. As a result two different organic gels were obtained with a total yield in the whole process of 45 wt%.

2.2. Sample characterization

Before characterization, the xerogels were outgassed (Micromeritics VacPrep 0.61) at 0.1 mbar and 120 ºC overnight in order to remove any humidity and other physisorbed gases.

2.2.1. Porous properties

The porosity of the samples was characterized by means of nitrogen adsorption-desorption isotherms and mercury porosimetry.

The nitrogen adsorption-desorption isotherms were measured at -196 ºC in a Tristar 3020 (Micromeritics) device. S_{BET} was determined from the N_2 adsorption branch and, in all cases; the number of points used to apply the BET equation was higher than 5. Vmicro was estimated by the Dubinin-Raduskevich method [39]. This method only takes into account micropore surfaces. The external surface area (S_{EXT}) was determined by applying the t-plot method developed by Lecloux et all. [40], which measures the external surface of the

meso-macropores but excludes the microporous surface area. These two techniques are therefore complementary. N_2 adsorption-desorption isotherms were only used to obtain information about microporosity (S_{BET}, Vmicro and mean micropore size) and the S_{EXT}. Parameters, such as porosity (%), pore size distribution (PSD), bulk density and mesopore/macropore volumes (Vmeso, Vmacro), were determined by means of mercury porosimetry, using an AutoPore IV 9500 (Micromeritics), which is able to measure from atmospheric pressure up to 228 MPa. In this study, the lowest limit of mesopores detected by this apparatus was 5.5 nm, whereas Vmacro referred to porosity ranging from 50 to 10000 nm. The surface tension and contact angle were 485 mN m^{-1} and 130 º, respectively, and the stem volume was between 45-58 % in all the analyses performed. In the low pressure step, the samples were evacuated up to 6.7 Pa. The equilibration time used was 10 seconds.

2.2.2. Elemental analysis

Determination of C, H and N was carried out in a LECO CHNS-932 analyzer. The oxygen content was determined using a LECO VTF-900 analyzer.

2.2.3. TPD analysis

The typology of the surface oxygen groups contained in the RF xerogels was evaluated by temperature programmed desorption (TPD) using a Chemisorption Autochem II 2920 device from Micromeritics. This equipment is a fully automated chemisorption analyzer, which includes a gas feeding system, a temperature-controlled reaction zone and a gas analyzer (mass spectrometer, OmniStar TM, Pfeiffer Vacuum). The amount of CO and CO_2 released was registered while the samples were subjected to heat treatment from room temperature to 1000 ºC at a heating rate of 10 ºC min^{-1} under an Ar flow of 50 mL min^{-1}.

2.2.4. FTIR analysis

Surface chemistry was also characterized by Fourier transform infrared spectroscopy (FTIR) in a Nicolet FTIR 8700 with DTGS detector. The data were recorded between 4000-400 cm^{-1}, using 64 scans and a resolution of 4 cm^{-1}.

2.2.5. Water vapour adsorption experiments

The procedure for measuring the capacity of water vapour adsorption and kinetics consisted in placing 0.6-0.8 g of sample inside a hermetic vessel at 25 ºC and 100 % humidity and recording changes in mass with time until constant values were reached.

Water vapour adsorption-desorption isotherms were obtained using a Hydrosorb 1000 multigas instrument (Quantachrome) at 25 ºC.

3. RESULTS AND DISCUSSION

3.1. Porous properties

For comparative purposes a commercial silica gel, commonly used as desiccant in laboratories, was selected (Sigma-Aldrich, 2-6 mm particle size). The data relating to the textural properties of the two RF organic xerogels and the selected desiccant reference (i.e. silica gel) are presented in Table 1. These differences on the porosity between these xerogels are consequence of the variables used for each sample during the synthesis process, as can be found in literature [17, 18, 21]. Differences between the micro-mesoporosities of the samples were determined from N_2 adsorption-desorption isotherms, as shown in Figure 1. The silica gel used for this study is a micro-mesoporous material with an average mesopore size of ca. 4 nm, a value extracted from the PSD obtained by applying the DFT method to the adsorption branch of the nitrogen isotherm (data not shown). The OX-10 xerogel yields an isotherm that can be classified as type I-IV according to the BDDT classification, although the

presence of a hysteresis loop at high relative pressures denotes the presence of a certain macroporosity (a deduction supported by the results of mercury porosimetry). Although the surface area of the silica gel is higher than that of OX-10 (338 versus 214 m^2 g^{-1} respectively), the total pore volume and the Sext of OX-10 is higher than that of the silica gel (Table 1), due to the differences in the pore size distributions. According to the N$_2$ adsorption isotherm corresponding to OX-2100, this sample shows almost no adsorption at all, which does not necessarily mean that it is a non-porous material, but the pore size is too large to be determined accurately by this technique. In this case, porosity was characterised by mercury porosimetry

Table 1. *Textural properties of the two RF xerogels and the reference silica gel.*

		OX-10	OX-2100	Silica gel
N$_2$ Isotherm	S_{BET} (±5, m^2 g^{-1})	214	9	338
	V_{DUB-N2} (±0.05, cm^3 g^{-1})	0.08	0.00	0.12
	V_p (±0.05, cm^3 g^{-1})	1.38	0.02	0.23
	S_{ext} (±5, m^2 g^{-1})	187	12	170
Hg porosimetry	ρ^a (±0.05, g cm^{-3})	0.47	0.34	-
	V_{meso} (±0.05, cm^3 g^{-1})	0.78	0.00	-
	V_{macro} (±0.05, cm^3 g^{-1})	0.56	2.15	-
	d_{pore} (±2, nm)	10	2100	-
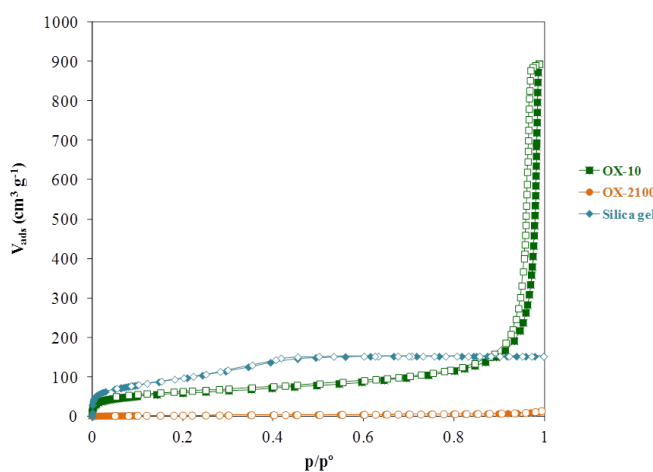
Figure 1. *N$_2$ adsorption–desorption isotherms of the organic xerogels and the reference silica gel sample.*

Figure 2 illustrates the cumulative volume vs. pore size obtained from the mercury porosimetry experiments. As the Autopore IV porosimeter cannot detect pores smaller than 5.5 nm, silica gel was not analysed by this technique since it has a narrower pore structure. In Figure 2a, it can be observed that the cumulative volume falls to a pore size of 10-20 nm, which implies that most of the pores in OX-10 are in the mesopore range. However, a small volume of pores larger than this are observed as well corresponding to the macropore range up to 120 nm. From Figure 2b, on the other hand it is clear that the OX-2100 xerogel has a larger pore size, due to a change in cumulative volume corresponding to a pore size of ca. 2100 nm, which denotes a macroporous material. (Figure S1 in Supplementary Material shows the pore size distributions for both RF xerogels: OX-10 and OX-2100).
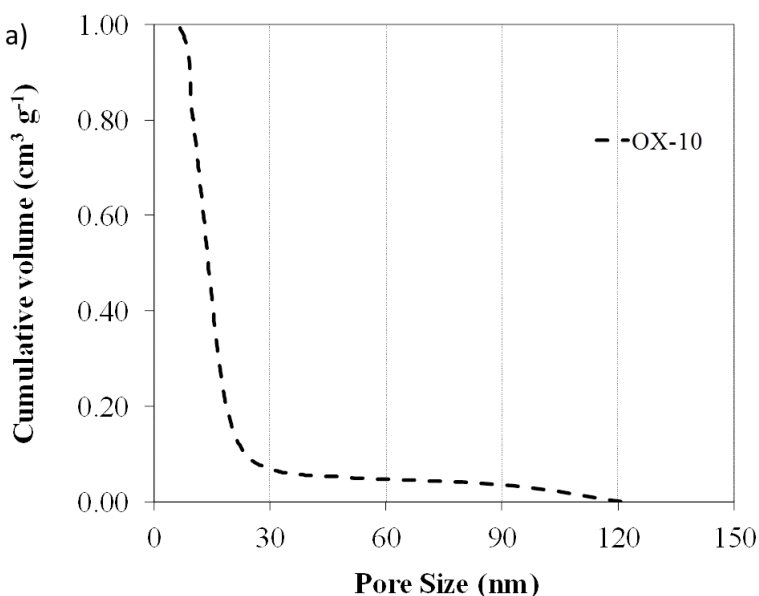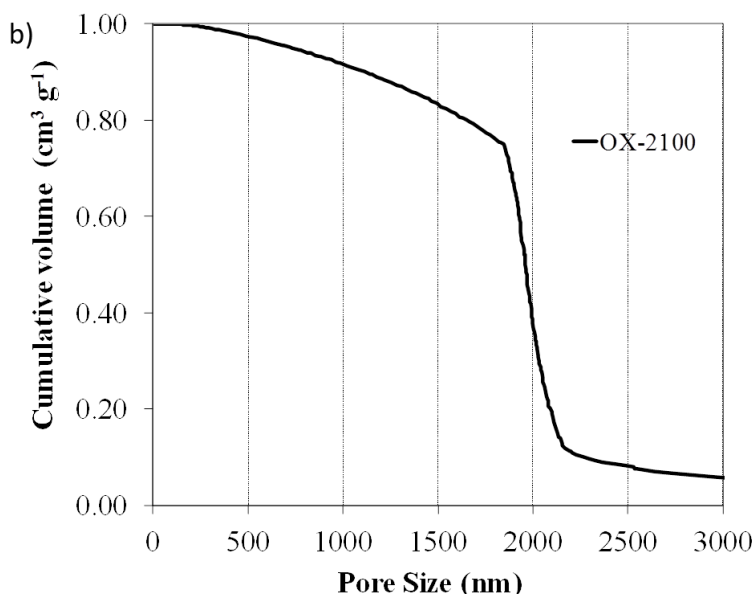
Figure 2. Cumulative volume vs. pore size obtained by mercury porosimetry for the RF xerogels: a) OX-10 and b) OX-2100.
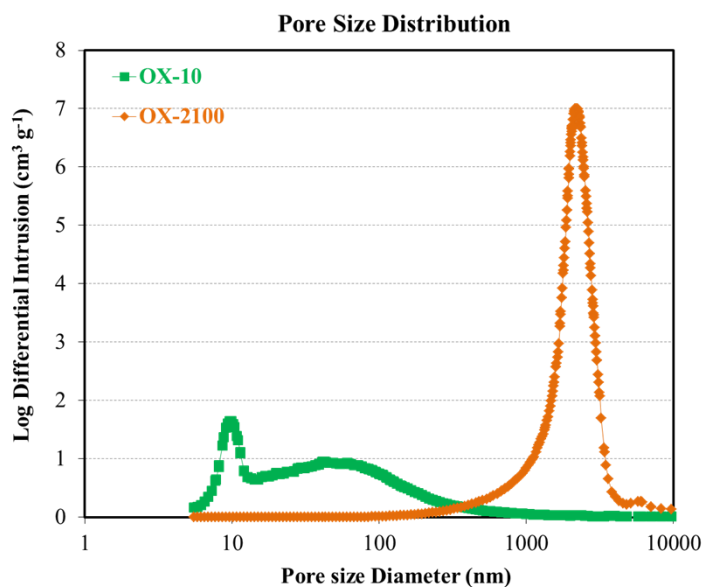
Figure S1. Pore size distribution of the organic xerogels obtained by mercury porosimetry.

In short, the three samples used in the present study possess totally different porous structures, as the silica gel is a micro-mesoporous material with narrow mesopores, OX-10 is micro-meso-macroporous while OX-2100 is entirely macroporous.

3.2. Chemical properties

The data obtained from the elemental analysis of the organic xerogels are presented in Table 2. As can be seen, the chemical composition is very similar in both samples. From the elemental analysis data it can be inferred that the O/C molar ratio for the organic xerogels is 0.35. Their high oxygen content makes it necessary to examine the typology of these groups in order to determine whether the different synthesis conditions affect the nature of the oxygenated groups.

Table 2. Elemental analysis results for the two organic xerogels (dry basis).

	OX-10	OX-2100
C (±0.2, wt. %)	64.7	66.3
H (±0.2, wt. %)	4.9	4.5
N (±0.2, wt. %)	0.3	0.3
O (±0.2, wt. %)	30.1	28.9

The quantity and type of oxygen functionalities in the organic xerogels can be determined from the TPD curves, since the oxygen groups decompose into CO and CO_2 upon heating. According to Figure 3, the evolving CO and CO_2 groups are virtually identical in both cases, which implies that not only is the proportion of oxygen very similar in both samples but that the type of oxygen functionality is practically identical as well. Therefore, to obtain RF xerogels with different surface chemistries, some post-treatments must be performed.
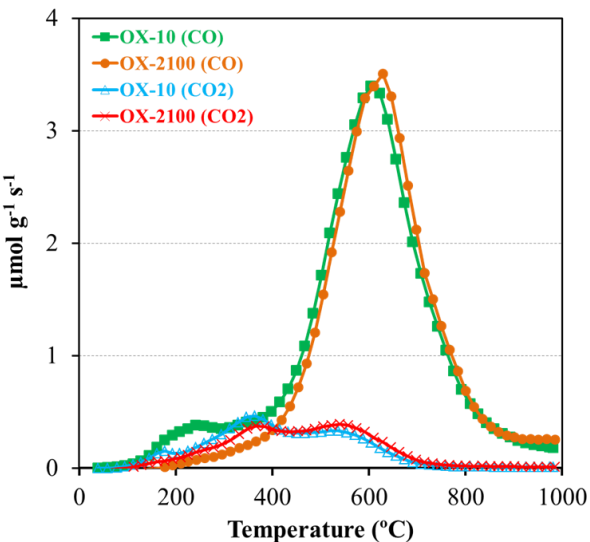
Figure 3. *CO and CO_2 TPD spectra of the two organic xerogels OX-10 and OX-2100.*

In general, it can be observed that both organic xerogels have a larger quantity of oxygen groups desorbing as CO, namely, neutral or basic groups (phenols, alcohols) [41, 42], which is in agreement to the most abundant oxygen surface groups in RF xerogels. In the CO evolution curves of Figure 3, both samples show a very pronounced peak centred at ca. 650 ºC, which can be assigned to phenols (-OH), since according to the literature groups of this type evolve as CO in a temperature range of 500-750 ºC [42].

The less stable and more acidic functionalities (carboxylic acids, anhydrides, lactones) produce CO_2 when the material is subjected to thermal treatment. The CO_2 spectrum indicates a clear less presence of the oxygen functionalities that release as CO_2. Two peaks can be recognized, one whose maximum is around 350 ºC, can be attributed to a small presence of carboxylic acids whereas the other centred at around 550 ºC, suggests the presence of carboxylic anhydride and/or lactone-type groups [41, 42]. These functionalities may be produced, in a small extent, during the drying step in air by microwave heating.

FTIR may also provide some information about the functionalities present in the samples studied. Figure 4 shows analogous spectra for the two organic xerogels, confirming the similar composition and functionalities of both samples. In both cases, there is a broad band between 3600 and 3000 cm^{-1} associated to the O-H stretching vibrations, originating from the phenol groups. Aliphatic stretching vibrations can be assigned to the band at 2900 cm^{-1}, whilst the corresponding aliphatic deformation vibration is located at ca. 1400 cm^{-1}. The well defined band at around 1600 cm^{-1} corresponds to the aromatic ring stretching vibration C=C. Bands at 1100 and 1200 cm^{-1} are assigned to methylene ether bridges C-O-C stretch and =C-O-C symmetric and asymmetric stretch. C-O stretching from alcohols also contribute with bands at 1100 cm^{-1}, whilst and small contribution from C=O carbonyl stretching from carboxylic acids, anhydrides, ester and ketones are assigned to band ca. 1700 cm^{-1}. All these oxygen functionalities are in agreement with the TPD results mentioned above.
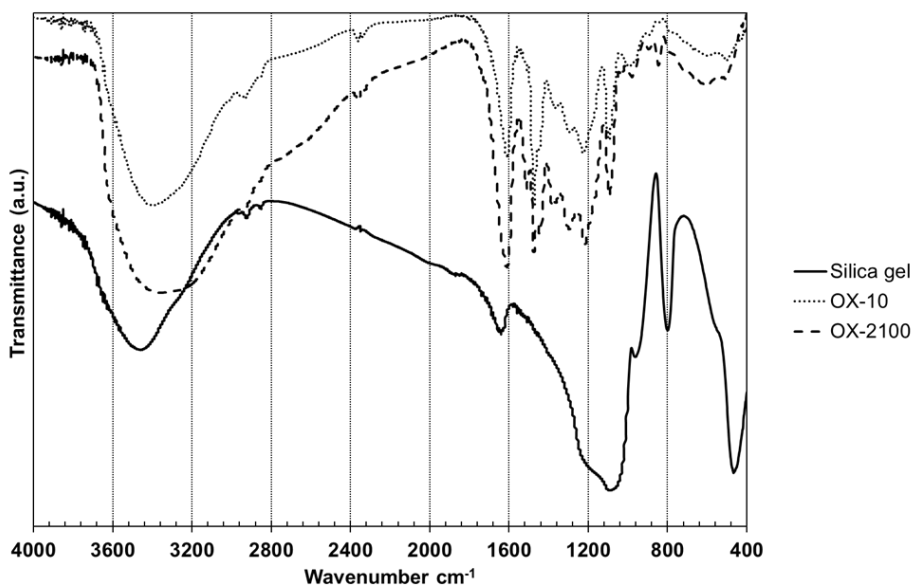
Figure 4. FTIR spectra of the two organic xerogels and the silica gel.

On the other hand, silica gel obviously presents a different spectrum. It can be observed a broad band at around 3400 cm^{-1} due to the hydroxyl group on the surface of the silica. The well defined bands at 470 and 790 cm^{-1} are ascribed to the Si-O-Si bending vibrations, whilst the broad band at ca. 1100 cm^{-1} is due to the Si-O stretching.

3.3. Desiccant behaviour

The desiccant properties of silica gel are due to the presence of hydroxyl groups in the surface of the material that endow it with a hydrophilic nature. Moreover, its porosity gives it a high water adsorption capacity so that moisture is attracted and retained in the surface of the material. The results of this study show that organic xerogels are materials with a potential desiccant capacity since they contain mainly phenolic groups on their surface (see Figures 3 and 4), and have a porous structure that can be tailored to optimize the adsorption of water.

The desiccant behaviour of the samples at 25 ºC under atmospheric pressure and 100 % humidity is illustrated in Figure 5. As can be observed, the slope of the organic xerogels curves during the first few hours is steeper, which implies that the speed of adsorption is faster in both samples. Taking into account that all the oxygen content may contribute to the hydrophilic character in a sample, it can be made a rough estimation of the oxygen content ratio in the samples studied. Thus, from the theoretical formula of silica gel (i.e., SiO_2 nH_2O) it can be estimated that the O/Si molar ratio may be considered as 2. In spite of the fact that the proportion of oxygen is lower in the case of xerogels (O/C = 0.35 for organic xerogels and O/Si = 2 for silica gel), water is more easily attracted to the surface of organic xerogels than in the case of silica, due to either their surface chemistry or their different porous structure which is characterised by the presence of feeder pores, or to a combination of both of these factors.
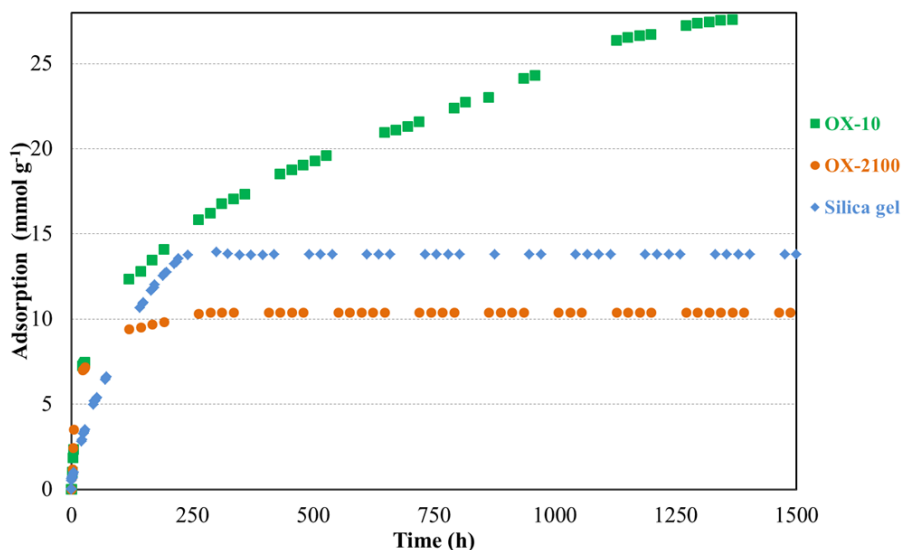
Figure 5. *Moisture adsorption isotherms at 25 ºC, atmospheric pressure and 100 % humidity corresponding to OX-10, OX-2100 and the silica gel.*

Once the first hours (ca. 48 h) have elapsed, greater differences between the samples become apparent. The RF xerogel labelled OX-2100, which is a totally macroporous sample, allows water molecules easy access to its surface but, once all of the surface is covered, the speed of adsorption decreases drastically and saturation point is reached at ca. 10 mmol/g. Silica gel starts with a lower rate of adsorption, and its capacity of adsorption is sharply reduced at around 14 mmol/g after 250 h. This could be because the water molecules experience greater difficulty accessing the narrow pores. Nevertheless its large surface area provides a readily available surface area covered with hydroxyl groups with an affinity for water molecules.

Not only does sample OX-10 show a faster rate of water adsorption but it also has a better water adsorption capacity than the other two samples. Although the rate of adsorption decreases progressively, the sample keeps adsorbing moisture for more than 1200 h. The OX-10 sample adsorbs ca. 27 mmol/g which amounts to 50 % of its own weight in water.

The desiccant materials employed in this study are substances whose performance as desiccants is based on surface interactions like those of adsorption processes. It is for this reason that these materials can be regenerated merely by heating, enabling them to be reused several times. Accordingly, the temperature of regeneration is a factor that must be taken into account especially when their application is intended for industrial scale. The advantage of silica gel and RF organic xerogels is that they can be regenerated by heating at relatively low temperatures (i.e.120 ºC), whilst other desiccants commonly used, such as alumina require higher regeneration temperatures.

It is well known that at ambient pressure water molecules do not condense in pores and fill the entire pore volume. This would suggest that the total pore volume is not the main factor that determines the desiccant behaviour of these materials. Nevertheless, despite the importance of hydroxyl surface groups in determining the hydrophilic character of the material, the pore structure is also relevant as this affects the rate of adsorption and the availability of the hydrophilic surface in desiccants.

Further insights into the hydrophilic behaviour of the materials were obtained from the water adsorption isotherms at 25 ºC (Figure 6). As expected, the maximum water uptakes measured during the dynamic (Figure 5) and equilibrium (Figure 6) experiments agree reasonably well (i.e. 27 vs 20 mmol g^{-1}, 14 vs 11 mmol g^{-1}, 10 vs 8 mmol g^{-1} for OX-10, Silica gel and OX-2100 in the dynamic vs equilibrium experiments). At low relative pressures (p/p0 < 0.25, Figure 6), the amount of water adsorbed on both the organic xerogels and the silica gel is essentially the same. This result indicates that differences in microporosity (see Table 1) are not determinant for the adsorption of water molecules. Adsorption by the silica gel increases smoothly from $p/p^0 > 0.25$, whereas the water adsorption isotherms of the two OXs remain identical up to $p/p^0 = 0.9$, probably due to the presence of wider pores in the organic xerogels. The silica gel has a narrow mesoporosity (mean pore size 4 nm according to DFT calculations), that comes into play at lower relative pressures. The presence of wider mesopores (i.e. mean pore size 10 nm according to mercury

porosimetry) in the OX-10 sample causes its water capacity to increase dramatically in the $0.9 < p/p^0 < 1$ interval, whilst sample OX-2100 displays the lowest total water adsorption capacity of the series studied due to the fact that its pores are too wide to play an important role in the adsorption of water. The water vapor adsorption isotherm obtained for this sample (OX-2100) is corroborated by others in the literature [43] corresponding to RF-xerogels with similar porosity that is not adequate for water adsorption applications. Therefore, although all RF-xerogels present hydrophilic character, not all of them can be used as desiccants but only the ones with the proper porosity.
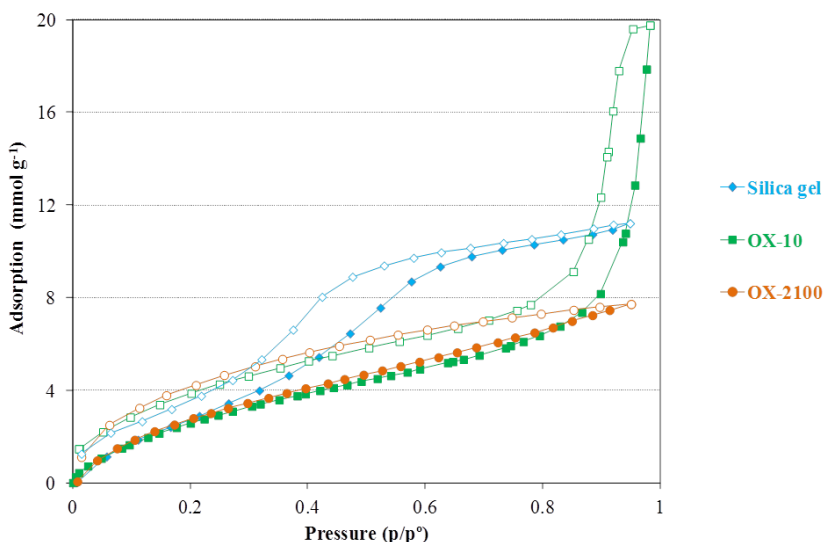
Figure 6. *Water adsorption isotherms at 25 ºC of the two organic xerogels and the reference silica gel.*

4. CONCLUSIONS

The desiccant behaviour of two organic xerogels with different porosities was studied and compared using silica gel as reference material. Although the presence of hydroxyl groups in the organic xerogels may be lower than in the silica gel, the former showed a higher rate of moisture adsorption. Pore

structure seemed to play an important role in water adsorption capacity. The OX-10 sample, whose porosity was mainly composed of micro-mesoporosity displayed a water adsorption capacity two times higher than the silica gel, and three times higher than OX-2100, a totally macroporous xerogel. Although the presence of oxygen surface groups is important as it determines the hydrophilic character of the material, the presence of feeder pores (mesopores) that facilitates access to the hydrophilic surface was found to be the key factor for ensuring a good desiccant behaviour. Neither the total pore volume nor the high surface area (i.e. high microporosity) of the desiccant sample has a greater influence than the mesopore structure.

Moreover, organic xerogels offer a series of important advantages: their light weight, the possibility of modifying the surface chemistry to adsorb (and eliminate) components other than moisture, chemical resistance to acids that may be present in the fluids to be treated, and the possibility of being applied without the need for a doping or carbonization/activation step, making them cost-effective materials.

In short, all organic xerogels are hydrophilic materials since its surface is absolutely covered by oxygenated groups, independently of the variables used during synthesis. The water absorption capacity, which endows these materials of a desiccant behaviour, depends on the porosity of the material which can be controlled with the variables used during the synthesis process. Therefore, not all of them can be used as desiccants since only a proper porosity provides them of this capacity. If porosity is properly designed, organic xerogels are efficient desiccant materials which offer a fast rate of adsorption, a good water adsorption capacity, and can be easily regenerated at low temperature.

ACKNOWLEDGEMENTS

REFERENCES

[1] R. Pekala, Organic aerogels from the polycondensation of resorcinol with formaldehyde, Journal of Materials Science, 24 (1989) 3221-3227.

[2] N. Job, F. Panariello, J. Marien, M. Crine, J.-P. Pirard, A. Léonard, Synthesis optimization of organic xerogels produced from convective air-drying of resorcinol–formaldehyde gels, Journal of Non-Crystalline Solids, 352 (2006) 24-34.

[3] J. Aguado-Serrano, M.L. Rojas-Cervantes, R.M. Martín-Aranda, A.J. López-Peinado, V. Gómez-Serrano, Surface and catalytic properties of acid metal–carbons prepared by the sol–gel method, Applied Surface Science, 252 (2006) 6075-6079.

[4] V.M. Gun'ko, V.M. Bogatyrov, O.I. Oranska, I.V. Urubkov, R. Leboda, B. Charmas, J. Skubiszewska-Zięba, Synthesis and characterization of resorcinol–formaldehyde resin chars doped by zinc oxide, Applied Surface Science, 303 (2014) 263-271.

[5] A. Léonard, S. Blacher, M. Crine, W. Jomaa, Evolution of mechanical properties and final textural properties of resorcinol–formaldehyde xerogels during ambient air drying, Journal of Non-Crystalline Solids, 354 (2008) 831-838.

[6] F. Pérez-Caballero, A.L. Peikolainen, M. Uibu, R. Kuusik, O. Volobujeva, M. Koel, Preparation of carbon aerogels from 5-methylresorcinol–formaldehyde gels, Microporous Mesoporous Mater., 108 (2008) 230-236.

[7] A. Szczurek, G. Amaral-Labat, V. Fierro, A. Pizzi, A. Celzard, The use of tannin to prepare carbon gels. Part II. Carbon cryogels, Carbon, 49 (2011) 2785-2794.

[8] A. Szczurek, G. Amaral-Labat, V. Fierro, A. Pizzi, E. Masson, A. Celzard, The use of tannin to prepare carbon gels. Part I: Carbon aerogels, Carbon, 49 (2011) 2773-2784.

[9] L.I. Grishechko, G. Amaral-Labat, A. Szczurek, V. Fierro, B.N. Kuznetsov, A. Pizzi, A. Celzard, New tannin–lignin aerogels, Industrial Crops and Products, 41 (2013) 347-355.

[10] K. Kraiwattanawong, H. Tamon, P. Praserthdam, Influence of solvent species used in solvent exchange for preparation of mesoporous carbon xerogels from resorcinol and formaldehyde via subcritical drying, Microporous Mesoporous Mater., 138 (2011) 8-16.

[11] A.M. ElKhatat, S.A. Al-Muhtaseb, Advances in Tailoring Resorcinol-Formaldehyde Organic and Carbon Gels, Advanced Materials, 23 (2011) 2887-2903.

[12] T. Yamamoto, T. Nishimura, T. Suzuki, H. Tamon, Effect of drying method on mesoporosity of resorcinol-formaldehyde drygel and carbon gel, Drying Technology, 19 (2001) 1319-1333.

[13] E. Gallegos-Suárez, A.F. Pérez-Cadenas, F.J. Maldonado-Hódar, F. Carrasco-Marín, On the micro- and mesoporosity of carbon aerogels and xerogels. The role of the drying conditions during the synthesis processes, Chemical Engineering Journal, 181–182 (2012) 851-855.

[14] A. Szczurek, G. Amaral-Labat, V. Fierro, A. Pizzi, E. Masson, A. Celzard, Porosity of resorcinol-formaldehyde organic and carbon aerogels exchanged and dried with supercritical organic solvents, Materials Chemistry and Physics, 129 (2011) 1221-1232.

[15] C. Liang, G. Sha, S. Guo, Resorcinol–formaldehyde aerogels prepared by supercritical acetone drying, Journal of Non-Crystalline Solids, 271 (2000) 167-170.

[16] N. Rey-Raap, J.A. Menéndez, A. Arenillas, Optimization of the process variables in the microwave-induced synthesis of carbon xerogels, Journal of Sol-Gel Science and Technology, 69 (2014) 488-497.

[17] N. Rey-Raap, J. Angel Menéndez, A. Arenillas, RF xerogels with tailored porosity over the entire nanoscale, Microporous Mesoporous Mater., 195 (2014) 266-275.

[18] N. Rey-Raap, J. Angel Menéndez, A. Arenillas, Simultaneous adjustment of the main chemical variables to fine-tune the porosity of carbon xerogels, Carbon, 78 (2014) 490-499.

[19] A.H. Moreno, A. Arenillas, E.G. Calvo, J.M. Bermúdez, J.A. Menéndez, Carbonisation of resorcinol-formaldehyde organic xerogels: Effect of temperature, particle size and heating rate on the porosity of carbon xerogels, J Anal Appl Pyrolysis, 100 (2013) 111-116.

[20] S.A. Al-Muhtaseb, J.A. Ritter, Preparation and Properties of Resorcinol–Formaldehyde Organic and Carbon Gels, Advanced Materials, 15 (2003) 101-114.

[21] I.D. Alonso-Buenaposada, N. Rey-Raap, E.G. Calvo, J. Angel Menéndez, A. Arenillas, Effect of methanol content in commercial formaldehyde solutions on the porosity of RF carbon xerogels, Journal of Non-Crystalline Solids, 426 (2015) 13-18.

[22] C. Alegre, D. Sebastián, E. Baquedano, M.E. Gálvez, R. Moliner, M. Lázaro, Tailoring Synthesis Conditions of Carbon Xerogels towards Their Utilization as Pt-Catalyst Supports for Oxygen Reduction Reaction (ORR), Catalysts, 2 (2012) 466.

[23] E.G. Calvo, N. Ferrera-Lorenzo, J.A. Menéndez, A. Arenillas, Microwave synthesis of micro-mesoporous activated carbon xerogels for high performance supercapacitors, Microporous Mesoporous Mater., 168 (2013) 206-212.

[24] L. Zubizarreta, A. Arenillas, J.J. Pis, Carbon materials for H2 storage, International Journal of Hydrogen Energy, 34 (2009) 4575-4581.

[25] C. Moreno-Castilla, F.J. Maldonado-Hódar, Carbon aerogels for catalysis applications: An overview, Carbon, 43 (2005) 455-465.

[26] C. Alegre, E. Baquedano, M.E. Gálvez, R. Moliner, M.J. Lázaro, Tailoring carbon xerogels' properties to enhance catalytic activity of Pt catalysts towards methanol oxidation, International Journal of Hydrogen Energy.

[27] J.P.S. Sousa, M.F.R. Pereira, J.L. Figueiredo, Carbon Xerogel Catalyst for NO Oxidation, Catalysts, 2 (2012) 447.

[28] A.K. Meena, G.K. Mishra, P.K. Rai, C. Rajagopal, P.N. Nagar, Removal of heavy metal ions from aqueous solutions using carbon aerogel as an adsorbent, Journal of Hazardous Materials, 122 (2005) 161-170.

[29] B. Yang, C. Yu, Q. Yu, X. Zhang, Z. Li, L. Lei, N-doped carbon xerogels as adsorbents for the removal of heavy metal ions from aqueous solution, RSC Adv., 5 (2015) 7182-7191.

[30] K.Y. Kang, S.J. Hong, B.I. Lee, J.S. Lee, Enhanced electrochemical capacitance of nitrogen-doped carbon gels synthesized by microwave-assisted polymerization of resorcinol and formaldehyde, Electrochemistry Communications, 10 (2008) 1105-1108.

[31] C. Alegre, D. Sebastián, M. Gálvez, R. Moliner, A. Stassi, A. Aricò, M. Lázaro, V. Baglio, PtRu Nanoparticles Deposited by the Sulfite Complex Method on Highly Porous Carbon Xerogels: Effect of the Thermal Treatment, Catalysts, 3 (2013) 744.

[32] S. Chandra, S. Bag, R. Bhar, P. Pramanik, Effect of transition and non-transition metals during the synthesis of carbon xerogels, Microporous and Mesoporous Materials, 138 (2011) 149-156.

[33] N. Mahata, M.F.R. Pereira, F. Suárez-García, A. Martínez-Alonso, J.M.D. Tascón, J.L. Figueiredo, Tuning of texture and surface chemistry of carbon xerogels, Journal of Colloid and Interface Science, 324 (2008) 150-155.

[34] E.G. Calvo, E.J. Juárez-Pérez, J.A. Menéndez, A. Arenillas, Fast microwave-assisted synthesis of tailored mesoporous carbon xerogels, J. Colloid Interface Sci., 357 (2011) 541-547.

[35] E.-P. Ng, S. Mintova, Nanoporous materials with enhanced hydrophilicity and high water sorption capacity, Microporous and Mesoporous Materials, 114 (2008) 1-26.

[36] R. Iler, The Chemistry of Silica; Solubility, Polymerization, Colloid and Surface Chemistry, and Biochemistry, John Wiley & Sons, New York1979.

[37] D.W. Breck, Zeolite molecular sieves: structure, Chemistry and Use, Wiley, New York, 636 (1974).

[38] E. Mathiowitz, J.S. Jacob, Y.S. Jong, T.M. Hekal, W. Spano, R. Guemonprez, A.M. Klibanov, R. Langer, Novel desiccants based on designed polymeric blends, Journal of applied polymer science, 80 (2001) 317-327.

[39] M. Dubinin, The potential theory of adsorption of gases and vapors for adsorbents with energetically nonuniform surfaces, Chemical Reviews, 60 (1960) 235-241.

[40] A. Lecloux, Texture of catalysts, Catalysis: science and technology, 2 (1981) 171-230.

[41] J.F. Vivo-Vilches, E. Bailón-García, A.F. Pérez-Cadenas, F. Carrasco-Marín, F.J. Maldonado-Hódar, Tailoring the surface chemistry and porosity of activated carbons: Evidence of reorganization and mobility of oxygenated surface groups, Carbon, 68 (2014) 520-530.

[42] J.L. Figueiredo, M.F.R. Pereira, The role of surface chemistry in catalysis with carbons, Catalysis Today, 150 (2010) 2-7.

[43] M. Wickenheisser, A. Herbst, R. Tannert, B. Milow, C. Janiak, Hierarchical MOF-xerogel monolith composites from embedding MIL-100(Fe,Cr) and MIL-101(Cr) in resorcinol-formaldehyde xerogels for water adsortion applications, Microporous and Mesoporous Materials, 215 (2015) 143-153.

PUBLICACIÓN VI

ON THE DESICCANT CAPACITY OF THE MESOPOROUS RF-XEROGELS

Isabel D. Alonso-Buenaposada, Ana Arenillas, J. Angel Menéndez, *Microporous and Mesoporous Materials, 248 (2017) 1-6.*

On the desiccant capacity of the mesoporous RF-xerogels

CrossMark

Isabel D. Alonso-Buenaposada, Ana Arenillas, J. Angel Menéndez[*]

Instituto Nacional del Carbón, CSIC, Apartado 73, 33080 Oviedo, Spain

ABSTRACT

Resorcinol-formaldehyde xerogels are ideal desiccant materials since the high concentration of hydroxyl groups on their surfaces confers on them a high hydrophilicity, which adsorbs moisture from their surroundings and their large porosity provides them with a high water sorption capacity. In this study, the porosity of organic xerogels was tailored by adjusting the proportion of methanol in the precursor solution in order to optimize their desiccant capability. It was found that, although an increase in microporosity improves the performance of the desiccant, mesoporosity is a more important property for this application. Organic xerogels are excellent desiccants which are able to adsorb more than 80 % of their own weight in moisture and function efficiently for more than 3000 h, when their porosity is optimized. This is a great improvement on the commonly used silica gels that become saturated after only 150 h and can only adsorb a maximum of 40 wt % of their own weight in moisture. Moreover, RF xerogels have the advantage that they are organic materials resistant to acid attack and this allows them to be used in processes where conventional inorganic desiccants would rapidly deteriorate.

Keywords: water sorption; desiccant materials; xerogels; hydrophilic materials

1. INTRODUCTION

Resorcinol-formaldehyde (RF) gels have been the most widely studied nanoporous organic gels in recent years [1-3]. However, other precursors can be used to produce materials with similar properties [4-9]. The synthesis process of these polymers consists of three steps: gelation, curing and drying. Depending on the type of drying method used in the synthesis process, (i.e., supercritical drying, freeze-drying or evaporative drying), they are classified as aerogels, cryogels or xerogels, respectively [10, 11]. In this study, microwave radiation was used as heating source to synthesize the xerogels described, as it is a simple, fast and cost-effective method to fabricate RF-xerogels in just one step using only one device [12].

The widely recognized advantage of RF xerogels is that it is possible to obtain materials whose porosity can be designed for a specific application by adjusting the variables used during the synthesis process (i.e., the pH of the precursor solution, dilution ratio, RF molar ratio, etc.) [13-16]. This versatility, in combination with the fact that they are light and cheap to produce, makes them suitable for a wide range of applications [17-21].

As already pointed out in a previous study, organic xerogels can be used as desiccant materials [22]. Any desiccant material, whose behaviour is determined by surface interactions and not by chemical reactions [23-25], requires two main properties to ensure its effectiveness [26]: i) hydrophilicity, i.e., its high affinity towards water and ii) a good sorption capacity, i.e., an ability to retain a large volume of water. In the case of RF xerogels, the high concentration of hydroxyl groups on their surfaces provides them with a high hydrophilicity that attracts surrounding moisture through hydrogen bonding, and their large porosity gives them their high water sorption capacity. Their hydrophilicity and suitability for use as desiccant materials have been demonstrated in a previous work [22]. However, in that study only two samples were evaluated and compared with a silica gel, a mesoporous xerogel and a macroporous RF xerogel with pore sizes of 10 and 2100 nm, respectively. There is a huge difference in pore size between 10 and 2100 nm, and although

pore size would seem to be the determinant factor for the performance of a desiccant, mesopores being more effective than others, there is still a need for pore-size optimization. Therefore, further studies on the influence of mesopore size on the desiccant behaviour of RF xerogels are required, as optimization of the mesopores is essential in light of the increasing use of desiccant materials for different applications in recent years [25, 27-29]. Moreover, the optimization of desiccant performance in combination with the chemical resistance of these RF xerogels (i.e. in acid or basic media), their light weight and their production in just one-step (without the need for any post-treatment or a large number of steps in the production line), make these materials highly cost-effective and competitive for scaling up.

Accordingly, in this work the influence of porous properties, in the mesopore range, on the water adsorption capacity of RF xerogels is studied in order to optimize their effectiveness as light-weight organic desiccants.

2. EXPERIMENTAL

2.1. Synthesis of organic xerogels

Organic xerogels were obtained by a process described in detail elsewhere [22]. Briefly, resorcinol (R), and formaldehyde (F) were mixed at a R/F molar ratio of 0.3. Water was added at a dilution ratio of 5, and the pH of the precursor solutions was adjusted to 5 using a 0.1 M NaOH solution (Titripac, Merck). As previously reported, the methanol (MeOH) content of formaldehyde solutions plays a determinant role in the formation of the porosity [14]. For this reason, formaldehyde solutions with: 2, 4, 13, 20, 30 and 40 % of MeOH were used in order to obtain different porosities. As the MeOH content is the only difference between the samples, the percentage of methanol is used in the nomenclature proceeded by OX in reference to the organic xerogel.

2.2. Sample characterization

Before characterization, the samples were outgassed (Micromeritics VacPrep 0.61) at 0.1 mbar and 120 ºC overnight in order to remove any humidity and other physisorbed gases.

2.2.1. Porous properties

The porosity of the samples was characterized by means of nitrogen adsorption-desorption isotherms and mercury porosimetry.

The nitrogen adsorption-desorption isotherms were measured at -196 ºC in a Tristar 3020 (Micromeritics) device. S_{BET}, micropore volume and pore size distribution were determined from the N_2 adsorption branch, by applying the Brunauer-Emmett-Teller equation, Dubinin-Raduskevich equation and DFT method, respectively. Total pore volume was estimated from the amount of nitrogen adsorbed at $p/p^0=0.99$.

Total pore volume and pore size were determined by means of mercury porosimetry, using an AutoPore IV 9500 (Micromeritics), which is able to measure from atmospheric pressure up to 228 MPa. In this study, the lowest limit of mesopores detectable by this apparatus was 5.5 nm. In accordance with the findings of previous studies [10], no alterations in the macro and mesoporosity were observed during the carbonization process (Figure S1a). Therefore, the organic xerogels were thermally treated under an inert atmosphere (700 ºC, 2 h) before mercury porosimetry characterization in order to avoid compression problems arising from the low mechanical resistance of these materials [30]. Figure S1 in the supplementary material shows the problems of mercury porosimetry characterization of the organic samples due to their poor mechanical properties.
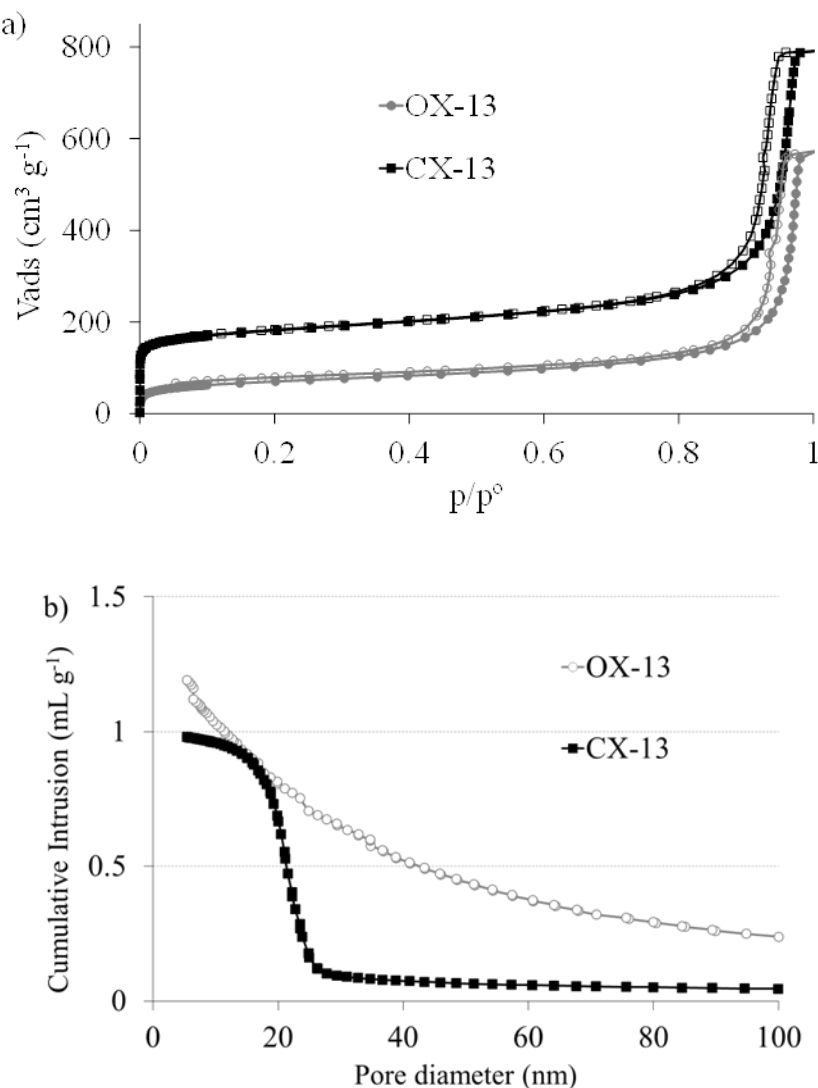
Figure S1. N_2 *adsorption-desorption of an organic xerogel and its carbonized counterpart (a) showing that the carbonization process only affect to the microporosity of the samples and has no influence on the meso-macroporosity; mercury porosimetry cannot be used as porosity characterization technique for organic xerogels due to their low mechanical properties and the compression problems shown (b).*

The bulk density and percentage of porosity of all the samples studied were determined by means of a Geopyc 1360 (Micromeritics) densitometer. A chamber with an internal diameter of 12.7 mm and a strength of 28 N over 20 cycles with conversion factor of 0.1284 (cm^3 mm^{-1}) was employed. The chamber

was filled with 0.8 g of Dryflow and a sample volume of ca. 50 % of the total volume.

2.2.2. Moisture adsorption capacity

For measuring the overall capacity of water vapour adsorption and kinetics, samples with a 2-3 mm particle size were kept in a sealed vessel in conditions of 100 % humidity at 25 ºC. Weight changes were recorded until a constant value was obtained.

On the other hand, water vapour adsorption-desorption isotherms were also evaluated by a volumetric method at 25 ºC using a Hydrosorb 1000 multigas instrument (Quantachrome). These isotherms were repeated five times for each sample in order to evaluate its regeneration capacity and the potential influence on moisture adsorption of the re-used desiccants. Samples were outgassed at 100 ºC under vacuum for 3 hours in the same analysis tube between subsequent water vapour isotherms.

2.2.3. Microscopy

A Zeiss DSM 942 scanning electron microscope was used to obtain micrographs of the RF xerogels. The samples were attached to an aluminium tap using conductive double-sided adhesive tape. An EDT Everhart-Thornley secondary electron detector, programmed to operate at an accelerating voltage of 25 kV, was employed for all the characterizations.

2.2.4. FTIR analysis

Fourier transform infrared spectroscopy (FTIR) was applied to evaluate the surface chemistry of the RF xerogels. A Nicolet FTIR 8700 fitted with a DTGS detector was employed. The data were recorded between 4000-400 cm^{-1}, over 64 scans at a resolution of 4 cm^{-1}.

3. RESULTS AND DISCUSSION

In a previous work [22] it was observed that xerogels of large pore size (macropores of ca. 2100 nm) show a poorer water adsorption capacity than those with a narrow mesoporosity (ca. 10 nm). Nevertheless, there are many possible pore sizes between these two options, and given that optimal water adsorption capability seems to be in the mesopore range, the search for a good desiccant should be based on finding the optimal mesopore size.

Table 1 shows the porous properties of RF xerogels synthesized with formaldehyde solutions with different concentrations of methanol. It can be observed that just by varying the methanol content mesopore materials with pore sizes of 8, 22 and 51 nm for samples OX-20, OX-13 and OX-4, respectively, can be obtained as well as a macroporous sample with narrow macropores centred at 79 nm (OX-2). Thus, the lower the concentration of methanol used, the higher the total pore volume and pore size achieved with the result that the density of the materials is reduced and their porosity is increased. The role of the methanol in the formaldehyde solution is to serve as a stabilizer, i.e. to prevent the formaldehyde molecules from precipitating. However, the methanol also acts as a retardant of the polymerization reaction between formaldehyde and resorcinol, which delays the crosslinking step and causes an increase in the size of the nodules (Figure 1a), generating wider pore inter-clusters and therefore less dense materials. As the methanol content increases, the nodules formed during the polymerization also decrease (Figures 1b and 1c) together with the pore size, resulting in denser materials.

Table 1. *Porous properties of the RF xerogels studied and the silica gel used as reference.*

Sample	Mercury porosimetry		Densitometer		N$_2$ adsorption-desorption isotherms		
	Pore volume (cm^{3}g^{-1})	Pore size (nm)	Bulk density (g cm^3)	Porosity (%)	S$_{BET}$ (m^2 g^{-1})	Micropore volume (cm^3 g^{-1})	Total pore volume (cm^3 g^{-1})
OX-2	2.07	79	0.30	79	169	0.07	0.38
OX-4	1.53	51	0.39	72	204	0.09	0.59
OX-13	0.98	22	0.48	66	261	0.10	0.88
OX-20	0.35	8	0.73	48	350	0.15	0.58
OX-30	0.33	7	0.70	50	600	0.23	0.72
OX-40	0	0	1.10	18	28	0.01	0.02
SG-760	n.a.	n.a.	1.21	42	760	0.28	0.42
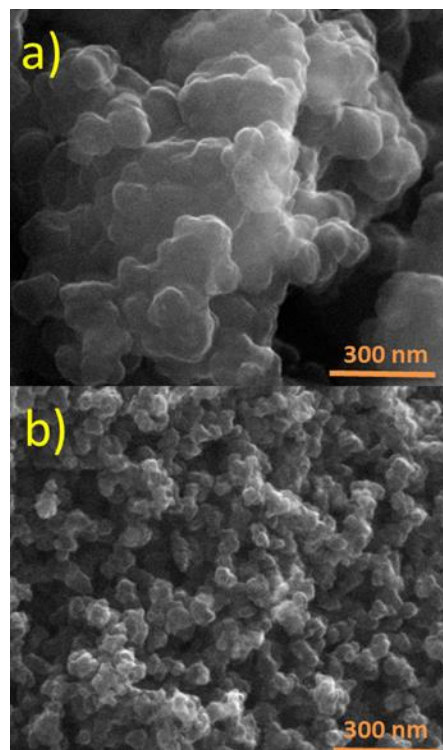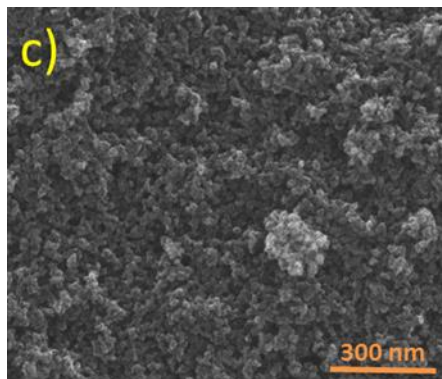
Figure.1. *SEM images showing the decrease in nodule size when the methanol content is increased for: a) OX-2, b) OX-13 and c) OX-20.*

It should also be mentioned that an excess of methanol during the synthesis of RF xerogels may result in such a weak structure that it may collapse during the drying step. This is the case of sample OX-40, which shows no porous properties (see Table 1).

Previous studies suggest that the methanol concentration has an influence only on meso and/or macroporosity, but not on micropore volume [14]. However, the nitrogen adsorption-desorption isotherms in Figure 2 show that the samples synthesized with very high concentrations of methanol experience an increase in volume adsorbed at low relative pressures, which indicates an increase in micropore volume and therefore, in the BET surface area (see Table 1), except for the sample with an excess of methanol (OX-40) that shows no N_2 adsorption. This effect on microporosity seems to be greater when larger concentrations of methanol are used. For example, an increase in methanol content of 11 wt% from OX-2 to OX-13 entails an increase of 92 m^2 g^{-1} in S_{BET} (Table 1). However, an increase of only 7 wt% of methanol from OX-13 to OX-20 also leads to an increase in S_{BET} of 91 m^2 g^{-1}. This could be due to the fact that the higher the concentration of methanol in the precursor mixture, the higher the concentration of residual methanol in the polymer that does not take part in the polymerization reaction. This residual compound may affect the drying step process, causing defects in the polymeric structure and in an increase in microporosity and S_{BET}. On the other hand, an excess of methanol

may result in such a weak structure that collapses, like OX-40. It is worth to be noted that the total pore volume determined by N_2 adsorption isotherms is underrated for samples with macroporsity (i.e. OX-2 and OX-4) as it is not the proper technique for these kind of pore characterization. On the other hand, samples with narrow mesoporosity may be underrated by the mercury porosimetry because this technique only characterizes pores bigger than 5.5 nm, and samples such as OX-20 and OX-30 have a considerable micropore volume (Table 1) and mesopores lower than 5 nm (Figure S2). Therefore, the combination of both techniques is mandatory for a complete porous properties characterization of series of samples with very different porosity.
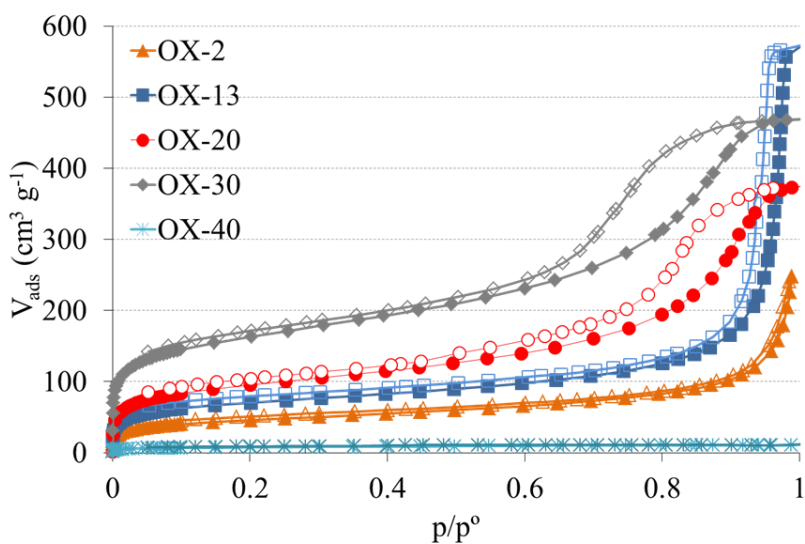
Figure.2. *N_2 adsorption-desorption isotherms of the samples synthesized with different concentrations of methanol.*
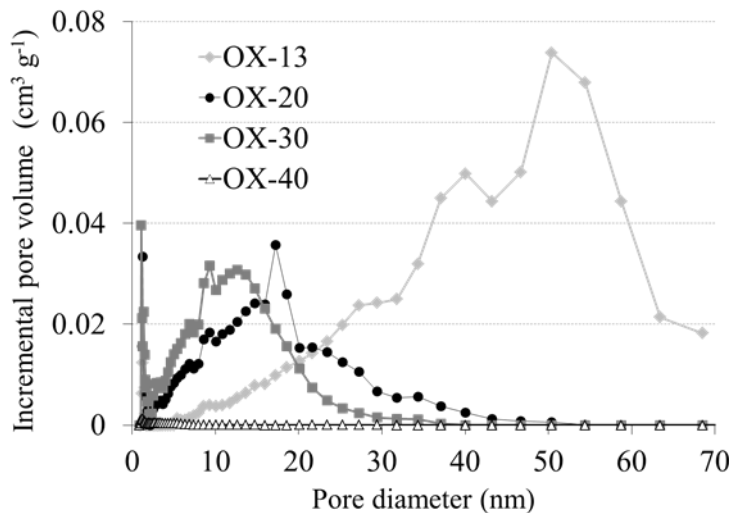
Figure S2. *Pore size distribution of the organic xerogels obtained from N_2 adosroption-desorption isotherms.*

In spite of all of the variations in the porosities of the samples synthesized with different methanol contents, the surface chemistry of the samples is almost identical in all cases. In Figure 3, the FTIR spectra of just two RF xerogels randomly selected are shown for purposes of clarity (all the samples studied show analogous spectra). It can be observed that the samples have similar functional groups. Both groups of spectra show two bands fixed at 2900 and 1400 cm^{-1} which correspond to aliphatic stretching and deformation vibrations, respectively. The stretching vibration from the aromatic ring of resorcinol is fixed at 1600 cm^{-1}. Moreover, the bands at 1100 and 1200 cm^{-1} correspond to methylene ether bridges formed during the polymerization. The wide band between 3600 and 3000 cm^{-1} is associated to O-H stretching vibrations from the phenolic groups of the resorcinol. These functional groups are the cause of the hydrophilicity of these materials since water molecules from the air are attracted by their surfaces through hydrogen bonding. Therefore, as the surface chemistry is the same in all the samples studied, any difference in their water sorption capacity must be caused by differences in their porous properties.
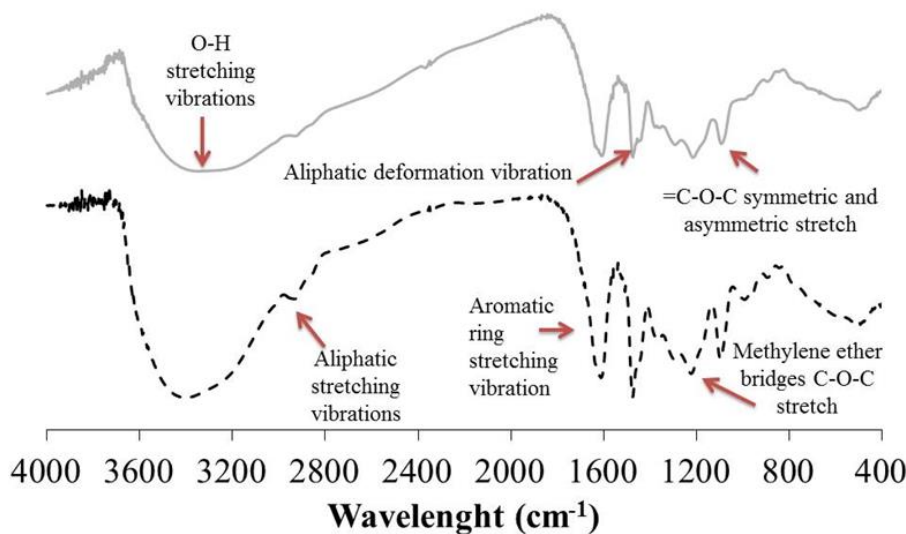
Figure. 3. FTIR spectra of two RF xerogels: OX-2 (top trace) and OX-20 (bottom trace).

Regarding the desiccant capability of these materials, Figure 4 shows that water adsorption performance at the beginning of the experiment is the same for all the samples, if they are exposed to the same humidity conditions (i.e. 100 %). This agrees with the fact that all the samples have the same surface chemistry (Figure 3), and therefore the same water affinity. It can be inferred therefore that, at the beginning of the experiment the porous properties, which differ significantly between samples, have no influence. However, as moisture adsorption takes place over the surface of the adsorbent, the role of the porous properties becomes more relevant. It is clear that samples with wider pores (i.e. 79 and 51 nm from OX-2 and OX-4, respectively), caused by introducing a lower methanol content, prove to be poorer desiccants because they become saturated even at very low percentages of moisture adsorption (ca. 20 wt%). It can be therefore affirmed that a good desiccant is characterized by its mesopore content and not by its macroporosity. Samples OX-13 and OX-20 show a greater water adsorption capacity, and the smaller the mesopore size is, the more water they adsorb (75 wt% and 83 % for 22 and 8 nm,

respectively). According to these results therefore, the water adsorption capacity is not favoured by a greater pore volume or greater percentage of porosity, but by the mesopore size. The sample with a pore size of ca. 8 nm (OX-20) seems to exhibit the highest adsorption capacity, although its pore volume is nearly 3 times lower than that of OX-13 (0.35 vs 0.98 cm^3 g^{-1} for OX-20 vs OX-13, respectively). However, this enhancement in desiccant performance could also be due to the micropore volume, as sample OX-20 also presents a higher S$_{BET}$ (350 vs 261 m^2 g^{-1} for OX-20 vs OX-13).
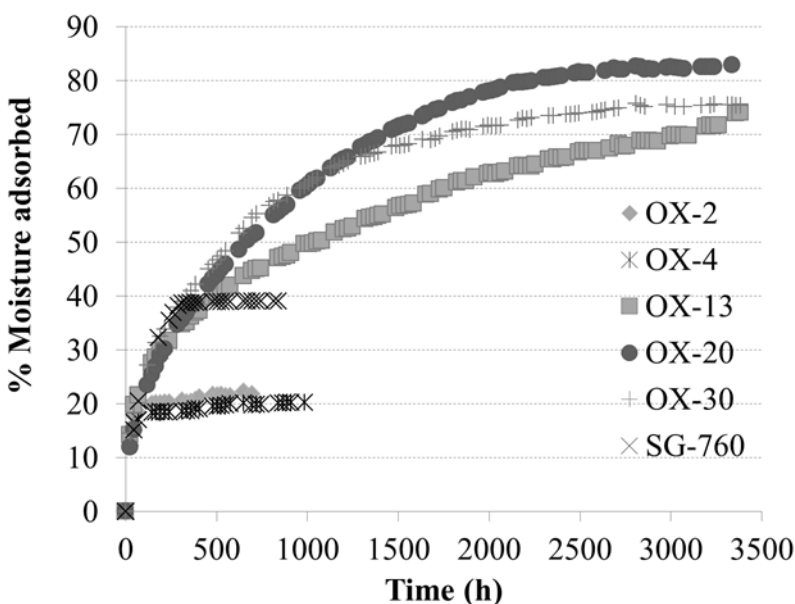
Fig. 4. *Moisture adsorption isotherms at 25 ºC, atmospheric pressure and 100 % humidity for organic xerogels with different pore sizes and the silica gel used as reference.*

The S$_{BET}$ (Table 1) and water adsorption data in Figure 4, indicate that the microporosity has no influence if the samples have wide pores (i.e. macropores). Thus, samples OX-2 and OX-4 have different S$_{BET}$ values (169 and 204 m^2 g^{-1}, respectively), but their adsorption capacities (Figure 4) are almost the same. However, if these samples are compared with OX-13 and OX-20, which have surface areas of 261 and 350 m^2 g^{-1}, it can be seen that the higher the microporosity is (i.e. the higher the S$_{BET}$) the greater the water adsorption capacity.

In order to determine the effect of microporosity on the desiccant performance an extra sample was synthesized and compared with the OX series. As mentioned before, all the RF xerogels have similar chemical compositions and so their surface chemistry cannot be considered a determinant variable in the water adsorption process. It is also well known that one of the main advantages of RF xerogels is that their porosity can be tailored by modifying the synthesis conditions. Therefore, a sample (OX-30) with the same surface chemistry and same mesoporosity as OX-20 was synthesized so that the only difference was in their microporosities. The porous characteristics and water adsorption performance of the OX-30 sample are shown in Table 1 and in Figure 4, respectively. It can be observed that the adsorption profile for the OX-13, OX-20 and OX-30 samples is very similar up to 500 h. At this stage the different microporosities of the samples have no influence at all on adsorption capacity. However, over longer periods of time the adsorption profiles of OX-20 and OX-30 increase more quickly than those of OX-13 due to the narrow mesoporosities of the former samples. Therefore, mesopores ca. 8 nm are preferable for this application. The adsorption profiles of OX-20 and OX-30 are very similar up to 1200 h of experimentation, due to their similar mesoporosities. At this point sample OX-20 shows a higher adsorption capacity than OX-30, even though its S_{BET} is smaller.

It is apparent that, although microporosity is important for the water adsorption, it is not the most important parameter. An increase in microporosity does not imply an increase in water adsorption capacity (see comparison of OX-20 profile to that of OX-30 in Figure 4). Like surface chemistry it is important for desiccant performance but it is not the most important parameter (see the OX-20 profile compared to the OX-2 profile in Figure 4). It is the presence of feeder pores in the mesoporosity range that is the most important parameter for optimal desiccant performance.

This implies that, although the micropore volume is important for this type of materials, it is the size and volume of the mesopores that make RF xerogels useful for water adsorption purposes. It is also worth pointing out that

sample OX-20, with mesopores of ca. 8 nm, adsorbs more than 80 % of its own weight in moisture and up to 20 % is adsorbed during the first 48 h. As one might expect, the rate of adsorption slows down with time as the surface becomes covered with water molecules; nevertheless it works effectively for more than 3000 h.

For comparative purposes, a new commercial silica gel from Sigma-Aldrich with a 2-6 mm particle size (SG-760), commonly used as desiccant material, was purchased. As the rest of the samples used in this work, this material was not previously used but outgassed, as described in the experimental section, before to carry out any experiment. The porous properties of this reference gel were also determined by N_2 adsorption-desorption isotherms (Figure S3). This material which is predominantly microporous has a pore volume of 0.32 cm^3 g^{-1}, a narrow mesopore size of 3 nm, and a S_{BET} of 760 m^2 g^{-1} (see Table 1). The water adsorption capacity of this reference gel was also evaluated in the same conditions as the series of RF xerogels (Figure 4). The results show that the commercial desiccant adsorbs less than 40 wt% and becomes saturated after 200 h of experimentation. It is clear that it is not the high microporosity of this sample that gives it its high water adsorption capacity, which suggests that microporosity is not the determinant factor here for producing an effective desiccant. However, it has to be taken into account that in this case the reference gel has a different chemistry to the RF xerogels, and therefore only a tentative comparison of the water adsorption process can be made.
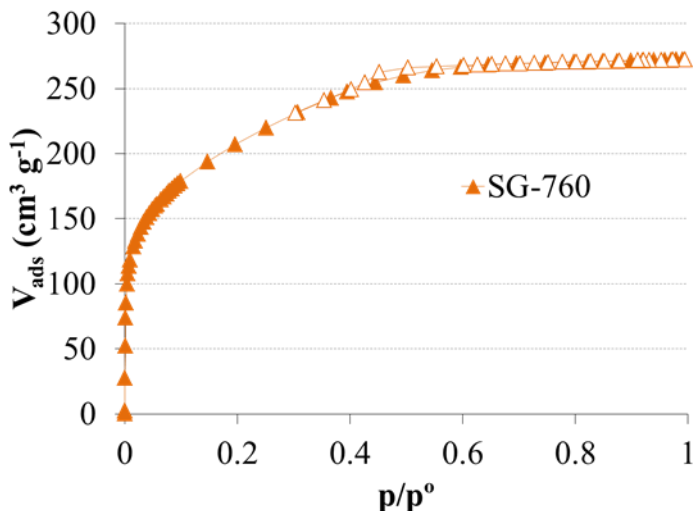
Figure S3. N_2 adsorption-desorption isotherm for the silica gel used as reference commercial desiccant.

The regeneration capacity of sample OX-20 was tested by saturating and regenerating the sample for 5 consecutive cycles, in the volumetric equipment mentioned in section 2.2.2. Given that part of the water retained in the porous structure of the sample cannot be desorbed by simply decreasing the pressure (see desorption branch in Figure 5), the sample was heated for regeneration at 100 ºC for 3 hour between cycles. The adsorption-desorption isotherms corresponding to cycles 1 and 5 are shown in Figure 5. As it can be observed, OX-20 preserves virtually intact its adsorption capacity after these 5 cycles. Therefore, it seems reasonable to assume that the optimised RF-xerogels have a good regeneration capacity.
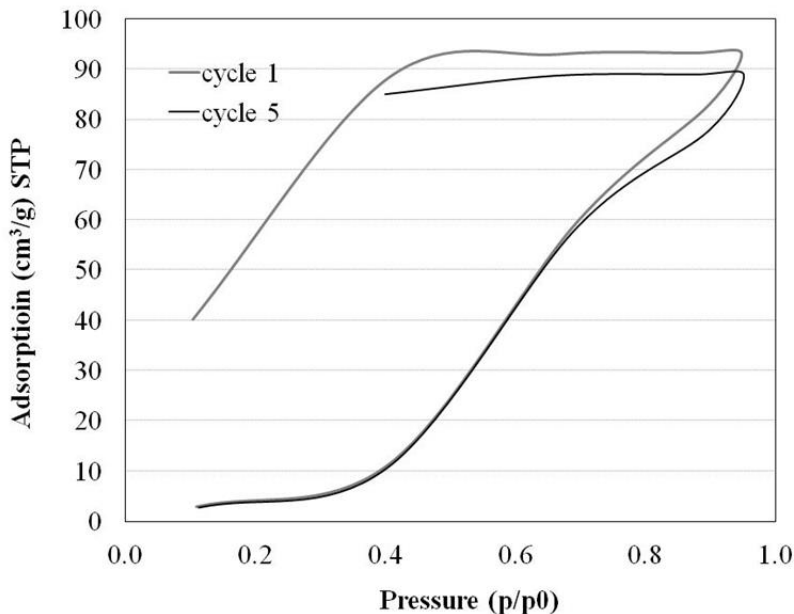
Fig. 5. *Water adsorption-desorption isotherms of sample OX-20 (pristine and after 5 cycles of adsorption/regeneration).*

4. CONCLUSIONS

Organic xerogels have demonstrated to be excellent desiccant materials which are able to adsorb more than 80 % of their own weight in moisture, up to 20 % of which is adsorbed during the first 48 h. In addition, they can work efficiently for more than 3000 h, once their porosity has been optimized. Although it is recognized that surface chemistry and microporosity are important features for this application, the key property for RF xerogels to function as an efficient desiccant material is mesopore size (i.e. pores ca. 8 nm). Moreover, the use of these organic materials as desiccants have other advantages such as their light weight and chemical resistance that make RF xerogels ideal for use in water removal processes.

ACKNOWLEDGEMENTS

REFERENCES

[1] J.J. Salazar-Rábago, M. Sánchez-Polo, J. Rivera-Utrilla, R. Leyva-Ramos, R. Ocampo-Pérez, F. Carrasco-Marin, Organic xerogels doped with Tris(2,2′-bipyridine) ruthenium(II) as hydroxyl radical promoters: Synthesis, characterization, and photoactivity, Chemical Engineering Journal, 306 (2016) 289-297.

[2] F. Orellana-García, M.A. Álvarez, M.V. López-Ramón, J. Rivera-Utrilla, M. Sánchez-Polo, M.Á. Fontecha-Cámara, Photoactivity of organic xerogels and aerogels in the photodegradation of herbicides from waters, Applied Catalysis B: Environmental, 181 (2016) 94-102.

[3] N. Rey-Raap, A. Arenillas, J.A. Menéndez, A visual validation of the combined effect of pH and dilution on the porosity of carbon xerogels, Microporous and Mesoporous Materials, 223 (2016) 89-93.

[4] K. Huang, S.-H. Chai, R.T. Mayes, S. Tan, C.W. Jones, S. Dai, Significantly increasing porosity of mesoporous carbon by NaNH2 activation for enhanced CO2 adsorption, Microporous and Mesoporous Materials, 230 (2016) 100-108.

[5] I. Naseri, A. Kazemi, A.R. Bahramian, M. Razzaghi Kashani, Preparation of organic and carbon xerogels using high-temperature–pressure sol–gel polymerization, Materials & Design, 61 (2014) 35-40.

[6] G. Amaral-Labat, L.I. Grishechko, V. Fierro, B.N. Kuznetsov, A. Pizzi, A. Celzard, Tannin-based xerogels with distinctive porous structures, Biomass and Bioenergy, 56 (2013) 437-445.

[7] C. Moreno-Castilla, M.B. Dawidziuk, F. Carrasco-Marín, Z. Zapata-Benabithe, Surface characteristics and electrochemical capacitances of carbon aerogels obtained from resorcinol and pyrocatechol using boric and oxalic acids as polymerization catalysts, Carbon, 49 (2011) 3808-3819.

[8] F.L. Braghiroli, V. Fierro, M.T. Izquierdo, J. Parmentier, A. Pizzi, L. Delmotte, P. Fioux, A. Celzard, High surface – Highly N-doped carbons from hydrothermally treated tannin, Industrial Crops and Products, 66 (2015) 282-290.

[9] W. Kiciński, M. Bystrzejewski, M.H. Rümmeli, T. Gemming, Porous graphitic materials obtained from carbonization of organic xerogels doped with transition metal salts, Bull Mater Sci, 37 (2014) 141-150.

[10] E.G. Calvo, A. Arenillas, J. Menéndez, Designing Nanostructured Carbon Xerogels, INTECH Open Access Publisher, Rijeka, 2011.

[11] N. Job, A. Théry, R. Pirard, J. Marien, L. Kocon, J.-N. Rouzaud, F. Béguin, J.-P. Pirard, Carbon aerogels, cryogels and xerogels: Influence of the drying method on the textural properties of porous carbon materials, Carbon, 43 (2005) 2481-2494.

[12] E.G. Calvo, E.J. Juárez-Pérez, J.A. Menéndez, A. Arenillas, Fast microwave-assisted synthesis of tailored mesoporous carbon xerogels, Journal of Colloid and Interface Science, 357 (2011) 541-547.

[13] N. Rey-Raap, J.A. Menéndez, A. Arenillas, Optimization of the process variables in the microwave-induced synthesis of carbon xerogels, J Sol-Gel Sci Technol, 69 (2014) 488-497.

[14] I.D. Alonso-Buenaposada, N. Rey-Raap, E.G. Calvo, J. Angel Menéndez, A. Arenillas, Effect of methanol content in commercial formaldehyde solutions on the porosity of RF carbon xerogels, Journal of Non-Crystalline Solids, 426 (2015) 13-18.

[15] N. Rey-Raap, J. Angel Menéndez, A. Arenillas, RF xerogels with tailored porosity over the entire nanoscale, Microporous and Mesoporous Materials, 195 (2014) 266-275.

[16] N. Job, C.J. Gommes, R. Pirard, J.-P. Pirard, Effect of the counter-ion of the basification agent on the pore texture of organic and carbon xerogels, Journal of Non-Crystalline Solids, 354 (2008) 4698-4701.

[17] M.R. Carrasco-Díaz, E. Castillejos-López, A. Cerpa-Naranjo, M.L. Rojas-Cervantes, On the textural and crystalline properties of Fe-carbon xerogels. Application as Fenton-like catalysts in the oxidation of paracetamol by H2O2, Microporous and Mesoporous Materials, 237 (2017) 282-293.

[18] C. Alegre, D. Sebastián, M.E. Gálvez, R. Moliner, M.J. Lázaro, Sulfurized carbon xerogels as Pt support with enhanced activity for fuel cell applications, Applied Catalysis B: Environmental, 192 (2016) 260-267.

[19] F.S. Dias, L.G. Tartuci, H.d.F. Gorgulho, W.S. Machado, Characterization of a carbon xerogel-based sensor for detection of acetone, ethanol, and methanol vapors, Sensors and Actuators B: Chemical, 231 (2016) 440-449.

[20] A.F. Léonard, C.J. Gommes, M.-L. Piedboeuf, J.-P. Pirard, N. Job, Rapid aqueous synthesis of ordered mesoporous carbons: Investigation of synthesis variables and application as anode materials for Li-ion batteries, Microporous and Mesoporous Materials, 195 (2014) 92-101.

[21] N. Job, S. Lambert, A. Zubiaur, C. Cao, J.-P. Pirard, Design of Pt/Carbon Xerogel Catalysts for PEM Fuel Cells, Catalysts, 5 (2015) 40.

[22] I.D. Alonso-Buenaposada, E.G. Calvo, M.A. Montes-Morán, J. Narciso, J.A. Menéndez, A. Arenillas, Desiccant capability of organic xerogels: Surface chemistry vs porous texture, Microporous and Mesoporous Materials, 232 (2016) 70-76.

[23] R. Iler, The Chemistry of Silica; Solubility, Polymerization, Colloid and Surface Chemistry, and Biochemistry, John Wiley & Sons, New York1979.

[24] D.W. Breck, Zeolite molecular sieves: structure, Chemistry and Use, Wiley, New York, 636 (1974).

[25] X. Zheng, T.S. Ge, R.Z. Wang, Recent progress on desiccant materials for solid desiccant cooling systems, Energy, 74 (2014) 280-294.

[26] E.-P. Ng, S. Mintova, Nanoporous materials with enhanced hydrophilicity and high water sorption capacity, Microporous and Mesoporous Materials, 114 (2008) 1-26.

[27] M. Wickenheisser, T. Paul, C. Janiak, Prospects of monolithic MIL-MOF@poly(NIPAM)HIPE composites as water sorption materials, Microporous and Mesoporous Materials, 220 (2016) 258-269.

[28] M. Wickenheisser, A. Herbst, R. Tannert, B. Milow, C. Janiak, Hierarchical MOF-xerogel monolith composites from embedding MIL-100(Fe,Cr) and MIL-101(Cr) in resorcinol-formaldehyde xerogels for water adsorption applications, Microporous and Mesoporous Materials, 215 (2015) 143-153.

[29] M.M. Rafique, P. Gandhidasan, H.M.S. Bahaidarah, Liquid desiccant materials and dehumidifiers – A review, Renewable and Sustainable Energy Reviews, 56 (2016) 179-195.

[30] N. Job, R. Pirard, J.P. Pirard, C. Alié, Non Intrusive Mercury Porosimetry: Pyrolysis of Resorcinol-Formaldehyde Xerogels, Particle & Particle Systems Characterization, 23 (2006) 72-81.

PATENTE

USO DE UN XEROGEL ORGÁNICO COMO DESECANTE

J. Angel Menéndez, Ana Arenillas, <u>Isabel D. Alonso-Buenaposada</u>, Esther G. Calvo, Natalia Rey-Raap, Miguel A. Montes-Morán, *Referencia: ES1641.1201. (2016). Extensión a solicitud internacional: PTC1641.1201*

Justificante de presentación electrónica de solicitud de patente

Este documento es un justificante de que se ha recibido una solicitud española de patente por vía electrónica, utilizando la conexión segura de la O.E.P.M. Asimismo, se le ha asignado de forma automática un número de solicitud y una fecha de recepción, conforme al artículo 14.3 del Reglamento para la ejecución de la Ley 11/1986, de 20 de marzo, de Patentes. La fecha de presentación de la solicitud de acuerdo con el art. 22 de la Ley de Patentes, le será comunicada posteriormente.

Número de solicitud:	P201630261
Fecha de recepción:	04 marzo 2016, 13:22 (CET)
Oficina receptora:	OEPM Madrid
Su referencia:	ES1641.1201
Solicitante:	CONSEJO SUPERIOR DE INVESTIGACIONES CIENTÍFICAS (CSIC)
Número de solicitantes:	1
País:	ES
Título:	USO DE UN XEROGEL ORGÁNICO COMO DESECANTE
Documentos enviados:	Descripcion.pdf (11 p.) package-data.xml Reivindicaciones-1.pdf (2 p.) es-request.xml Dibujos-1.pdf (1 p.) application-body.xml Resumen-1.pdf (1 p.) es-fee-sheet.xml OLF-ARCHIVE.zip feesheet.pdf FEERCPT-1.pdf (1 p.) request.pdf
Enviados por:	CN=ENTIDAD PONS PATENTES Y MARCAS INTERNACIONAL SL - CIF B84921709 - NOMBRE PONS ARIÑO ANGEL - NIF 50534279J,OU=703015345,OU=fnmt clase 2 ca,O=FNMT,C=es
Fecha y hora de recepción:	04 marzo 2016, 13:22 (CET)
Codificación del envío:	2F:DB:64:CB:3B:D1:AF:24:35:C4:5A:E7:3C:95:A7:B7:A6:BE:37:28

AVISO IMPORTANTE

Las tasas pagaderas al solicitar y durante la tramitación de una patente o un modelo de utilidad son las que se recogen en el Apartado "Tasas y precios públicos" de la página web de la OEPM (http://www.oepm.es/es/propiedad_industrial/tasas/). Consecuentemente, si recibe una comunicación informándole de la necesidad de hacer un pago por la inscripción de su patente o su modelo de utilidad en un "registro central" o en un "registro de internet" posiblemente se trate de un fraude.

La anotación en este tipo de autodenominados "registros" no despliega ningún tipo de eficacia jurídica ni tiene carácter oficial.

En estos casos le aconsejamos que se ponga en contacto con la Oficina Española de Patentes y Marcas en el correo electrónico informacion@oepm.es.

ADVERTENCIA: POR DISPOSICIÓN LEGAL LOS DATOS CONTENIDOS EN ESTA SOLICITUD PODRÁN SER PUBLICADOS EN EL BOLETÍN OFICIAL DE LA PROPIEDAD INDUSTRIAL E INSCRITOS EN EL REGISTRO DE PATENTES DE LA OEPM, SIENDO AMBAS BASES DE DATOS DE CARÁCTER PÚBLICO Y ACCESIBLES VÍA REDES MUNDIALES DE INFORMÁTICA.

Para cualquier aclaración puede contactar con la O.E.P.M.

/Madrid, Oficina Receptora/

MINISTERIO
DE INDUSTRIA, ENERGÍA
Y TURISMO

Oficina Española
de Patentes y Marcas

(1) MODALIDAD:		
	PATENTE DE INVENCIÓN	[✓]
	MODELO DE UTILIDAD	[ ]

(2) TIPO DE SOLICITUD:		
	PRIMERA PRESENTACIÓN	[✓]
	ADICIÓN A LA PATENTE EUROPEA	[ ]
	ADICIÓN A LA PATENTE ESPAÑOLA	[ ]
	SOLICITUD DIVISIONAL	[ ]
	CAMBIO DE MODALIDAD	[ ]
	TRANSFORMACIÓN SOLICITUD PATENTE EUROPEA	[ ]
	PCT: ENTRADA FASE NACIONAL	[ ]

(3) EXP. PRINCIPAL O DE ORIGEN:		
	MODALIDAD:	
	N.º SOLICITUD:	
	FECHA SOLICITUD:	

4) LUGAR DE PRESENTACIÓN:		
		OEPM, Presentación Electrónica

(5-1) SOLICITANTE 1:		
	DENOMINACIÓN SOCIAL:	CONSEJO SUPERIOR DE INVESTIGACIONES CIENTÍFICAS (CSIC)
	UNIVERSIDAD PÚBLICA	[ ]
	NACIONALIDAD:	España
	CÓDIGO PAÍS:	ES
	NIF/NIE/PASAPORTE:	Q2818002D
	CNAE:	
	PYME:	
	DOMICILIO:	C/ Serrano, nº 117
	LOCALIDAD:	Madrid
	PROVINCIA:	28 Madrid
	CÓDIGO POSTAL:	28006
	PAÍS RESIDENCIA:	España
	CÓDIGO PAÍS:	ES
	TELÉFONO:	
	FAX:	
	CORREO ELECTRÓNICO:	
	PERSONA DE CONTACTO:	
MODO DE OBTENCIÓN DEL DERECHO:	INVENCIÓN LABORAL:	[✓]
	CONTRATO:	[ ]
	SUCESIÓN:	[ ]
	PORCENTAJE DE TITULARIDAD:	100,00 %

(6-1) INVENTOR 1:		
	APELLIDOS:	MENÉNDEZ DÍAZ
	NOMBRE:	J. ÁNGEL
	NACIONALIDAD:	España
	CÓDIGO PAÍS:	ES
	NIF/NIE/PASAPORTE:	
(6-2) INVENTOR 2:		
	APELLIDOS:	ARENILLAS DE LA PUENTE
	NOMBRE:	ANA
	NACIONALIDAD:	España
	CÓDIGO PAÍS:	ES
	NIF/NIE/PASAPORTE:	
(6-3) INVENTOR 3:		
	APELLIDOS:	DÍAZ

	ALONSO-BUENAPOSADA
NOMBRE:	ISABEL
NACIONALIDAD:	España
CÓDIGO PAÍS:	ES
NIF/NIE/PASAPORTE:	

(6-4) INVENTOR 4:

APELLIDOS:	GÓMEZ CALVO
NOMBRE:	ESTHER
NACIONALIDAD:	España
CÓDIGO PAÍS:	ES
NIF/NIE/PASAPORTE:	

(6-5) INVENTOR 5:

APELLIDOS:	REY-RAAP
NOMBRE:	NATALIA
NACIONALIDAD:	España
CÓDIGO PAÍS:	ES
NIF/NIE/PASAPORTE:	

(7) TÍTULO DE LA INVENCIÓN:

USO DE UN XEROGEL ORGÁNICO COMO DESECANTE

(8) PETICIÓN DE INFORME SOBRE EL ESTADO DE LA TÉCNICA:

SI [ ]
NO [✓]

(9) SOLICITA LA INCLUSIÓN EN EL PROCEDIMIENTO ACELERADO DE CONCESIÓN

SI [ ]
NO [✓]

(10) EFECTUADO DEPÓSITO DE MATERIA BIOLÓGICA:

SI [ ]
NO [✓]

(11) DEPÓSITO:

REFERENCIA DE IDENTIFICACIÓN:
INSTITUCIÓN DE DEPÓSITO:
NÚMERO DE DEPÓSITO:
ACCESIBILIDAD RESTRINGIDA A UN EXPERTO (ART. 45.1. B):

(12) DECLARACIONES RELATIVAS A LA LISTA DE SECUENCIAS:

LA LISTA DE SECUENCIAS NO VA MÁS ALLÁ DEL CONTENIDO DE LA SOLICITUD [ ]
LA LISTA DE SECUENCIAS EN FORMATO PDF Y ASCII SON IDENTICOS [ ]

(13) EXPOSICIONES OFICIALES:

LUGAR:
FECHA:

(14) DECLARACIONES DE PRIORIDAD:

PAÍS DE ORIGEN:
CÓDIGO PAÍS:
NÚMERO:
FECHA:

(15) AGENTE DE PROPIEDAD INDUSTRIAL:

APELLIDOS:	PONS ARIÑO
NOMBRE:	ÁNGEL
CÓDIGO DE AGENTE:	0499/5
NÚMERO DE PODER:	20081765

(16) RELACIÓN DE DOCUMENTOS QUE SE ACOMPAÑAN:

DESCRIPCIÓN:	[✓] N.º de páginas: 11
REIVINDICACIONES:	[✓] N.º de reivindicaciones: 17
DIBUJOS:	[✓] N.º de dibujos: 1
RESUMEN:	[✓] N.º de páginas: 1
FIGURA(S) A PUBLICAR CON EL RESUMEN:	[ ] N.º de figura(s):
ARCHIVO DE PRECONVERSION:	[✓]
DOCUMENTO DE REPRESENTACIÓN:	[ ] N.º de páginas:
JUSTIFICANTE DE PAGO (1):	[✓] N.º de páginas: 1

LISTA DE SECUENCIAS PDF:	[ ] N.º de páginas:
ARCHIVO PARA LA BUSQUEDA DE LS:	[ ]
OTROS (Aparecerán detallados):	
(17) EL SOLICITANTE SE ACOGE AL APLAZAMIENTO DE PAGO DE TASA PREVISTO EN EL ART. 162 DE LA LEY 11/1986 DE PATENTES, DECLARA: BAJO JURAMIENTO O PROMESA SER CIERTOS TODOS LOS DATOS QUE FIGURAN EN LA DOCUMENTACIÓN ADJUNTA:	[ ]
DOC COPIA DNI:	[ ] N.º de páginas:
DOC COPIA DECLARACIÓN DE CARENCIA DE MEDIOS:	[ ] N.º de páginas:
DOC COPIA CERTIFICACIÓN DE HABERES:	[ ] N.º de páginas:
DOC COPIA ÚLTIMA DECLARACIÓN DE LA RENTA:	[ ] N.º de páginas:
DOC COPIA LIBRO DE FAMILIA:	[ ] N.º de páginas:
DOC COPIA OTROS:	[ ] N.º de páginas:
(18) NOTAS:	
(19) FIRMA: FIRMA DEL SOLICITANTE O REPRESENTANTE: LUGAR DE FIRMA: FECHA DE FIRMA:	

MINISTERIO DE INDUSTRIA, ENERGIA Y TURISMO	Oficina Española de Patentes y Marcas	TASA en materia de Propiedad Industrial CODIGO 511	Modelo 791

Identificación

	Ejercicio:	2016
	Nro Justificante:	7915111336343

Sujeto Pasivo

NIF:

Apellidos y Nombre o Razón Social:

Agente o Representante legal (1):

NIF: 50534279J

Apellidos y Nombre o Razón Social: ÁNGEL PONS ARIÑO

Código de Agente o Representante (2):   0499

Autoliquidación

Titular del expediente si es distinto del pagador: CSIC

Modalidad Expediente: P   Número Expediente: Tipo (3):

Clave: IE01   Año: 2016   Concepto: SOL. DE INVENCION O REAHABILITACIÓN POR INTERNET

Unidades: 1   Importe: 63,68

Referencia OEPM: 88129418085

909992100200188129418085

Declarante

Fecha: 4/03/16 13:05

Firma: ÁNGEL PONS ARIÑO

Ingreso

Importe en euros: 63,68   Adeudo en cuenta: ⊗

NRC Asignado: 7915111336343000000001

Modelo 791

(1) Solo cuando el pago se realice con cargo a la cuenta corriente del representante o agente.
(2) En el caso de que tenga asignado un número por la OEPM.
(3) En el caso de patentes europeas, se pondrá una P si es el número de publicación o una S si es el número de solicitud.

OEPM, Paseo de la Castellana, 75, 28071 Madrid   NIF: Q2820005C

TBP

MINISTERIO
DE INDUSTRIA, ENERGÍA
Y TURISMO

Oficina Española
de Patentes y Marcas

OFICINA ESPAÑOLA DE PATENTES Y MARCAS

Hoja informativa sobre pago de tasas de una solicitud de patente o modelo de utilidad

1. REFERENCIA DE SOLICITUD	ES1641.1201	
2. TASAS	**Importe (en euros)**	
Concepto	**Código de barras asignado**	**Importe**
IE01 Solicitud de demanda de depósito o de rehabilitación.	88129418085	63,68
IE02 Solicitud de cambio de modalidad en la protección		0,00
IE04 Petición IET		0,00
IE06 Prioridad extranjera (0)		0,00
El solicitante se acoge al aplazamiento de tasas previsto en el art. 162 de la Ley 11/1986 de Patentes El solicitante es una Universidad pública	❏ ❏	
Importe total		63,68
Importe abonado		63,68

Se ha aplicado el 15% de descuento sobre la tasa de solicitud de acuerdo con la D. Adic. 8.2 Ley de Marcas.

DESCRIPCIÓN

La presente invención se refiere al uso como desecante de un xerogel orgánico, preferiblemente un xerogel de resorcinol/formaldehído (xerogel RF), de alta porosidad y alto contenido de oxígeno.

ESTADO DE LA TÉCNICA

Los geles orgánicos son materiales nanoporosos obtenidos por la polimerización de bencenos hidroxilados y aldehídos en presencia de un disolvente (ver Pekala, R. Organic aerogels from the polycondensation of resorcinol with formaldehyde. Journal of Materials Science 1989, 24, 3221-3227).

Los materiales desecantes son sólidos higroscópicos que inducen o mantienen un estado de sequedad del medio que les rodea. Con el fin de ser considerado como un buen material desecante poroso, no sólo tiene que ser un material hidrófilo sino que además es necesario que posea una alta capacidad de adsorción de agua (ver Ng, E.-P.; Mintova, S. Nanoporous materials with enhanced hydrophilicity and high water sorption capacity. Microporous and Mesoporous Materials 2008, 114, 1-26). La capacidad hidrófila hace referencia a su afinidad por el agua, mientras que su capacidad de adsorción depende principalmente de la porosidad. Por ejemplo, algunos materiales basados en carbono considerados como hidrófilos muestran una alta capacidad de adsorción de agua debido a su química superficial rica en grupos oxigenados, pero su velocidad de adsorción es baja debido a que su porosidad no es la adecuada, por lo que no pueden ser considerados como desecantes.

En términos generales, existen dos tipos de materiales desecantes: (i) sustancias cuyo comportamiento como desecante se debe a una reacción química de hidratación, tales como P_4O_{10}, $MgSO_4$; y (ii) sustancias cuyo comportamiento desecante se basa en interacciones de superficie, como procesos de adsorción, tales como tamices moleculares, geles de sílice, arcillas y almidones (ver por ejemplo, Iler, R. The chemistry of silica; solubility,

polymerization, colloid and surface chemistry, and biochemistry. John Wiley & Sons, New York: 1979; y Breck, D.W. Zeolite molecular sieves: Structure. Chemistry and Use, Wiley, New York 1974, 636).

Los desecantes se han utilizado durante las últimas décadas en una amplia gama de aplicaciones, con el objetivo de controlar la humedad en el aire cuando es necesario un ambiente libre de humedad, para controlar el nivel de agua en las corrientes de gas industriales, en los sistemas de aire acondicionado, para almacenar y proteger las mercancías en contenedores de transporte contra el daño de la humedad (Mathiowitz, E.; Jacob, J.S.; Jong, Y.S.; Hekal, T.M.; Spano, W.; Guemonprez, R.; Klibanov, A.M.; Langer, R. Novel desiccants based on designed polymeric blends. Journal of applied polymer science 2001, 80, 317-327).

Un desecante de uso generalizado es el gel de sílice. Su buena capacidad de adsorción de humedad se debe a sus propiedades porosas y la presencia de grupos hidroxilo en la superficie que dota a estos materiales de naturaleza hidrófila. Las moléculas de agua son atraídas por esta química superficial rica en oxígeno y almacenadas en los poros del material.

La gel de sílice no puede ser utilizada para eliminar humedad en medios ácidos por presentar una estructura sensible a éstos.

Por tanto, sería deseable disponer de un agente desecante que permita eliminar la humedad de una forma rápida y que, por tanto, presente una alta velocidad de absorción de humedad además de una alta capacidad de absorción de humedad; que sea resistente a los ácidos que puedan estar presentes en los fluidos a tratar; y que sean modificables estructuralmente para poder eliminar otros componentes a parte aparte de la humedad.

DESCRIPCIÓN DE LA INVENCIÓN

Como se ha mencionado anteriormente, la presente invención se refiere al uso como desecante de un xerogel orgánico, preferiblemente un xerogel RF, de alta porosidad y gran cantidad de grupos superficiales oxigenados.

Así, en un primer aspecto, la presente invención se refiere al uso de un xerogel orgánico como desecante, donde:

o el tamaño medio de poro de dicho xerogel orgánico es de entre 2 nm y 50 nm; y

o el contenido de oxígeno de dicho xerogel orgánico es de al menos el 25 % en peso.

En otra realización la invención se refiere al uso definido anteriormente, donde la porosidad total está comprendida entre el 60 % y el 70 %.

En otra realización la invención se refiere al uso definido anteriormente, donde al menos el 55 % de dicha porosidad se debe a poros cuyo tamaño de poro está comprendido entre los 2 nm y los 50 nm.

En otra realización la invención se refiere al uso definido anteriormente, donde el 58 % de dicha porosidad se debe a poros cuyo tamaño de poro está comprendido entre los 2 nm y los 50 nm.

En otra realización la invención se refiere al uso definido anteriormente, donde la porosidad total es del 61%.

En otra realización la invención se refiere al uso definido anteriormente, donde:

o la porosidad total está comprendida entre el 60 % y el 90 %; y

o al menos el 50 %, preferiblemente el 58 %, de dicha porosidad se debe a poros cuyo tamaño de poro está comprendido entre los 2 nm y los 50 nm.

En otra realización la invención se refiere al uso definido anteriormente, donde.

- o la porosidad total está comprendida entre el 60 % y el 70 %; y

- o al menos el 55 % de dicha porosidad se debe a poros cuyo tamaño de poro está comprendido entre los 2 nm y los 50 nm.

En otra realización la invención se refiere al uso definido anteriormente, donde:

- o la porosidad total es del 61 %; y

- o el 58 % de dicha porosidad se debe a poros cuyo tamaño de poro está comprendido entre los 2 nm y los 50 nm.

En otra realización la invención se refiere al uso definido anteriormente, donde el xerogel orgánico resulta de la polimerización, preferiblemente de la polimerización en microondas, entre un aldehído y un benceno hidroxilado.

En otra realización la invención se refiere al uso definido anteriormente, donde el aldehído se selecciona de formaldehído y furfural.

En otra realización la invención se refiere al uso definido anteriormente, donde el benceno hidroxilado se selecciona de resorcinol, fenol y catecol.

En otra realización la invención se refiere al uso definido anteriormente, donde:

- o el aldehído se selecciona de formaldehído y furfural; y

- o el benceno hidroxilado se selecciona de resorcinol, fenol y catecol.

En otra realización la invención se refiere al uso definido anteriormente, donde el xerogel orgánico se selecciona de xerogel resorcinol/formaldehído y xerogel fenol/formaldehído.

En otra realización la invención se refiere al uso definido anteriormente, donde el xerogel orgánico es un xerogel resorcinol/formaldehído.

En otra realización la invención se refiere al uso definido anteriormente, donde la polimerización se lleva a cabo a un pH comprendido entre 4 y 8, y preferiblemente a un pH de 5.8.

En otra realización la invención se refiere al uso definido anteriormente, donde el xerogel resorcinol/formaldehído se obtiene mediante una etapa de polimerización en microondas de una mezcla de resorcinol (R), formaldehído (F), agua y un catalizador.

En otra realización la invención se refiere al uso definido anteriormente, donde el xerogel resorcinol/formaldehído se obtiene mediante una etapa de polimerización en microondas de una mezcla de resorcinol (R), formaldehído (F), agua y un catalizador de naturaleza básica.

En otra realización la invención se refiere al uso definido anteriormente, donde el xerogel resorcinol/formaldehído se obtiene mediante una etapa de polimerización en microondas de una mezcla de resorcinol (R), formaldehído (F), agua y un catalizador de naturaleza básica; y dicho catalizador de naturaleza básica es inorgánico, y preferiblemente se selecciona de $Na(OH)_2$, $Ca(OH)_2$, Na_2CO_3,$NaHCO_3$, NH_4NO_3 y NH_4Cl.

En otra realización la invención se refiere al uso definido anteriormente, donde el xerogel resorcinol/formaldehído se obtiene mediante una etapa de polimerización en microondas de una mezcla de resorcinol (R), formaldehído (F), agua y un catalizador de naturaleza básica; y dicho catalizador de naturaleza básica es orgánico, y preferiblemente se selecciona de urea, melamina, pirona, piridina, metil-amina y dimetil-amina.

En otra realización la invención se refiere al uso definido anteriormente, donde la relación molar entre el resorcinol (R) y el formaldehído (F) es de entre el 0.5 y el 0.7, y preferiblemente de 0.5.

En otra realización la invención se refiere al uso definido anteriormente, donde el xerogel orgánico se obtiene tras un post-tratamiento en aire a una temperatura de entre 100 ºC y 300 ºC, y preferiblemente a una temperatura de 100 ºC.

A lo largo de la presente invención, el término "desecante" se refiere a una sustancia que se usa para eliminar humedad del aire u otro medio gaseoso o de alguna otra sustancia.

El término "gel orgánico" se refiere a un polímero sólido de naturaleza orgánica que se obtiene mediante un proceso sol-gel de polimerización de uno o varios precursores (monómeros) de naturaleza orgánica, y posterior eliminación del disolvente en el que se ha llevado a cabo la polimerización.

El término "xerogel orgánico" se refiere un tipo de gel orgánico que se obtiene a presión atmosférica y a temperaturas próximas a las ambientales (nunca negativas y como máximo a unos 100 ºC). Ejemplos incluyen cualquier xerogel resultante de la polimerización entre un aldehído y un benceno hidroxilado (un anillo de benceno sustituido en cualquiera de sus posiciones disponibles por de uno a cuatro grupos hidroxilo). Ejemplos de aldehído incluyen entre otros resorcinol, fenol y cocatecol. Ejemplos de aldehído incluyen entre otros furfural y formaldehído.

El término "xerogel RF" o "xerogel resorcinol/formaldehído" se refiere a un gel orgánico obtenido a partir de la polimerización de resorcinol (R) y formaldehido (F) en el que el disolvente es eliminado por evaporación, y preferiblemente eliminando el disolvente por evaporación en horno microondas.

Los xerogeles a los que se refiere la invención presentan una cinética, o velocidad de adsorción, superior a la del gel de sílice, por lo que puede considerarse que es un desecante que actúa de una forma rápida.

El término "porosidad" o "fracción de huecos", se refiere a la medida de los espacios vacíos en un material, y es una fracción del volumen de huecos sobre el volumen total del material, expresado como un porcentaje entre 0 % y 100 %. La porosidad de los xerogeles de la invención es de entre el 60 % y el 90 %, preferiblemente de entre el 60 % y 70 % y más preferiblemente del 61 %.

El término "catalizador de naturaleza básica" se refiere a una sustancia de naturaleza orgánica o inorgánica cuyo pH en disolución acuosa es superior a 7. Ejemplos de catalizador de naturaleza inorgánica incluyen, entre otros,

Na(OH), Ca(OH)$_2$, Na$_2$CO$_3$, NaHCO$_3$, NH$_4$NO$_3$ y NH$_4$Cl. Ejemplos de catalizador de naturaleza orgánica incluyen, entre otros urea, melamina, pirona, piridina, metil-amina y dimetil-amina.

El término "post-tratamiento en aire" se refiere a un tratamiento a temperatura superior a 100 ºC e inferior a 300 ºC, presión atmosférica y atmósfera de aire, que se hace después de la síntesis del xerogel. Este post-tratamiento puede llevarse a cabo en una estufa convencional o en cualquier otro tipo de dispositivo capaz de elevar la temperatura del material hasta la temperatura del post-tratamiento.

A lo largo de la descripción y las reivindicaciones la palabra "comprende" y sus variantes no pretenden excluir otras características técnicas, aditivos, componentes o pasos. Para los expertos en la materia, otros objetos, ventajas y características de la invención se desprenderán en parte de la descripción y en parte de la práctica de la invención. Los siguientes ejemplos y figuras se proporcionan a modo de ilustración, y no se pretende que sean limitativos de la presente invención.

BREVE DESCRIPCIÓN DE LAS FIGURAS

FIG. 1 muestra las isotermas de adsorción de vapor de agua obtenidas a 25 ºC y a una humedad relativa (del aire) del 100 %

EJEMPLOS

A continuación se ilustrará la invención mediante unos ensayos realizados por los inventores, que ponen de manifiesto la efectividad del producto de la invención.

Síntesis de xerogeles orgánicos

Los xerogeles orgánicos utilizados en este estudio fueron sintetizados mediante la polimerización de resorcinol (R) y formaldehído (F), utilizando agua desionizada como disolvente y NaOH como catalizador de la reacción. En primer lugar, resorcinol (Indspec, 99,6 %) se disolvió en agua desionizada usando un vaso de vidrio sin sellar y agitación magnética hasta su completa disolución. Después, se añadió una solución de formaldehído hasta obtener una solución homogénea. Se añadió una solución de NaOH (0,1 M, Titripac, Merck) gota a gota para ajustar el pH deseado. La proporción de cada reactivo se selecciona de tal manera que se obtienen dos porosidades diferentes (Tabla 1). Las soluciones precursoras se colocaron en un horno microondas a 85 °C durante aproximadamente 3 horas. Durante este tiempo tiene lugar la polimerización y curado de los xerogeles. Posteriormente, los polímeros se secaron por calentamiento en un horno microondas hasta registrar una pérdida de masa de más de 50 %, lo que se corresponde con la eliminación total del disolvente, siendo el tiempo total de síntesis inferior a 5 h. Como resultado se obtuvieron dos geles orgánicos diferentes (Tabla 2). Finalmente los xerogeles se sometieron a un post-tratamiento en aire a una temperatura de 100 °C durante una hora.

Caracterización de las muestras

Antes de que cualquier caracterización, los xerogeles se desgasificaron (Micromeritics VacPrep 0,61) a 0,1 mbar y 120 °C durante una noche, con el fin de eliminar la humedad y otros gases adsorbidos.

Propiedades porosas

La porosidad de las muestras estudiadas se caracterizó por medio de isotermas de adsorción-desorción de nitrógeno y porosimetría de mercurio.

Las isotermas de adsorción-desorción de nitrógeno se midieron a -196 ºC en un Tristar 3020 (Micromeritics). La superficie BET se determinó a partir de la rama de adsorción de N_2 y, en todos los casos; el número de puntos utilizados para aplicar la ecuación BET fue superior a 5. El volumen de microporos (V_{micro}) se estimó por el método de Dubinin-Raduskevich. Este método sólo incluye superficies de microporos. Por lo tanto, ambas técnicas son complementarias. Las isotermas de adsorción-desorción de N_2 solamente se utilizaron para obtener información acerca de microporosidad (superficie BET, V_{micro}). Parámetros tales como la porosidad (%), la distribución de tamaño de poro (PSD), densidad aparente y volúmenes de mesoporos y macroporos (V_{meso}, V_{macro}), se determinaron mediante porosimetría de mercurio, con el equipo AutoPore IV 9500 (Micromeritics), que es capaz de medir desde la presión atmosférica hasta 228 MPa. En el caso de la caracterización de los mesoporos el límite inferior de este equipo es de 5.5 nm. Del mismo modo, en este estudio, el Vmacro se refiere a la porosidad que oscila desde 50 hasta 10000 nm. La tensión superficial y ángulo de contacto que se tomaron para el mercurio fueron de 485 mN m^{-1} y 130º respectivamente, y el volumen de llenado del vástago estuvo entre 45-58 % en todos los análisis realizados. Inicialmente, en la etapa de baja presión, las muestras fueron evacuadas a 6.7 Pa y el tiempo de equilibrio utilizado fue de 10 segundos. Posteriormente, la presión se aumentó gradualmente hasta el valor máximo, evaluándose la intrusión de mercurio.

Análisis elemental

La determinación de C, H y N se llevó a cabo en un analizador LECO CHNS-932. El contenido de oxígeno se determinó usando el analizador LECO VTF-900.

Experimentos de adsorción de vapor de agua

El procedimiento para medir la capacidad de adsorción de vapor de agua y la cinética consistió en colocar de 0.6 a 0.8 g de muestra dentro de un recipiente hermético a 25 ºC y 100 % de humedad relativa del aire y registrar los cambios de masa con el tiempo hasta valores constantes.

El xerogel RF se obtiene en un proceso que comprende dos etapas. La primera consiste en la polimerización en microondas de una mezcla de resorcinol, formaldehido, agua y un catalizador. La obtención del xerogel orgánico en microondas está descrita en ES 2354782 "Procedimiento de obtención de xerogeles orgánicos de porosidad controlada". No obstante, la mezcla precursora que se somete a este tratamiento posee unas características particulares (pH superior a 5.5, relación molar disolvente/reactivos entre 5 y 9 y relación molar resorcinol/formaldehido menor de 0.7). De otra manera, los xerogeles resultantes no poseen la porosidad adecuada (superior al 60 % y con tamaños medios de poro situados entre 2 y 50 nm, es decir mesoporos) que les dota de gran capacidad de adsorción de la humedad ambiental.

Estas características de la disolución precursora han sido optimizadas y no son, por tanto, evidentes a priori. Por ejemplo, si el tratamiento se lleva a cabo fuera de los rangos de pH, relación resorcinol/formaldehido y/o dilución, la porosidad resultante no sería adecuada y la capacidad de adsorción de humedad disminuiría notablemente. Por ejemplo, en la Figura 1 se presentan las capacidades desecantes de los xerogeles denominados A y B, así como la del gel de sílice tomado como referencia. Estas capacidades desecantes se expresan como la variación de los milimoles de agua adsorbidos por gramo de material con el tiempo; a una temperatura de 25 ºC y en unas condiciones de humedad relativa del aire del 100 %. En la mencionada Figura puede verse que el xerogel B, a pesar de poseer una porosidad mayor que el xerogel A, su capacidad de adsorción de vapor de agua es ligeramente superior a los 10 milimoles por gramo (18 % en peso), frente a los casi 30 milimoles por gramo

(54 % en peso) del xerogel A; es decir, éste último presenta prácticamente el triple de capacidad de adsorción. Se ve, por tanto, que si el xerogel se sintetiza fuera de las condiciones anteriormente descritas su capacidad desecante es notablemente inferior.

La segunda etapa del procedimiento de obtención consiste en un post-tratamiento en aire a una temperatura comprendida entre 100 y 300 ºC; aunque preferiblemente de 100 ºC. Este tratamiento tiene por objeto estabilizar el xerogel. Adicionalmente, también contribuye a generar grupos superficiales oxigenados que aumentan la capacidad de adsorción de agua.

El material presenta una capacidad desecante (adsorción de humedad del ambiente) superior a la del gel de sílice (material tomado como desecante comercial de referencia). Por ejemplo, en la Figura 1 puede verse como el xerogel orgánico denominado A posee una capacidad de adsorción próxima a los 30 milimoles por gramo (54 % en peso), mientras que la capacidad de adsorción del gel de sílice en las mismas condiciones es de tan solo 14 milimoles por gramo (25 % en peso). Es decir, la capacidad desecante del xerogel orgánico duplica la del material de referencia.

La velocidad promedio a la que se produce esta adsorción puede llegar a representar, dependiendo de las condiciones de humedad y temperatura, 2 veces la del gel de sílice. Así por ejemplo, en la Figura 1 puede observarse como el tiempo necesario para adsorber 10 milimoles de agua es de 75 horas para el xerogel A, mientras que el gel de sílice tarda 140 horas en adsorber la misma cantidad de agua. Es decir, el xerogel A es casi 2 veces más rápido que el gel de sílice.

Es un material orgánico resistente al ataque de ácidos, lo que le diferencia de la mayoría de materiales desecantes que son de naturaleza inorgánica, por ejemplo el gel de sílice.

El material presenta una porosidad superior al 60 % mientras que la porosidad del gel de sílice, por ejemplo, está en torno al 30 %. Estos datos se muestran en la Tabla 2. Esta diferencia en porosidad total da lugar a un

material con mayor capacidad desecante en el caso del xerogel tipo A, como se muestra en el ejemplo de la Figura 1. Esta porosidad está compuesta mayoritariamente por poros cuyos tamaños están comprendidos entre 2 nm y 50 nm, también denominados mesoporos. Por ejemplo, en la Tabla 2 se muestra como en el caso del xerogel A el 58 % de la porosidad total son mesoporos. Un porcentaje inferior de mesoporos, aunque la porosidad total sea superior, da lugar a un material con una capacidad desecante notablemente inferior a la del material descrito en esta patente. Caso, por ejemplo del xerogel B. Esto se ilustra en el ejemplo que se presenta en la Figura 1.

La microporosidad, aun siendo un factor con cierta influencia, no es un factor relevante para un buen desecante, ya que el gel tipo A y el gel de sílice presentan similares valores de volumen de microporos y superficie específica: 0.1 cm^3/g y 300 m^2/g para ambos materiales.

Tabla 1. *Condiciones de síntesis de los xerogeles A y B.*

Xerogel	pH	Relación molar disolvente/reactivos	Relación molar R/F	Capacidad desecante
A	5.8	6.4	0.5	> gel de sílice
B	4.8	8.0	0.7	< gel de sílice

Tabla 2. *Características porosas y químicas del xerogel desecante (A), un xerogel que no es un buen desecante (B), un material desecante de referencia (gel de sílice.)*

Material	% Porosidad	% de poros con tamaños entre 2 nm y 50 nm	%C	%H	%O	% Impurezas inorgánicas
A	61	58	64.8	4.9	30.3	< 0.1
B	69	0	66.3	4.5	29.2	< 0.1
Gel de sílice	31	50	-	-	53.3	No aplicable

El material está compuesto mayoritariamente por carbono, que se encuentra siempre en una proporción superior al 60 %. Posee, además una cantidad importante de grupos superficiales oxigenados, con un contenido en oxígeno siempre superior al 25 % en peso. Esa característica favorece la adsorción de moléculas de agua. El material también presenta un pequeño

contenido en hidrógeno, en cantidades comprendidas entre el 4 y el 5 %. Es importante mencionar que no se han detectado ningún tipo de restos inorgánicos, por lo que el nivel de impurezas de este material es menor de 0.1 % en peso. En la Tabla 2 se muestran las características químicas del xerogel denominado A. Las características químicas del xerogel denominado B son similares; sin embargo su textura porosa diferente hace que este material no sea un buen desecante. Por tanto, para que el material presente buenas características como desecante es necesaria la adecuada combinación de propiedades químicas y porosas.

El material presenta una buena consistencia y puede obtenerse en forma granular o incluso en forma de monolitos conformados. También puede molerse y presentarse en forma de polvo fino, pudiendo de esta manera ser incorporado a tintas, pinturas u otros medios que permitan su aplicación a superficies o incluso ser usado en fabricación aditiva.

REIVINDICACIONES

1. Uso de un xerogel orgánico como desecante, donde:

➢ el tamaño medio de poro de dicho xerogel orgánico es de entre 2 nm y 50 nm; y

➢ el contenido de oxígeno de dicho xerogel orgánico es de al menos el 25 % en peso.

2. El uso según la reivindicación 1, donde:

➢ la porosidad total está comprendida entre el 60 % y el 90 %; y

➢ al menos el 50 % de dicha porosidad se debe a poros cuyo tamaño de poro está comprendido entre los 2 nm y los 50 nm.

3. El uso según cualquiera de las reivindicaciones 1 ó 2, donde la porosidad total está comprendida entre el 60 % y el 70 %.

4.   El uso según cualquiera de las reivindicaciones 1 a 3, donde al menos el 55 % de dicha porosidad se debe a poros cuyo tamaño de poro está comprendido entre los 2 nm y los 50 nm.

5.   El uso según la reivindicación 4, donde el 58 % de dicha porosidad se debe a poros cuyo tamaño de poro está comprendido entre los 2 nm y los 50 nm.

6.   El uso según cualquiera de las reivindicaciones 1 a 5, donde la porosidad total es del 61 %.

7.   El uso según cualquiera de las reivindicaciones 1 a 6, donde el xerogel orgánico resulta de la polimerización entre un aldehído y un benceno hidroxilado.

8.   El uso según la reivindicación 7, donde el aldehído se selecciona de formaldehído y furfural.

9.   El uso según cualquiera de las reivindicaciones 7 u 8, donde el benceno hidroxilado se selecciona de resorcinol, fenol y catecol.

10.   El uso según cualquiera de las reivindicaciones 1 a 7, donde el xerogel orgánico se selecciona de xerogel resorcinol/formaldehído y xerogel fenol/formaldehído.

11.   El uso según la reivindicación 10, donde el xerogel orgánico es un xerogel resorcinol/formaldehído.

12.   El uso según la reivindicación 7, donde la polimerización se lleva a cabo a un pH comprendido entre 4 y 8.

13.   , El uso según la reivindicación 12, donde la polimerización se lleva a cabo a un pH de 5.8.

14.   El uso según cualquiera de las reivindicaciones 7 a 13, donde la relación molar entre el aldehído y el benceno hidroxilado es de entre el 0.5 y el 0.7.

15.   El uso según la reivindicación 14, donde la relación molar entre el aldehído y el benceno hidroxilado es de 0.5.

16.   El uso según cualquiera de las reivindicaciones 1 a 15, donde el xerogel orgánico se obtiene tras un post-tratamiento en aire a una temperatura de entre 100 ºC y 300 ºC.

17.   El uso según la reivindicación 16, donde el xerogel orgánico se obtiene tras un post-tratamiento en aire a una temperatura 100 ºC.
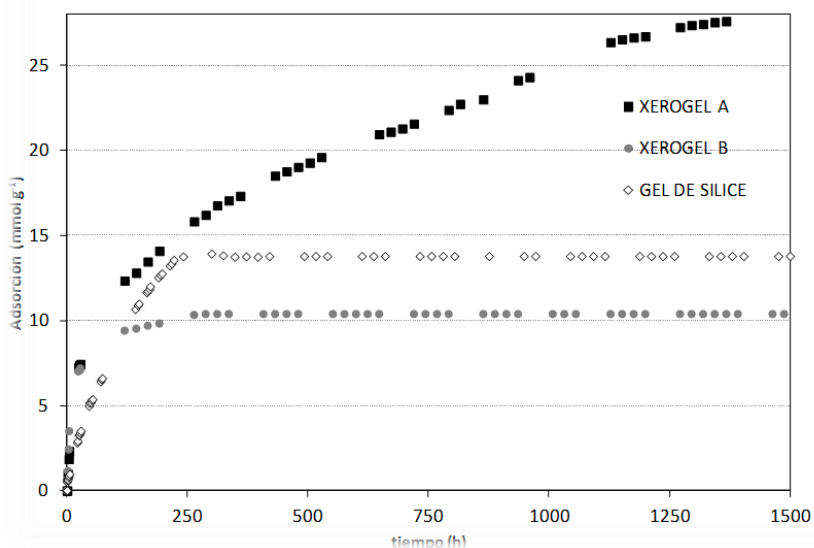
FIGURAS

Figura 1

RESUMEN

Uso de un xerogel orgánico como desecante

La presente invención se refiere al uso de un xerogel orgánico como desecante de alta porosidad y alto contenido de oxígeno.

5.2. Modificación superficial de los xerogeles resorcinol-formaldehído

La mojabilidad de los materiales afecta de forma directa sobre su eficacia en las distintas aplicaciones. Como se ha desarrollado en el apartado anterior, los xerogeles RF son materiales con una gran capacidad de adsorción de humedad. Sin embargo, esta propiedad no siempre es favorable, como es el caso de la utilización de xerogeles orgánicos en aislamiento térmico [24], donde la adsorción de humedad implica un aumento de la conductividad térmica, o en la adsorción de aceites, donde se requiere de una superficie apolar para obtener la máxima eficacia. De esta manera, surge la necesidad de obtener xerogeles orgánicos de naturaleza hidrófoba (del griego, *hydro* = agua + *fobos* = horror), que eviten esta atracción por el agua.

El fenómeno de mojabilidad ha sido estudiado en profundidad desde hace años [52]. La forma más común de determinación de la hidrofilia/fobia de un material es a través de su *ángulo de contacto*, que hace referencia al ángulo formado entre la interfase de un sólido y un líquido (ver *Capítulo 3*). Fue Young and Laplace [53] quien determinó por primera vez una teoría de mojabilidad consistente para sólidos planos y químicamente homogéneos. Sin embargo, la mayoría de los materiales tienen una superficie químicamente y/o físicamente irregular o son porosos. Fue entonces cuando Wenzel [54] determinó que la rugosidad de un material afecta al ángulo de contacto, ya que la gota colocada en la superficie de un material se esparce hasta que encuentra un estado de equilibrio, por lo que el ángulo de contacto es distinto al de una superficie ideal. Para este tipo de materiales, es posible encontrar superficies denominadas *superhidrófobas* las cuales muestran máxima repulsión al agua y ángulos de contacto superiores a 150 º [55]. Además, si el sólido es suficientemente rugoso, pueden incluso encontrarse burbujas de aire encerrado entre la gota y el material, factor tenido en cuenta en el modelo de Cassie [56, 57].

Aunque es muy larga la lista de autores que han participado en el estudio de estas propiedades [58-61], la conclusión común es que para obtener

unos materiales superhidrófobos se necesita que su superficie sea rugosa y con baja energía superficial. En el caso de los xerogeles RF la rugosidad viene dada por su textura porosa, mientras que para la baja energía superficial se requiere de reacciones de pasivado para cubrir la superficie con grupos apolares.

5.2.1. Xerogeles hidrófobos mediante pasivado con silanos

Existen en la bibliografía numerosos estudios donde se modifica la naturaleza hidrófila de los geles de sílice, mediante reacciones de silanación, con el fin de evitar el colapso de la estructura durante la etapa de secado [62, 63], mejorar la difusión de ciertos disolventes [64, 65] o aumentar la vida útil de estos materiales [66]. Los geles de sílice guardan una gran similitud con los xerogeles RF, ya que ambos poseen una superficie cubierta de grupos hidroxilo y una gran porosidad. Por lo tanto, los procedimientos llevados a cabo en este estudio para la obtención de xerogeles RF de naturaleza hidrófoba tienen su origen en los estudios encontrados en la bibliografía sobre geles de sílice.

En esta Tesis Doctoral se ha evaluado y optimizado la obtención de xerogeles RF hidrófobos a través de la reacción de pasivado con silanos y su estabilidad en condiciones ambientales.

5.2.1.1. Objetivos

Los objetivos planteados para realizar el estudio fueron:

➢ Evaluar la posibilidad de obtención de xerogeles orgánicos hidrófobos a través de su reacción con:

- o Trimetilclorosilano (TMCS).
- o Trimetilmetoxisilano (TMMS).
- o Hexametildisilazano (HMDZ).

➢ Evaluar el efecto de la modificación de la química superficial sobre la textura porosa del material.

➢ Establecer el tiempo mínimo necesario para obtener el máximo grado de repulsión del agua para dos tamaños de poro muy distintos.

➢ Evaluar la durabilidad de este tratamiento en condiciones ambientales.

5.2.1.2. Estudio

Para llevar a cabo este estudio se sintetizaron dos xerogeles orgánicos con distintos tamaños de poro: i) OX-60, que es un material mesoporoso cuyo tamaño de poro coincide con el óptimo para su utilización en aislamiento térmico, y ii) OX-6000, material macroporoso, que posee un tamaño de poro apropiado para su utilización en adsorción de aceites, dos aplicaciones potenciales para los que este tratamiento superficial sería requerido. Se utilizaron 3 compuestos distintos para la obtención del material hidrófobo (TMCS, TMMS y HMDZ) y se optimizaron los tiempos de síntesis para cada tamaño de poro.

5.2.1.3. Resultados

Los detalles experimentales y la discusión de los resultados obtenidos se hallan en la *Publicación VII*, incluida al final de esta sección. Los principales resultados de este estudio se detallan a continuación:

➢ La modificación superficial sólo se logró para el HMDZ debido a que su naturaleza básica hace posible que la reacción tenga lugar. Para el TMCS y TMMS sería necesaria la adición de un catalizador.

➢ El ángulo de contacto aumenta progresivamente según aumenta el tiempo de reacción hasta un máximo de 125 º.

➢ A mayor tamaño de poro menor tiempo de reacción es necesario para la obtención de una superficie hidrófoba.

➢ La modificación superficial no afecta a la textura porosa del material.

➢ La modificación superficial es reversible con el tiempo en condiciones ambientales, debido a que sufre reacciones de hidrólisis con la humedad

del aire. La pérdida de hidrofobicidad es más rápida cuanto mayor es el tamaño del poro.

5.2.1.4. Conclusión

La obtención de xerogeles orgánicos hidrófobos con porosidad a medida es posible a través de su modificación superficial con HMDZ. Esta modificación es fácilmente reversible mediante hidrólisis (Figura 19).
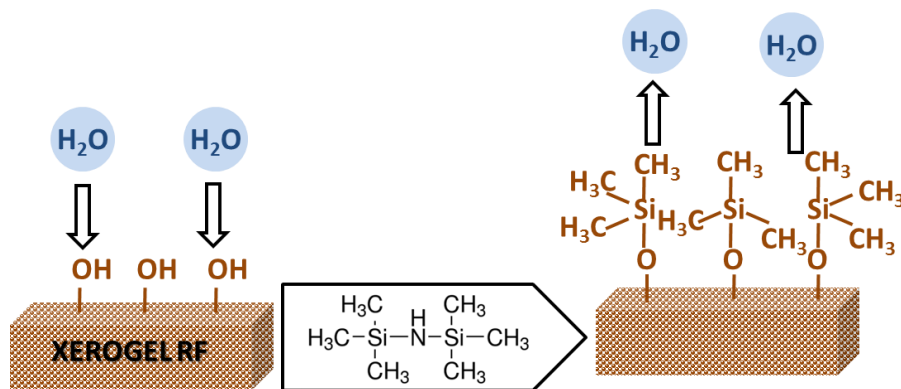

Figura 19.   *Modificación superficial de xerogeles orgánicos con HMDZ.*

PUBLICACIÓN VII

HYDROPHOBIC RF XEROGELS SYNTHESIS BY GRAFTING WITH SILANES

<u>Isabel D. Alonso-Buenaposada</u>, Miguel A. Montes-Morán, J. Angel Menéndez, Ana Arenillas, *Enviado*.

Enviada

Hydrophobic RF xerogels synthesis by grafting with silanes

Isabel D. Alonso-Buenaposada, Miguel A. Montes-Morán, J. Angel Menéndez, Ana Arenillas*

Instituto Nacional del Carbón, CSIC, Apartado 73, 33080 Oviedo, Spain

ABSTRACT

Hydrophilic organic xerogels were transformed into hydrophobic materials by treating them with hexamethyldisilazane at 80 ºC and at atmospheric pressure in absence of catalyst. Hexamethyldisilazane reacts with dangling hydroxyl surface groups, blocks the oxygen with methylsilane groups, and prevents the formation of hydrogen bonds with water molecules. In this way, the hydrophilic surface of the organic xerogel is transformed into a hydrophobic one. However, the graft is not permanent and reverses with time in the presence of water. It was found that the wider the pores of the organic xerogel are, the quicker the grafting process is, but also that this modification of the surface nature is less durable under a humid atmosphere.

Keywords: RF xerogels; hydrophobic materials; surface chemistry; porosity; silanes

1. INTRODUCTION

Resorcinol-formaldehyde (RF) organic xerogels with a predetermined and purpose-designed pore texture can be obtained by selecting suitable physical and chemical variables during the synthesis process [1-3]. The use of microwave radiation as heating source as an alternative to conventional synthesis offers the possibility of obtaining a tailored porous structure by a simple, fast and cost-effective method suitable for producing RF xerogels on a large scale and has led to an increase in interest in these polymers [4].

Although the physical conditions used during the synthesis process may affect the porosity of the RF xerogels [5, 6], the size and volume of their pores are mainly determined by chemical variables, i.e., i) the pH of the precursor solution [7], ii) the dilution ratio [8], i.e. the reactant/solvent ratio, ii) the resorcinol/formaldehyde molar ratio [9] and iv) the percentage of methanol used as stabilizer in the formaldehyde solution [10]. RF xerogels are usually thermally treated in an inert or reactive atmosphere to produce carbon materials called carbon xerogels or activated carbon xerogels [11, 12] that are useful for many applications due to their thermal and chemical stability. Under adequate synthesis conditions, these carbon materials preserve the pore structure of the RF precursors. The combination of these variables offers a wide range of possible porosities, enabling RF and carbon xerogels to be used in several very different applications (e.g., hydrogen storage, thermal insulation, as electrodes in supercapacitors, as catalytic supports, etc.) [13-16].

RF xerogels not only have the advantage of a purpose-designed porosity but also of a very rich surface chemistry (i.e. a large oxygen surface group content) [17], making them suitable for a wide range of applications. Moreover, high-temperature post-treatments are not required for RF xerogels, leading to a notable reduction in manufacturing process costs. What is more, the high concentration of hydroxyl groups which covers the surface of RF xerogels provides them with a high hydrophilicity which attracts moisture from the air, while their large pores improve their water sorption capacity, making them suitable to use as desiccant materials [17]. RF xerogels could also be

employed as thermal insulators since, by tailoring their pore size and volume, it is possible to minimize their convective and conductive heat transfer capacity [18]. In this case, a hydrophilic surface in RF xerogels would be a disadvantage since adsorbed water increases the conductivity of the material considerably. A hydrophobic surface is clearly preferable if the RF xerogels are going to be used as oil spill cleaners or for other non-polar compound adsorption in cleaning or separation processes. In short, the possibility of tailoring the porosity (i.e. pore size and volume) of RF xerogels for a specific application is the main advantage of these synthetic materials. Nevertheless, surface chemistry may also play an important role, and the possibility of controlling its hydrophilic or hydrophobic nature will also be determinant for optimal performance in a specific application.

There are already in the literature several reports on a wide range of procedures for covering hydrophilic surfaces with very diverse materials to make them hydrophobic. Some authors [19, 20] have reported performing such surface modifications by using colloidal silica particles and fluoroalkylsilane as a silylating precursor in sol–gel processes. Another reported option [21] consists in preparing a two-tier roughness using silicon, followed by fluorination of the silicon surface. Other authors have used dopamine to carry out this in imitation of the technique of mussel coating [22], while yet others have used chemical vapour deposition techniques [23] or plasma etching treatments [24]. The generation of hydrophobic polymeric surfaces can be carried out by several techniques (i.e., layer-by-layer deposition, electrodeposition / electropolymerization, plasma and laser treatments, electrospining, etc. [25]), most of which are quite complex and tedious processes.

Like RF xerogels, silica gels also have hydroxyl groups covering their surface, which makes them a suitable and very commonly used desiccant material. The surface modification of silica gels has also been studied. The most common way of obtaining hydrophobic silica gels is to introduce methylsilane groups into the wet gel covering the surface, although other procedures such as post-synthesis treatments in liquid or gas phase can also

be used [26, 27]. The aims of such surface modifications are to prevent the collapse of pores during the drying step [28, 29], to improve the diffusion of certain solvents [30, 31], to obtain a solid suitable for use in oil-spill cleaning [32, 33] or to increase the durability of the material [34], among others. The compounds most commonly used to modify the surface of silica gels so that they become hydrophobic materials are trimethylchlorosilane (TMCS) [24, 35], trimethyl-methoxysilane (TMMS) [26, 36] and hexamethyldisilazane (HMDZ) [30, 37]. Moreover, these silanes are also commonly employed for the protection of alcohols in organic chemistry synthesis [38]. The ideal protecting group for an active hydrogen moiety such as alcohol would be one that could be introduced in a high yield, remain stable in certain conditions but could be selectively removed in a high yield in other conditions without modifying the other functional groups in the organic molecule.

The aim of the present work is to modify the hydrophilic surface of RF xerogels without causing any additional modification of their chemistry, which to the best of our knowledge has not been achieved before. To this end, RF xerogels were treated with silanes in an effort to develop a simple and low-cost process without using a catalyst or any other additional compound, which would complicate and make the process more expensive. In order to evaluate the possible influence of the pore size of the xerogel on the grafting process, two RF xerogels with very different porosities were evaluated and compared on the basis of the effectiveness (hydrophobic strength) and time of treatment required, and the treatment durability over time.

2. EXPERIMENTAL SECTION

2.1. Synthesis of resorcinol-formaldehyde xerogels

Two RF xerogels with average pore sizes of ca. 60 nm and 6000 nm (i.e. OX-60 and OX-6000, respectively) were evaluated for grafting with silanes.

In order to obtain xerogel OX-60, 16.33 g of resorcinol (Indspec, 99 %) was dissolved in 83.36 mL of deionized water until total dissolution under magnetic stirring. After that, 100.31 mL of formaldehyde (37 wt. % in water, stabilized by the addition of 12.5 wt. % of methanol, supplied by Merck) was added. The pH of this solution was 3.25 and the proportions selected corresponded to a dilution ratio of 5.7 (i.e. the molar ratio of the total solvent to the reactants) and a R/F molar ratio of 0.12. In the case of OX-6000, 43.71 g of resorcinol (Indspec, 99 %) was dissolved in 110.38 mL of deionized water until total dissolution under magnetic stirring. After that, 45.90 mL of formaldehyde (37 wt. % in water, stabilized by adding 0.7 wt. % of methanol, supplied by Química S.A.U) was added. To this precursor solution, drops of a 5 M NaOH solution (prepared from AnalaR Normapur, 99.9 %) were added until a pH of 5 was obtained. The proportions selected corresponded to a dilution ratio of 8 and R/F molar ratio of 0.7.

Each precursor solution was placed in a microwave oven (in-lab designed and constructed [4]) at 85 ºC for 3 hours to allow gelation and curing to take place. After the formation of the polymeric structure, all excess water was eliminated by heating the gel in the same device continuously until a mass loss of 50 wt. % was attained. This drying step lasted ca. 2 hours. Each material was kept in the oven at 100 ºC overnight to remove any traces of moisture and unreacted compounds and so obtain a completely stable material.

The final material was ground and sieved to under < 212 μm in order to obtain a homogeneous powder suitable for the treatments.

2.2. Grafting with silanes

The following silanes were employed for the RF xerogel grafting process: trimethylchlorosilane (TMCS), trimethyl-methoxysilane (TMMS) and hexamethyldisilazane (HMDZ). Suspensions of 8 g of each RF xerogel in 100 mL of each silane compound were stirred at 80 ºC and at atmospheric pressure. Aliquots of the resulting material were extracted at different reaction times in

order to measure the progression of the reaction. In order to remove any residual reagent from the pores of the xerogel, the aliquots were dried overnight in a stove at 80 ºC before characterization.

2.3. Sample characterization

2.3.1. Porous properties characterization

Before characterization, the samples were outgassed (Micromeritics VacPrep 0.61) at 0.1 mbar and 120 ºC overnight in order to remove any humidity and other physisorbed gases. The textural properties were characterized by means of nitrogen adsorption-desorption isotherms, mercury porosimetry and density analysis.

The nitrogen adsorption-desorption isotherms were measured at -196 ºC in a Tristar 3020 (Micromeritics) device. The pore volume and mean pore size were determined by mercury porosimetry, using an AutoPore IV 9500 (Micromeritics) from atmospheric pressure up to 228 MPa. The range of pore sizes evaluated was from 5.5 to 2000 nm. The surface tension and contact angle were 485 mN m^{-1} and 130º, respectively, and the stem volume was between 45-60 % in all of the analyses. In the low pressure step, the samples were evacuated up to 6.7 Pa and the equilibration time used was 10 seconds. In order to determine the bulk density and the percentage of porosity of the samples, a Geopyc 1360 (Micromeritics) device was set to a Dryflow of 0.8 g and a sample volume of around 50 % of the total volume. A chamber with an internal diameter of 12.7 mm and a strength of 28 N for 20 cycles with a conversion factor of 0.1284 (cm^3 mm^{-1}), was used.

2.3.2. Contact angle determination

In order to determine the hydrophobic nature of the RF xerogel surface, the contact angle between a drop of deionized water and the surface of the material was measured using a Krüss 62/G40 optical tensiometer. Each drop of

water (ca. 6 mm in diameter) was deposited onto a completely flat surface using a micrometric syringe. A pellet of 10 mm diameter was prepared from the sample powders (< 212 µm particle size) applying a pressure of 10 Tons for 25 s. In all cases, three different pellets from each sample were evaluated and the average of the contact angles was selected as the final value.

3. RESULTS AND DISCUSSION

In this study, two RF xerogels with very different porosities were selected to be used in two different applications: OX-60 with a pore size and properties suitable for use as a thermal insulator [18] and OX-6000 with a pore size and properties suitable for oil spill cleaning. Given that the surface chemistry of both samples was analogous [17], potential differences detected during the grafting process with silanes could only be due to the porosity of the samples. Table 1 shows the main porous characteristics of the two samples studied. As can be seen, both samples have a similar bulk density and open porosity (i.e. ca 0.3 g cm^{-1} and ca. 75 %, respectively) but very different pore sizes and volumes. Their microporosities also differ, since BET surface areas of 244 m^2 g^{-1} and 20 m^2 g^{-1} were recorded for OX-60 and OX-6000, respectively.

Table 1. *Porous properties of the two RF xerogels studied.*

Sample	Mercury porosimetry		Densitometry		N$_2$ adsorption-desorption
	Pore volume (cm^3 g^{-1})	Mean pore size (nm)	Bulk density (g cm^{-3})	Porosity (%)	S$_{BET}$ (m^2 g^{-1})
OX-60	0.83	59	0.31	77	244
OX-6000	1.61	5694	0.34	76	20

The three silanes (TMCS, TMMS and HMDZ) grafted onto the RF xerogels were tested under the same operational conditions. However, because of the acidic surface of the xerogels (i.e. pH$_{PZC}$ of around 3) reaction with TMCS and TMMS is not favoured. A basic booster is required since an initial

deprotonation reaction needs to occur before the grafting reaction starts. In contrast, the reaction with HMDZ was favoured due to the basicity of this particular silane reagent (pKa=7.5). The nitrogen in HMDZ would extract the hydrogen from the hydroxyl groups in the RF xerogel, giving rise to their anionic form. This anionic group would then act as a nucleophile with the electron pair in the oxygen reacting with the silicon atoms in the HMDZ via a SN$_2$ reaction, resulting in O-Si bonds (see reaction mechanism in Figure 1). The ammonia produced in the reaction is eliminated as the reaction proceeds and as a consequence of this, the resultant material contains no nitrogen groups. Consequently, a RF xerogel with a surface covered with nonpolar alkyl groups is obtained.
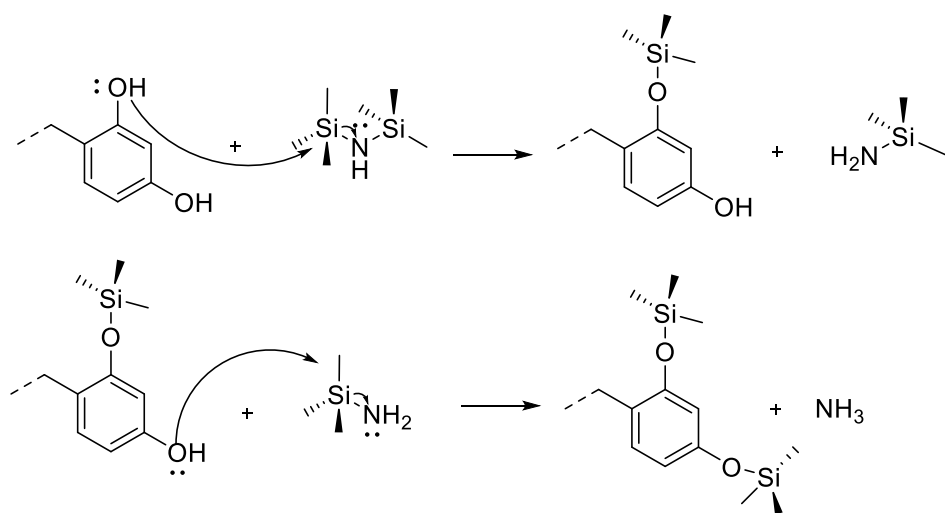

Figure 1. *Grafting reaction mechanism between RF xerogel surface groups and hexamethyldisilazane (HMDZ).*

The parameter to evaluate the effectiveness of the grafting of silane onto the RF xerogels was the contact angle between a drop of deionized water and the surface of the material using an optical tensiometer. Figure 2 shows the contact angle measured at different reaction times for the three silanes. When using TMCS and TMMS as grafting agents, no change in the contact angle was detected for the resulting samples at any time throughout the reaction. The contact angle for these samples, as well as for the pristine RF xerogel is

considered to be 0º since the drops of water were quickly absorbed by the pellets. This indicates that either TMCS or TMMS did not react with the surface chemistry of the RF xerogels and therefore the materials remained hydrophilic after the treatment.

However, in the case of HMDZ a change in the contact angle was observed (Figure 2; for the purpose of brevity, the HMDZ-grafted OX-60 and OX-6000 have been labelled Si-OX-60 and Si-OX-6000, respectively). In fact, when a RF xerogel with large pore size (OX-6000) was treated with HMDZ, the material turned from hydrophilic (α < 90º) to hydrophobic (α > 90º) after a grafting reaction of only one minute and maximum hydrophobicity (ca. α = 125º) was achieved after only 8 minutes. In contrast, the OX-60 sample needed a larger reaction time, as can be seen from Figure 2, where no hydrophobicity is observed until after 1 hour of reaction. In this case the maximum hydrophobicity, again α = 125º, was only attained after 8 h of treatment. The difference in these grafting reaction times is due to the fact that it was more difficult for HMDZ to diffuse along the narrow pores of OX-60, than along the wider pores of OX -6000. However the maximum hydrophobicity finally attained by both RF xerogels was the same due to the analogous surface chemistries of the samples.
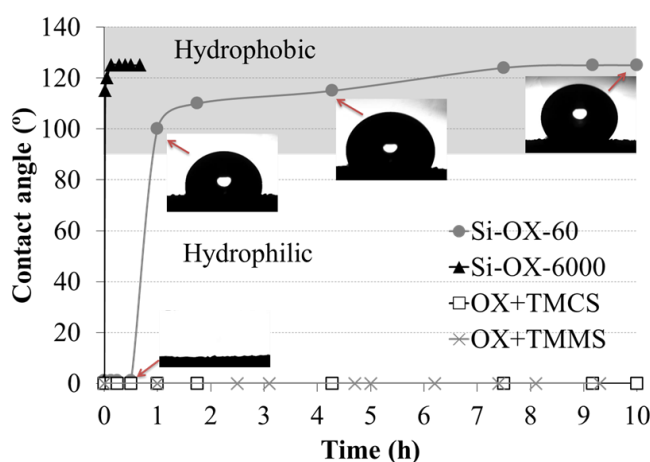

Figure 2. *Evolution of the contact angle, as measured by an optical tensiometer, with grafting reaction times for the silanes tested. Si-OXs samples are RF xerogels grafted with HMDZ (see text).*

The attachment of alkyl groups to the RF xerogel may cause changes in the porous properties of the samples. As mentioned before, being able to tailor the porosity of the RF xerogels is the main advantage of these materials. For this reason, it is essential to check for possible changes in porosity after each treatment.

Figure 3 shows the pore size distributions of the original and grafted samples as measured by Hg porosimetry. An increase in the pore volume and mean pore size of the treated samples can be observed after the treatment. The pore volume of Si-OX-6000 and Si-OX-60 is 2.08 and 0.97 cm^3 g^{-1}, respectively. This means an increase in pore volume of 29 % for OX-6000, and 18 % for OX-60 (see Table 1). On the other hand, the average pore size increases from 59 to 70 nm in the case of Si-OX-60 and from 5694 to 6160 nm for Si-OX-6000. However, these increments have to be treated with caution, as the RF xerogels studied have poor mechanical strengths and therefore they are very sensitive to the changes in pressure levels used in mercury porosimetry. Other authors have observed that compression problems in the analyses of these materials can lead to overestimations of the pore volume and size [39]. Thus, it should be concluded that the porosities of the RF xerogels in this study were not greatly affected by the grafting treatment applied. This can be seen from the fact that sample OX-60 and its counterpart have a pore volume of around 0.9 cm^3 g^{-1} and a pore size of 60 nm, whilst OX-6000 and its counterpart have twice the pore volume (ca. 2 cm^3 g^{-1}) and a pore size of around 6000 nm.
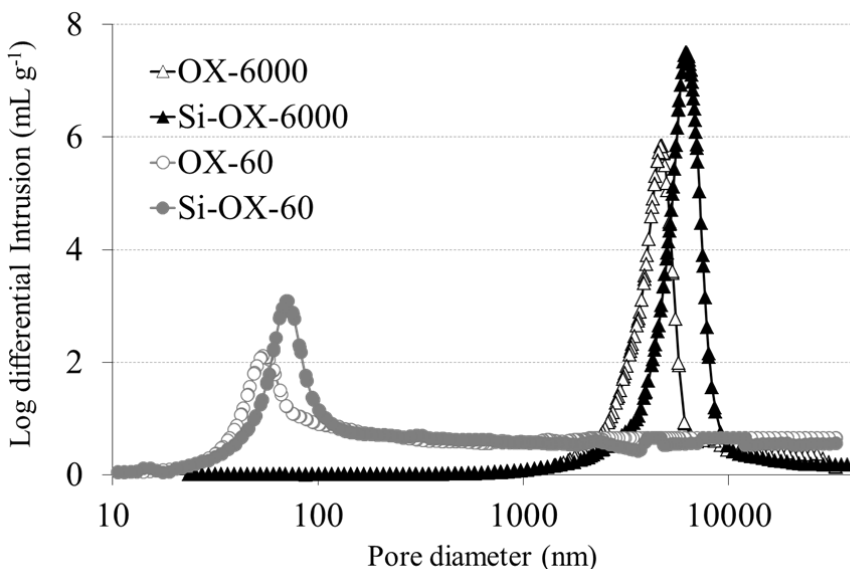
Figure 3. *Pore size distribution of the RF xerogels before and after treatment with HMDZ.*

Now that it has been shown that initially hydrophilic RF xerogels can be converted into hydrophobic materials without experiencing almost any change in their porous properties, it might be worthwhile evaluating the modifications of the surface properties with time under atmospheric exposure. For this purpose both grafted samples were exposed to ambient conditions (i.e. 20 ºC and 80 % humidity) and the contact angle was checked periodically over a period of several days. Figure 4 confirms that the surface modification of both samples is not permanent. The hydrolysis of the silane surface groups due to the humidity in the atmosphere seems to be responsible for the gradual transition from hydrophobic back to hydrophilic xerogels. Trimethylsilanes are relatively easy to hydrolyze [38, 40]. Sample Si-OX-6000 becomes hydrophilic again after 19 days of exposure to ambient humid conditions. In the case of the sample with narrow pores, Si-OX-60, after 19 days the sample is still hydrophobic (α > 90º), although a decrease in the contact angle is noticeable after 2 weeks. After 4 weeks of exposure of Si-OX-60 to ambient humid conditions the surface is hydrophilic (α < 90º), presumably due to the loss of many of the alkyl surface groups introduced during the treatment with HMDZ, but it is still possible to measure a contact angle. However, after 35 days of ambient exposure the

material is again highly hydrophilic to the point that it resembles the initial sample (see Figure 4). In short, it can be said that the easier the alkyl groups are to introduce, the easier they are to remove and the hydrolysis reaction of RF xerogels with HMDZ is favoured, especially in the wider pore sample (Si-OX-6000).
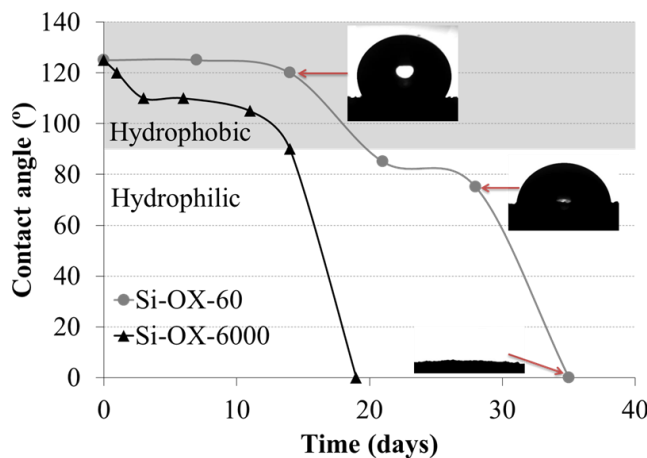
Figure 4. Loss of hydrophobicity with time of exposure to ambient humid conditions (20 ºC and 80 % humidity).

Samples Si-OX-60 and Si-OX-6000 are hydrophobic, at least for several days. These materials avoid any contact with water (Figure 5a). However, if the sample/water suspension is shaken overnight a good dispersion of the sample can be obtained (Figure 5b).
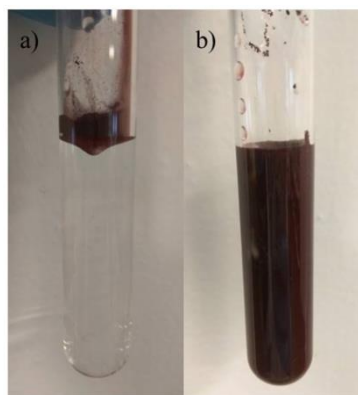
Figure 5. Proof of hydrophobicity of RF xerogels grafted with silanes (a). The materials become hydrophilic again after overnight shaking of the water suspension (b).

Thus, the surface modification of the RF xerogels can easily be reversed by simply hydrolyzing the methylsilane groups. On the other hand, if kept away from moisture, their hydrophobicity remains intact. This property of RF xerogels could be very useful for applications, such as the separation of non-polar compounds by adsorption or the elimination of non-polar contaminants, where the adsorbate can be easily desorbed and then concentrated elsewhere by a simple process of water scrubbing.

4. CONCLUSIONS

The surface nature of RF xerogels can be easily converted from hydrophilic to hydrophobic by grafting hexamethyldisilazane onto the RF xerogels in one simple step. No extra compounds or catalyst are needed. The duration of the modification process depends on the porous properties of the RF xerogel due to diffusional factors. The wider the pore size, the quicker the process of obtaining a hydrophobic surface. The tailored porosity of the RF xerogels is not substantially modified by the treatments. Depending on the final application of the xerogels (i) their hydrophobicity can be maintained if exposure to moisture is avoided, or (ii) it can be easily reversed by a simple hydrolysis process.

ACKNOWLEDGMENTS

REFERENCES

[1] S.A. Al-Muhtaseb, J.A. Ritter, Preparation and Properties of Resorcinol–Formaldehyde Organic and Carbon Gels, Advanced Materials, 15 (2003) 101-114.

[2] F.L. Conceição, P.J.M. Carrott, M.M.L. Ribeiro Carrott, New carbon materials with high porosity in the 1–7 nm range obtained by chemical activation with phosphoric acid of resorcinol–formaldehyde aerogels, Carbon, 47 (2009) 1874-1877.

[3] S. Morales-Torres, F.J. Maldonado-Hódar, A.F. Pérez-Cadenas, F. Carrasco-Marín, Textural and mechanical characteristics of carbon aerogels synthesized by polymerization of resorcinol and formaldehyde using alkali carbonates as basification agents, Physical Chemistry Chemical Physics, 12 (2010) 10365-10372.

[4] E.G. Calvo, E.J. Juárez-Pérez, J.A. Menéndez, A. Arenillas, Fast microwave-assisted synthesis of tailored mesoporous carbon xerogels, Journal of Colloid and Interface Science, 357 (2011) 541-547.

[5] J. Menéndez, A. Arenillas, B. Fidalgo, Y. Fernández, L. Zubizarreta, E. Calvo, J. Bermúdez, Microwave heating processes involving carbon materials, Fuel Processing Technology, 91 (2010) 1-8.

[6] N. Rey-Raap, J.A. Menéndez, A. Arenillas, Optimization of the process variables in the microwave-induced synthesis of carbon xerogels, J Sol-Gel Sci Technol, 69 (2014) 488-497.

[7] N. Job, R. Pirard, J. Marien, J.-P. Pirard, Porous carbon xerogels with texture tailored by pH control during sol–gel process, Carbon, 42 (2004) 619-628.

[8] Z. Zapata-Benabithe, C. Moreno-Castilla, F. Carrasco-Marín, Effect of dilution ratio and drying method of resorcinol–formaldehyde carbon gels on their electrocapacitive properties in aqueous and non-aqueous electrolytes, Journal of Sol-Gel Science and Technology, 75 (2015) 407-412.

[9] N. Rey-Raap, J. Angel Menéndez, A. Arenillas, Simultaneous adjustment of the main chemical variables to fine-tune the porosity of carbon xerogels, Carbon, 78 (2014) 490-499.

[10] I.D. Alonso-Buenaposada, N. Rey-Raap, E.G. Calvo, J. Angel Menéndez, A. Arenillas, Effect of methanol content in commercial formaldehyde solutions on the porosity of RF carbon xerogels, Journal of Non-Crystalline Solids, 426 (2015) 13-18.

[11] M.S. Contreras, C.A. Páez, L. Zubizarreta, A. Léonard, S. Blacher, C.G. Olivera-Fuentes, A. Arenillas, J.-P. Pirard, N. Job, A comparison of physical activation of carbon xerogels with carbon dioxide with chemical activation using hydroxides, Carbon, 48 (2010) 3157-3168.

[12] A.H. Moreno, A. Arenillas, E.G. Calvo, J.M. Bermúdez, J.A. Menéndez, Carbonisation of resorcinol–formaldehyde organic xerogels: Effect of temperature, particle size and heating rate on the porosity of carbon xerogels, Journal of Analytical and Applied Pyrolysis, 100 (2013) 111-116.

[13] L. Zubizarreta, J.A. Menéndez, N. Job, J.P. Marco-Lozar, J.P. Pirard, J.J. Pis, A. Linares-Solano, D. Cazorla-Amorós, A. Arenillas, Ni-doped carbon xerogels for H2 storage, Carbon, 48 (2010) 2722-2733.

[14] V. Celorrio, J. Flórez-Montaño, R. Moliner, E. Pastor, M.J. Lázaro, Fuel cell performance of Pt electrocatalysts supported on carbon nanocoils, International Journal of Hydrogen Energy, 39 (2014) 5371-5377.

[15] D. Fairén-Jiménez, F. Carrasco-Marín, C. Moreno-Castilla, Adsorption of Benzene, Toluene, and Xylenes on Monolithic Carbon Aerogels from Dry Air Flows, Langmuir, 23 (2007) 10095-10101.

[16] P. Staiti, A. Arenillas, F. Lufrano, J.Á. Menéndez, High energy ultracapacitor based on carbon xerogel electrodes and sodium sulfate electrolyte, Journal of Power Sources, 214 (2012) 137-141.

[17] I.D. Alonso-Buenaposada, E.G. Calvo, M.A. Montes-Morán, J. Narciso, J.A. Menéndez, A. Arenillas, Desiccant capability of organic xerogels: Surface chemistry vs porous texture, Microporous and Mesoporous Materials, 232 (2016) 70-76.

[18] E. Cuce, P.M. Cuce, C.J. Wood, S.B. Riffat, Toward aerogel based thermal superinsulation in buildings: A comprehensive review, Renewable and Sustainable Energy Reviews, 34 (2014) 273-299.

[19] M. Hikita, K. Tanaka, T. Nakamura, T. Kajiyama, A. Takahara, Super-Liquid-Repellent Surfaces Prepared by Colloidal Silica Nanoparticles Covered with Fluoroalkyl Groups, Langmuir, 21 (2005) 7299-7302.

[20] H.M. Shang, Y. Wang, S.J. Limmer, T.P. Chou, K. Takahashi, G.Z. Cao, Optically transparent superhydrophobic silica-based films, Thin Solid Films, 472 (2005) 37-43.

[21] X. Yao, L. Xu, L. Jiang, Fabrication and characterization of superhydrophobic surfaces with dynamic stability, Advanced Functional Materials, 20 (2010) 3343-3349.

[22] S.M. Kang, I. You, W.K. Cho, H.K. Shon, T.G. Lee, I.S. Choi, J.M. Karp, H. Lee, One-step modification of superhydrophobic surfaces by a mussel-inspired polymer coating, Angewandte Chemie International Edition, 49 (2010) 9401-9404.

[23] A. Hozumi, O. Takai, Preparation of ultra water-repellent films by microwave plasma-enhanced CVD, Thin Solid Films, 303 (1997) 222-225.

[24] S. Mahadik, D.B. Mahadik, M.S. Kavale, V.G. Parale, P.B. Wagh, H. Barshilia, S. Gupta, N.D. Hegde, A.V. Rao, Thermally stable and transparent superhydrophobic sol–gel coatings by spray method, Journal of Sol-Gel Science and Technology, 63 (2012) 580-586.

[25] N.J. Shirtcliffe, G. McHale, M. I Newton, The superhydrophobicity of polymer surfaces: recent developments, Journal of Polymer Science Part B: Polymer Physics, 49 (2011) 1203-1217.

[26] S.H. Li, X.D. Sun, L.-j. Wang, W.-b. Gu, W.-m. Wang, Z.Y. Yang, Y. Wang, J.H. Zhu, Fabricating hydrophobic nanoparticles within mesoporous channel of silica for efficient TSNA removal, Microporous and Mesoporous Materials, 237 (2017) 237-245.

[27] G. Eris, D. Sanli, Z. Ulker, S.E. Bozbag, A. Jonás, A. Kiraz, C. Erkey, Three-dimensional optofluidic waveguides in hydrophobic silica aerogels via supercritical fluid processing, J. Supercritical Fluids, 73 (2013) 28-33.

[28] P.B. Sarawade, J.-K. Kim, A. Hilonga, H.T. Kim, Preparation of hydrophobic mesoporous silica powder with a high specific surface area by surface modification of a wet-gel slurry and spray-drying, Powder Technology, 197 (2010) 288-294.

[29] A.P. Perissinotto, C.M. Awano, F.S. de Vicente, D.A. Donatti, A. Mesquita, L.F. da Silva, D.R. Vollet, Structure and diffuse-boundary in hydrophobic and sodium dodecyl sulfate-modified silica aerogels, Microporous and Mesoporous Materials, 223 (2016) 196-202.

[30] J.L. Gurav, A.V. Rao, D.Y. Nadargi, H.H. Park, Ambient pressure dried TEOS-based silica aerogels: Good absorbents of organic liquids, J Mater Sci, 45 (2010) 503-510.

[31] A. Bisson, E. Rodier, A. Rigacci, D. Lecomte, P. Achard, Study of evaporative drying of treated silica gels, Journal of Non-Crystalline Solids, 350 (2004) 230-237.

[32] O. Manna, S.K. Das, R. Sharma, K.K. Kar, Superhydrophobic and Superoleophobic Surfaces in Composite Materials, Composite Materials, Springer2017, pp. 647-686.

[33] P. Guo, S.-R. Zhai, Z.-Y. Xiao, F. Zhang, Q.-D. An, X.-W. Song, Preparation of superhydrophobic materials for oil/water separation and oil absorption using PMHS–TEOS-derived xerogel and polystyrene, Journal of Sol-Gel Science and Technology, 72 (2014) 385-393.

[34] L.-J. Wang, S.-Y. Zhao, M. Yang, Structural characteristics and thermal conductivity of ambient pressure dried silica aerogels with one-step solvent exchange/surface modification, Materials Chemistry and Physics, 113 (2009) 485-490.

[35] A. Ślosarczyk, M. Barełkowski, S. Niemier, P. Jakubowska, Synthesis and characterisation of silica aerogel/carbon microfibers nanocomposites dried in supercritical and ambient pressure conditions, Journal of Sol-Gel Science and Technology, 76 (2015) 227-232.

[36] K. Kanamori, Liquid-phase synthesis and application of monolithic porous materials based on organic–inorganic hybrid methylsiloxanes, crosslinked polymers and carbons, Journal of Sol-Gel Science and Technology, 65 (2013) 12-22.

[37] W.J. Malfait, S. Zhao, R. Verel, S. Iswar, D. Rentsch, R. Fener, Y. Zhang, B. Milow, M.M. Koebel, Surface Chemistry of Hydrophobic Silica Aerogels, Chem. Mater., 27 (2015) 6737-6745.

[38] P. Patschinski, C. Zhang, H. Zipse, The Lewis Base-Catalyzed Silylation of Alcohols—A Mechanistic Analysis, The Journal of Organic Chemistry, 79 (2014) 8348-8357.

[39] N. Job, R. Pirard, J.P. Pirard, C. Alié, Non Intrusive Mercury Porosimetry: Pyrolysis of Resorcinol-Formaldehyde Xerogels, Particle & Particle Systems Characterization, 23 (2006) 72-81.

[40] K.P.C. Vollhardt, N.E. Schore, Organic Chemistry, W. H. Freeman2010.

5.2.2. Xerogeles superhidrófobos transpirables mediante pasivado con metanol en fase vapor

La aparición de materiales repelentes al agua líquida, pero transpirables al vapor, han supuesto un gran avance en campos como la ropa deportiva, donde el agua de lluvia no atraviesa la tela pero permite salir el sudor generado por el deportista. Este tipo de materiales provocan un efecto tamiz donde las gotas de agua que exceden los 0.1 mm no pasan a través de su porosidad, e incluso son repelidas, mientras que las moléculas de agua de 0.4 nm de diámetro sí atraviesan el material [67, 68]. El control de la porosidad de los xerogeles RF les convierte en buenos candidatos para este fin. Sin embargo, su química superficial es rica en grupos fenólicos que les dotan de una naturaleza hidrófila y retienen el agua (*Publicación V y VI*).

Por lo tanto, en esta Tesis Doctoral se ha evaluado la modificación superficial de los xerogeles RF, a través de la reacción de pasivado con metanol en fase vapor, para la obtención de materiales superhidrófobos estables en condiciones ambientales, transpirables y fácilmente regenerables.

5.2.2.1. Objetivos

Los objetivos planteados para realizar el estudio fueron:

➢ Evaluar la posibilidad de obtención de xerogeles orgánicos superhidrófobos a través de reacción con metanol en fase vapor.

➢ Evaluar el efecto de la modificación superficial sobre la textura porosa del material.

➢ Establecer el tiempo mínimo necesario para obtener el máximo grado de repulsión del agua para cinco tamaños de poro distintos.

➢ Evaluar la durabilidad de este tratamiento en condiciones ambientales.

➢ Evaluar la capacidad de adsorber/desorber vapor de agua.

➢ Estudiar su capacidad de regeneración y su eficacia con los ciclos de uso.

5.2.2.2. Estudio

Para llevar a cabo este estudio se sintetizaron cinco xerogeles orgánicos con distintos tamaños de poro de 70 a 6000 nm. Se estudió su afinidad por el agua en fase líquida a través de medida del ángulo de contacto de una gota de agua y su afinidad por agua en fase gas por ganancia de peso en condiciones de saturación de humedad.

5.2.2.3. Resultados

Los detalles experimentales y la discusión de los resultados obtenidos se hallan en la *Publicación VIII*, incluida al final de este capítulo. Los principales resultados de este estudio se detallan a continuación:

➢ El tiempo requerido para llevar a cabo la modificación superficial sigue una tendencia exponencial, requiriendo tiempos muy largos a tamaños de poro pequeños.

➢ El ángulo de contacto cambia de forma radical de 0 º a > 150 º, sin pasos intermedios.

➢ Esta modificación superficial da lugar a materiales superhidrófobos que presentan una repelencia extrema al agua líquida y provocan que la gota de medida del ángulo de contacto ruede por la superficie del material sin posibilidad de obtener una medida exacta.

➢ Únicamente una parte de los grupos hidroxilo de la superficie reaccionan ante este tratamiento. No obstante, es suficiente para mostrar un comportamiento superhidrófobo al agua líquida.

➢ La modificación superficial no afecta a la textura porosa del material.

➢ La modificación superficial es estable en condiciones ambientales y durante largos periodos de tiempo.

➢ Los materiales son capaces de adsorber/desorber vapor de agua, por lo que son considerados transpirables.

5.2.2.4. Conclusión

Se obtuvieron xerogeles orgánicos superhidrófobos estables a la humedad capaces de intercambiar vapor de agua con su entorno dependiendo de las condiciones ambientales que le rodeen (Figura 20).
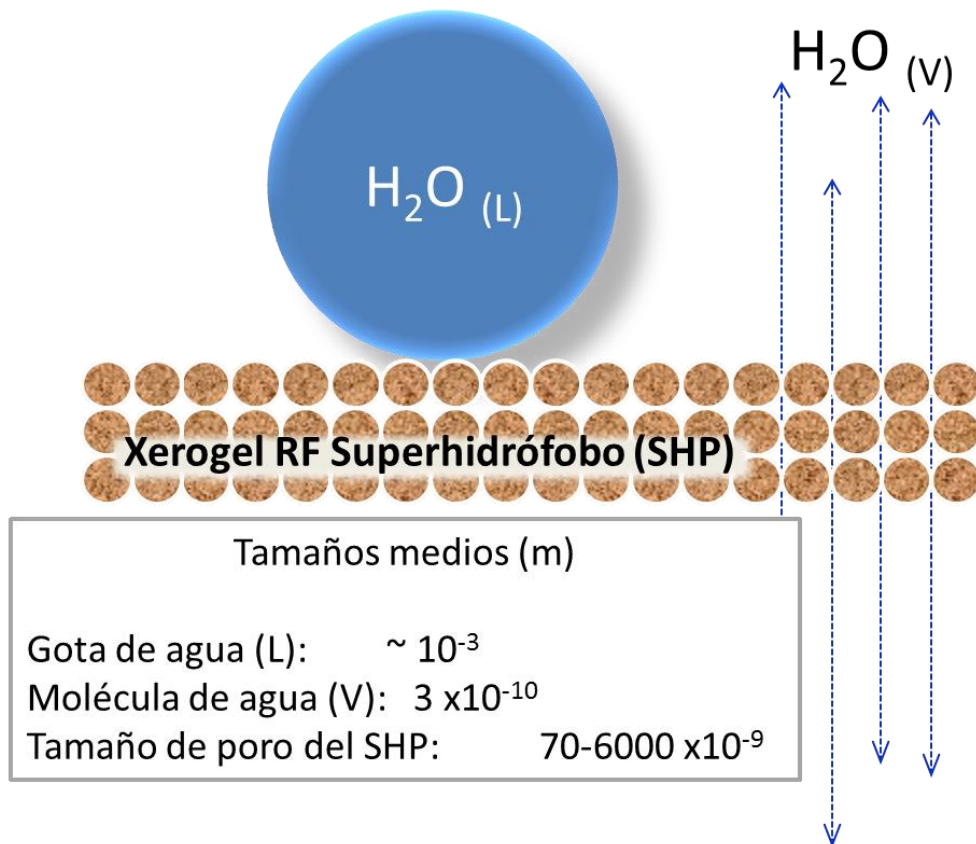

Figura 20. *Mecanismo explicativo del comportamiento superhidrófobo transpirable de los xerogeles RF con superficie modificada.*

PUBLICACIÓN VIII

SUPERHYDROPHOBIC AND BREATHABLE RESORCINOL-FORMALDEHYDE XEROGELS

Isabel D. Alonso-Buenaposada, Ana Arenillas, Miguel A. Montes-Morán, J. Angel Menéndez, *Enviada*.

Enviada

Superhydrophobic and Breathable Resorcinol-Formaldehyde Xerogels

Isabel D. Alonso-Buenaposada, Ana Arenillas, Miguel A. Montes-Morán, J. Angel Menéndez

Instituto Nacional del Carbón, CSIC, Apartado 73, 33080 Oviedo, Spain

ABSTRACT

A new macroporous, waterproof and breathable material has been synthetized. The synthesis of these materials consists in a modified version of the classical resorcinol-formaldehyde (RF) xerogels synthesis. This new process includes a further treatment, after the gelation-curing-drying process, with methanol at 240 ºC in order to passivate the hydrophilic phenolic groups of the surface of the RF xerogel. It was found that the treatment time strongly depends on the pore size of the xerogels. After reaching this threshold time, the hydrophilic materials become superhydrophobic. It is postulated that the exohedral inner surface of the porous xerogels, different from most porous materials, is responsible for this behavior. Although the materials exhibit a superhydrophobic behavior against liquid water and maintain its waterproofness for a long period of time, they are able to adsorb/desorb water vapor, which makes them also breathable.

Keywords: xerogels; hydrophobicity; surface chemistry; passivation

1. INTRODUCTION

Waterproof and breathable materials or composites are essential in a number of processes and commodities, including protective clothing, sports apparel, and membrane contactors [1-6]. For all these applications, materials are required to combine conflicting properties such as avoiding liquid water to penetrate and allowing the vapor water to pass through at the same time. In any case, the combination of waterproofness and breathability is essentially a size discrimination issue. Thus, a waterproof and breathable material (or laminate) should be able to repel water droplets normally exceeding 105 nm in diameter (i.e., 0.1 mm) and to let through water molecules in the vapor phase with ca. 0.4 nm in diameter. The transport properties of water and moisture through a given material will determine its final performance in this type of applications [2, 7].

So far, two successful approaches, in terms of commercial products, have been developed to cope with this sieving effect, namely porous and hydrophilic membranes/coatings [1, 8]. Hydrophilic membranes are virtually non-porous materials through which the water molecules diffuse following an anomalous mechanism [1, 9]. This type of membranes/coatings are based on copolymers of poly(ethylene oxide), poly(vinyl alcohol), polyurethane, etc. On the other hand, porous membranes are made of hydrophobic materials with an adequate porous texture to both withstand penetration by liquid water and maximize the transfer of water vapor molecules [1, 2, 7]. Polymers used for these porous membranes include polyolefins, polyurethanes and poly(tetrafluoroethylene), amongst others. Porosity in these materials can be attained either during the polymer synthesis or by using post-treatments such as mechanical frothing or fibrillation [1, 10].

In addition to these two well-established methodologies, research in the field is still much in progress. Different approaches try to overcome drawbacks such as materials cost [10-12], durability [12-14], and a finer control of the porous structure in the case of porous membranes/coatings. Regarding this last subject, it is generally accepted that pore diameters in the 102-104 nm interval are required for effective waterproofness and breathability [15]. Still, the control

of the porosity of the hydrophobic polymers is very imperfect due to the limitations of the conventional processing. Alternatives include new polymeric formulations [15, 16], and the use of more exotic polymer processing technologies such as electrospinning.[17-19]

Organic gels in general, and resorcinol/formaldehyde (RF) resins in particular, are polymeric systems that show tremendous versatility in terms of developing tailored porous textures. Since the seminal work of Pekala [20], a number of works have detailed the effect of different synthesis variables on the final three-dimensional structure of the RF gels [21-26], which in turn determines the porosity of the materials. As a consequence, RF gels are nowadays synthesized with pore sizes and volumes adapted to the requirements of a given application. Furthermore, the use of microwave radiation to assist the synthesis of RF xerogels has dramatically shorten the production times, hence the costs [27], The tight control of the porosity of the RF xerogels would make them an ideal candidate polymer for waterproof/breathable applications. However, the surface chemistry of the organic xerogels is rich in phenolic groups, which provides them with a high hydrophilicity. This property, which in conjunction with their textural properties allows these materials to be used as desiccant materials [28] will not favor the water repellency required for this new application. Thus, to fulfil requirements of water repellency a passivating post-treatment of the RF xerogel surfaces would be eventually required.

There already exist several procedures for chemically modifying a micro-/nanostructured surface to give rise to low-surface energy materials (fluorinated substrates, coating mesh films, etc) [29-32], as well as methods to impart roughness to hydrophobic solid surfaces such as crystallization control [33], phase separation [34], electrochemical deposition [35], and chemical vapour deposition [36, 37]. Hydrophilic silica gels, which also have surfaces rich on hydroxyl groups resembling that of RF xerogels, have been turned into hydrophobic materials by grafting methylsilane compounds on their surface [30, 38, 39]. However, the use of silane compounds to this aim has not been

considered a suitable procedure due to the possible hydrolysis reactions that could likely take place at ambient conditions, which would limit the range of final applications of the resulting materials. A much more attractive alternative of surface passivation of surface hydroxyl groups has been described in a previous work, in which surface methoxylation was carried out using methanol vapor [40].

In this work, a similar one-step methoxylation reaction of the phenolic groups of RF xerogels has been carried out. The resulting methoxylated xerogels are superhydrophobic materials that, at the same time, absorb and desorb significant quantities of water vapor. The process was studied using different RF xerogels with average pore sizes covering a wide range of macroporosity (from 70-6000 nm) in order to explore the potential of this material in waterproof, breathable applications. Possible porosity alterations after the treatment were evaluated as well as the durability of the treatment over time.

2. EXPERIMENTAL

2.1. Materials

Resorcinol (Indspec, 99.6 wt. %), formaldehyde (Química S.A.U., aqueous solution with 37 wt. % formaldehyde and 0.7 wt. % methanol), deionized water, methanol (AnalaR Normapur, 99 %) and sodium hydroxide solutions made up from solid NaOH, (AnalaR Normapur, 99.9 %).

2.2. Synthesis of RF-xerogels

Resorcinol-formaldehyde xerogels were prepared according to Pekala's method described elsewhere [22,40]. Briefly, solid resorcinol was dissolved by magnetic stirring in deionized water until total solution. At the same time the formaldehyde is mixed with the methanol in another glass baker. Both solutions

were mixed and stirred to ensure homogeneity. The pH of the resulting solution was modified by dropping NaOH in order to achieve the desired final pH. The proportion of each reagent depends on the variables selected in order to give rise each textural properties which was previously designed (Table 1). Each precursor solution was placed in a microwave oven for 10000 seconds (2 h and 47 min) in order to induce gelation and curing to take place. The final material was dried until a loss of mass of 50 % weight was achieved.

Table 1. *Experimental variables used in the preparation of the organic xerogels (pH of the precursor solution; molar ratio of the total solvent to reactants, D; molar ratio resorcinol/formaldehyde and percentage of methanol in the formaldehyde solution).*

Sample	pH	D	R/F	% MeOH
OX-6000	5.0	8	0.7	0.7
OX-2000	5.5	8	0.7	0.7
OX-500	3.1	5.6	0.5	12.5
OX-150	3.3	5.6	0.5	12.5
OX-70	3.3	5.7	0.1	12.5

2.3. Surface modification

Each RF-xerogel was grinded and sieved under < 212 µm and finally heated at 100 ºC overnight to eliminate completely the residual moisture and unreacted compounds. The hydrophilic RF-xerogel was placed inside a quartz reactor. A nitrogen flow of 100 mL min^{-1} was bubbled in liquid methanol at 80 ºC in a vessel flask and introduced in the reactor at 240 ºC. Different dwelling times were carried out to study the effect of the time of treatment on the wetting properties of the resulting materials. Prior testing, methoxylated RF samples were heated in an oven for 1 h at 80 ºC to remove residual methanol.

2.4.   Sample characterization

Pore size and volume were determined by means of mercury porosimetry (AutoPore IV 9500, Micromeritics) from atmospheric pressure up to 228 MPa. That pressure ensures pores of 5.5 nm as the minimum pore size detectable by the equipment. The surface tension and contact angle values for Hg in all the characterizations were 0.485 N m^{-1} and 130º, respectively. Prior to these analyses, samples were outgassed (Micromeritics VacPrep 0.61) at 0.1 mbar and 120 ºC overnight.

The morphology was observed by means of scanning electron microscopy (SEM). Prior to this characterization, the xerogels were carbonized at 700 ºC under nitrogen atmosphere (100 mL min^{-1}) for 2 h. The morphology of the sample do not change notably by the carbonisation process, but the electrical conductivity of the samples increases and so the SEM image quality is improved notably [21].

In order to determine the wettability of each sample, contact angle measurements were performed using a Krüss 62/G40 optical tensiometer. To this end, a water droplet (ca. 6 mm of diameter) was placed on the surface of a pellet of the RF xerogels with a glass micrometric syringe. Pellets of 10 mm diameter were obtained by comprising sample powders (< 212 μm particle size) using a pressure of 10 Tons for 25 s.

Fourier transform infrared spectroscopy (FTIR) was carried out in a Nicolet FTIR 8700 (Thermo Scientific) spectrometer fitted with a DTGS (deuterated triglycine sulphate) detector. The data were recorded between 4000-400 cm^{-1}, over 64 scans at a resolution of 4 cm^{-1}. Determination of C, H and N was carried out in a LECO CHNS-932 analyzer. The oxygen content was determined using a LECO VTF-900 analyzer.

Temperature programmed desorption (TPD) experiments were performed by thermogravimetry (DSC Q600 TA Instruments) coupled with a mass spectrometer (ThermoStar Pfeiffer). The sample was heated in the

thermobalance at 5 ºC min^{-1} up to 300 ºC, whilst the m/z signals (from 1 to 50) were registered in the mass spectrometer.

Moisture absorption capacity of each sample was tested by exposing them to saturated (100 % relative humidity) air at 25 ºC. Controlled amounts (200 mg) of RF xerogels were placed in 2 cm diameter glass vials. Weight changes were recorded until a constant mass was obtained. Thermogravimetric analysis was performed in order to corroborate these results by means of a TA instrument DSC Q600 analyzer. Changes in the weight of each sample were recorded in the temperature range of 25 to 350 ºC under nitrogen flow of 20 mL min^{-1} and at a heating rate of 10 ºC min^{-1}.

3. RESULTS AND DISCUSSION

The nanostructure of RF-xerogels is composed of packed quasi-spherical nodules, with small holes between them that constitute the porosity of these materials. Moreover, the size of these nodules, and therefore the size of the pores, can be pre-set, by selecting the appropriate synthesis conditions.[20] As an example of this, Figure 1 shows how different conditions of preparation (see Table 1) determine the nanometric structure of the OX-70, OX-500 and OX-2000 samples used in this study.
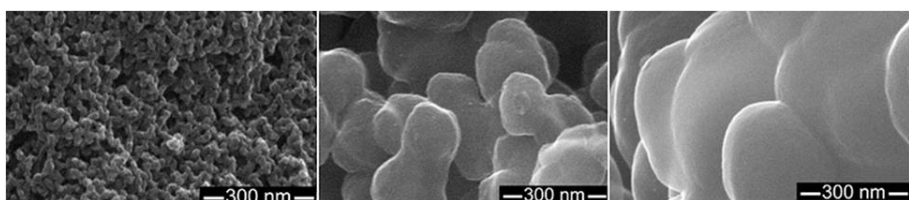

Figure 1. *SEM images of carbonized RF-xerogels: OX-70, OX-500 and OX-2000 (from left to right). Carbonized samples were used to increase de electrical conductivity and so have better SEM pictures. Nevertheless, the structure of the organic xerogels is virtually identical except by some minimum shrinking of the nodules after carbonization.*

The main porous characteristics of the different RF-xerogels are summarized in Table 2. Results show that it is possible to obtain RF xerogels with different pore size in the range of macropores (i.e. from ca. 70 to 6000 nm)

and with a relatively narrow pore size distribution (Figure 2). Obviously, the pore volume increases with the pore size, with values for the sample OX-6000 almost doubling that for OX-70 (i.e., 2 vs 1 cm^3 g^{-1}, Table 2). As a consequence, samples with higher pore size present a lower bulk density. The porosity of all the samples ranges between 50-70 % (Table 2).

Sample	Pore volume (cm^3 g^{-1})	Average pore size (nm)	Bulk density (g cm^{-3})	% Porosity
OX-6000	2.01	6260	0.34	69
OX-2000	2.17	2292	0.33	70
OX-500	1.57	522	0.42	65
OX-150	1.56	172	0.43	66
OX-70	1.04	65	0.45	47

Table 2. *Selected textural properties, determined by Hg porosimetry, of the RF-xerogels.*
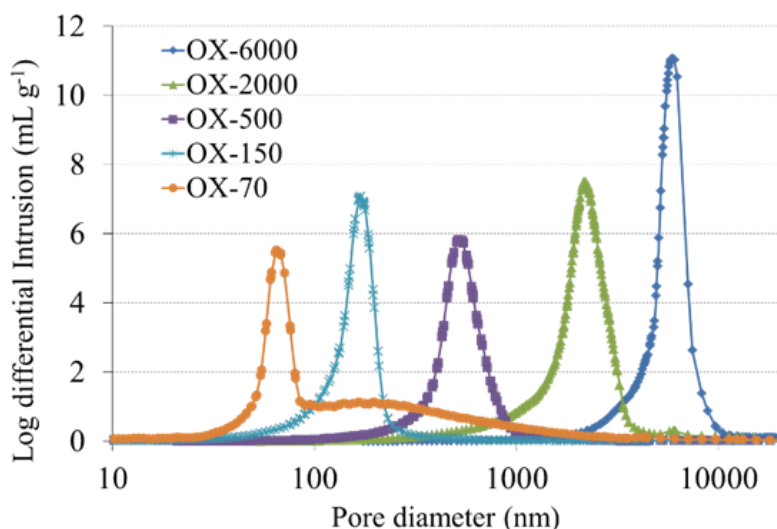

Figure 2. *Pore size distribution, obtained by mercury porosimetry, of the RF-xerogels.*

Regarding the surface chemistry of these materials, it is well established that the surface of the RF-xerogels is covered with some dangling phenolic groups (see Figure 3) [41]. The passivating mechanism that would transform those hydrophilic sites into hydrophobic is also depicted in Figure 3. According to the methoxylation reaction shown in Figure 3, hydrophobic methyl ether

groups will decorate the passivated surface of the treated RF xerogels. The contact angle measurements carried out on the passivated RF-xerogels corroborate this, i.e., all the materials except OX-70 eventually become superhydrophobic (i.e. contact angle > 150 º, Figure 4). Moreover, measuring the contact angle on these samples is, most of times, a tough task since the water drops are repelled away from the sample surface (see video in the supplementary material).
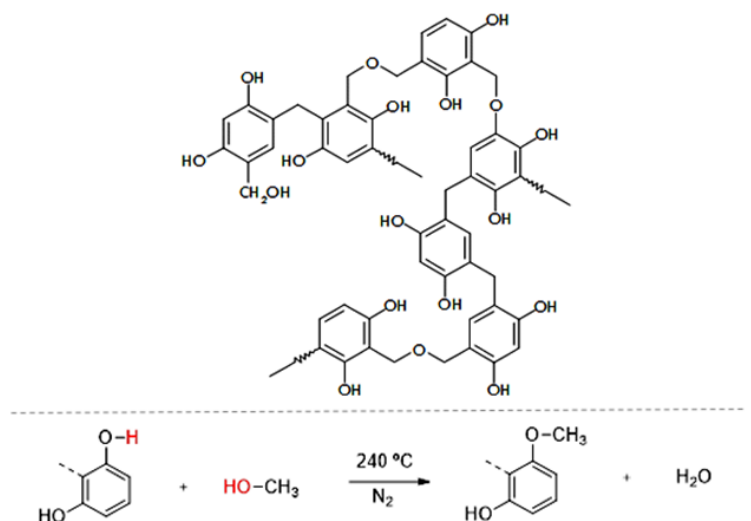
Figure 3. *Chemical structure of RF-xerogels (top) and passivation of hydrophilic sites of the xerogel surface by the reaction of alcohol condensation between methanol and hydroxyl groups (down).*
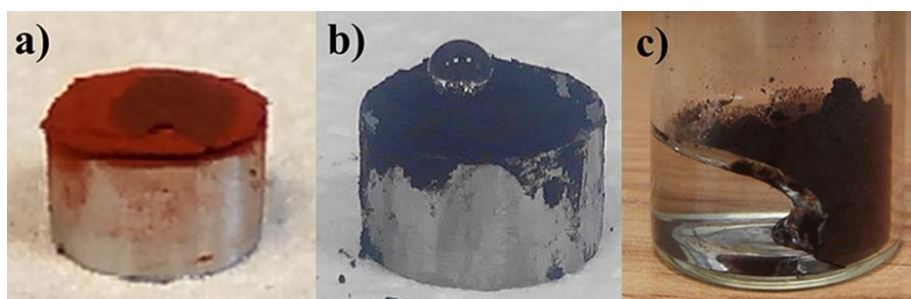
Figure 4. *Behavior of a drop of water over compacted powders of (a) hydrophilic (non-treated) and (b) superhydrophobic (passivated) RF xerogel. (c) Powder suspensions of the superhydrophobic xerogel after vigorous shaking; a bubble of air is clearly standing between liquid and solid phases.*

The time of the treatment with methanol required for transforming the RF-xerogels into superhydrophobic materials (SHP) is different for each material. Interestingly, this time increases as decreasing the pore size in a nearly exponentially way (Figure 5). Thus, while ca. 1 h of treatment is enough to passivate the OX-6000 surface and to transform it into SHP-6000, OX-150 needs 27 hours for changing its hydrophilic surface to the superhydrophobic of SHP-150 and OX-70 remains hydrophilic even after 100 hours of treatment.
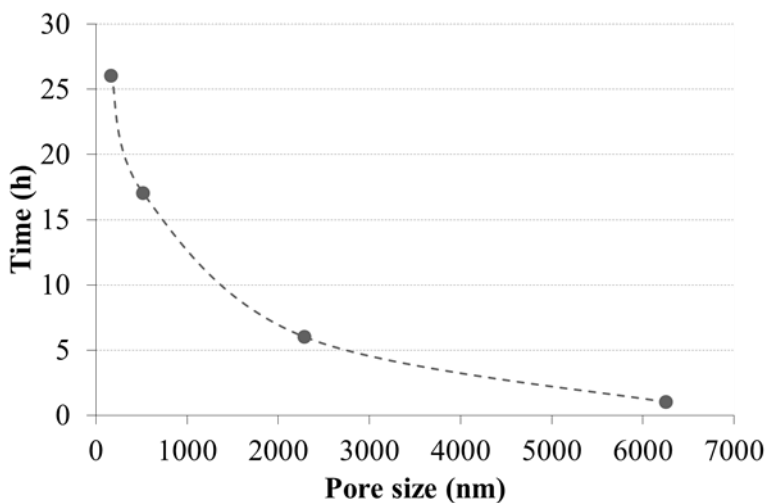

Figure 5. *Time necessary for passivate the RF-xerogels surface transforming it into a superhydrophobic surface (contact angle > 150º), as a function of their average pore size.*

Given the big differences in size between the molecule of methanol (0.46 nm) [42], and the mean pore size of these materials (70 - 6000 nm), this strong dependence of the time of passivation with the size of the pores is, somehow, surprising. There are two facts, however, that could explain it. The first one is related to the particular shape of the pores of the RF-xerogels. As schematized in Figure 6, the internal surface of RF-xerogels has a positive curvature, which differs from most porous materials with cylindrical or slit shaped pores, with a negative or null curvature, respectively [43] This particular porous texture of the RF-xerogels implies that, although the size of the pore may be large enough, pores are connected through bottlenecks formed by the contact points between spheres (see Figure 6). The number of these

bottlenecks increases and their size becomes narrower as the clusters are smaller (i.e., the mean pore size of the RF xerogel is smaller), thus hindering the access of the methanol molecules to the inner surface area. The second fact that would account for the increasing difficulty of methanol to passivate the RF-xerogel surfaces as their average pore size decreases is that, as the passivation proceeds, polar hydroxyl groups are being substituted by the nonpolar methyl groups. Since methanol is an amphipathic molecule, the passivation of the hydroxyl groups of the RF-xerogel would turn a polar surface into nonpolar as the reaction proceeds. Nonpolar (dispersive) interactions between the methanol molecules and the passivated surface would increase progressively, thus competing with the main reaction pathway depicted in Figure 3 and slowing down the methoxylation. This phenomenon would become more important in small pores (or in the aforementioned bottlenecks) where methyl groups would be closer to each other.
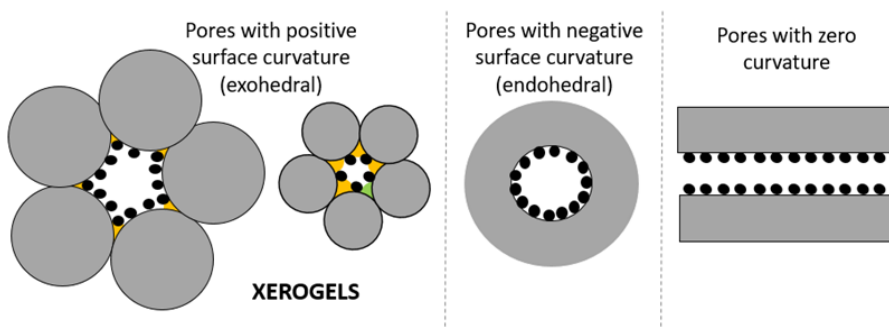
Figure 6. *Different pore models according to the surface curvature on the inner surface or the pore.*

Another surprising fact is that after a certain treatment time, the RF-xerogels shift abruptly from hydrophilic to superhydrophobic. Indeed, the treatments with methanol were stopped at different times and contact angle tests carried out (Figure 7). Angles measured were either 0 º or 180 º. This suggests that there is a threshold in the proportion of passivated phenolic groups above which the RF-xerogels surface repels liquid water completely.
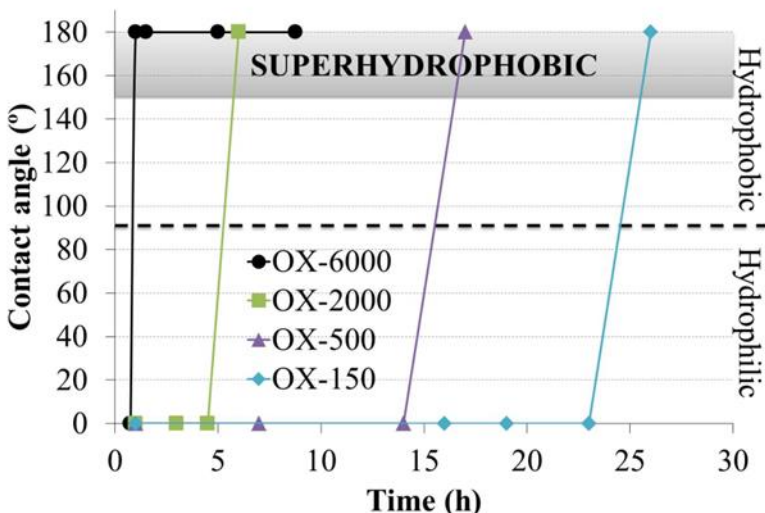
Figure 7. *Variation of the contact angle with the time of passivation.*

So far it has been demonstrated that the hydrophilic surfaces of the macroporous RF xerogels can be made superhydrophobic by a simple passivation with methanol. However, as one of the advantages of RF xerogels is the possibility to design and adjust the porosity for a determined application, it would be necessary to check if this tailored porosity is modified by the methanol treatment. For this purpose, mercury porosimetry was carried out on the passivated samples. Figure 8 shows the plots of cumulative intrusion of Hg vs pore diameter comparing two RF xerogels with very different mean pore size (OX-2000 and OX-150) and their passivated counterparts (SHP-2000 and SHP-150, respectively). The curves of each pair of materials are essentially identical, i.e., the treatment with methanol does not change the pore size distribution of the original OX samples. It should be pointed out that although it is clear that the main steps in the cumulative intrusion plots occur around 150 and 2000 nm for both pair of samples OX-150/SHP-150 and OX-2000/SHP-2000, respectively, the increasing in the intrusion volume observed at the beginning of the analysis (i.e., low pressure conditions corresponding to high pore diameters, Figure 8) should be ascribed to interparticular porosity and/or compressive effects of organic xerogels. In any case, the intrusion profiles are always

identical (including all effects) for samples before and after the methanol treatment.
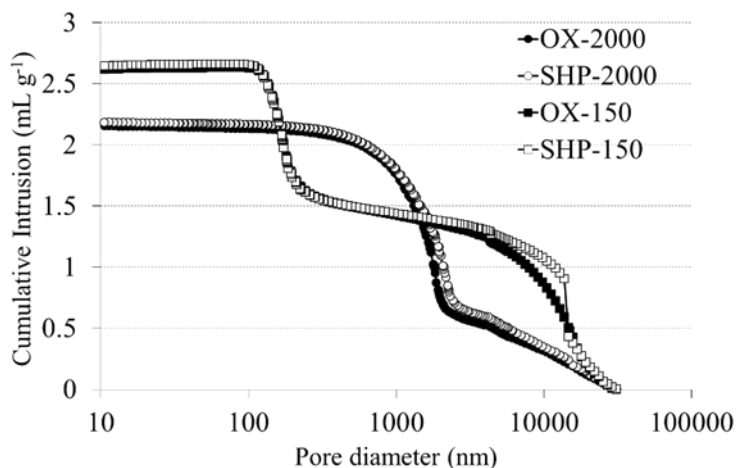
Figure 8. *Cumulative intrusion vs pore size obtained by mercury porosimetry of two RF-xerogels before and after the methoxylation reaction.*

Changes in the surface chemistry after the passivation treatment have already been advanced and they are expected to take place according to the passivation reaction shown in Figure 3. However, to verify that passivation mechanism and to what extent it takes place: (i) elemental chemical analysis, (ii) FTIR characterization and (iii) Temperature Programmed Desorption (TPD) coupled with mass spectrometry were performed on treated and untreated samples.

Results of the elemental analyses (Table 3) reveals that the SHP-samples contains approximately 2 wt% more carbon than pristine samples and that the H/O and C/O ratios increase after the passivation. This is consistent with the incorporation of methyl groups blocking hydrophilic sites to form methoxy ($O-CH_3$) groups, considering that the number of atoms of O would remain unaltered during the treatment (Figure 3).

Table 3. *Elemental analysis results for two treated and non-treated xerogels and their molar ratios.*

	OX-6000	SHP-6000	OX-150	SHP-150
C (±0.2, wt. %)	65.7	67.6	66.1	68.4
H (±0.2, wt. %)	4.0	4.0	4.4	4.2
O (±0.2, wt. %)	30.3	28.4	29.5	27.4
H/O molar ratio	2.11	2.25	2.34	2.43
C/O molar ratio	2.89	3.17	2.99	3.32

The FTIR spectra of samples OX-6000 and SHP-6000 are shown in Figure 9. The most notable difference is the decrease of the relative intensity of the broad band at 3600-3000 cm^{-1} (that corresponds to the OH groups) after the passivation treatment. All bands below 1700 cm^{-1}, which have been already identified in RF xerogels [27] are also present after the methoxylation. In order to have an estimation of the decrease of the relative intensity of the OH band corresponding to the phenolic groups, the aromatic C=C absorption band centered at 1605 cm^{-1}, which should remain unaltered during the reaction, was taken as reference. Thus, comparing the ratios of the intensities of these two absorption bands it can be concluded that the intensity reduction of the OH band after the treatment is ca. 24 % with respect to the band of the original OX-6000 xerogel. Beyond this "semi-quantitative" result, it should be noticed that the treatment with methanol passivates only part of the phenolic groups, which, in any case, seems to be enough to make the material superhydrophobic.
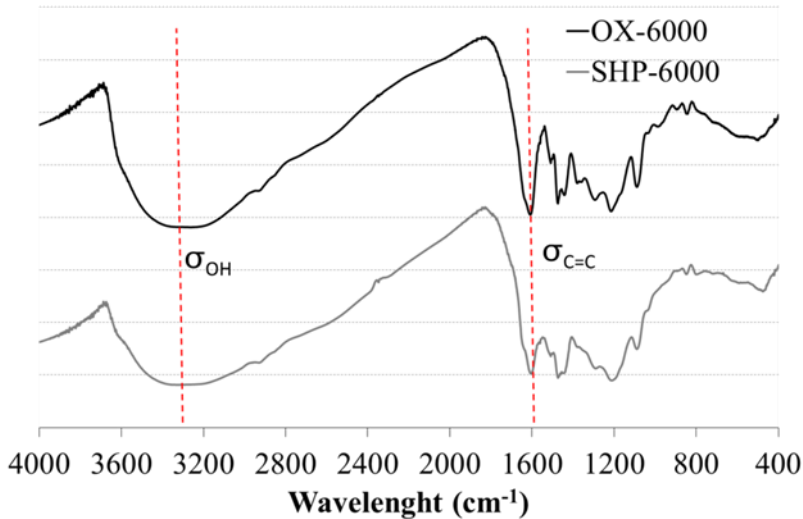
Figure 9. *FTIR spectra of the RF xerogels before (OX-6000) and after (SHP-6000) the surface modification.*

During the TPD analysis by TGA-MS, the m/z 31 corresponding to methoxy groups, was recorded with the increasing temperature. As an example representative of all passivated RF-xerogels, Figure 10 shows the results of the OX-500 and SHP-500 materials. The passivated xerogel exhibits a pronounced peak at temperatures between 50 and 200 °C, with a maximum centered at 120 °C, ascribed to the evolution of the methoxy groups. As expected, this peak does not appear in the original sample. Additional information regarding the thermal stability of the methoxy groups introduced with the passivation treatment can be inferred from this plot. Thus, it might be expected that the SHP-xerogels would keep their superhydrophobicity, at least, up to 50 °C.
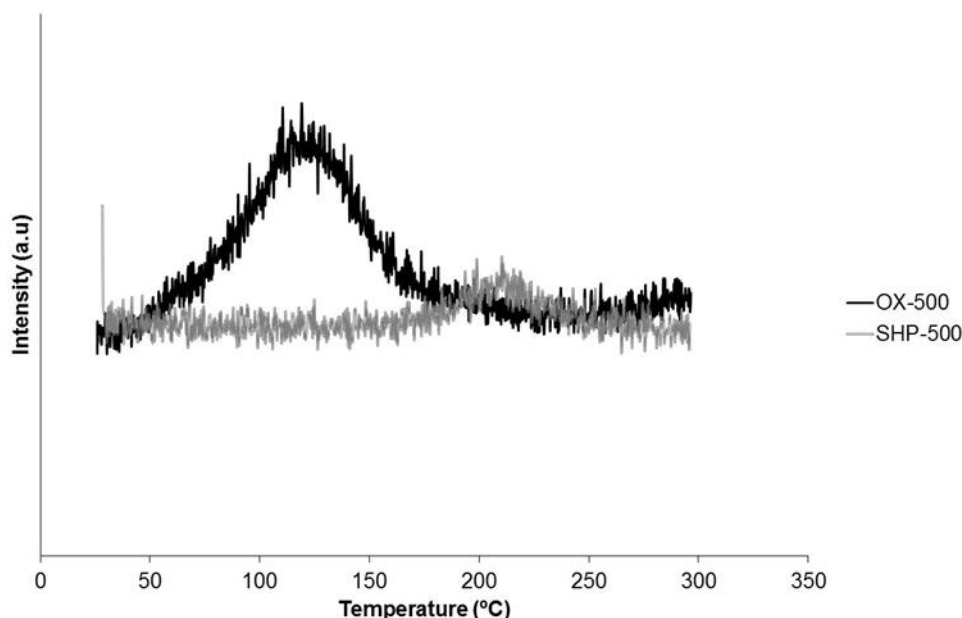
Figure 10. *Evolution of methoxy (O-CH$_3$) groups during TPD analysis for samples OX-500 and SHP-500.*

Another question regarding the SHP-materials concerns the stability/reversibility of the methoxylation treatment in terms of the durability of the superhydrophobic property of the passivated samples. In order to find this out, samples of the SPH-xerogels were exposed to an atmosphere saturated with a 100 % of humidity for 40 days, and aliquots of those samples were taken periodically for contact angle measurements. The optical tensiometer shows that the contact angle of all aged samples remained higher than 150 º (Table 4). Furthermore, it was found a weight gain in the time, which indicated that the samples were adsorbing moisture from the atmosphere (Table 4). This indicates that the passivated xerogels were able to retain a certain degree of moisture inside its porosity, in spite of their waterproofness. The water vapor absorption was found to be relatively fast, with most of the moisture absorbed in the first day of exposure (see Table 4).

Table 4. Variations on the moisture uptake and contact angle of the SHP-xerogels during 40 days exposure to 100 % relative humidity air

Days	0	1	10	20	30	40
Moisture uptake (wt%)						
SHP-6000	0	13	13	13	14	15
SHP-2000	0	13	17	18	19	19
SHP-500	0	13	15	16	17	18
SHP-150	0	11	11	12	12	13
Contact angle (α)						
SHP-6000	>150°	>150°	>150°	>150°	>150°	>150°
SHP-2000	>150°	>150°	>150°	>150°	>150°	>150°
SHP-500	>150°	>150°	>150°	>150°	>150°	>150°
SHP-150	>150°	>150°	>150°	>150°	>150°	>150°

Whether this absorption of moisture is a reversible process or not was also checked by subjecting the soaked samples (after 40 days exposure) to a certain vacuum (10 Pa) at 25 ºC and for 24 h and quantifying then the moisture retained (or released). The moisture retained in the different samples was: 1.6 wt% for SHP-6000, 1.7 wt% for SHP-2000, 1.9 wt% for SHP-500 and 2.9 wt% for SHP-150. Additionally, aliquots of the saturated samples were put in a desiccator containing silica gel for 3 days at 25 ºC and atmospheric pressure. The moisture retained by the samples after this experiment was: 3.2 wt% for SHP-6000, 3.9 wt% for SHP-2000, 4.0 wt% for SHP-500 and 4.9 wt% for SHP-150. In sum, under the above mentioned conditions the adsorption of moisture by the SHP-xerogels is reversible up to an 80-90 %. Therefore, if environmental moisture can enter and leave the sample by simply modifying the pressure or the humidity of the environment, it can be considered that SHP-xerogels are breathable. The effect of the average pore size on the ability of the SHP samples for absorbing/releasing moisture is only noticeable for low pore size values. Hence, SHP-150 moisture uptake per gram and day is slower than that of SHP-500, but further increase of the pore size from 500 to 6000 nm renders similar values (Table 4).

The mechanism that would explain why the SHP-xerogels are superhydrophobic but, at the same time, breathable is depicted in the sketch of Figure 11.
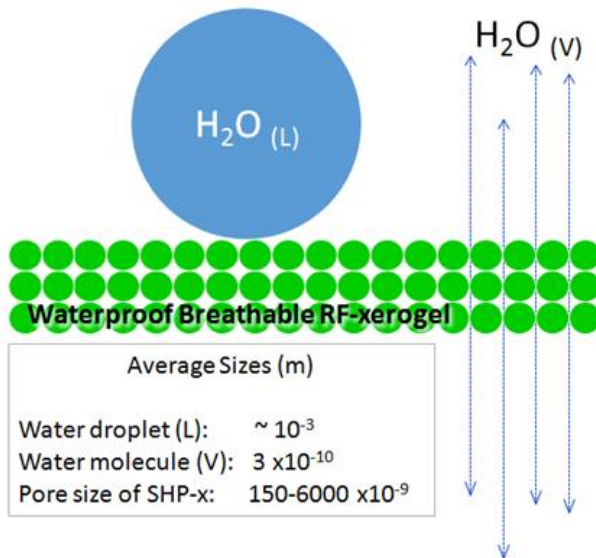
Figure 11. *Proposed mechanism explaining the waterproofing and breathability of the passivated RF-xerogels.*

As the most external, and most accessible, surface of the material is completely passivated by the treatment with methanol, the liquid water drops are repelled. Furthermore, the diameter of these water drops is, at least, one order of magnitude larger than the pores of the material, which contributes to the superhydrophobicity exhibited against liquid water. On the other hand, water molecules of vapor are, at least, one order of magnitude smaller than the pores of the materials, so they can pass through it. There are, however, some phenolic groups inside the pores that were not passivated (see Figure 9), so part (ca. 20 %) of the moisture is retained inside the pores. Nevertheless, these hydroxyl groups are sufficiently far away from the outer surface to promote the absorption of the liquid water drops.

4. CONCLUSIONS

A simple methoxylation treatment transforms highly hydrophilic RF-xerogels into superhydrophobic materials. The treatment time for shifting to superhydrophobic highly depends on the pore size of the material and occurs suddenly, without passing through intermediate states. This is attributed to repulsive/dispersive interactions, magnified by the exohedral shape of the pores, between the nonpolar passivated surface and the methanol. Changes on the surface chemistry of the particles did not affect the porosity of the original xerogels. This is a very important outcome as far as the porosity of this type of materials can be easily controlled during the synthesis, thus opening the possibility of tuning the porosity for a given application. Furthermore, it has been demonstrated that the superhydrophobic xerogels still retain the ability of interchanging water vapor between atmospheres with different vapor activities. This breathable behavior is mainly controlled by the hydrophilic groups that remain unreacted in the inner pore surfaces, with the average pore size being only relevant below 500 nm.

ACKNOWLEDGMENT

REFERENCES

[1] G.R. Lomax, Breathable polyurethane membranes for textile and related industries, Journal of Materials Chemistry, 17 (2007) 2775-2784.

[2] W. Jeong, S. An, The transport properties of polymer membrane-fabric composites, Journal of materials science, 36 (2001) 4797-4803.

[3] S. Zhao, P.H. Feron, L. Deng, E. Favre, E. Chabanon, S. Yan, J. Hou, V. Chen, H. Qi, Status and progress of membrane contactors in post-combustion carbon capture: A state-of-the-art review of new developments, Journal of Membrane Science, 511 (2016) 180-206.

[4] Z. Fu, K. Li, L. Pu, B. Ge, Z. Chen, Waterproof Breathable Membrane Used as Gas Diffusion Layer in Activated Carbon Air Cathode Microbial Fuel Cells, Fuel Cells, 16 (2016) 839-844.

[5] D. Xing, Y. Tang, X. Mei, B. Liu, Electricity generation of microbial fuel cell with waterproof breathable membrane cathode, Journal of Power Sources, 300 (2015) 491-495.

[6] A. Gugliuzza, E. Drioli, New performance of hydrophobic fluorinated porous membranes exhibiting particulate-like morphology, Desalination, 240 (2009) 14-20.

[7] J. Huang, A new test method for determining water vapor transport properties of polymer membranes, Polymer testing, 26 (2007) 685-691.

[8] Q.B. Meng, S.-I. Lee, C. Nah, Y.-S. Lee, Preparation of waterborne polyurethanes using an amphiphilic diol for breathable waterproof textile coatings, Progress in Organic Coatings, 66 (2009) 382-386.

[9] E.Y. Kim, J.H. Lee, D.J. Lee, Y.H. Lee, J.H. Lee, H.D. Kim, Synthesis and properties of highly hydrophilic waterborne polyurethane-ureas containing various hardener content for waterproof breathable fabrics, Journal of Applied Polymer Science, 129 (2013) 1745-1751.

[10] Y. Li, Z. Zhu, J. Yu, B. Ding, Carbon nanotubes enhanced fluorinated polyurethane macroporous membranes for waterproof and breathable application, ACS applied materials & interfaces, 7 (2015) 13538-13546.

[11] J.B. You, Y. Yoo, M.S. Oh, S.G. Im, Simple and Reliable Method to Incorporate the Janus Property onto Arbitrary Porous Substrates, ACS applied materials & interfaces, 6 (2014) 4005-4010.

[12] J. Sheng, M. Zhang, Y. Xu, J. Yu, B. Ding, Tailoring Water-Resistant and Breathable Performance of Polyacrylonitrile Nanofibrous Membranes Modified by Polydimethylsiloxane, ACS Applied Materials & Interfaces, 8 (2016) 27218-27226.

[13] H. Wang, Y. Xue, J. Ding, L. Feng, X. Wang, T. Lin, Durable, Self-Healing Superhydrophobic and Superoleophobic Surfaces from Fluorinated-Decyl Polyhedral Oligomeric Silsesquioxane and Hydrolyzed Fluorinated Alkyl Silane, Angewandte Chemie International Edition, 50 (2011) 11433-11436.

[14] H. Zhou, H. Wang, H. Niu, A. Gestos, X. Wang, T. Lin, Fluoroalkyl silane modified silicone rubber/nanoparticle composite: a super durable, robust superhydrophobic fabric coating, Advanced materials, 24 (2012) 2409-2412.

[15] W. Zhaohui, G. Zhenya, A study on novel waterproof and moisture-permeable poly (vinylidene fluoride) micropore membrane-coated fabrics, Journal of applied polymer science, 79 (2001) 801-807.

[16] A. Gugliuzza, G. Clarizia, G. Golemme, E. Drioli, New breathable and waterproof coatings for textiles: effect of an aliphatic polyurethane on the

formation of PEEK-WC porous membranes, European Polymer Journal, 38 (2002) 235-242.

[17] A. Stolz, S. Le Floch, L. Reinert, S.M.M. Ramos, J. Tuaillon-Combes, Y. Soneda, P. Chaudet, D. Baillis, N. Blanchard, L. Duclaux, A. San-Miguel, Melamine-derived carbon sponges for oil-water separation, Carbon, 107 (2016) 198-208.

[18] F.S. NV, J. Gopinathan, B. Indumathi, S. Thomas, A. Bhattacharyya, Morphology and hydroscopic properties of acrylic/thermoplastic polyurethane core–shell electrospun micro/nano fibrous mats with tunable porosity, RSC Advances, 6 (2016) 54286-54292.

[19] B. Yoon, S. Lee, Designing waterproof breathable materials based on electrospun nanofibers and assessing the performance characteristics, Fibers and Polymers, 12 (2011) 57-64.

[20] R. Pekala, Organic aerogels from the polycondensation of resorcinol with formaldehyde, Journal of Materials Science, 24 (1989) 3221-3227.

[21] N. Rey-Raap, A. Arenillas, J.A. Menéndez, A visual validation of the combined effect of pH and dilution on the porosity of carbon xerogels, Microporous and Mesoporous Materials, 223 (2016) 89-93.

[22] I.D. Alonso-Buenaposada, N. Rey-Raap, E.G. Calvo, J. Angel Menéndez, A. Arenillas, Effect of methanol content in commercial formaldehyde solutions on the porosity of RF carbon xerogels, Journal of Non-Crystalline Solids, 426 (2015) 13-18.

[23] Z. Zapata-Benabithe, C. Moreno-Castilla, F. Carrasco-Marín, Effect of dilution ratio and drying method of resorcinol–formaldehyde carbon gels on their electrocapacitive properties in aqueous and non-aqueous electrolytes, J Sol Gel Sci Technol, 75 (2015) 407-412.

[24] N. Job, C.J. Gommes, R. Pirard, J.-P. Pirard, Effect of the counter-ion of the basification agent on the pore texture of organic and carbon xerogels, Journal of Non-Crystalline Solids, 354 (2008) 4698-4701.

[25] L. Zubizarreta, A. Arenillas, J.J. Pis, Preparation of Ni-doped carbon nanospheres with different surface chemistry and controlled pore structure, Applied Surface Science, 254 (2008) 3993-4000.

[26] J. Choma, K. Jedynak, W. Fahrenholz, J. Ludwinowicz, M. Jaroniec, Microporosity development in phenolic resin-based mesoporous carbons for enhancing CO2 adsorption at ambient conditions, Applied Surface Science, 289 (2014) 592-600.

[27] E.G. Calvo, E.J. Juárez-Pérez, J.A. Menéndez, A. Arenillas, Fast microwave-assisted synthesis of tailored mesoporous carbon xerogels, Journal of Colloid and Interface Science, 357 (2011) 541-547.

[28] I.D. Alonso-Buenaposada, E.G. Calvo, M.A. Montes-Morán, J. Narciso, J.A. Menéndez, A. Arenillas, Desiccant capability of organic xerogels:

Surface chemistry vs porous texture, Microporous and Mesoporous Materials, 232 (2016) 70-76.

[29] M. Hikita, K. Tanaka, T. Nakamura, T. Kajiyama, A. Takahara, Super-Liquid-Repellent Surfaces Prepared by Colloidal Silica Nanoparticles Covered with Fluoroalkyl Groups, Langmuir, 21 (2005) 7299-7302.

[30] A.V. Rao, E. Nilsen, M.-A. Einarsrud, Effect of precursors, methylation agents and solvents on the physicochemical properties of silica aerogels prepared by atmospheric pressure drying method, Journal of non-crystalline solids, 296 (2001) 165-171.

[31] L. Feng, Z. Zhang, Z. Mai, Y. Ma, B. Liu, L. Jiang, D. Zhu, A super-hydrophobic and super-oleophilic coating mesh film for the separation of oil and water, Angewandte Chemie International Edition, 43 (2004) 2012-2014.

[32] H. Guo, M. Ulbricht, The effects of (macro)molecular structure on hydrophilic surface modification of polypropylene membranes via entrapment, Journal of Colloid and Interface Science, 350 (2010) 99-109.

[33] M. Pantoja, J. Abenojar, M.A. Martinez, Influence of the type of solvent on the development of superhydrophobicity from silane-based solution containing nanoparticles, Applied Surface Science.

[34] H. Li, R. Wang, H. Hu, W. Liu, Surface modification of self-healing poly(urea-formaldehyde) microcapsules using silane-coupling agent, Applied Surface Science, 255 (2008) 1894-1900.

[35] H. Tian, T. Yang, Y. Chen, Fabrication and characterization of superhydrophobic thin films based on TEOS/RF hybrid, Applied Surface Science, 255 (2009) 4289-4292.

[36] J. Becerra, G. Sudre, I. Royaud, R. Montserret, B. Verrier, C. Rochas, T. Delair, L. David, Tuning the Hydrophilic/Hydrophobic Balance to Control the Structure of Chitosan Films and Their Protein Release Behavior, AAPS PharmSciTech, (2016) 1-14.

[37] X. Feng, L. Jiang, Design and creation of superwetting/antiwetting surfaces, Advanced Materials, 18 (2006) 3063-3078.

[38] P. Suresh Kumar, J. Sundaramurthy, D. Mangalaraj, D. Nataraj, D. Rajarathnam, M.P. Srinivasan, Enhanced super-hydrophobic and switching behavior of ZnO nanostructured surfaces prepared by simple solution – Immersion successive ionic layer adsorption and reaction process, Journal of Colloid and Interface Science, 363 (2011) 51-58.

[39] C.D. Esplin, A. Bowden, B. Jensen, Super-hydrophobic and Anti-Microbial Surfaces via Carbon Infiltrated-Carbon Nanotubes, (2017).

[40] T. Supakar, M. Moradiafrapoli, G.F. Christopher, J.O. Marston, Spreading, encapsulation and transition to arrested shapes during drop impact onto hydrophobic powders, Journal of Colloid and Interface Science, 468 (2016) 10-20.

[41] X. Zhang, D. Wang, Preparation and activity of ionic liquid catalysts grafted on hydrophobic silica gel, in: 3rd International Conference on Manufacturing Science and Engineering, ICMSE 2012, Xiamen, 2012, pp. 2621-2624.

[42] S.H. Li, X.D. Sun, L.-j. Wang, W.-b. Gu, W.-m. Wang, Z.Y. Yang, Y. Wang, J.H. Zhu, Fabricating hydrophobic nanoparticles within mesoporous channel of silica for efficient TSNA removal, Microporous and Mesoporous Materials, 237 (2017) 237-245.

[43] K.-H. Lee, S.-Y. Kim, K.-P. Yoo, Low-density, hydrophobic aerogels, Journal of Non-Crystalline Solids, 186 (1995) 18-22.

Capítulo 6

Conclusiones

6. Conclusiones

En la presente memoria, compilación de distintos documentos (artículos científicos y una patente), se muestran los estudios realizados para lograr un control total de las propiedades porosas y químicas de los xerogeles RF de manera que puedan ser diseñados a medida de forma específica y minuciosa para cualquier aplicación.

Las conclusiones más relevantes de las publicaciones relacionadas con el **diseño de las propiedades porosas** de los xerogeles son las siguientes:

✓ La proporción de metanol contenida en la disolución de formaldehído comercial afecta, de forma relevante, a la porosidad final de los xerogeles RF. Por lo tanto, aparece como nueva a variable a tener en cuenta a la hora de diseñar estos materiales con una porosidad final definida.

✓ La utilización de un catalizador ácido en la disolución precursora como acelerante de la reacción de polimerización permite obtener materiales con propiedades porosas y químicas similares a las obtenidas mediante el catalizador básico común. Además, mediante este proceso no se incluyen impurezas metálicas a la estructura final del material y permite obtener materiales con tamaños de poro mayores a los conseguidos con catalizadores básicos. Este mecanismo refuerza el papel del efecto del metanol de la disolución de formaldehído ya que es la única manera

de obtener tamaños de poro menores de 50 nm, rango donde se encuentran la mayoría de las aplicaciones.

✓ El control minucioso de las propiedades porosas de los xerogeles de carbono les convierte en materiales potenciales para ser utilizados como soportes de biomoléculas, como en este caso el Citocromo C, ya que su porosidad es diseñada a medida de la biomolécula que se quiere soportar. A través de este procedimiento es posible recuperar y reutilizar proteínas de alto valor económico.

Las conclusiones más relevantes de las publicaciones relacionadas con el **diseño de la química superficial** de los xerogeles RF son las siguientes:

✓ Los xerogeles orgánicos han mostrado ser unos excelentes materiales desecantes que absorben más de un 80 % de su peso en humedad. Además son de fácil manejo debido a su baja densidad, se regeneran a bajas temperaturas (100 ºC), se pueden fabricar a bajo coste, ya que no requieren de procesos de carbonización, y son resistentes a ataques con ácido.

✓ Los xerogeles RF pueden cambiar su naturaleza hidrófila a hidrófoba mediante un tratamiento de modificación superficial con HMDZ. Esta modificación es reversible mediante hidrólisis.

✓ Se pueden obtener xerogeles RF superhidrófobos transpirables a través de un tratamiento de modificación superficial con metanol en fase vapor. Además, son resistentes a exposiciones prolongadas en atmósfera húmeda y pueden ser regenerados fácilmente sin perder efectividad en su uso.

Por lo tanto la **CONCLUSIÓN GENERAL** que se obtiene de esta Tesis Doctoral es que los xerogeles RF pueden ser diseñados con las propiedades porosas y químicas a medida de la aplicación deseada a través de procedimientos rápidos, sencillos y de bajo coste, lo que les hace materiales que pueden ser fabricados a escala industrial.

Capítulo 7

Referencias

7. Referencias

[1] E.G. Calvo, E.J. Juárez-Pérez, J.A. Menéndez, A. Arenillas, Fast microwave-assisted synthesis of tailored mesoporous carbon xerogels, Journal of Colloid and Interface Science, 357 (2011) 541-547.

[2] S.A. Al-Muhtaseb, J.A. Ritter, Preparation and Properties of Resorcinol–Formaldehyde Organic and Carbon Gels, Advanced Materials, 15 (2003) 101-114.

[3] L. Zubizarreta, A. Arenillas, J.A. Menéndez, J.J. Pis, J.P. Pirard, N. Job, Microwave drying as an effective method to obtain porous carbon xerogels, Journal of Non-Crystalline Solids, 354 (2008) 4024-4026.

[4] N. Rey-Raap, A. Arenillas, J.A. Menéndez, A visual validation of the combined effect of pH and dilution on the porosity of carbon xerogels, Microporous and Mesoporous Materials, 223 (2016) 89-93.

[5] C. Scherdel, R. Gayer, G. Reichenauer, Porous organic and carbon xerogels derived from alkaline aqueous phenol–formaldehyde solutions, Journal of Porous Materials, 19 (2012) 351-360.

[6] B.B. Garcia, S.L. Candelaria, D. Liu, S. Sepheri, J.A. Cruz, G. Cao, High performance high-purity sol-gel derived carbon supercapacitors from renewable sources, Renewable Energy, 36 (2011) 1788-1794.

[7] W. Kicinski, M. Bystrzejewski, M.H. Rümmeli, T. Gemming, Porous graphitic materials obtained from carbonization of organic xerogels doped with transition metal salts, Bulletin of Materials Science, 37 (2014) 141-150.

[8] N. Esmaeili, M. Zohuriaan-Mehr, S. Mohajeri, K. Kabiri, H. Bouhendi, Hydroxymethyl furfural-modified urea–formaldehyde resin: synthesis and properties, European Journal of Wood and Wood Products, 75 (2017) 71-80.

[9] G. Amaral-Labat, L.I. Grishechko, V. Fierro, B.N. Kuznetsov, A. Pizzi, A. Celzard, Tannin-based xerogels with distinctive porous structures, Biomass and Bioenergy, 56 (2013) 437-445.

[10] E.G. Calvo, A. Arenillas, J. Menéndez, Designing Nanostructured Carbon Xerogels, INTECH Open Access Publisher, Rijeka, 2011.

[11] E.J. Juárez-Pérez, E.G. Calvo, A. Arenillas, J.A. Menéndez, Precise determination of the point of sol–gel transition in carbon gel synthesis using a microwave heating method, Carbon, 48 (2010) 3305-3308.

[12] N. Rey-Raap, J.A. Menéndez, A. Arenillas, Optimization of the process variables in the microwave-induced synthesis of carbon xerogels, Journal of Sol-Gel Science and Technology, 69 (2014) 488-497.

[13] N. Job, R. Pirard, J. Marien, J.-P. Pirard, Porous carbon xerogels with texture tailored by pH control during sol–gel process, Carbon, 42 (2004) 619-628.

[14] E.G. Calvo, J.A. Menéndez, A. Arenillas, Influence of alkaline compounds on the porosity of resorcinol-formaldehyde xerogels, Journal of Non-Crystalline Solids, 452 (2016) 286-290.

[15] N. Rey-Raap, J. Angel Menéndez, A. Arenillas, Simultaneous adjustment of the main chemical variables to fine-tune the porosity of carbon xerogels, Carbon, 78 (2014) 490-499.

[16] I.D. Alonso-Buenaposada, N. Rey-Raap, E.G. Calvo, J. Angel Menéndez, A. Arenillas, Effect of methanol content in commercial formaldehyde solutions on the porosity of RF carbon xerogels, Journal of Non-Crystalline Solids, 426 (2015) 13-18.

[17] N. Job, F. Sabatier, J.-P. Pirard, M. Crine, A. Léonard, Towards the production of carbon xerogel monoliths by optimizing convective drying conditions, Carbon, 44 (2006) 2534-2542.

[18] N. Rey-Raap, A. Arenillas, J.A. Menéndez, Formaldehyde in the Synthesis of Resorcinol-Formaldehyde Carbon Gels in Formaldehyde: Synthesis, Applications and Potential Health Effects, (2015) 31.

[19] A.H. Moreno, A. Arenillas, E.G. Calvo, J.M. Bermúdez, J.A. Menéndez, Carbonisation of resorcinol–formaldehyde organic xerogels: Effect of temperature, particle size and heating rate on the porosity of carbon xerogels, Journal of Analytical and Applied Pyrolysis, 100 (2013) 111-116.

[20] E.G. Calvo, C. Ania, L. Zubizarreta, J. Menéndez, A. Arenillas, Exploring new routes in the synthesis of carbon xerogels for their application in electric double-layer capacitors, Energy & Fuels, 24 (2010) 3334-3339.

[21] C. Alegre, L. Calvillo, R. Moliner, J.A. González-Expósito, O. Guillén-Villafuerte, M.V.M. Huerta, E. Pastor, M.J. Lázaro, Pt and PtRu electrocatalysts supported on carbon xerogels for direct methanol fuel cells, Journal of Power Sources, 196 (2011) 4226-4235.

[22] V. Celorrio, J. Flórez-Montaño, R. Moliner, E. Pastor, M.J. Lázaro, Fuel cell performance of Pt electrocatalysts supported on carbon nanocoils, International Journal of Hydrogen Energy, 39 (2014) 5371-5377.

[23] L. Zubizarreta, J.A. Menéndez, N. Job, J.P. Marco-Lozar, J.P. Pirard, J.J. Pis, A. Linares-Solano, D. Cazorla-Amorós, A. Arenillas, Ni-doped carbon xerogels for H_2 storage, Carbon, 48 (2010) 2722-2733.

[24] N. Rey-Raap, E. Calvo, J. Menéndez, A. Arenillas, Exploring the potential of resorcinol-formaldehyde xerogels as thermal insulators, Microporous and Mesoporous Materials, 244 (2017) 50-54.

[25] N. Rey-Raap, S. Rodríguez-Sánchez, I.D. Alonso-Buenaposada, E.G. Calvo, J.A. Menéndez, A. Arenillas, The enhancement of porosity of carbon xerogels by using additives, Microporous and Mesoporous Materials, 217 (2015) 39-45.

[26] W.J. Frederic, Stabilization of formaldehyde solutions, Google Patents 1935.

[27] D.M. Pozar, Microwave engineering, John Wiley & Sons 2009.

[28] B.L. Hayes, Microwave synthesis: chemistry at the speed of light, Cem Corporation 2002.

[29] L. Masschelein-Kleiner, Los solventes, Santiago, Chile: Centro Nacional de Conservación y Restauración (2004).

[30] N. Rey-Raap, J. Angel Menéndez, A. Arenillas, RF xerogels with tailored porosity over the entire nanoscale, Microporous and Mesoporous Materials, 195 (2014) 266-275.

[31] S.J. Taylor, M.D. Haw, J. Sefcik, A.J. Fletcher, Gelation mechanism of resorcinol-formaldehyde gels investigated by dynamic light scattering, Langmuir, 30 (2014) 10231-10240.

[32] M.L.C. Piedboeuf, A.F. Léonard, K. Traina, N. Job, Influence of the textural parameters of resorcinol-formaldehyde dry polymers and carbon xerogels on particle sizes upon mechanical milling, Colloids and Surfaces A: Physicochemical and Engineering Aspects, 471 (2015) 124-132.

[33] S. Morales-Torres, F.J. Maldonado-Hódar, A.F. Pérez-Cadenas, F. Carrasco-Marín, Structural characterization of carbon xerogels: From film to monolith, Microporous and Mesoporous Materials, 153 (2012) 24-29.

[34]. C. Scherdel, R. Gayer, G. Reichenauer, Porous organic and carbon xerogels derived from alkaline aqueous phenol-formaldehyde solutions, Journal of Porous Materials, 19 (2012) 351-360

[35] E.G. Calvo, N. Ferrera-Lorenzo, J.A. Menéndez, A. Arenillas, Microwave synthesis of micro-mesoporous activated carbon xerogels for high performance supercapacitors, Microporous and Mesoporous Materials, 168 (2013) 206-212.

[36] N. Job, C.J. Gommes, R. Pirard, J.-P. Pirard, Effect of the counter-ion of the basification agent on the pore texture of organic and carbon xerogels, Journal of Non-Crystalline Solids, 354 (2008) 4698-4701.

[37] C. Alegre, D. Sebastián, E. Baquedano, M.E. Gálvez, R. Moliner, M.J. Lázaro, Tailoring synthesis conditions of carbon xerogels towards their utilization as Pt-catalyst supports for oxygen reduction reaction (ORR), Catalysts, 2 (2012) 466-489.

[38] D. Fairén-Jiménez, F. Carrasco-Marín, C. Moreno-Castilla, Porosity and surface area of monolithic carbon aerogels prepared using alkaline carbonates and organic acids as polymerization catalysts, Carbon, 44 (2006) 2301-2307.

[39] R. Moussaoui, M.B. Mosbah, K. Elghniji, E. Elaloui, Y. Moussaoui, Sol-gel synthesis of microporous carbon using resorcinol and formaldehyde, Journal of Chemical Research, 40 (2016) 209-212.

[40] P.J.M. Carrott, L.M. Marques, M.M.L. Ribeiro Carrott, Core-shell polymer aerogels prepared by co-polymerisation of 2,4-dihydroxybenzoic acid, resorcinol and formaldehyde, Microporous and Mesoporous Materials, 158 (2012) 170-174.

[41] C. Moreno-Castilla, F.J. Maldonado-Hódar, Carbon aerogels for catalysis applications: An overview, Carbon, 43 (2005) 455-465.

[42] Y. Cho, J. Bailey, Immobilization of enzymes on activated carbon: properties of immobilized glucoamylase, glucose oxidase, and gluconolactonase, Biotechnology and Bioengineering, 20 (1978) 1651-1665.

[43] T. Kyotani, Control of pore structure in carbon, Carbon, 38 (2000) 269-286.

[44] L. Bayne, R.V. Ulijn, P.J. Halling, Effect of pore size on the performance of immobilised enzymes, Chemical Society Reviews, 42 (2013) 9000-9010.

[45] J. Huang, X. Li, Y. Zheng, Y. Zhang, R. Zhao, X. Gao, H. Yan, Immobilization of Penicillin G Acylase on Poly [(glycidyl methacrylate)-co-(glycerol monomethacrylate)]-Grafted Magnetic Microspheres, Macromolecular Bioscience, 8 (2008) 508-515.

[46] T.D. Lazzara, I. Mey, C. Steinem, A. Janshoff, Benefits and limitations of porous substrates as biosensors for protein adsorption, Analytical Chemistry, 83 (2011) 5624-5630.

[47] S. Hudson, J. Cooney, E. Magner, Proteins in mesoporous silicates, Angewandte Chemie International Edition, 47 (2008) 8582-8594.

[48] S. Hudson, E. Magner, J. Cooney, B.K. Hodnett, Methodology for the immobilization of enzymes onto mesoporous materials, The Journal of Physical Chemistry B, 109 (2005) 19496-19506.

[49] D. Fairén-Jiménez, F. Carrasco-Marín, C. Moreno-Castilla, Adsorption of Benzene, Toluene, and Xylenes on Monolithic Carbon Aerogels from Dry Air Flows, Langmuir, 23 (2007) 10095-10101.

[50] E.G. Calvo, N. Rey-Raap, A. Arenillas, J. Menéndez, The effect of the carbon surface chemistry and electrolyte pH on the energy storage of supercapacitors, RSC Advances, 4 (2014) 32398-32404.

[51] E.-P. Ng, S. Mintova, Nanoporous materials with enhanced hydrophilicity and high water sorption capacity, Microporous and Mesoporous Materials, 114 (2008) 1-26.

[52] D. Quéré, Wetting and roughness, Annual Review of Materials Research, 38 (2008) 71-99.

[53] A.W. Adamson, A.P. Gast, Physical chemistry of surfaces, (1967).

[54] R.N. Wenzel, Surface Roughness and Contact Angle, The Journal of Physical Chemistry, 53 (1949) 1466-1467.

[55] O. Manna, S.K. Das, R. Sharma, K.K. Kar, Superhydrophobic and Superoleophobic Surfaces in Composite Materials, Composite Materials, Springer 2017, pp. 647-686.

[56] A. Nakajima, K. Hashimoto, T. Watanabe, Recent studies on super-hydrophobic films, Monatshefte für Chemie/Chemical Monthly, 132 (2001) 31-41.

[57] A. Cassie, Contact angles, Discussions of the Faraday Society, 3 (1948) 11-16.

[58] R.E. Johnson Jr, R.H. Dettre, Contact angle hysteresis, ACS Publications1964.

[59] R.D. Hazlett, Fractal applications: wettability and contact angle, Journal of Colloid and Interface Science, 137 (1990) 527-533.

[60] J. Drelich, Static contact angles for liquids at heterogeneous rigid solid surfaces, Polish Journal of Chemistry, 71 (1997) 525-549.

[61] G. Wolansky, A. Marmur, The actual contact angle on a heterogeneous rough surface in three dimensions, Langmuir, 14 (1998) 5292-5297.

[62] P.B. Sarawade, J.-K. Kim, A. Hilonga, H.T. Kim, Preparation of hydrophobic mesoporous silica powder with a high specific surface area by surface modification of a wet-gel slurry and spray-drying, Powder Technology, 197 (2010) 288-294.

[63] A.P. Perissinotto, C.M. Awano, F.S. de Vicente, D.A. Donatti, A. Mesquita, L.F. da Silva, D.R. Vollet, Structure and diffuse-boundary in hydrophobic and

sodium dodecyl sulfate-modified silica aerogels, Microporous and Mesoporous Materials, 223 (2016) 196-202.

[64] J.L. Gurav, A.V. Rao, D.Y. Nadargi, H.H. Park, Ambient pressure dried TEOS-based silica aerogels: Good absorbents of organic liquids, J Mater Sci, 45 (2010) 503-510.

[65] A. Bisson, E. Rodier, A. Rigacci, D. Lecomte, P. Achard, Study of evaporative drying of treated silica gels, Journal of Non-Crystalline Solids, 350 (2004) 230-237.

[66] L.-J. Wang, S.-Y. Zhao, M. Yang, Structural characteristics and thermal conductivity of ambient pressure dried silica aerogels with one-step solvent exchange/surface modification, Materials Chemistry and Physics, 113 (2009) 485-490.

[67] W. Jeong, S. An, The transport properties of polymer membrane-fabric composites, Journal of materials science, 36 (2001) 4797-4803.

[68] J. Huang, A new test method for determining water vapor transport properties of polymer membranes, Polymer testing, 26 (2007) 685-691.

Anexo

Anexo

Comunicaciones a congresos

Los resultados obtenidos a lo largo de la presente Tesis Doctoral han dado lugar a diferentes trabajos presentados de forma oral o en forma de poster en distintos congresos nacionales e internacionales, los cuales se citan a continuación.

1

Autores: <u>Isabel D. Alonso-Buenaposada</u>, A. Arenillas, J.A. Menéndez

Título: Efecto de la proporción de metanol en disoluciones de formaldehído sobre la porosidad de xerogeles de carbono *(Poster)*

Congreso: XII Reunión del Grupo Español del Carbón, GEC

Lugar: Alicante (España)   **Fecha**: Octubre 2015

2

Autores: Alejandro Concheso, <u>Isabel D. Alonso-Buenaposada</u>, J.Angel Menéndez, Ana Arenillas, Miguel A. Montes-Morán

Título: Xerogel derived carbons with tuneable porosity for hosting biomolecules *(Poster)*

Congreso: Carbon

Lugar: Pensilvania (Estados Unidos)   **Fecha**: Julio 2016

3

Autores: <u>Isabel D. Alonso-Buenaposada</u>, Natalia Rey-Raap, Ana Arenillas, Esther G. Calvo, Miguel A. Montes-Morán, J.Angel Menéndez.

Título: Microwave heating applied to polymer science

Congreso: 3rd Global Congress on Microwave Energy Applications *(Poster)*

Lugar: Cartagena (España)   **Fecha**: Julio 2016

4

Autores: H. García,* L.A. Ramírez-Montoya, <u>I.D. Alonso-Buenaposada</u>, J. Ángel Menéndez, Ana Arenillas, M.A. Montes-Morán.

Título: Biocatalizadores soportados en xerogeles de carbono *(Comunicación Oral)*

Congreso: Sociedad Española de Catálisis (SECAT)

Lugar: Oviedo (España)   **Fecha**: Junio 2017

5

Autores: L.A. Ramírez-Montoya, * H. García, <u>I.D. Alonso-Buenaposada</u>, A. Arenillas, J.A. Menéndez, M.A. Montes-Morán.

Título: Xerogeles orgánicos como soportes de biocatalizadores enzimáticos *(Poster)*

Congreso: Sociedad Española de Catálisis (SECAT)

Lugar: Oviedo (España)   **Fecha:** Junio 2017

6

Autores: A. Arenillas, <u>I.D. Alonso-Buenaposada</u>, J.A. Menéndez.

Título: Mesopore size of RFxerogels for optimal water sorption capacity

Congreso: 19th International Sol-Gel Conference *(Poster)*

Lugar: Lieja (Bélgica)   **Fecha**: Septiembre 2017

7

Autores: L.A. Ramírez-Montoya, H. García, <u>I.D. Alonso-Buenaposada</u>, J.A. Menéndez, A. Arenillas, M.A. Montes-Morán.

Título: Fraccionamiento proteico en xerogeles de carbono mesoporosos *(Comunicación oral)*

Congreso: XIII Reunión del Grupo Español del Carbón, GEC

Lugar: Málaga (España)   **Fecha**: Octubre 2017

8

Autores: H. García, L.A. Ramírez-Montoya, <u>I.D. Alonso-Buenaposada</u>, J.A. Menéndez, A. Arenillas, M.A. Montes-Morán.

Título: Xerogeles de carbono como soporte para biocatalizadores *(Comunicación oral)*

Congreso: XIII Reunión del Grupo Español del Carbón, GEC

Lugar: Málaga (España)   **Fecha**: Octubre 2017

9

Autores: Luis A. Ramírez-Montoya*, Alejandro Concheso, <u>Isabel D. Alonso-Buenaposada</u>, Héctor García, J. Ángel Menéndez, Ana Arenillas, Miguel A. Montes-Morán.

Título: Carbon xerogels with tuneable porosity for cytochrome C adsorption *(Poster)*

Congreso: 10th World Congress of Chemical Engineering

Lugar: Barcelona (España)   **Fecha**: Octubre 2017